



HAL
open science

Study of new exchangers for boron removal from water containing high concentration of boron

Thi Thu Hien Nguyen

► **To cite this version:**

Thi Thu Hien Nguyen. Study of new exchangers for boron removal from water containing high concentration of boron. Other. Institut National Polytechnique de Toulouse - INPT, 2017. English. NNT : 2017INPT0138 . tel-04228531

HAL Id: tel-04228531

<https://theses.hal.science/tel-04228531v1>

Submitted on 4 Oct 2023

HAL is a multi-disciplinary open access archive for the deposit and dissemination of scientific research documents, whether they are published or not. The documents may come from teaching and research institutions in France or abroad, or from public or private research centers.

L'archive ouverte pluridisciplinaire **HAL**, est destinée au dépôt et à la diffusion de documents scientifiques de niveau recherche, publiés ou non, émanant des établissements d'enseignement et de recherche français ou étrangers, des laboratoires publics ou privés.



Université
de Toulouse

THÈSE

En vue de l'obtention du

DOCTORAT DE L'UNIVERSITÉ DE TOULOUSE

Délivré par :

Institut National Polytechnique de Toulouse (INP Toulouse)

Discipline ou spécialité :

Sciences des Agroressources

Présentée et soutenue par :

Mme THI THU HIEN NGUYEN

le mercredi 12 juillet 2017

Titre :

Study of some sorbents for boron removal from water containing high concentration of boron

Ecole doctorale :

Sciences de la Matière (SDM)

Unité de recherche :

Laboratoire de Chimie Agro-Industrielle (L.C.A.)

Directeur(s) de Thèse :

M. PHILIPPE BEHRA

M. PIERRE YVES PONTALIER

Rapporteurs :

M. HERVE GALLARD, UNIVERSITE DE POITIERS

M. MICHEL SARDIN, UNIVERSITÉ LORRAINE

Membre(s) du jury :

M. SYLVAIN OUIILLON, UNIVERSITE TOULOUSE 3, Président

Mme ISABELLE LE HECHO, UNIVERSITE DE PAU ET DES PAYS DE L ADOUR, Membre

M. PHILIPPE BEHRA, INP TOULOUSE, Membre

M. PIERRE YVES PONTALIER, INP TOULOUSE, Membre

RESUME EN FRANÇAIS

Le bore est nécessaire pour le développement des plantes supérieures (structuration de la paroi végétale). Il pose cependant des problèmes (défoliation, pourriture et chute des fruits mûrs). Pour l'homme, sa toxicité se traduit par des nausées, des diarrhées, des troubles du développement intellectuel, neurologique et physique.

La pénurie en eau douce conduit à dessaler l'eau de mer pour augmenter la quantité en eau destinée à la consommation humaine, l'industrie et l'agriculture. Lors de ce procédé, il faut éliminer les ions majeurs mais aussi le bore présent à des concentrations élevées ($> 4,5 \text{ mg L}^{-1}$, environ $0,45 \text{ mM}$). Son usage dans l'industrie et son rejet dans l'environnement conduisent à la pollution des eaux souterraines et de surface. Son élimination est donc indispensable, sachant que l'Organisation Mondiale de la Santé recommande une valeur guide de $0,5 \text{ mg L}^{-1}$ dans l'eau potable et une valeur maximale de $0,3 \text{ mg L}^{-1}$ dans l'eau utilisée pour l'irrigation.

Cette thèse porte sur l'étude cinétique et thermodynamique des échanges du bore à la surface de différents matériaux en fonction de paramètres physico-chimiques (pH, concentration initiale ...) à l'aide d'essais en réacteurs fermés et en colonnes.

Deux types de résines commerciales ont été choisies : (i) les résines échangeuses d'anions Ambersep 900-OH et Amberlite IRA 402 Cl avec des fonctions ammonium, (ii) les résines spécifiques Amberlite IRA 743 et Diaion CRB 03 ayant des fonctions méthylglucamine.

Les premières essais en réacteurs fermés montrent que les échanges liquide-solide sont rapides avec une élimination du bore $> 96\%$ pour $t < 30 \text{ min}$ pour Amberlite IRA 743, Diaion CRB 03 et Ambersep 900-OH. Pour $t > 2 \text{ h}$, un équilibre est observé pour toutes les résines. Le modèle du pseudo-second ordre permet de décrire la cinétique de sorption pour les 4 résines. A l'équilibre, l'adsorption est maximum d'une part dans une gamme de pH compris entre 6 et 12 pour les 2 résines sélectives Amberlite IRA 743 et Diaion CRB 03, et d'autre part pour un pH de 8 pour la résine Ambersep 900-OH et un pH 10 pour la résine Amberlite IRA 402 Cl. Au pH initiale 8, l'affinité de bore pour les résines a diminué comme suit: Ambersep 900-OH ($1,6 \text{ mmol g}^{-1}$), Amberlite IRA 743 ($1,3 \text{ mmol g}^{-1}$), Diaion CRB 03 ($0,9 \text{ mmol g}^{-1}$) and Amberlite IRA 402 Cl ($0,2 \text{ mmol g}^{-1}$). Dans la gamme des concentrations de bore étudiées, (i) la relation de type Langmuir a été appliquée aux résines Ambersep 900-OH et Diaion CRB 03 pour l'ajustement de la capacité de sorption maximale et du coefficient de type Langmuir qui sont de 2,2 et $0,87 \text{ mmol g}^{-1}$ respectivement. (ii) la relation de type BET a été utilisée pour décrire le comportement du bore en présence de la résine Amberlite IRA 743 et pour estimer le coefficient de type BET et la capacité de sorption du bore ($0,43 \text{ mmol g}^{-1}$); et (iii) le modèle de type Henry a été utilisé pour adapter le comportement à la sorption du bore dans le cas de l'Amberlite IRA 402 Cl.

Les résines Ambersep 900-OH, échangeuse d'anions, et Amberlite IRA 743, sélective, ont été utilisées pour les essais en colonnes en fonction de la concentration en bore et du temps de séjour. Pour la résine spécifique, le temps de séjour dans la colonne affecte fortement le comportement du bore : lorsqu'il diminue, son élution est rapide suivie d'une longue traînée ; lorsqu'il augmente, la courbe de percée correspond à un système à l'équilibre. Pour un temps de séjour

élevé, les résultats confirment la non-linéarité observée lors des essais en réacteurs fermés. Pour la résine échangeuse d'anions, la non-linéarité est aussi confirmée. Ces essais permettent de différencier le comportement du bore lors de sa désorption. La régénération est obtenue après des traitements acides et basiques pour la résine spécifique alors qu'un traitement alcalin est suffisant pour la résine anionique. Des modèles optimisés et des modèles non linéaires sont étudiés pour construire un modèle d'échange pour prédire le devenir de bore.

La fixation du bore sur des pectines et sa rétention par des membranes d'ultrafiltration (membranes de seuil de coupure différent) a aussi été étudiée. Les pectines ont été caractérisées (composition en sucre et en bore présent initialement) et la viscosité des solutions pectiques mesurée. Des essais de filtration ont permis de déterminer l'efficacité de production et de rétention du bore sur ces matériaux.

RESUME EN ANGLAIS

Boron is an element, which is necessary as essential nutrient for living organisms, especially for plants where it is involved in cell wall composition. But boron excess can cause some problems on the development of plants (defoliation, decay and fall unripe fruits), of humans and animals such as nausea, diarrhoea, dermatitis, lethargy. Boron toxicity also changes blood composition, caused disorder in neurological, physical, intellectual development.

Nowadays, due to the shortage of fresh water sources, seawater desalination has been becoming an alternative fresh water supply. However, the presence of boron in seawater is quite high (4.5 mg L^{-1} , around 4.5 mM). Moreover, the increasing use of boron in industries and its discharge to the environment has led to the contamination of surface and ground waters. As the result, boron removal, in production of drinking water becomes very important. Therefore, the World health organization has recommended a guideline of $0.5 \text{ mg L}^{-1} \text{ B}$ in drinking water and a maximum limit of $0.3 \text{ mg L}^{-1} \text{ B}$ in fresh water used for irrigation.

The objective of this thesis is to study the mechanisms of boron surface exchange on different materials *versus* time and at equilibrium depending on some physicochemical parameters such as pH, initial boron concentration, reaction time in order to find a new exchanger for boron removal. Boron removal was carried out by ion exchange process using 2 types of resins: Amberlite IRA 743, Diaion CRB 03 as boron selective resins with methylglucamine functions, and Ambersep 900-OH and Amberlite IRA 402 Cl as anionic exchange resins with ammonium functions. From batch studies, fast exchange between resin surface and liquid phase was observed with boron removal up to at least 96% within 30 min for Amberlite IRA 743, Diaion CRB 03 and Ambersep 900-OH. The reaction between resin surface and boron solution reached equilibrium after 2 h for all the resins. The pseudo-second order kinetic model was used to well describe the sorption kinetic process of the resins. At equilibrium, the experimental results showed that the maximum adsorption was observed to be achieved at pH 8 for Ambersep 900-OH, pH 10 for Amberlite IRA 402 Cl and independent on pH range from 6 to 12 for the 2 boron selective resins Amberlite IRA 743 and Diaion CRB 03. At initial pH 8, the boron affinity for resins decreased as follow: Ambersep 900-OH (1.6 mmol g^{-1}), Amberlite IRA 743 (1.3 mmol g^{-1}), Diaion CRB 03 (0.9 mmol g^{-1}) and Amberlite IRA 402 Cl (0.2 mmol g^{-1}). In the range of boron concentrations studied, (i) the Langmuir-type relationship was applied to the Ambersep 900-OH and Diaion CRB 03 resins for fitting the maximum sorption capacity and the Langmuir-type coefficient which are 2.2 and 0.87 mmol g^{-1} respectively; (ii) the BET-type relationship was used for describing the boron behaviour in the presence of the Amberlite IRA 743 resin and for estimating the BET-type coefficient and the boron sorption capacity (0.43 mmol g^{-1}); and (iii) the Henry-type model was used for fitting boron sorption behaviour in the case of the Amberlite IRA 402 Cl.

Column experiments were performed with the anionic resin Ambersep 900-OH and the selective one Amberlite IRA 743 by studying both the influence of boron concentration and the residence time. For the selective resin, if the residence time decreases, the boron breakthrough is fast followed by a long tail. For larger residence time, local equilibrium seems to be assumed. Results

are thus consistent with batch experimental data. For the anionic resin, the non-linear behaviour is also confirmed. Moreover, column experiments showed a strong difference during desorption. To regenerate resins, acid and basic treatments are necessary for the selective resin although a basic solution is enough for the anionic resin. Optimized models and non - linear models are studied to build an exchange model for predicting boron fate.

Finally, characterization of pectins was also performed. Its composition (sugar and boron content) and the viscosity of pectin solutions were quantified. Filtration experiments allowed testing the efficiency of such material to remove boron too.

Acknowledgements

First of all, I would like to express my deepest gratitude to my thesis supervisors: professor Philippe Behra and doctor PierreYves Pontalier. It is my honor to have chance to work with them more than 4 years in Laboratoire de Chimie Agro-Industrielle (LCA), ENSIACET, INPT. From them, I learned a lot from their way of analyzing, solving problems as well as a meticulous, careful characteristic, which is one of the most extremely important factors in research field.

I am very much thankful to other colleagues in LCA, Romain and Remy, who has supported me a lot whenever I need more chemicals or equipment to do my experiments.

I am grateful to the participant of the following interns who has helped me very much in doing manipulation, especially for my column experiments which take lots of time and labor: Mohamed Badis Ayadi, Maria Nassarruiz, Elie Beros, Bou Rania, Paul Chaboureau, Falba Pierre, Carole Mailhan, BE Ngoc Diep. Without them, I couldn't imagine how can I finish a huge amount of experiment during my thesis.

It is also my pleasure to thank other PhD students in LCA who has shared with me not only their work experience but also the stress I met during my thesis: Mogni Assad, Benjamin Moras, BORIES Cecile, Alan Castillo Villa, Marian Anaya Castro, Pablo Lopez Hurtado, ORIEZ Vincent, Beaufils Nicolas. My thesis could be well done because of your great distribution and correction also.

Thank to Vietnamese friends in LCA: Quang Hung, Mai Anh, Nhật Mai, Thuỳ Dung, Thanh Tâm, Ngọc Diệp, Ngọc Hà, Minh Huy and two others in LGC: Văn Nhất, Trung Dũng for sharing with me other activities: travelling, having lunch, relaxing...

Nothing could be greater than the support from my beloved family: my husband who always listened to me and encouraged me to get over every hardest moment, my parents, my parents in law, my brother and sisters who live thousands miles far away from me but always believe in me and give me a hand whenever I need.

Toulouse, 24/09/2017

NGUYEN Thi Thu Hien

Table of contents

List of abbreviations	XIII
INTRODUCTION.....	1
Chapter 1 STATE OF THE ART	7
1.1. Boron presentation	9
1.1.1. Introduction of boron.....	9
1.1.2. Sources of boron.....	9
1.1.2.1. Natural sources.....	9
1.1.2.2. Boron sources from human activities.....	10
1.1.3. Boron and its effect on life development	10
1.2. Boron in water production	11
1.2.1. Water resources	11
1.2.2. Boron chemistry in aqueous solution	12
1.2.3. Desalination plant for water production	13
1.2.3.1. Types of desalination plants.....	13
1.2.3.2. Membrane plant design	13
1.3. Study of boron removal technologies	15
1.3.1. Reverse osmosis method	15
1.3.1.1. Reverse osmosis principles	15
1.3.1.2. Membrane separation mechanisms	16
1.3.1.3. Effects of each parameter on boron rejection	17
1.3.2. Ion exchange methods	19
1.3.2.1. Boron selective resins	19
1.3.2.1.1. Fixation mechanisms	19
1.3.2.1.2. Resin structure development	20
1.3.2.1.3. Effects of each parameter on boron rejection.....	23
1.3.2.2. Non boron selective resins	24
1.3.2.2.1. Ion exchange mechanism.....	24

1.3.2.2.2. Effect of each parameter on boron rejection	25
1.3.2.3. Other adsorbents	26
1.3.3. Hybrid methods	30
1.3.3.1. PEUF – Polymer enhanced ultrafiltration method	30
1.3.3.2. AMF – Adsorption membrane filtration	31
1.3.4. Other methods	33
1.3.4.1. Electrocoagulation method (EC).....	33
1.3.4.2. Donnan dialysis method (DD)	33
1.3.4.3. Capacitive deionization method (CDI)	33
1.3.4.4. Direct contact membrane distillation method (DCMD)	34
1.3.4.5. Conclusion	34
1.4. Theoretical models for batch and column systems.....	36
1.4.1. Kinetic and adsorption models	36
1.4.1.1. Kinetic models	36
1.4.1.2. Sorption model theory.....	37
1.4.2. Non-linear chromatography theory for column experiment.....	39
1.4.3. Optimized modeling of breakthrough curves	42
1.4.3.1. Pseudo first order modeling	42
1.4.3.2. Pseudo second order modeling	44
1.5. Pectins - New adsorbents	44
1.5.1. Pectins.....	44
1.5.1.1. Pectins presentation and functions	44
1.5.1.1. Pectins structure and properties	45
1.5.1.2. Application of pectins on industry	49
1.5.2. Membrane filtration.....	49
1.5.2.1. Principle and limiting factors	50
1.5.2.1.1. Principles	50
1.5.2.1.2. Limiting parameters of membrane filtration	51

1.5.2.1.3. Membrane configurations and modules	53
1.5.3. Conclusion.....	56
Chapter 2 MATERIAL AND METHODS.....	58
2.1. Boron analysis methods	60
2.2. Experiments on batch system.....	60
2.2.1. Resins	60
2.2.2. Experiment procedures	63
2.2.2.1. Kinetic experiments	63
2.2.2.1. pH effect experiments	63
2.2.2.2. Isotherm experiments	63
2.3. Experiments on column system	64
2.3.1. Material and experimental set-up	64
2.3.2. Experimental procedure.....	65
2.3.2.1. Pore volume (V_p) determination	65
2.3.2.2. Boron adsorption experiment.....	66
2.4. Experiments on hybrid system.....	67
2.4.1. Material.....	67
2.4.2. Experimental procedure.....	68
2.4.2.1. Pectin characterization	68
2.4.2.1.1. Pectin hydrolysis.....	68
2.4.2.1.2. Sugar and galacturonic acid analysis.....	68
2.4.2.1.3. Viscosity measurement.....	69
2.4.2.2. Boron fixation on hybrid method.....	69
2.4.2.2.1. Ultrafiltration evaluation on Amicon cell and hollow-fiber system.....	69
2.4.2.2.2. Boron fixation at different pH	70
2.4.2.2.2.1. Pectin with Milli-Q water.....	70
2.4.2.2.2.2. Pectin with boron solution	70

Chapter 3	BORON FIXATION ON SYNTHETIC RESINS WITH BATCH-MODE SYSTEM..	73
3.1.	Introduction.....	75
3.2.	Sorption kinetic and isotherm theory.....	78
3.3.	Material and methods.....	81
3.3.1.	Materials.....	81
3.3.2.	Methods.....	81
3.3.2.1.	Kinetic experiments.....	81
3.3.2.2.	pH effect experiments.....	82
3.3.2.3.	Isotherm experiments.....	82
3.3.3.	Boron analysis.....	82
3.4.	Results.....	83
3.4.1.	Kinetic sorption experiments.....	83
3.4.2.	Effect of pH on the boron adsorption.....	87
3.4.3.	Isotherm experiments.....	88
3.5.	Discussion.....	91
3.6.	Conclusion.....	96
Chapter 4	BORON FIXATION ON SYNTHETIC RESINS WITH FLOW - THROUGH REACTOR.....	98
4.1.	Introduction.....	100
4.2.	Materials and methods.....	101
4.2.1.	Materials.....	101
4.2.2.	Methods.....	101
4.2.2.1.	Boron analysis.....	101
4.2.2.2.	Column experiments.....	102
4.2.2.2.1.	Pore volume (V_p) Determination.....	102
4.2.2.2.2.	Boron experiments.....	103
4.3.	Results.....	103
4.3.1.	Pore volume (V_p) determination.....	103
4.3.1.1.	Ambersep 900-OH resin.....	103

4.3.1.2. Amberlite IRA 743 resin.....	106
4.3.2. Boron fixation experiments	108
4.3.2.1. Ambersep 900-OH.....	108
4.3.2.1.1. Influence of boron concentration.....	108
4.3.2.1.2. Influence of flow rate	109
4.3.2.1.3. Influence of resin bed volume	110
4.3.2.2. Amberlite IRA 743.....	111
4.3.2.2.1. Influence of flow rate	111
4.3.2.3. Comparison between two resins	112
4.3.2.4. pH and conductivity evolution.....	115
4.3.2.4.1. Ambersep 900-OH.....	115
4.3.2.4.2. Amberlite IRA 743	117
4.3.3. Optimized models.....	120
4.3.3.1. Pseudo first order breakthrough curve modeling.....	120
4.3.3.2. Pseudo-second order breakthrough curve modeling.....	122
4.3.4. Non-linear chromatography modeling	124
4.3.4.1. Non-linear model	124
4.3.4.2. Non-linear modeling	127
4.3.5. Conclusion.....	131
Chapter 5 PECTIN EXTRACTS FOR BORON REMOVAL IN WATER.....	133
5.1. Introduction.....	135
5.2. Materials and methods	138
5.2.1. Materials.....	138
5.2.2. Methods	139
5.2.2.1. Pectins characterization.....	139
5.2.2.1.1. Pectin hydrolysis.....	139
5.2.2.1.2. Sugar and galactorunic acid analysis.....	140
5.2.2.1.3. Viscosity measurement.....	140

5.2.2.1. Boron fixation on hybrid method.....	141
5.2.2.1.1. Ultrafiltration evaluation on Amicon cell and hollow-fiber system.....	141
5.2.2.1.2. Boron fixation at different pH	142
5.2.2.1.2.1. Pectin with Milli-Q water.....	142
5.2.2.1.2.2. Pectin with boron solution	142
5.3. Results and discussion	142
5.3.1. Pectin characterization.....	142
5.3.2. Ultrafiltration.....	143
5.3.2.1. Membranes screening	143
5.3.2.1.1. Membrane permeability.....	143
5.3.2.1.2. Influence of the pressure.....	146
5.3.2.2. Membrane performance evaluation	146
5.3.2.2.1. Batch extracted pectin	147
5.3.2.2.2. Twin-screw extracted pectin.....	147
5.3.2.3. Discussion	148
5.3.3. Boron fixation.....	149
5.3.3.1. Fixation experiment	149
5.3.3.1.1. Twin-screw extracted pectin.....	149
5.3.3.1.2. Batch extracted pectin	151
5.3.3.2. Discussion	152
5.3.4. Conclusion.....	152
CONCLUSIONS AND PERPECTIVES	155
5.4. Conclusions and perspectives	157
5.5. Future works	160

List of figures

Fig. 1.1. Boric acid speciation as a function of pH	12
Fig. 1.2. Presentation of the complete flowsheet of a desalination plant.....	14
Fig. 1.3. Boron removal processes of seawater desalination	15
Fig. 1.4. Osmosis and reverse osmosis model	16
Fig. 1.5. Mechanism of water transport through reverse osmosis membrane by performing bridges of hydrogen	17
Fig. 1.6. The distribution of boric acid and borate in seawater by the changes of each parameter. ..	18
Fig. 1.7. Structure of borate complex.....	19
Fig. 1.8. Reactions during boron complex formation.	19
Fig. 1.9. Reactions during boron complex formation	20
Fig. 1.10. Structure of boron selective resins containing N-methyl-D-glucamine.....	22
Fig. 1.11. Ion exchanger types	25
Fig. 1.12. Synthesis of N-methylglucamine-type cellulose derivatives.....	27
Fig. 1.13. Group configurations in cotton cellulose.....	27
Fig. 1.14. Boron fixation reaction on cotton cellulose.....	27
Fig. 1.15. Synthesis of cross – linked chitosan and N-methylglucamine.	28
Fig. 1.16. Flow sheet of the adsorption membrane filtration system.....	31
Fig. 1.17. Schematic representation of the response of the chromatographic column for linear adsorption isotherms.	40
Fig. 1.18. Examples of Golden’s rule.	41
Fig. 1.19. Relation between the shape of an adsorption isotherm and the shape of the breakthrough curve.....	42
Fig. 1.20. The structures of two possible isomers of the reversible RG-II-Boron diester found in the walls of plant.....	48
Fig. 1.21. The concentration polarization in filtration process.	52
Fig. 1.22. different resistances including concentration polarization and clogging.....	53
Fig. 1.23. The dead-end and cross-flow geometries	54
Fig. 1.24. Spiral wound membrane module	55
Fig. 1.25. Hollow fiber membrane modules (outside-in mode).....	55

Fig. 2.1. Batch experiment design.....	64
Fig. 3.1. Proposed mechanisms for the binding of boron by chelating resins	76
Fig. 3.2. N-methylglucamine group	77
Fig. 3.3. Kinetic experiments of boron fixation on the four resins: IRA 743, CRB 03, IRA 402 Cl and Ambersep 900-OH at initial pH 8	84
Fig. 3.4. Fitting of sorption boron kinetic experiments with the pseudo-first order kinetic model from 0 to 15 min the anionic Ambersep 900-OH resin and for the boron selective resin Amberlite IRA 743	85
Fig. 3.5. Fitting of sorption boron kinetic experiments with the pseudo-second order kinetic model for B sorption on the 4 resins.....	86
Fig. 3.6. pH Adsorption-edge experiments of boron adsorbed on the 4 resins, Amb 900-OH, CRB 03, IRA 743, IRA 402 Cl at pH 8	88
Fig. 3.7. Adsorption isotherms of boron with the selective and anionic resins for initial pH 8	89
Fig. 3.8. Comparison between Langmuir-type fitting (line: —) and experimental data (dots) for boron sorption on the resins: (a) Amberlite IRA 743, (b) Diaion CRB 03, (c) Ambersep 900-OH; and (d) linear-type fitting for the anionic resin Amberlite IRA 402 Cl.....	91
Fig. 3.9. Two first-step mechanisms for explaining BET-type behavior of boron sorption on the specific resin Amberlite IRA 743 taking into account diborate ion complexation supported by bond analyses of borates	95
Fig. 4.1. Adsorption of NaCl 0.05 M, pH 8.8 and NaCl 0.1 M, pH 9.0 on 100 mL Ambersep 900-OH resin, the first time, flow rate of 10 BV h ⁻¹ (1 L h ⁻¹).....	104
Fig. 4.2. Determination of V _p of 100 mL Ambersep 900-OH dry resin	105
Fig. 4.3. Adsorption of NaCl 0.05 M, pH 8.8 and NaCl 0.1 M, pH 8.9 on 100 mL Ambersep 900-OH resin, the second and the third time, flow rate of 10 BV h ⁻¹ (1 L h ⁻¹).....	106
Fig. 4.4. Adsorption of 0.05 M NaCl, pH 8.0 and 0.1 M NaCl, pH 8.9 on 100 mL Amberlite IRA 743 resin, flow rate of 30 BV h ⁻¹ (3 L h ⁻¹).	107
Fig. 4.5. Effect of boron concentration on boron breakthrough in the presence of Ambersep 900-OH. Experimental conditions: 9.0 mM and 1.8 mM boron solutions, 10 BV h ⁻¹ (1 L h ⁻¹), pH 8.....	108
Fig. 4.6. Effect of flow rate on boron breakthrough in the presence of Ambersep 900-OH.....	109
Fig. 4.7. Adsorption of 0.05 M NaCl, pH 8.0 and 0.1 M NaCl, pH 8.9 on 100 mL Amberlite IRA 743 resin, flow rate of 30 BV h ⁻¹ (3 L h ⁻¹).	110
Fig. 4.8. Breakthrough curve for desorption of 9.54 mM B solution, at flow rate of 16 BV h ⁻¹ (6.4 L h ⁻¹), pH 13.....	111

Fig. 4.9. Effect of flow rate on boron breakthrough in the presence of Amberlite IRA 743	112
Fig. 4.10. Comparison of boron breakthrough for the two types of resin, the specific IRA 743 and the anionic Ambersep 900-OH ones.	113
Fig. 4.11. Breakthrough curves of [B] versus [OH ⁻] for adsorption and desorption process of 1.8 mM boron solution, 10 BV h ⁻¹ (1.0 L h ⁻¹), pH 8.....	116
Fig. 4.12. Breakthrough curves of [B] versus C for adsorption and desorption process of 1.8 mM boron solution, 10 BV h ⁻¹ (1.0 L h ⁻¹), pH 8..	116
Fig. 4.13. Breakthrough curves of [B] versus [OH ⁻] for desorption process of 1.8 mM boron solution, 10 BV h ⁻¹ (1.0 L h ⁻¹), pH 12.6.....	117
Fig. 4.14. Breakthrough curves of boron and hydroxide versus elution volume for adsorption process of 8.62	118
Fig. 4.15. Breakthrough curves of boron and conductivity versus elution volume for adsorption process of 8.62 mM boron solution, 10 BV h ⁻¹ (1.0 L h ⁻¹), pH 8.	119
Fig. 4.16. Breakthrough curves of boron and pH versus elution volume for desorption process 8.62 mM boron solution, 10 BV h ⁻¹ , using 0.5 M H ₂ SO ₄ and 0.25 M NaOH.....	120
Fig. 4.17. Linear plot of time vs. ln(C/(C ₀ -C)) at 9.54 mM, 400 mL resin, 16 BV h ⁻¹ , Amb 900-OH resin.....	121
Fig. 4.18. Comparison between experimental and predicted breakthrough curves according to Yoon and Nelson model ([B]: 9.54 mm, 400 ml resin, 16 BV h ⁻¹ , Amb 900-OH resin)	121
Fig. 4.19. Linear plot of time vs ln(C/(C ₀ -C)) at 8.62 mM, 100 mL resin, 10 BV h ⁻¹ , Amb IRA 743	121
Fig. 4.20. Comparison between experimental and predicted breakthrough curves according to Yoon and Nelson model ([B]: 8.62 mM, 100 ml resin, 10 BV h ⁻¹ , Amb IRA 743)	121
Fig. 4.21. Linear plot of volume vs ln((C ₀ -C)/C) at 9.54 mM, 400 mL resin, 16 BV h ⁻¹ , Amb 900-OH.....	123
Fig. 4.22. Comparison between experimental and predicted breakthrough curves according to Thomas model ([B]: 9.54 mM, 400 ml resin, 16 BV h ⁻¹ , Amb 900-OH)	123
Fig. 4.23. Linear plot of volume vs ln((C ₀ -C)/C) at 8.62 mM, 100 mL resin, 10 BV h ⁻¹ , Amb IRA 743	123
Fig. 4.24. Comparison between experimental and predicted breakthrough curves according to Thomas model ([B]: 8.62 mM, 100 ml resin, 10 BV h ⁻¹ , Amb IRA 743).....	123
Fig. 4.25. Comparison of boron fixation fronts of model, optimized model and experiment with Ambersep 900-OH	127
Fig. 4.26: Comparison of boron elution of of model, optimized model and experiment with Ambersep 900-OH.....	128

Fig. 4.27. Comparison of model and experiment for boron fixation front with Ambersep IRA 743.	129
Fig. 5.1. Description of the interaction between pectin and boron.	137
Fig. 5.2. The illustration of boron complexation with RG-II.....	138
Fig. 5.3. Influence of the stirring velocity on the membrane permeability during the filtration of water with three membranes.	144
Fig. 5.4. Permeate flux evolution versus the stirring velocity during the filtration of a 5 g L ⁻¹ pectin solution with three membranes	144
Fig. 5.5. Influence of the pressure during the filtration of pectin solution.....	146
Fig. 5.6. Influence of the pressure on the permeate flux at steady state during the filtration of a 5 g L ⁻¹ pectin solution at 25 °C. Pectin has been extracted in batch condition.	147
Fig. 5.7. Influence of the pressure on the permeate flux at steady state during the filtration of a 5 g L ⁻¹ pectic solution at 25 °c. Pectin have been extracted by twin-screw extrusion.	148

List of table

Table 1.1. Some designed N-Methyl- D -glucamine resins.....	21
Table 1.2. Functional groups for anion exchangers	25
Table 1.3. The list of boron removal technologies.....	35
Table 1.4. Pectin content of some fruits.....	46
Table 1.5. The classification of membrane separation techniques.....	51
Table 2.1. Typical chemical and physical characteristics of four resins.....	61
Table 2.2. Mass and length in column of 100 ml each resin.....	65
Table 2.3. Properties of the sodium chloride solutions before elution.....	65
Table 2.4. Boron adsorption column experiment planning.....	66
Table 2.5. Suggested concentration ranges for calibration standards.....	69
Table 2.6. List of chemicals	71
Table 3.1. Rate constant k_1 , amount of boron adsorbed at equilibrium q_e and half-time of boron sorption reaction	85
Table 3.2. Rate constant k_2 , amount of boron adsorbed at equilibrium q_e and half-time of boron sorption reaction	87
Table 3.3. Maximum adsorption capacity, Langmuir-type coefficient, distribution coefficient and correlation coefficients estimated from the Langmuir-type relationship for the two selective resins and the anionic resin Ambersep 900-OH. For the Amberlite IRA 402-Cl, linear-type relationship was applied.....	90
Table 4.1. Properties of the sodium chloride solutions before elution.....	103
Table 4.2. Properties of the NaCl solutions for the second and third elutions.....	105
Table 4.3. Properties of the NaCl solutions for V_p determination of IRA 743	107
Table 4.4. Column utilization performance for each resin.....	114
Table 4.5. Boron adsorption capacities on each resin	115
Table 4.6. Properties of the boron feed solutions used for adsorption on Ambersep 900-OH	115
Table 4.7. Properties of the boron feed solution used for adsorption on Amberlite IRA 743	118
Table 4.8. Properties of the desorption solutions.....	120
Table 4.9. Yoon and nelson model parameters compared to pseudo-first order model parameters	122

Table 4.10. Yoon and nelson model parameters compared to pseudo-first order model parameters	124
Table 4.11. Mass and length in column of 100 mL each resin.....	126
Table 4.12: Calculation of the influence of the concentration on the boron retardation factor on the resin Ambersep IRA 900-OH.	128
Table 4.13: Comparison of the influence of the concentration on the boron retardation factor for model and experiment results of Simonnot and co-workers.....	130
Table 5.1. Suggested concentration ranges for calibration standards	140
Table 5.2. Composition of the pectin extracts used for the boron fixation.....	143
Table 5.3. The hydraulic permeabilities of the membrane with water and pectic solutions	145
Table 5.4. Boron in pectin, boron adsorbed by pectin, initial & final pH of adsorption experiment between boron solution and dry twin-screw pectin	150
Table 5.5. Influence of the pressure during the filtration of pectin solution.....	150
Table 5.6. Influence of the pressure on the permeate flux at steady state during the filtration of pectin solution. Pectin has been extracted in batch condition.....	151
Table 5.7. Boron in pectin, boron adsorbed by pectin, initial & final pH of adsorption experiment between boron solution and dry batch extracted pectin.....	152

List of abbreviations

Abbreviation	Fullname
AAS	Atomic absorption spectrometry
Amberlite IRA 400 Cl	IRA 400 Cl
Amberlite IRA 743	Amb IRA 743
Ambersep 900-OH	Amb 900-OH
AMF	Adsorption membrane filtration
BET	Brunauer-Emmett-Teller
BSRs	Boron selective resins
CDI	Capacitive deionization method
CRC	<i>Caulerpa racemosa</i> var. <i>cylindracea</i>
DCMD	Direct contact membrane distillation method
DD	Donnan dialysis method
DE	Degree of esterification
Diaion CRB 03	CRB 03
DVB	divinyl benzene
EC	Electrocoagulation method
ED	Electrodialysis
EDTA	Ethylenediaminetetraacetic acid
EU	European Union
GalA	Galacturonan acid
GMA	Glycidyl methacrylate
H/D	Height/Diameter
H/D	Height/Diameter
HG	Homogalacturonan
HM	High-methoxy
HPLC	High Performance Liquid Chromatography

ICP-AES	Inductively coupled plasma - Atomic emission spectroscopy
IUPAC	International Union of Pure and Applied Chemistry
LM	Low-methoxy
LOD	Limit of detection
LOQ	Limit of quantification
LTV	Long-tube vertical distillation
MD	Membrane distillation
MED	Multiple-effect evaporation/distillation
MENA	The Middle East and North African
MMA	Methyl methacrylate
MSF	Multi-stage flash evaporation/distillation
MWCO	Molecular weight cut-off
NMDG	N-methyl-D-glucamine
NRA	Nuclear reaction analytical
NREL	National Renewable Energy Laboratory
PEUF	Polymer enhanced ultrafiltration method
pKa	Acid dissociation constant
PTFE	Polytétrafluoroéthylène
RG	Rhamnogalactorunan
RO	Reverse osmosis
SRS	Sugar recovery standards
TIMS	Thermal ionization mass spectrometry
UK	United Kingdom
VCD	Vapor compression distillation
Vp	Pore volume
WHO	World Health Organization
WNM	Waste natural materials

INTRODUCTION

Fresh water is one of the most essential compounds necessary for the development of life on Earth. Fresh water plays an important role for the vital needs of human, animals and plants. Water content ranges from 60% to 95% in living organisms, in which humans are about 60 % water. To maintain health, humans need to drink 1.5 L to 2.5 L water per person per day. Moreover, people use fresh water for many purposes: Daily activities, raising livestock, or industrial production such as food, textile, etc. The presence of water is mandatory in most of development processes of plants such as photosynthesis, growth and reproduction. Different crops consume different level of water (from 300 to 2000 L) to produce one kilogram of dry matter (Pimentel *et al.* 2004). However, available fresh water source is very limited. Water all over the world has distributed mainly as seawater on the ocean with 97.5%, 1.7% as fresh water in icecap and only 0.8% as available fresh water which can be found as ground water or surface water in streams, lakes, or rivers (Shiklomanov and Rodda, 2003). Nowadays, water shortage is becoming a serious problem all over the world because of climate change and human impacts. The high water demand because of population rapid increasing, coupled with the heavy water pollution, due to the leakage of industrial sewage into the environment, are the crucial reasons. Besides, low annual rainfall level plus hardly water-stored geological characteristic like in Middle East North Africa are also the main factors for the lack of fresh water. In addition, with the global warming, drought exists longer in many areas while people, animal and plant as well need more fresh water to sustain their lives. Therefore, it is necessary to find alternative fresh water sources to respond the high demand of water of society. Desalted water produced from seawater desalination is one of the feasible solutions.

Water desalting is usually performed from seawater by water evaporation and by membrane plants where reverse osmosis is the desalting step. This latter technology is widely used because water production is cheaper. Unfortunately, desalted water contains a high concentration of boron. Normally, boron concentration in seawater is about 4.6 mg L⁻¹, higher in Mediterranean Sea (9.6 mg L⁻¹) (Xu and Jiang, 2008). After desalination, boron concentration decreased but still higher than 1.0 mg L⁻¹. Even with surface water or ground water, boron concentration can be high because of the contamination of boron appearing from discharge of wastewater due to using boron containing products in daily life such as soaps, glass production, fertilizer, etc. Hence, there is a problem with water containing low salt concentration but boron that must be removed.

Boron is one of the essential elements for the development of animals and plants but excess boron also cause some health and ecological damages. For the animals, boron toxicity limits cell formation, weakens the bones, retards growth and creates disorders of the reproductive system. For the plant, it is poisonous, shows adversely physical effects, for example, the reduction of root cell division, the inhibition of photosynthesis, the decrease of the chlorophyll. Consequently, it is very important to control boron concentration in water to get a guaranty water source for human living and irrigation. As the results, boron limitation was set up in drinking water is 0.5 mg L⁻¹ by WHO and 1.0 mg L⁻¹ by EU. For some sensitive crops such as citrus trees, the boron limitation is lowered to 0.3 mg L⁻¹ in irrigation water (WHO, 1998; WHO, 2011).

However, boron removal is a not easy solving problem. Many researches were carried out to find the best ways to remove boron but each of them still have its own disadvantages. The

methods such as sedimentation, coagulation, adsorption on clays are not effective because they can remove only small amount of boron or cannot remove at all. Membrane methods can reduce the boron content to permissible level with 98 - 99% efficiency. However, this technology needs to add alkali into the solution to increase the pH to 10 – 11, from that boric acid will be transformed to borate ions, which are favorable for the separation process. Additionally, the increase of alkalinity of solution is a good environment to produce precipitation of magnesium, calcium hydroxides on the membrane surface which cause scaling phenomena.

The last method is the boron fixation on resins, by adsorption or ion exchange. Conventional ion exchange presents low selectivity in the presence of other ions and need an additional chemical to increase pH of solution due to the poor ionization of boric acid in natural condition. Boron selective resins are widely used for boron removal because of high selectivity, by the formation of stable complex between boric acid or borate ions and cis-diol groups on the surface of resin. However, this method encounters with resin regeneration problem, because solution containing concentrated acidic and alkali with high boron concentration is generated after one or several regeneration cycles. Utilization of boron compounds from these solutions is inexpedient, thus they becomes the secondary contamination source to the environment.

The use of hybrid system opens a new approach of boron removal which can take the advantages of both adsorption and membrane methods. These methods are based on the following principle; boron is fixed on particulates that are removed by membrane filtration. With this technology, the boron removal could be effective without the scaling problem of membrane. To develop some ecofriendly boron removal methods, some natural sorbents such as cellulose, sawdust, chitosan, seaweed, tannin etc., with structure modifications were investigated to remove boron from aqueous solution. These materials contain polysaccharides, which have chelating properties, and amino groups, that are necessary for the process of boric acid complexing. However, research reported various results from inefficiency (sawdust) to fast and high efficiency (tannin gel, chitosan resin).

Beet pulp, the solid residue produced after sugar extraction, is usually dried before to be milled in pellets for animal feed. This residue contains a large amount of polysaccharide cellulose but also pectins. In the context of plant biorefinery, and valorization of biomass into biofuel, cellulose from beet pulp is very attractive but required pectin removal before fermentation. Hence the valorization of this latter fraction becomes crucial for the whole valorization of the beet pulp. Pectin has been identified as the polymer involved in the boron fixation in the plants and could be therefore applied for boron removal from water.

The Laboratoire de Chimie Agro-industrielle has been working on the plant fractionation, and particularly has demonstrated how to produce refined cellulose from beet pulp and optimized the pectin extraction. The valorization of this fraction could be possible as soil fertilizer, bringing the required dose of boron for the plants.

The first step of this work was to better understand the possible fixation mechanisms between boron and sorbent materials. Thus, properties and adsorption behavior of ion exchange resins and boron selective resins were investigated. Four synthetic resins were chosen including two anionic resins (Ambersep 900-OH and Amberlite IRA 402 Cl), and two boron selective resins

(Amberlite IRA 743 and Diaion CRB 03). During the second step, pectin extracts were characterized and then the efficiency of a hybrid system using these pectin extracts were studied.

This thesis is organized in 5 chapters as follow:

Chapter 1 is a state of the art which summaries knowledge related to boron. It describes in detail boron in environment, its impact on life development, its existence and properties in aqueous solution. A list of different boron removal technologies is presented and compared, based on their advantages and drawbacks. A specific part discusses mainly about the natural boron sorbents, which were already studied. A detail description of fixation mechanism of ion exchange and boron selective resin was found in this chapter with the kinetic and isotherm adsorption theory. The relationship between the isotherm shape in batch experiments and the breakthrough curves in column experiment was explained. Pectin extract as new adsorbents are presented with its occurrence in nature, composition, structure and its role in the development of plant.

Chapter 2 introduces the material and methods used in all experiments. It focuses on the batch and column experimental set-ups and then on the ultrafiltration systems. It describes the analytical and experimental procedures.

Chapter 3 presents results and discussion of boron fixation from kinetic and isotherm experiments on synthetic resins using batch reactors as a publication. The influence of pH on sorption isotherm is investigated in order to better understand the sorption mechanisms at different pH and at which pH, the maximum adsorption is achieved for each resin. Different kinetic and isotherm models are evaluated. The best fitting ones are chosen, and their parameters are calculated.

Chapter 4 shows the results of boron fixation on synthetic resins using column reactors with only two resins, the anionic resin Ambersep 900-OH and the boron selective resin, Amberlite IRA 743. This chapter presents the determination of pore volume of each resin, and then the influence of boron concentration and flow rate on the resin fixation efficiency. A comparison of reaction rate, retardation factor, boron adsorption capacities is done between the two resins. Final conclusion is given with respect to the main difference between two resins applying on continuous system. Different models are used to interpret data.

Chapter 5 summaries the boron removal from water using new adsorbents such as pectin extracts. Two types of pectin extract powders are characterized and compared. Solutions produced from these powders are filtrated, with different molecular weight cut-off membranes, in an agitated filtration cell. Influence of stirring and pressure allows selecting the best membrane that is characterized at larger scale with a hollow fiber membrane. Boron fixation using the two pectin extracts is operated in different pH conditions.

The last part is dedicated to the final conclusions followed by a presentation of future works.

Chapter 1
STATE OF THE ART

1.1. Boron presentation

1.1.1. Introduction of boron

Boron is a rare chemical element on the Earth, which is originally formed due to the Big Bang and the Stars. Its presence on the Earth's crust only accounts for 0.001% (10 mg L^{-1}), never in the elemental form (Rudnick and Gao, 2005). In the high oxygen environment on Earth, boron is fully oxidized to borate, which is highly soluble in water. In aquatic environment, it can be mainly found in combined compounds such as borate and boric acid.

Boron was first discovered independently in 1808 by a British chemist Humphry Davy and a French chemist Joseph Louis Gay-Lussac, and then clearly identified as a chemical element in 1824 by Jöns Jacob Berzelius, a Swedish scientist (Lussac and Thenard, 1808; David *et al.*, 1809). In Mendeleev periodic table, the letter B with atomic number 5 symbolizes for boron. Boron is metalloid element, which is light but very hard. The molar mass of boron is 10.81. Its electron configuration is $1s^2 2s^2 2p^1$. Because of having an empty orbital, boron has trend to make bonding with other rich electron elements to form different boron compounds. There are two popular allotropes of boron: amorphous form exists in brown powder form while crystalline boron is black and extremely hard (Cividini *et al.*, 2009).

1.1.2. Sources of boron

Boron is released into the environment by both natural processes and anthropic sources.

1.1.2.1. Natural sources

Most common naturally occurring boron compounds are borate minerals, which are deposited from volcanic gases or hot springs near volcanic activities. There are more than 200 minerals in the world with two predominant deposits (borax and sassolite), which consist of different compounds of boron with sodium, calcium and magnesium, for example, kernite ($\text{Na}_2\text{O} \cdot 2\text{B}_2\text{O}_3 \cdot 4\text{H}_2\text{O}$), colemanite ($\text{Ca}_2\text{B}_6\text{O}_{11} \cdot 5\text{H}_2\text{O}$), ulexite ($\text{NaCaB}_5\text{O}_9 \cdot 8\text{H}_2\text{O}$), sassolite (H_3BO_3) and boracite ($\text{Mg}_3\text{B}_7\text{O}_{13}\text{Cl}$) (Indian Bureau of Mines, 2014). Boron can be found in rock, at a concentration of 5 mg L^{-1} in basalt to 100 mg L^{-1} in sedimentary shale or in soil ($10 - 20 \text{ mg L}^{-1}$). Moreover, boron also can be found in ambient air (average 20 ng m^{-3}) (Smallwood *et al.*, 1998).

Boron is also found naturally in seawater with average value of 4.6 mg L^{-1} . This value varied substantially depending on geography and location of ocean bodies such as in the Mediterranean Sea, the boron concentration is as high as 9.6 mg L^{-1} . The concentration of boron in fresh water is usually from less than 0.01 mg L^{-1} to 1.5 mg L^{-1} depending on the influence of geochemical nature of the drainage area, proximity to marine coastal regions. Concentrations in surface and groundwater are generally in the order of a few tenths of 1 mg L^{-1} , in rainwater typically below $10 \text{ } \mu\text{g L}^{-1}$ but depend on input from industrial and municipal effluents (Wolska and Bryjak, 2013).

Besides, boron is found in plant, animal and human bodies as essential element, which is required for structural development. Different crop types are suitable with different doses of boron, from less than 1.0 mg L⁻¹ for sensitive crops to above 2.0 mg L⁻¹ for tolerant crops. For mammalian organism like animal and human, the safe and adequate dose for health ranges from 1 to 13 mg L⁻¹ which is defined by World Health Organization (Wolska and Bryjak, 2013).

1.1.2.2. Boron sources from human activities

During industrial process, a big amount of boron has been introduced into environment as a waste. Hundreds years ago, boron has been utilized for making glass by Roman or borax clay product by Chinese. Nowadays, boron has wider application on variety industrial fields, for instance, glass fiber and porcelain as two major uses with durability improvement role, medicine, leather processing, adhesive, flame retardant, food grain preservation, soap, detergents, cleaners, fertilizer, herbicides, insecticides, gems manufacture due to its hardness property, textile industry as decolorizing agent, toothpaste and mouth wash solution due to germicidal nature, neutron absorber in nuclear reactor, boron neutron capture as an important treatment method for curing some cancers and arthritis (Smallwood *et al.*, 1998)

Boron appears in surface water as the consequence of the discharge of treated sewage effluent. Its concentration varies in different regions, for example, the average value in Europe is smaller than 0.6 mg L⁻¹, below 0.3 mg L⁻¹ in Japan, South Africa and South America and below 0.1 mg L⁻¹ in North American waters (Indian Minerals Yearbook, 2015).

1.1.3. Boron and its effect on life development

Boron has been known for many years as an essential micronutrient element for the growing process of fruits and vegetables. It is vital to plant health due to its role in forming and strengthening cell walls, transporting sugar, developing hormone and nutrition balancing with others such as nitrogen, phosphorous, calcium and potassium. Therefore, adequate B nutrition is critical for high yields and quality of crops. However, it is not easy to control the proper amount of boron for each type of plant because the gap between deficiency and excess for this element is very narrow. Boron deficiency inhibits plant from the growth of meristematic tissue, cell formation and delays enzymatic reactions while boron toxicity shows the signs of yellow tips of leaves, defoliation, spots on fruits, decay and fall of unripe fruit. Consequently, these influences result in death of plants (Melnik *et al.*, 2005). So, in agricultural production, boron in irrigation water should not exceed 0.3 – 4.0 mg L⁻¹ depending on the crop type and soil characteristic to avoid boron excess problem. To deal with the lack of boron in plant, proper type of fertilizer is considered making up the compensation. Different plants have different demands of boron for their development. There are three kinds of boron tolerances which are corresponding to three level of boron sensitivity of plants: sensitive plants: < 1.0 mg L⁻¹, semi-sensitive plants: 1.0 – 2.0 mg L⁻¹, tolerant plants: > 2.0 mg L⁻¹ (Tu *et al.*, 2010).

Numerous researches have indicated the necessary presence of boron in the physical and intellectual growth of animals and human even the amount should be provided every day is quite small, about 1 to 13 mg according to WHO. Nielsen reported that boron is a dynamic trace element which is required for bone development, brain and immune function, energy substrate

utilization and micro mineral metabolism (Nielsen *et al.*, 1997). It is noted that boron deficiency has negative effects on composition and function of many parts of human and animal body. The lack of boron in animals can cause the reduction of other minerals absorption such as calcium, copper or nitrogen. Mammalian organisms that have excessive boron suffered from problems of cardiovascular, coronary, nervous and reproductive systems. It can change blood composition, caused disorder in neurological, physical, intellectual development. Particularly, excess of boron is very dangerous for pregnant women as it increases the risk of birth pathology. Greater dose of boron (> 500 mg/d) may cause nausea, vomiting, weight loss and diarrhea (Wolska and Bryjak, 2013).

1.2. Boron in water production

1.2.1. Water resources

Around 97% of the water in the world is in the oceans and approximately 2%- 2.5% of the water is in ice stored in glaciers and polar ice, although global warming is reducing this reservoir of fresh water. Hence, of all the water in the world, a mere 0.5%-1% is fresh water available for the needs of all plant, animal and human life (Haden *et al.*, 2005; Shiklomanov *et al.*, 1993). The over-exploitation of existing fresh water supplies is becoming a problem in many parts of the world. There are many causes in which the principal ones are known such as population growth, demands for higher living standards, growth of both agriculture and industry, and climate change. Globally, the main water consumption sectors are irrigation, urban, and manufacturing industry, especially irrigation in agriculture. It becomes more and more serious in the countries which are already suffered from increasing water shortages such as Greece, Spain, Southern Europe in general and the Middle East and North African (MENA) countries (Reid *et al.*, 2010; El-Dessouky and Ettouney, 2002).

There is a number of ways in which the problem of increasing water shortage can be tackled such as the more economical use of water by reduction in wastage; the increased recycling of water by both industrial and domestic users; by the transfer of water from areas rich in water resources to areas of need - for example, the proposed use of a pipeline from Turkey to Israel and the use of canals and rivers in the UK to transfer water from one area to another (DEFRA, 2000), for example the use of the Cotswold Canals as a route for water to be pumped from the River Severn to the River Thames (Thames Water, 2014). Another way is the production of fresh water from brackish and seawater by a process called "desalination". Desalination refers to those processes that reduce the quantity of dissolved substances in the water fed to the process. Seawater tastes excessively salty and that in normal circumstances it cannot be drunk or used for normal domestic purposes such as washing and cooking. However, if this salt content could be reduced, it would then be possible to produce water suitable for drinking and other domestic purposes.

Nowadays, fresh water production is usually managed from seawater or polluted surface water. Consequently to the boron harmful effect, the WHO recommended the value of boron concentration in drinking water to be below 0.5 mg L⁻¹ but the value in the guideline however has been revised to 2.4 mg L⁻¹. Although this new change seems more relaxed for the drinking water than before, the requirement of 0.5 mg L⁻¹ is still kept for irrigation water since the boron

demonstrates the herbicidal effect (Wei *et al.*, 2011). As the boron can be high in many water resources, for example, in seawater it is around 4.5 mg L⁻¹ (Xu and Jiang, 2008), water desalination requires high percentage removal for fresh water production.

1.2.2. Boron chemistry in aqueous solution

In aqueous solution, boron is normally present as boric acid H₃BO₃ and borate anions (H₂BO₃⁻ or B(OH)₄⁻). Boric acid appears predominantly in aquatic environment with pH around 7 or 8. It is a water-soluble substance with solubility of 55 g L⁻¹ at 25 °C. Boric acid acts as a weak Lewis acid due to the electron deficiency of boron, thus it tends to combine with one OH⁻ ion to become B(OH)₄⁻ in high pH medium (Wolska and Bryjak, 2013). There is formation of polyborates such as B₅O₆(OH)₄⁻, B₃O₃(OH)₄, B₃O₃(OH)₅²⁻ and B₄O₅(OH)₄²⁻ in solution at high concentration (> 1000 mg L⁻¹) and at pH between 6 to 11 (Öztürk and Kavak, 2005).

Equilibrium of boric acid and borate (pKa = 9.2) can be expressed as follow:



The pKa values indicates that with pH is smaller than 9.2, boron is mainly as boric acid species in the solution and borate ion becomes predominant fraction in alkaline conditions FIG. 1.1.

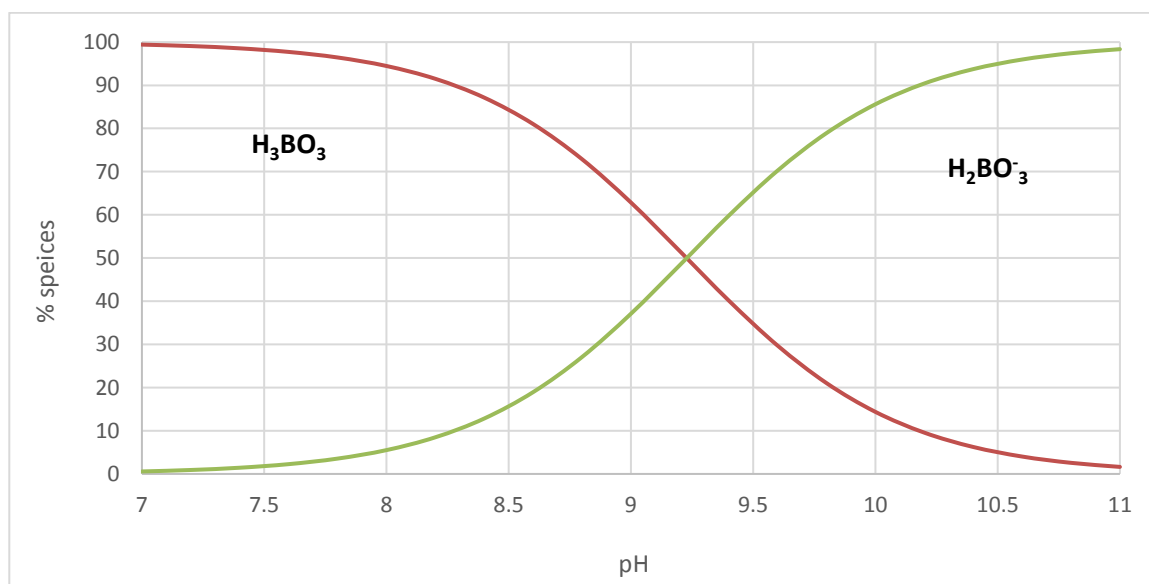


Fig. 1.1. Boric acid speciation as a function of pH

(Calculation with VminteqA2)

Previous investigations showed that pKa is dependent on ionic strength and temperature of the solution. When the ionic strength increased, pKa is decreased due to change in borate ion activity and pKa changes from 9.08 to 9.38 as the solution changes from 10 °C to 50 °C due to the change in the pK of water (pKw) (Hilal *et al.*, 2011; Oo *et al.*, 2012).

1.2.3. Desalination plant for water production

1.2.3.1. Types of desalination plants

Water desalination is one of the ways to solve the problem of the water resource limitation for the production of drinking water. There are, approximately, over 23,000 desalination plants in more than 150 countries treating over 85,000 m³/d with over half of them in the Middle East. The number of desalination plant is continuously growing in 2013-2014, about 564 new plants were contracted (Pankratz *et al.*, 2014). Two kinds of desalination plants can be considered depending on the process, thermal plant and membrane plant.

In thermal desalination, the process is the distillation in which the heat is used to generate steam from the seawater that is then condensed to form water with a low salinity that can be used for domestic and industrial purposes or for irrigation (El-Dessouky and Ettouney, 2002). There are three main desalination techniques that use the principle of distillation and a couple of methods that have still to be proved on a commercial scale:

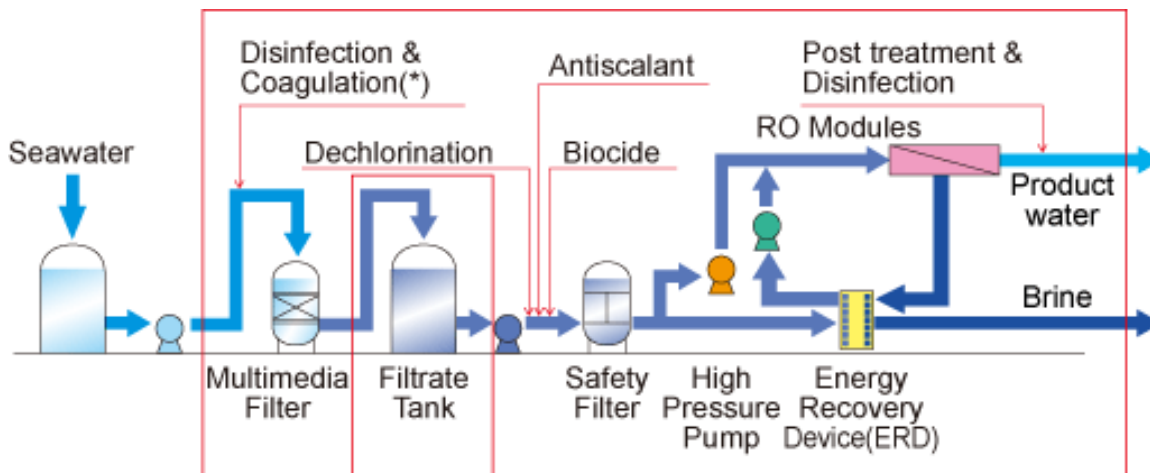
- Multi-stage flash evaporation/distillation (MSF)
- Multiple-effect evaporation/distillation (MED) also known as long-tube vertical distillation (LTV)
- Vapor compression distillation (VCD)
- Solar distillation
- Rapid spray evaporation.

In membrane desalination process, there are two categories. The first one is reverse osmosis (RO) where fresh water permeates under high pressure through the semi-permeable membranes to be separated from the highly concentrated brine solution. The second one is electrodialysis (ED) in which under the electrical current, the electrically charged salt ions are separated through selective ion exchange membrane, leaving the low salinity water flow. Between two processes, reverse osmosis is more common use in industrial applications.

1.2.3.2. Membrane plant design

A membrane desalination plant is generally composed of reverse osmosis membranes as the core of the desalination process. Nevertheless, the required and completed process is complex and implies many steps as shown in FIG. 1.2.

a) **Complete flowsheet**



Optimal *

Fig. 1.2. Presentation of the complete flowsheet of a desalination plant

(From Toray-Innovation by Chemistry, 2006)

At the first stage water must be disinfected before removal of the suspended matter, after coagulation if necessary. Usually disinfection is achieved through chlorine treatment and thus it is important to remove the free chlorine prior any membrane treatment. This step is usually done by adsorption with activated carbon that has the problem of releasing fine particle. A final filtration step is then required to prevent any blocking problem during reverse osmosis. Antiscalant and biocide are finally added before a preservative filtration.

b) **Desalination configuration**

Produced water using single stage RO can achieve boron concentration of $0.9 - 1.8 \text{ mg L}^{-1}$. Newly seawater reverse osmosis membrane has been reported to obtain boron removal up to 91 – 93% while conventional RO membrane rejects boron at the level of 40 – 78% (Glueckstern and Priel, 2003; Koseoglu *et al.*, 2008). In order to get low boron concentration in RO permeate, numerous designs has been developed. Typical designs involved the first stage of RO treatment with either a second stage of RO treatment or boron selective resin. The model is shown in the FIG. 1.3 below.

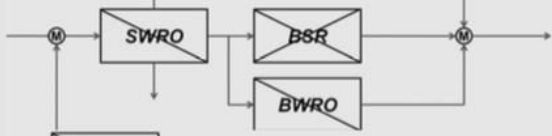
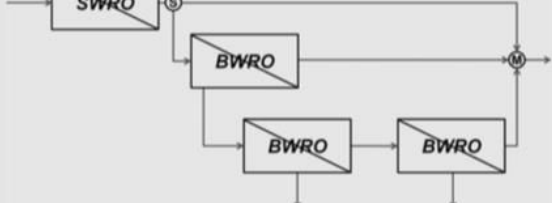
Design concept	Achievable concentration and cost	Examples of simplified schematic diagram
1 pass SWRO (with/without pH changes)	0.8–1.0 mg/L (0.38–0.52 \$/m ³)	
2 pass with increased pH	0.4–0.5 mg/L (0.45–0.55 \$/m ³)	
2 pass with BSR	Less than 0.4 mg/L (0.50–0.55 \$/m ³)	
Cascade design (IDE process)	Less than 0.4 mg/L (0.47–0.52 \$/m ³)	

Fig. 1.3. Boron removal processes of seawater desalination

From (Redondo *et al.*, 2003)

1.3. Study of boron removal technologies

1.3.1. Reverse osmosis method

1.3.1.1. Reverse osmosis principles

Osmosis is a process whereas a spontaneous transport of solvent from a dilute solution to a concentrated solution across an ideal semi-permeable membrane. The membrane impedes the passage of the solute but allow the flow of the solvent permeating it. This flow can be reduced by exerting a pressure on the high concentration solution (Fig. 1.4) (Öztürk *et al.*, 2008). Osmotic pressure is the pressure on solution side of membrane at which the equilibrium is reached. When the exerting pressure is greater than the osmotic pressure, the flow reverses. The pure solvent will pass from the high concentration side to the low concentration side. This phenomenon is the basis of reverse osmosis (RO) of seawater desalination and water treatment. The raw water, product water and concentrated reject are called the feed, permeate and concentrate, respectively. Hence, reverse osmosis technology utilizes a pressure that is higher than osmotic pressure to force water passing through the semi-permeable membrane while rejecting dissolved species.

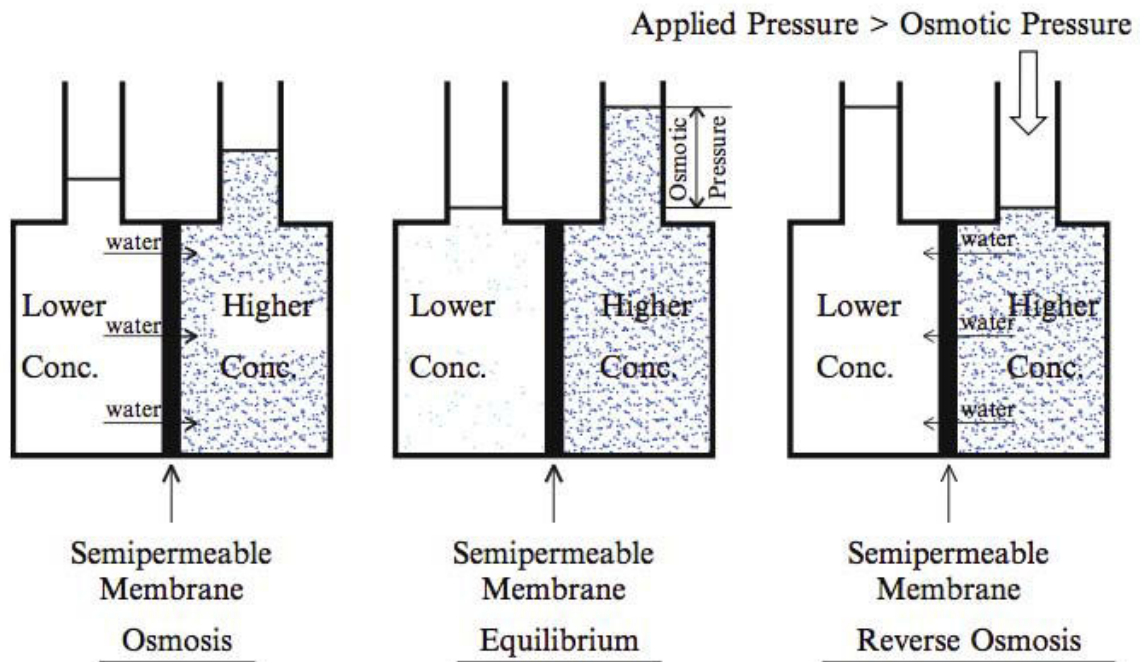


Fig. 1.4. Osmosis and reverse osmosis model

From (Lawrence *et al*, 2011)

1.3.1.2. Membrane separation mechanisms

Reverse osmosis membranes are supposed to be dense membrane. Thus, transfer of solvent and solute through the membrane is achieved by diffusion. Separation efficiency of the membranes depends on the difference of diffusivities of each molecule. Usually water diffusion is high while for larger molecule diffusion is low, and hence the rejection of the solutes appears very high at more than 99%. The transfer requires the dissolution of the molecule in the membrane material before diffusion as describe in the following figure for water. Hence, the interactions between the membrane and solute govern the efficiency of reverse osmosis and explain their large selectivity.

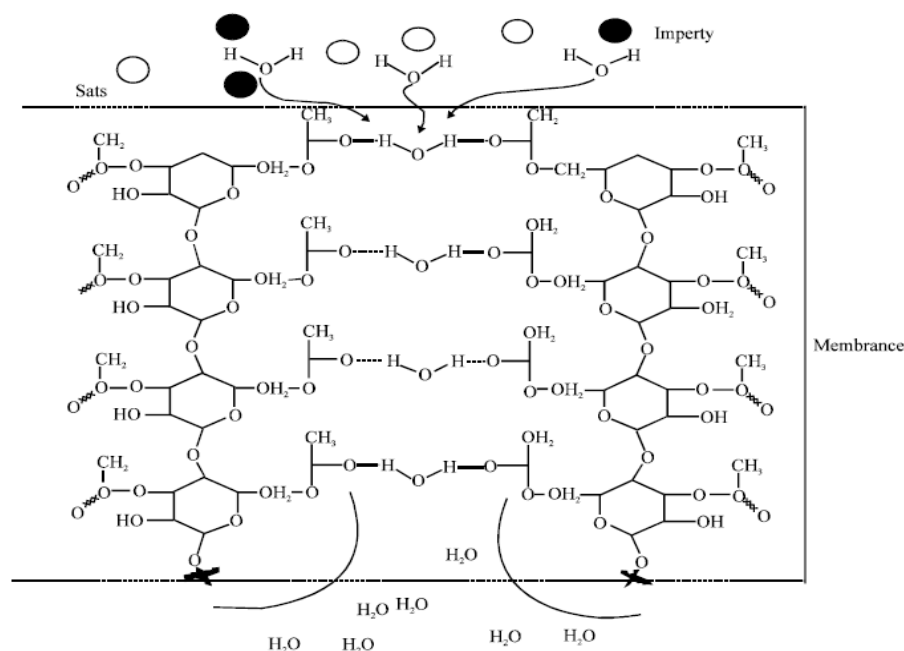


Fig. 1.5. Mechanism of water transport through reverse osmosis membrane by performing bridges of hydrogen

From (Rodríguez *et al.*, 2001)

Usually charged molecule diffusion is low, and hence the rejection of the salt appears very high at more than 99%. But for neutral molecules the rejection rate by reverse osmosis is lower and sometimes there is almost no rejection. This mechanism explains the problem for boron removal during desalination process. The passage of non-dissociated boric acid to water through the membrane is high. The better rejection of borate ions can be understood according to the charge repulsion and size exclusion on the membrane. The dissociated borate form is fully hydrated in the solution that results in a larger radius and a charged enhancement of the ions. Therefore, ionized borates are more impeded on the negatively charge membrane. However, for neutrally charged boric acid form, the hydration causes smaller size of the molecule, thus less rejection is obtained. Boric acid in low pH solution, is able to make hydrogen bridge with the active groups of the membrane and diffuse in a similar way to that of water (Ezechi *et al.*, 2012; Kabay *et al.*, 2010).

1.3.1.3. Effects of each parameter on boron rejection

The influence of affecting parameters such as pH, temperature, pressure, salinity or ionic strength, initial concentration and feed flow rate was considered in order to develop a reliable design to optimize the boron removal process.

Boron rejection has strong dependence on pH while initial concentration and feed flow rate seems to be negligible. Keseoglu and co-workers reported that a much higher boron rejection was reached at pH of 10.5 (> 98%) than those at natural seawater pH of 8.2 (about 85%- 90%) (Koseoglu *et al.*, 2008). Boron rejection performance has been studied using different type of membranes (BW30LE, ESPA 2, ESPA B) and different transmembrane pressures (24, 30, 40 bars) at different pH (ph 7.6 and 9.6). It has also showed that boron removal efficiency

significantly increased from pH 7.6 to pH 9.6 (Teychene *et al.*, 2013). At high pH, there is a transformation from boric acid to borate ion, which is in bigger size and easily impeded on the surface of membrane. Additionally, there is also strong repulsion between negatively charged active group of membrane and dissociated borate, results in higher rejection (Bonnélye *et al.*, 2007). But at higher pH, the precipitation of calcium carbonate and magnesium hydroxide can block and degrade the membrane then after, reduce the filtration efficiency (Cengeloglu *et al.*, 2008). In the solution of pH range 7 to 8, the boron rejection decreases to 50 – 70% due to the diffusion of dominant uncharged boric acid in the membrane (Hilal *et al.*, 2011).

Increased feed salinity and/or temperature shows a decrease in boron removal Fig. 1.6. According to Oo and Song (2009), it might be explained as the effect of charge neutralization or hindering of membrane surface potential at high salt concentration. The decline of removing boron would be due to the electrostatic repulsion between borate ion and membrane surface is less dominant. Similar to salinity, increased temperature shows higher amounts of boron in permeate despite of higher portion of borate ion in the solution. It is possible to explain this phenomenon by the increase of total flux through RO membrane including salt flux at higher temperature (Magara *et al.*, 1998; Bick and Oron, 2005).

Increasing applied pressure also increases the permeate flux as well as the boron rejection (Bonnélye *et al.*, 2007). Furthermore, complexation reaction can be a choice for enhancing boron rejection by adding mannitol or Fe which can cause the formation of large complexes in the solution (Qin *et al.*, 2005; Geffen *et al.*, 2006).

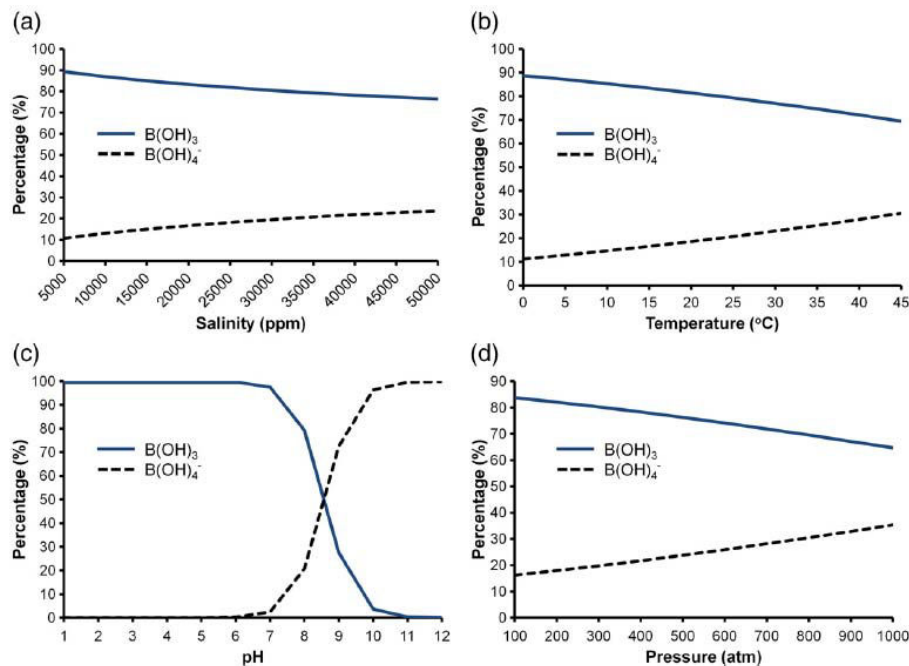


Fig. 1.6. The distribution of boric acid and borate in seawater by the changes of each parameter. (a) pH = 8, T = 25 °C, pressure = 1 atm (b) pH = 8, salinity = 35 000 ppm, pressure = 1 atm (c) T = 25 °C, salinity = 35 000 ppm, pressure = 1 atm (d) pH = 8, T = 25 °C, salinity = 34 800 ppm.

From (Hilal *et al.*, 2011)

At industrial scale the solution that has been applied the addition of an extra reverse osmosis step after desalination, specific for boron removal, after pH increasing to 10.5. This procedure is expensive because it also required adding acid to neutralize the high pH to the water pH.

1.3.2. Ion exchange methods

Several adsorbents are investigated and developed such as ion exchange resins, polysaccharides, oxides, synthesized clay, fly ash, layer double hydroxides, natural polymers but the most used are boron selective resins.

1.3.2.1. Boron selective resins

1.3.2.1.1. Fixation mechanisms

Chelating resins or boron selective resins (BSRs) are the most effective and popular sorbents in boron adsorption techniques. Their component consists of two main parts: macroporous polymer supports and functional groups. Functional group consists of vis-diols and N-methyl-D-glucamine (NMDG) groups. Vis-diols groups, adjacent hydroxyl groups located in cis position, have high selectivity with boron by making different borate stable complexes (FIG. 1.7 to FIG. 1.9). Glucamine group controls pH of solution by capturing proton liberating during dissociated reaction, thus the pH of the solution is kept to be unchanged or insignificantly changed (Li *et al.*, 2011; Xu and Jiang, 2008).

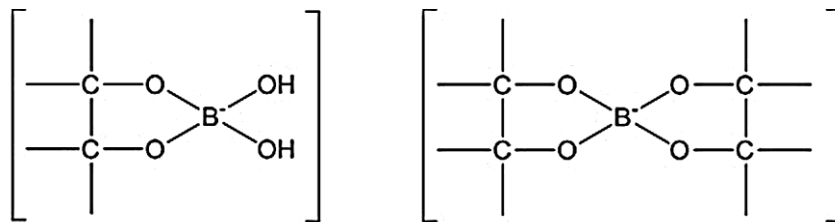
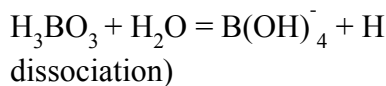


Fig. 1.7. Structure of borate complex

From (Wang *et al.*, 2014)



(Boric acid)

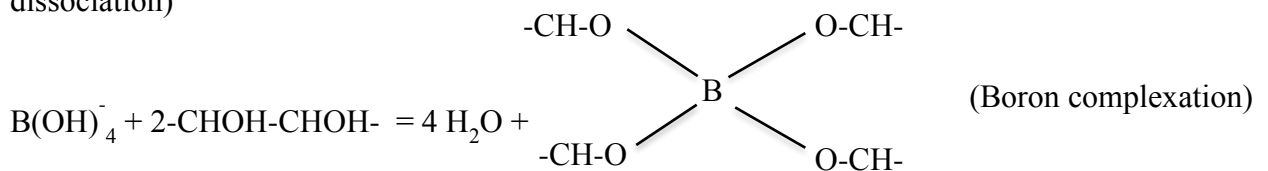


Fig. 1.8. Reactions during boron complex formation.

Adapted from (Yılmaz *et al.*, 2005)

Borate complexes are formed in different steps

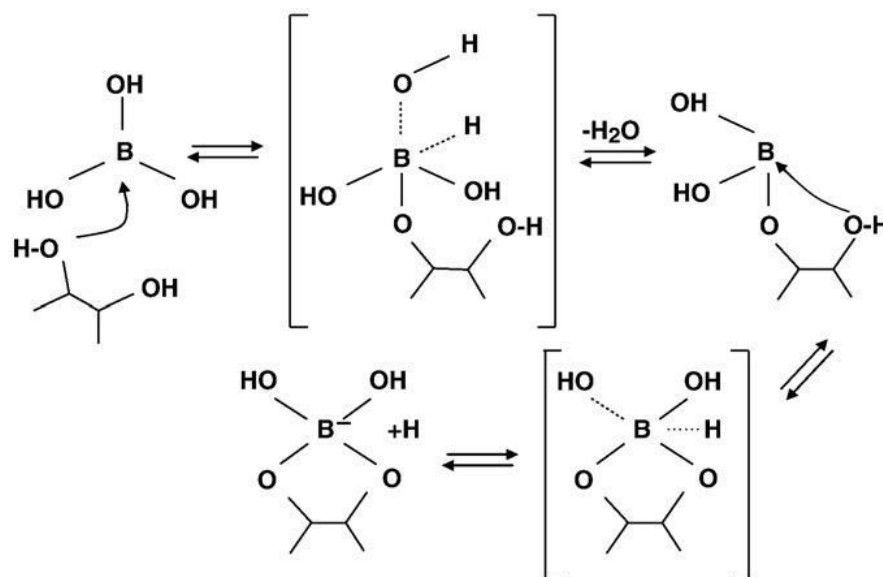


Fig. 1.9. Reactions during boron complex formation

Adapted from (Kabay *et al.*, 2010)

Researches that showed efficient adsorption performance of several boron selective resins has been published such as Amberlite IRA 743 (Amberlite XE 243), Amberlite IRN – 78 (Yılmaz *et al.*, 2005), Diaion CRB 02, Dowex XUS 43594.00, Purolite S108 and S110 (Kabay *et al.*, 2010).

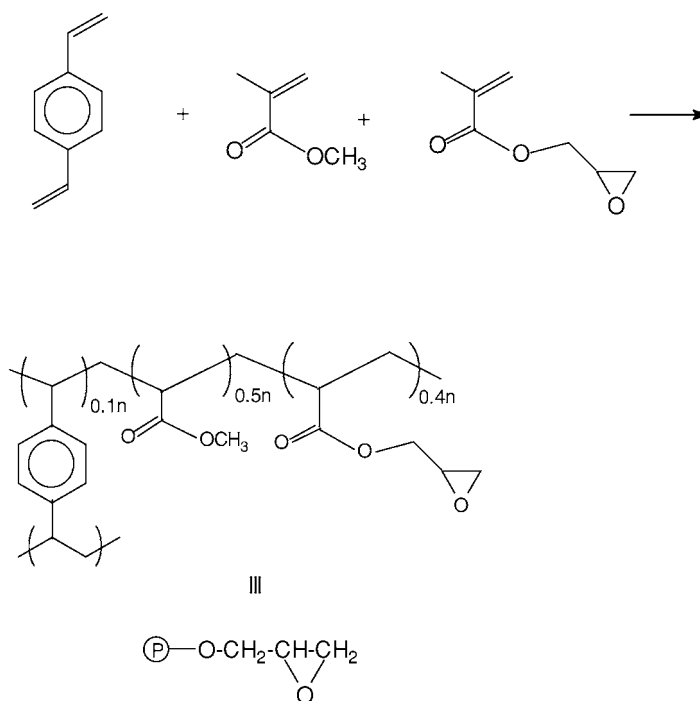
1.3.2.1.2. Resin structure development

The conventional ion exchange polystyrene resin had been used for boron adsorption but it exposes two main disadvantages such as hydrophobic skeleton structure and small specific area surface. For more detail, hydrophobic structure is not favorable for the mass transfer process, which limits the efficiency of boron removal in aqueous media. Specific surface area is the factor that can increase adsorption quality through raising the crosslink rate of the functional group. Therefore, in order to improve the ability of boron adsorption of boron selective resins, two crucial features of supports, hydrophilic matrix and big specific surface area, are optimized. Numerous studies have been done to produce hydrophilic supports with large specific surface area such as polyacrylic acid resin, macroporous solid material, etc. Some NMDG-resins was modified on different polymers as new adsorbents, which obtained high obtaining boron adsorption capacity (10 mg g^{-1} to 25 mg g^{-1}). A list of modified NMDG - resins is reported in TABLE 1.1 (Wang *et al.*, 2014).

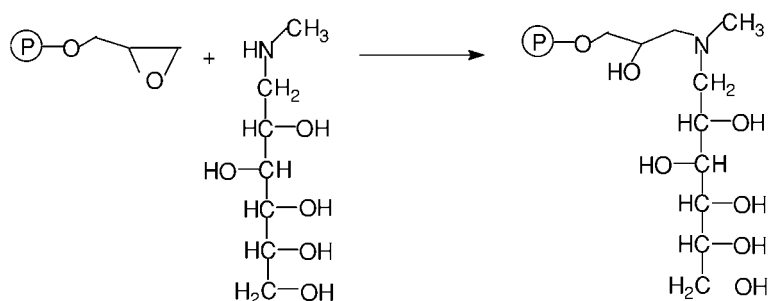
Table 1.1. Some designed N-Methyl- D -Glucamine resins. From (Wang *et al.*, 2014).

Polymer support	Capacity (mg g ⁻¹)
Glycidyl methacrylate-methyl methacrylate-divinyl benzene (GMA-MMA-DVB)	22.34
Glycidyl methacrylate-co-trimethylolpropane trimethacrylate (GMA-co-TRIM)	14.90
Polyethylene styryl sulfonamide	25.57
Cellulose	11.90
Glucamine-modified MCM-41	8.650
Polyol-functionalized SBA-15	6.810
Tetraethoxysilane, (3-glycidoxypropyl) trimethoxysilane (TEOS-GPTMS)	12.40
Silica-polyallylamine composite (SPC)	16.76
Chitosan (CCTS)	35.13
6-Nylon fiber-GMA	12.00
Calyx 4 arene based magnetic sporopollenin	12.32

Biçak *et al.* (2001) has produced terpolymers from glycidyl methacrylate (GMA), methyl methacrylate (MMA) and divinyl benzene (DVB). The obtained terpolymers have been perfectly in spherical bead forms which have been then modified with NMDG by a 4 h reaction at 80 °C. After sorption and elution test, the authors have concluded that the resin gained hydrophilic property, with specific surface area of 0.368 m² g⁻¹ using BET method. The produced resin has been applied for both batch and column mode sorption and archived promising capacity values of 2.15 mmol g⁻¹ and 1.2 mmol g⁻¹, respectively. Besides, new resin also had other advantages over common polymeric boron sorbents, for example, high regeneration cycle (> 20 times), no interference form Ca (II), Mg (II), Fe (III) and no particle disintegration in long term uses. The chemical structure of BSRs containing NMDG is shown in the FIG. 1.10.



a, Production of cross-linked polymer using GMA, MMA, DVB



b, Addition of N-methyl-D-glucamine group on the cross-linked polymer

Fig. 1.10. Structure of boron selective resins containing N-Methyl-D-Glucamine

From (Biçak *et al.*, 2001)

Parschova and co-workers (Parschová *et al.*, 2007) have carried out an experiment which has compared the performance of four adsorbents possessing the same NMDG functional groups but different polymeric supports. Three fibrous matrices have been selected, polypropylene – styrene, polypropylene – GMA, viscose GMA, polystyrene – DVB (Purolite D-4123). Test has been carried out in dynamic column. Polypropylene and viscose fibers, have grafted with glycidyl methacrylate (GMA) has showed different boron uptake efficiencies. Even, polypropylene fiber and viscose fiber has had the same total capacity (1.2 mol kg^{-1}), viscose fibers have exhibited higher breakthrough capacity than polypropylene fiber. The structure has grafted and functionalized viscose fiber probably enables better access of borate ions from solution to the functional groups compared to the polypropylene fiber. In regards of sorption kinetics, fibrous sorbents demonstrated much faster rate than commercial Purolite D-4123, however, sorption capacity has been lower than that of classical bead sorbent at flow rate range 6 BV h^{-1} to 60 BV h^{-1} . Additionally, fibrous sorbents have been easy to be regenerated,

especially viscose fiber, column has packed by this particle (glass column of inner diameter 1 cm, 5 mL of sorbent) could be regenerated with 0.1 mol L⁻¹ hydrochloric acid.

Beside NMDG functional groups, researches on other functional group with chelating resin have been developed. Senkal and Bicak (2003) have reported that polymer has supported iminodipropylene glycol functions showed very good efficiency for boron adsorption. In their research, the supported polymer has been also prepared from glycidyl methacrylate (GMA), methyl methacrylate (MMA) and divinyl benzene (DVB) using the same method used in Bicak (Biçak *et al.*, 2001). The spherical beads have been initially modified by an excess of ethylene diamine, and then reacted with glycidol to give resin with aminopropylene glycol functions. The resulting resin has exhibited a high boron loading capacity of 32 mg g⁻¹, good regenerability and reasonable rapid sorption ability prove by almost completely removal of boron in 10 mL of 50 mg L⁻¹ boric acid less than 12 min using 0.5 g of polymeric resin.

Sorbitol is a well-known substance for making a stable chelating structure with boric acid in aqueous solution. In order to make the use of this property, Bicak and Senkal (Biçak and Şenkal, 1998) has investigated a resin which is formed from crosslink polystyrene – 10% divinylbenzene (DVB) as polymeric support and sorbitol as the functional group. Obtained results from the study revealed that this sorbitol – containing polymer was an efficient boron removal adsorbent with high capacity of 13.18 mg g⁻¹. Moreover, due to the hydrolytic stability of the sulfamide linkage, the resinous polymer could be regenerated without loss of reactivity. Besides, one more special point on this polymer chain was the oxirane ring offered many functionalization possibilities due to the ring opening ability in mild condition.

1.3.2.1.3. Effects of each parameter on boron rejection

Boron removal from aqueous solution using different BSRs depends on various affecting factors, which have been investigated through many studies to find the optimized operating condition in order to archive the best adsorption percentage. These studies have been both applied on batch and column mode sorption.

Boncukcuoglu (Boncukcuoğlu *et al.*, 2004) has used resin Amberlite IRA 743 and considered different influence factors such as ratio between resin and boron solution, initial boron concentration, stirring speed and particle size. He has concluded from his investigation that boron removal ability improved when rising resin/solution ratio and lowering initial boron concentration. The rate of reaction has been proved to be very fast at the beginning as well. Besides, it was demonstrated that stirring speed has no significant effect on boron adsorption. Kabay (Kabay *et al.*, 2008) has had the same conclusion about the effect of stirring speed from 350 to 750 rpm on boron removal by employing two resins, Diaion CRB 02 and Dowex – XUS 43594.00 but he has proclaimed additional result on effect of resin size on boron sorption. It has showed that high percentage of boron rejection was reached when particle size has decreased due to increase of surface area and the improvement of diffusion rate.

Yan (Yan *et al.*, 2008) has showed that the removal rate of boron decreased with increasing the flow rate in a column packed with boron specific resin XUS-800. The contact time has been

shorter as the flow rate increased; hence the breakthrough point has reached with a low removal level of boron. It has been demonstrated that adsorption capacity of boron improved as increasing temperature and pH of feed solution. Raising temperature has accelerated the random movement of boron in the column, which has promoted the exchange process while increasing pH donated more borate species in the feed solution, which has been also favorable for ion exchange reaction with resin. In high chloride anions concentration medium, there has been a competition between chloride and borate ions with exchange sites on the resin surface resulted in a reduction in efficiency of boron removal. As far as the effect of initial boron concentration has been concerned, it had reported that the time to get breakthrough point has markedly decreased when a high concentration of boron solution has been applied. This phenomenon has been simply explained by the lack of active sites on the resin compared to an excessive amount of present boron species. Height/diameter (H/D) was the final key factor, which had an important effect on boron sorption. It is clearly indicated by Yan that boron adsorption capacity significantly rose up with an enhancement of H/D because of the improvement of the liquid distribution and the contact time of the liquid – solid phase.

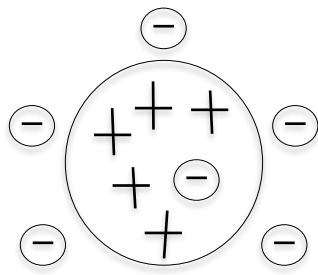
However, reversed conclusion about the influence of ionic strength on the removal of boron has been found in the publication of Simonnot and co-workers who have used another boron selective resin Ambertile IRA 743 in column experiment (Simonnot *et al.*, 2000). She has carried out column test with 0 – 0.292 g NaCl/mg B at pH ranges of 5.5 to 8, instead of 1.25 – 2.5 g NaCl/mg B at pH 4 to 12 like in Yan's work (Yan *et al.*, 2008). The result has indicated there has not been significant effect of ionic strength on boron rejection process. It has also been concluded that no pH effect on the boron adsorption efficiency in the range pH 5.5 to 8. The possible reasons might be the difference in operating condition of pH and NaCl level and type of resins (Hilal *et al.*, 2011).

1.3.2.2. Non boron selective resins

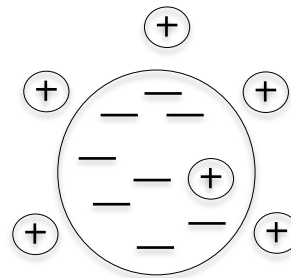
1.3.2.2.1. Ion exchange mechanism

Boron non – selective resin is known as ion exchanger, which is comprised of two main parts: matrix and functional group. The matrix is insoluble which is usually made based on inorganic compound, synthetic resin or polysaccharide. The matrix is covalently bonded with charged groups, which are associated with mobile counter ions. These counter-ions can be reversibly exchanged with other ions of the same charge without altering the matrix. There are two types of ion exchanger: anion and cation exchangers. Anion exchanger that has positively charged groups and negatively charged counter ions (Cl^- , OH^- ...) is used for boron removal. The characteristics of the matrix determine its chromatographic properties such as efficiency, capacity, recovery as well as its chemical stability, mechanical strength and flow properties.

The presence of charged groups is a fundamental property of an ion exchanger. The type of charged groups determines the type and strength of the ion exchanger. Their total number and availability of charged group determines the capacity of the exchanger. There is a variety of charged groups for anion exchanger that could be used to remove boron in aqueous solution Table 1.2.



Anion exchanger with
exchangeable counter ion



Cation exchanger with
exchangeable counter ions

Fig. 1.11. Ion exchanger types

Adapted from (GE healthcare, 2010)

Table 1.2. Functional groups for anion exchangers

From (GE healthcare, 2010)

Anion exchangers	Functional group
Diethylaminoethyl (DEAE)	$-O-CH_2-CH_2-N^+H(CH_2CH_3)_2$
Quaternary aminoethyl (QAE)	$-O-CH_2-CH_2-N^+(CH_3)_2-CH_2-CHOH-CH_3$
Quaternary ammonium (Q)	$O-CH_2-CHOH-CH_2-O-CH_2-CHOH-CH_2-N^+(CH_3)_3$

1.3.2.2.2. Effect of each parameter on boron rejection

Ozturk and Köse (2008) have carried out researches on boron removal using Dowex 2 x 8 anion exchange resin on batch-wise system. Boron fixation percentage has increased with the amount of resin applied in the reaction due to enhancement of specific surface area. When the temperature rises from 25 °C to 45 °C boron removal efficiency decreases, but higher temperature has indicated stimulation in reaction rate, thus equilibrium attained sooner at high temperature. The boron removal percentage has been determined as 55, 40, 33.3 % at temperature of 25, 35 and 45 °C, respectively. Similar to the influence of resin dosage, the increase in initial boron concentration (100 – 1000 mg L⁻¹) results in the increase in the amount of sorbed boron (0.37 – 1.43 mmol g⁻¹). The test of pH influence on boron adsorption has been performed at pH from 2 to 10 at 25 °C. The maximum adsorption (1.57 mmol g⁻¹) obtained at pH 9, has been explained by the predominance of borate ions in the aqueous medium at alkaline condition. It is also observed that there has been a considerable influence of foreign ions presented in the solution like Ca²⁺, Na⁺, Cl⁻, SO₄²⁻. The sorption of boron has significantly decreased by adding of other ions due to the competition between them and borate ions on adsorption sites. The Langmuir and Freundlich isotherm relationships have been applied for the sorption equilibrium. Results have indicated that the Langmuir isotherm was adequately

described the equilibrium relation between the resin and liquid phases of the ion exchange process.

The boron sorption has been studied at 39 and 45 mL h⁻¹ flow rates with the same resin. The results indicate that the breakthrough capacities have obtained from two flow rates are quite similar, 13.9 and 13.1 mg mL⁻¹ for 39 and 45 mL h⁻¹, respectively. The breakthrough point has shifted to the longer time when the flow rate decreased. Borate ions do not have enough time to react with the resin at high flow rate, which consequently results in less volume of effluent to reach the breakthrough point. Breakthrough capacity values have increased for the second (22.95 mg mL⁻¹) and third cycle (21.79 mg mL⁻¹) has compared to that of the first cycle (13.13 mg mL⁻¹). This could be due to activation of functional sites on the resin by reconditioning with NaOH during the regeneration step.

For boron concentrations ranging from 28 to 100 mg L⁻¹, IRA 93, a weak basic anion resin, removes only small quantity of boric acid while IRA 400 and Wofatit L 150, two strong basic anion resins, remove more effectively boric acid (Ristić and Rajaković, 1996). Wofatit L 150 exhibited a significant uptake of boron with capacity of 0.16 mmol g⁻¹ while these values for IRA 400 and IRA 93 have been 0.056 and 0.036 mmol g⁻¹, respectively. The boron sorption has improved for all the resins, from 0.16 to 0.24 and 0.20 mg g⁻¹ with citric and tartaric acid, respectively, in the feed solution for the Wofatit L 150 resin. The impregnation of anion-exchange resins with citric and tartaric acids could lead a modification of their affinity toward boron.

1.3.2.3. Other adsorbents

Waste natural materials (WNM) such as sawdust, coconut husk, sugarcane, bagasse, tealeaf, rice hull has been investigated for the fixation of molecules because it could be more economical to widening their application. Moreover, proper use of WNM can also limit the use of petroleum derivatives as raw material and hence avoid water pollution by hazardous substances (Orlando *et al.*, 2003). Their composition in cellulose, hemicellulose, lignin, tannin, pectin contributes to the development of exchange because of the abundance of co-planar cis-diol groups that have chelating properties with boron in aqueous solution.

Cellulose

New natural polymer adsorbents, which were derived from synthesis of cellulose with N-methylglucamine, have been developed for boron sorption. Two forms of cellulose (powder and fiber) were first used to make graft polymerization with a vinyl monomer having epoxy groups, then transformed in N-methylglucamine cellulose derivatives FIG. 1.12.

Results from this research demonstrated that cotton was a cost-effective biosorbent for boron removal as the post-treatment in a desalination plant with good capacity (1.05 mmol g^{-1}) at neutral pH (pH 7) of seawater. The Freundlich isotherm model has described efficiently the boron adsorption into cotton. .

Chitosan

Chitosan is one of abundant, cheap and environmental – friendly biopolymers, which can be obtained by deacetylation of chitin from shrimp, crab and other crustaceans. Chitosan has a lot of amine and hydroxyl groups as primary site for surface modification, which has wide application on biomedical engineering and water treatment (Wei *et al.*, 2011).

Chitosan can serve as base material to develop a natural resin with N-methylglucamine (Sabarudin *et al.*, 2005). This resin, which has made of cross-linked chitosan and N-methylglucamine (NMDG) also has had faster adsorption compared to synthetic resins. In this work, chitosan-NMDE has been synthesized into two steps, first has been the cross-linking of chitosan, and second has been the introduction of NMDG into the chitosan through the arm of chloromethylloxirane (FIG. 1.15).

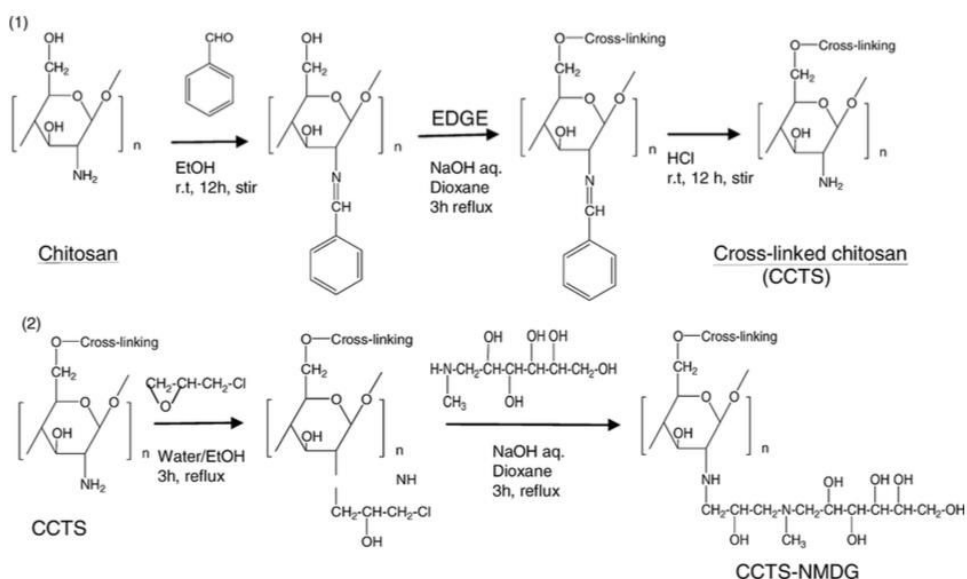


Fig. 1.15. Synthesis of cross – linked chitosan and N-methylglucamine.

From (Sabarudin *et al.*, 2005)

The boron adsorption has been evaluated in a packed mini column by passing water samples (tap water, river water, estuarine and ground water) and measuring the remaining boron in eluate. The results have showed that new synthesized chitosan resin had higher boron sorption capacity and faster boron sorption kinetic than commercial boron synthetic resins. This investigation also revealed an efficient fixation of boron at neutral pH. Chitosan bio-based resin has also been produced by atom transfer radical polymerization (Wei *et al.*, 2011). Boron sorption has showed that at neutral pH, the maximum sorption capacity was 3.25 mmol g^{-1} with almost 90% boron removed within 8 h. The behavior has been well described by an intraparticle surface diffusion model. Moreover, the presence of ions (sodium, nitrate and chloride) has proved to have no effect on boron removal. The average boron concentration in seawater has reduced from 4.8 mg L^{-1} to 0.5 mg L^{-1} when a sorbent dosage of 1.2 g L^{-1} has been applied. In

these studies, the production method has been complex and no regeneration has evaluated (Demey *et al.*, 2014; Gazi and Shahmohammadi, 2012). Chitosan can be encapsulated during the formation of regular beads of nickel (II) hydroxide by sodium hydroxide addition (Turek *et al.*, 2007). The maximum adsorption capacity has been 61.4 mg g^{-1} at 298 K and pH of 8 – 9 for the bead obtained by the procedure. Langmuir model well fitted with the sorption isotherm and the pseudo- – second order rate equation best described the kinetic profile of reaction. Desorption studies was successful with five consecutive cycles at pH 12 which confirmed high efficiency for boron recovery ($> 90\%$ uptake).

Algal adsorbents

Caulerpa racemosa var. cylindracea (CRC) is invasive marine seaweed that cell wall is composed polymers having functional groups consist of hydroxyl and amine groups. Powder obtained from this alga has been evaluated for boron fixation. Optimum condition obtained from batch experiment using 25 mL of boric acid for contact time, temperature, adsorbent dosage (from 0.05 g to 0.3 g CRC), initial boron concentration, pH, ionic strength was 2.5 h, 318 K, 0.2 g, 8 mg L^{-1} , pH 7.5, 0.1 M NaCl. The maximum adsorption was achieved about 63% (0.25 mg g^{-1} at 45°C). It was also observed that the maximum adsorption capacity of CRC is higher than those of cotton cellulose (Bursali *et al.*, 2009).

Several types of available, low cost, natural residues have used such as wheat, rice and green shell of walnut (Jalali *et al.*, 2015). The optimum pH, contact time and isotherm experiment has tested. The maximum B sorption by walnut shell and rice residues have attained at pH 7, while that for wheat residues was at pH 8. The maximum adsorption value of 2.9 mg g^{-1} has obtained by the utilization of rice residues. The research data has demonstrated that the boron sorption equilibrium is established after 48 h. The carboxylic and phenolic acids have been two main reactive surface groups that play an important role on boron sorption. The fixation has been rather slow because boron must diffuse into the porous structure of the biomass but this study revealed that biomass residues could be considered as an available, cost- – effective and environmentally friendly strategy to remove excessive boron in water.

Other typical adsorbents

Besides natural adsorbents, some materials with low cost as fly ash and tailing are also used (Polowczyk *et al.*, 2013). The boron adsorption on fly ash agglomerates with particle size of 1.0 – 1.6 mm has increased with increasing temperature ($25\text{--}45^\circ\text{C}$). The maximum adsorption capacity has achieved is 0.64 mmol g^{-1} for 0.0025 g mL^{-1} adsorbent-to-solute ratio. For 100 mg L^{-1} initial boron concentration, the maximum removal has been 90% for 0.75 adsorbent-to-solute ratio.

Another low cost candidate for boron removal is calcined magnesite tailing (Kıpçak and Özdemir, 2012). It has reported that the optimum calcination temperature was 600°C and the optimum pH was 6. The contact time to reach adsorption equilibrium was about 420 min. The maximum boron loading capacity of magnesite is 6.09 mmol g^{-1} at 45°C has demonstrated that the magnesite was an effective adsorbent for boron removal from aqueous solutions. Layer double hydroxides (LDHs) are a group of clay minerals, which have lots of divalent cations. These cations can be replaced by trivalent cations causing a net positive charge, which can be changed with anions in the layered structure (Theiss *et al.*, 2013). Ferreira (Ferreira *et al.*, 2006)

used Mg/Al and Mg/Fe LDHs to remove boron from wastewater with maximum capacity was 14.0 mg g^{-1} according to Langmuir model. Kentjono and co-workers (Kentjono *et al.*, 2010) have also used Mg/Al LDHs to remove boron from optoelectronic wastewater with high boron concentration (Kentjono *et al.*, 2010). The maximum boron loading capacity has been 3.51 mmol g^{-1} at pH 9.

Besides, boron removal has also studied using many other adsorbents such as cerium oxide (Öztürk and Kavak, 2008), activated carbon (Rajaković and Ristić, 1996), activated alumina (Bouguerra *et al.*, 2008), Al_2O_3 based materials (Seki *et al.*, 2006), activated carbon impregnated with salicylic acid (Çelik *et al.*, 2008), iron-rich natural clays (Seyhan *et al.*, 2007), activated sludge (Fujita *et al.*, 2005), neutralized red mud (Cengeloglu *et al.*, 2008) and composite magnetic particles (Liu *et al.*, 2009). For these materials, it has reported that the adsorption was pH, adsorbent dose dependent. Different adsorbents have different adsorption capacities such as activated carbon (0.19 mg g^{-1}), activated alumina (0.44 mg g^{-1}), minespoils ($0.002 - 0.004 \text{ mg g}^{-1}$), neutralized red mud (6.0 mg g^{-1}) (Ezechi *et al.*, 2012).

1.3.3. Hybrid methods

Hybrid method is the combination of sorption process and membrane filtration. Solutes like boron species and other harmful substances in water are first adsorbed by fine sorbents that are then removed by membrane filtration. The advantages of this technique over other methods are better performance, lower cost, no pressure drop like conventional sorption system. Two most popular methods are PEUF and AMF, which are describe below.

1.3.3.1. PEUF – Polymer enhanced ultrafiltration method

In PEUF method, borate will react with soluble water polymers to form complex in the solution following by a membrane ultrafiltration process to get the separation. This technique can be operated under lower pressure than nanofiltration method but obtains higher flux, thus higher adsorption efficiency and separation (Smith *et al.*, 1999). Rivas (Rivas *et al.*, 2011) has reported that PEUF using water soluble polymers which contain one or several functional group on their backbone or side chain such as amine, amide, carboxylic acid, hydroxyl, phosphoric acid quaternary ammonium salts, and sulfonic acid have ability to remove pollutant ions from aqueous solution. Base on his results, it has indicated that ion removal efficiency depends on variable factors like pH, ionic strength, polymer concentration, chemical properties of species of interest. Water-soluble polymers with high retention capacity for ion removal are poly [2-(acryloyloxy) ethyl] trimethylammonium chloride, P (CIAETA), at pH 8. Besides, arsenic removal was tried with different water soluble polymers, for instance, poly [3-(acryloylamino) propyl] trimethylammonium chloride P (CIVBTA), poly (4-vinyl-1-methyl-pyridinium) bromide P (BrVMP), poly (diallyl dimethyl ammonium) chloride P (CIDDA).

Polyvinyl alcohol has been selected to use as the boron complexing agent (Dilek *et al.*, 2002). All operating parameter were considered such as metal/polymer ratio, pH of system, and polymer characteristics as molecular weight, degree of hydrolysis. High retention could be achieved by increasing pH, decreasing degree of hydrolysis and decreasing loading values while molecular weight of polymer had no effect on retention capacity. It has been concluded that

there had been no problem with concentration polarization, fouling, and gel formation thus high reproducibility was obtained. In summary, PEUF had been proved to be an alternative method of boron removal.

A novel boron specific copolymer with quaternary amine, poly (vinyl amino-N, N'-bis-propane diol-co-DADMAC) (GPVA-co-DADMAC), has been synthesized in three comonomer ratios (2%, 5% and 10%). This polymer has been indicated efficiently exploited for boron removal via PEUF by Zerze *et al.* (2013). Boron concentration could be reduced from 10 mg L⁻¹ to 0.8 mg L⁻¹ at pH 9 with mass ratio of 0.001. Owing high boron binding affinity at high pH and easy decomplexation ability at low pH, the synthesized copolymer was useful for large scale water treatment. It is described that the polymers selective for boron adsorption, were synthesized by attaching sugar – like ligand to the polymeric chain by Smith *et al.* (2005). PEUF has advantages over other techniques with efficient boron rejection, high separation efficiency and fast kinetics. However, it still encounters with some drawbacks such as complex process, high cost because of membrane fouling, using of high molecular weight water soluble molecular and polymer regeneration (Wolska and Bryjak, 2013).

1.3.3.2. AMF – Adsorption membrane filtration

Nowadays, one of the best boron removal approaches for the hybrid configuration is AMF system, which consists of microspherical sorbents and microfiltration membranes. It has been found that microfiltration did not need a high pressure to run and the membranes could work below their critical flux conditions without being fouled by the particles. Moreover, AMF is known as an efficient method for boron rejection due to capability of using fine small sorbents that increases surface area and the adsorption kinetic performances (Hilal *et al.*, 2011).

Several systems of AMF has been developed to examine the suitability and performance of hybrid process (Hilal *et al.*, 2011; Kabay *et al.*, 2006). FIG. 1.16 shows a detail system of boron removal procedure.

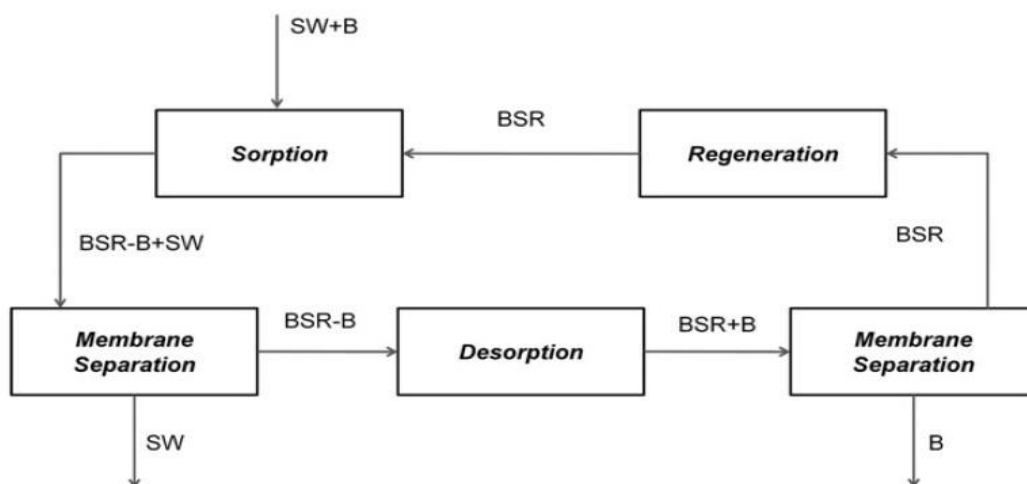


Fig. 1.16. Flow sheet of the adsorption membrane filtration system

From (Hilal *et al.*, 2011)

The above figure describes the 5 – step process of boron removal: 1, Boron sorption by BSRs; 2, Membrane separation mixture of BSR-B and water; 3, Boron desorption using acid; 4, Membrane separation of BSR and boron; 5, Regeneration of BSR using base.

Two BSRs have selected for boron adsorption, Diaion CRB 02 and Dowex XUS – 43594.00. A flat – type hydrophobic Teflon-fluoropore membrane with a thickness of 200 μm and pore diameter of 0.2 μm has employed for the second stage. The kinetic behavior of both resins has investigated. It has concluded that two chelating agents were rapid enough to participate in the hybrid process. Diaion CRB 02 required 5 min to get 50 percentage reductions from initial concentration while Dowex type resin took 30 min. Furthermore, it has observed that boron removal was improved after five cycles due to the better access to functional groups through the regeneration of resins with the NaOH solution. Another research of the same author has been described a boron sorption process utilizing two boron selective resins, Diaion CRB 02 and BSR 1 (Wolska *et al.*, 2010). Membrane filtration modules were microfiltration polypropylene capillary membranes with a pore diameter of 0.4 μm . The hybrid system was applied on several boron solution types such as geothermal water, boric acid from artificial solution and permeates on the first stage of SWRO treatment. Effect of different process parameters on boron removal efficiency have considered, for example, particle size, slurry rate delivery, resins concentration and volume of permeates flux. Finally, as the results, it has reported that sorbent particle size had a markedly influence on the sorption of membrane hybrid system. In addition, a significant reduction of boron concentration in first 15 min was also observed.

A hollow fiber polypropylene membrane with pore diameter of 0.4 μm has been used as a filtration material on the AMF system by Yimaz (Yilmaz *et al.*, 2006). Taking the advantage of low energy requirement of this material, hollow fiber was tested with two boron specific resins, Diaion CRB 02 and XUS – 43594.00. Ultimately, the obtained data has demonstrated that CRB 02 was more favorable for AMF system because of taking less time to reach steady state, resulted in faster boron adsorption kinetics. It is realized that it is important to investigate a high acid resistant membrane which is contacted with low pH solution after desorption step. Onderkova (Onderková *et al.*, 2009) carried out an boron sorption with AMF process utilizing a tubular ceramic microfiltration membrane Membralox with an inner diameter of 7 mm and a length of 0.25 m. From experiment, it was concluded that the ceramic membrane is applicable for the AMF application.

The AMF system should run with small size particles for avoiding the abrasion and low size dispersity. However, most current commercial sorbent have been now produced in pore diameter range of 300 to 500 μm which has been possible to be grinded into smaller size, consequently larger size heterogeneity and shaper edge, resulted in membrane surface's hurt (Blahušiak and Schlosser, 2009). Finally, this factor will cause a negative effect on stability and reliability of the system. There has been several ways utilized to obtain polymeric microspheres such as crystallization, precipitation or polymerization of emulsion or suspension but among of them, membrane emulsification of monomer followed by emulsion polymerization seems to be the most attractive ways due to a better particle size control than others. This method has been tested by Wolska and Bryjak (Wolska and Bryjak, 2011) to synthesized polymeric particle from vinylbenzyl chloride-styrene-divinylbenzene monomers. It was noted good boron uptake and shape stability was achieved when sorbents were exposed in acid and basic solution.

1.3.4. Other methods

1.3.4.1. Electrocoagulation method (EC)

Coagulation is one of the most important physio-chemical reactions used in water treatment. The precipitation of ions (heavy metals) and colloids (organic and inorganic) are carried out in solution by charges neutralization. An electrocoagulation process undergoes three steps: 1. Coagulant formation by anode electrical oxidation, 2. Destabilization of pollutants and suspended by emulsion breaking, 3. Combining instable particles to form flocs (Wolska and Bryjak, 2013).

EC is considered as one of the simplest method because it requires simple equipment, consume small amount of chemical and is easy to operate. EC process applied for boron removal from aqueous solution was efficient, at high concentration (100 mg L^{-1}) even (Sayiner *et al.*, 2008). Aluminum and iron have been used as cathode and anode, respectively. After 50 min of retention, it was reported that 70% boron was removed by aluminum and 62% of that was removed by iron electrode. EC system strongly depends on the current density, initial concentrations, and time. Studying on the same technique but utilizing zinc and stainless steel as electrode material, Vasudevan (Vasudevan *et al.*, 2013) has indicated in his research that optimum removal efficiency of 93.2 % was achieved at a current density of 0.2 A dm^{-2} , at pH of 7.0 with the energy consumption of 1.007 kWh m^{-3} . The adsorption of boron onto Zn(OH)_2 has been found to be spontaneous and endothermic thermodynamically.

1.3.4.2. Donnan dialysis method (DD)

DD is one of the ion exchange membrane processes used for purification or concentration of the dilute solution (Akretche and Kerdjoudj, 2000). The principle of this technique is making the use of difference in chemical potential between two compartments, which were separated by an ion exchange membrane. Boron removal from aqueous solution has been studied through Neosepta-AHA membrane by Ayyildiz (Ayyildiz and Kara, 2005) as a function of concentration, pH, conduct time, membrane structure and effect of accompanying ions. It has showed from the experiment that high boron could be obtained with the feed solution pH of 9.5. Beside Neosepta-AHA, different types of anion exchange membranes have been examined such as Neosepta AHA, AFN and AMH. Membrane sometimes was modified with plasma in order to improvement the boron removal efficiency (Kir *et al.*, 2011). The surface of membrane has been treated by electron cyclotron resonance plasma (ECR) to enhance the performance. The boron solution has been selected with two concentrations, 0.1 and 0.001 M. Finally, it has demonstrated that ECR plasma treatment effectively improved the AFX anion-exchange membrane surface's performance. Another research of anion exchange AMX (Neosepta) membrane was investigated through multiple regression methods and proved to be an efficient technology for boron adsorption (Turek *et al.*, 2009).

1.3.4.3. Capacitive deionization method (CDI)

CDI serves as energy – efficient method for the desalination of brackish water (Anderson *et al.*, 2010). In CDI process, two high surface – area activated carbon electrodes comprising from

fibers or C aerogel are used. A high enough potential (< 1.23 V) has been applied in CDI cell that forms hydronium or hydroxide ions due to a red-ox reaction on the surface of electrodes, consequently leads to a slight change in pH in aqueous solution near the electrodes. Simultaneously, boric acid is fed through or along the electrodes. At the negative electrode, boric acid has been dissociated in to borate anion, which has had highly reversible electrostatic adsorbed on the positively charged electrode (Avraham *et al.*, 2011). In summary, boron removal from aqueous solution has taken place in two steps: boric dissociation on the negative electrode due to the formation of local pH and electro-adsorption of borate anion on the positive electrode.

1.3.4.4. Direct contact membrane distillation method (DCMD)

Membrane distillation (MD) is a thermally driven process that delivers water vapor through a porous hydrophobic membrane. Hot feed solution is introduced on one side of the membrane and a cool permeate is charged on another side. The vapor is forced to go through the membrane pores due to the partial pressure difference forming from the temperature difference through the membrane. The condensation of vapor obtained from the permeate side gives the produced water (Winter *et al.*, 2011). Direct contact membrane distillation (DCMD) is the best-known configuration of MD, in which the hydrophobic membrane directly separates the feed and the distillate. An investigation using poly(vinylidene fluoride) hollow fiber membrane to remove boron from aqueous solution. DCMD process had high boron removal efficiency ($> 99.8\%$), even with high initial boron concentration (750 mg L^{-1}) solution. Influence of feed temperature was neglected while that of pH and salt concentration was less than in reverse osmosis. Ground water sample of 12.7 mg L^{-1} has been tested with DCMD. As the result, the permeate boron has kept below $20 \text{ } \mu\text{g L}^{-1}$ whether the feed has been acidified or not but a pre-acidification has recorded to be helpful in maintaining the permeate flux stability (Hou *et al.*, 2010).

1.3.4.5. Conclusion

There are many potential techniques for boron removal with their own advantages and disadvantages, which are shown in TABLE 1.3. In general, the most widespread methods using now are reverse osmosis filtration and fixation on specific resins because of their efficiency, short time reaction and simplicity. However, regard to the main drawback of each method, for example, the strong pH dependent of reverse osmosis and the problems of high cost and the production of polluting effluent during regeneration of boron selective resins, companies are searching to produce a new adsorbents which is cheap, biodegradable and effective for boron removal process.

Table 1.3. The list of boron removal technologies

Technologies	Advantages	Disadvantages	
Reverse Osmosis	+ High removal efficiency (> 98%) at pH > 10.5)	+ High pH needed + Fouling, scaling which reduces membrane lifetime	
Boron selective resins	+ High removal efficiency > 99% at natural pH (6.5 – 8.5) + pH of solution is stable before and after adsorption + Sorption rate is fast + Easy boron recovering	+ Need to regenerate resin by strong acid and basic solution + Expensive	
Non boron selective resins	+ Not expensive	+ Removal efficiency is low (about 55%) at high temperature (45 °C) + Dependent on interfering ions + High pH required	
Hybrid methods	+ High removal efficiency + No pressure drop + Operated at natural pH + Fast sorption rate + Reduce regeneration solution for BSRs	+ Complex procedure + Fouling, scaling	
Others	Natural adsorbents	+ Fast sorption rate + High efficiency + Environmental friendly	+ Complicated preparation procedure
	Fly ash, calcined magnesite taling	+ Low cost + Slow sorption rate	+ Easy influence by pH, interfering ions, temperature
	Electrocoagulation method (EC), Donnan dialysis method (DD), Capacitive deionization method (CDI)	+ Adsorption equilibrium reaches within 1 hour + Boron removal efficiency from 60% - 90%	+ High level of pretreatment + Frequent electrode replacement + Easy influence by pH of samples, salinity
	Direct contact membrane distillation method (DCMD), Microwave hydrothermal method (MHM)	+ High efficiency (> 90%) + Fast reaction	+ Need to add acid in the feed solution to maintain stability of permeate flux to reduce the dissolution of boron precipitation of MHM

1.4. Theoretical models for batch and column systems

1.4.1. Kinetic and adsorption models

1.4.1.1. Kinetic models

Several kinetic models can be used to predict the mechanism of sorption processes such as Lagergren pseudo-first order, the pseudo-second order of equation and parabolic diffusion model (Stone and Morgan, 1990; Ho and McKay, 1999; Öztürk and Kavak, 2005). Among them, the pseudo-first and pseudo-second order models are the most frequently used (Stone and Morgan, 1990; Kabay *et al.*, 2007; Yang *et al.*, 2014; Sigg *et al.*, 2014).

The pseudo-first order rate equation of Lagergren has been applied in the cases of diffusion through a boundary liquid film and adsorption kinetics as a chemical phenomenon. If film diffusion is rate controlling, the constant of the equation will vary inversely with the particle size and the film thickness. If the exchange is chemically rate controlled, the constant of the equation will be independent of particle diameter and flow rate and will depend only on the concentrations of the ions in solutions (Stone and Morgan, 1990; Ho and MacKay, 1999).

The pseudo-first order model is based on the following equation:

$$\frac{dq_t}{dt} = k_1(q_e - q_t) \quad \text{EQ 1.2}$$

where q_t and q_e represent the amounts of boron adsorbed (mmol g^{-1}) at time t and equilibrium, respectively; k_1 is the sorption rate constant (min^{-1}); q_e is estimated by taken the maximum value of experimental data.

That means

$$\frac{dq_t}{q_e - q_t} = k_1 dt \quad \text{EQ 1.3}$$

Taking the integral of EQ 1.3 with respect to the boundary conditions:

$q = 0$ when $t = 0$, and

$q = q_t$ when $t = t$,

We obtained the following relationship:

$$\log(q_e - q_t) = \log(q_e) - \frac{k_1}{2.303} t \quad \text{EQ 1.4}$$

Sorption rate constant k_1 (min^{-1}) can be estimated by plotting $\log(q_e - q_t)$ with time.

Multiple pseudo-first order kinetics has been used in some sorption systems such as protein silica (Ho and McKay, 1999). Basically, it means that a plot of $\ln(q_e - q_t)$ vs. time can be divided into two or three linear sections, each linear section meaning a pseudo-first order reaction mechanism. One step is assumed to correspond to the initial binding of the molecules with the active site of the solid surface by removal or organization of surface bound water. The other step represents the denaturation and reorganization of the bound polymer (Ho and McKay, 1999). In the case of two kinetic steps, the first sorption one is faster than the second one, and the sorption rate is controlled by either film diffusion or an intraparticle diffusion mechanism. Intraparticle diffusion was found to be a rate limiting step following the pseudo-first order sorption rate expression of Lagergren (Ho and Mac Kay, 1999).

The pseudo-second order kinetics is described as follows:

$$\frac{dq_t}{dt} = k_2(q_e - q_t)^2 \quad \text{EQ 1.5}$$

where q_t and q_e represent the amounts of boron adsorbed (mmol g^{-1}) at time t and equilibrium, respectively; k_2 is the sorption rate constant ($\text{g mmol}^{-1} \text{min}$). Rearranging the variables in the equation EQ 1.5 and integrating in the boundary as above, one gets:

$$q_t = \frac{k_2 q_e^2 t}{1 + k_2 q_e t} \quad \text{EQ 1.6}$$

Parameters can be estimated either by non-linear regression by using dedicated software or by re-writing equation EQ 1.6 as the reverse ratio of both sides multiplied then by t . In the latter case, it comes:

$$\frac{t}{q_t} = \frac{1}{k_2 q_e^2} + \frac{1}{q_e} t \quad \text{EQ 1.7}$$

The sorption rate constant k_2 ($\text{g mmol}^{-1} \text{min}$) and q_e (mmol g^{-1}) can be calculated by plotting q_t with t .

1.4.1.2. Sorption model theory

The Langmuir model (Langmuir, 1918): has been developed to study the equilibrium at gas-solid interface. Owing to similar shaped isotherms, this model has been extended for probing the sorption phenomenon at liquid-solid interface (Stumm, 1992). Some mathematic relationships have been adopted for fitting the experimental data (Sigg *et al.*, 2014). Monolayer adsorption between liquid and solid phases is usually described by Langmuir-type isotherm model with the following assumptions (Farley *et al.*, 1985; Sontheimer *et al.*, 1985; Sigg *et al.*, 2014).

- Homogeneous surface sites (same energy)
- Each site can occupy at most one molecule (all sites are identical and equivalent)
- No repulsion or attraction due to molecules already adsorbed

- A maximum of a monolayer can be formed at the surface of the adsorbent

The adsorption process can be express as follow:



where A is solute, = S is surface sites, = S - A is adsorbate occupying one surface site.

The Langmuir-type constant (K_L) is expressed (Sigg *et al.*, 2014):

$$K_L = \frac{\{=S-A\}}{[A]\{=S\}} \quad \text{EQ 1.9}$$

The total surface site is expressed as:

$$S_{\text{tot}} = \{=S\} + \{= S - A\} \quad \text{EQ 1.10}$$

Use equation EQ 1.9 and EQ 1.10, it comes:

$$\{=S-A\} = S_{\text{tot}} \frac{K_L [A]}{1 + K_L [A]} \quad \text{EQ 1.11}$$

with [A] is solute concentration in aqueous solution at equilibrium (mmol L^{-1}), $\{= S - A\}$ is the concentration of solute adsorbed on the resin at equilibrium (mmol g^{-1}), S_{tot} is the total adsorption capacity (or total surface site concentration) (mol g^{-1}), K_L is Langmuir constant (L mol^{-1}).

As shown in Sigg *et al.* (2014) and Charrière *et al.* (2015), the Langmuir-type relationship can be deduced from physical-chemical reactions at solid-liquid interfaces such as surface complexation or ionic exchange reactions.

BET sorption model: Multilayer adsorption has been often described by Brunauer-Emmett-Teller isotherm (BET) (Brunauer *et al.*, 1938). It has been applied for liquid-solid interface (Sontheimer *et al.*, 1985) as BET-type isotherm, especially if surface precipitation is assumed to occur at the solid-liquid interface (Farley *et al.*, 1985; Lützenkichen, 1996; Sigg *et al.*, 2014):

$$q_e = \frac{q_s C_{\text{BET}} C_e}{(C_s - C_e) \left[1 + (C_{\text{BET}} - 1) \left(\frac{C_e}{C_s} \right) \right]} \quad \text{EQ 1.12}$$

where C_{BET} is BET constant (L mmol^{-1}), C_e is solute concentration in aqueous at equilibrium (mol L^{-1}), q_e is solute concentration on resin (mol g^{-1}), C_s is solute monolayer saturation concentration (mol L^{-1}), q_s is equilibrium adsorption capacity (mol L^{-1}).

As C_{BET} and $C_{\text{BET}} (C_e/C_s)$ are much greater than 1, equation EQ 1.12 becomes:

$$q_e = \frac{q_s}{1 - \frac{C_e}{C_s}} \quad \text{EQ 1.13}$$

For both models, different ways can be used for parameter estimation, either by linearizing equation or by using specific software dedicated to solve non-linear equations.

1.4.2. Non-linear chromatography theory for column experiment

Description of adsorption processes of chemicals from a fluid phase onto a solid matrix always plays an important role in environmental science because this information is very essential to estimate the mobility of pollutants. The sorption equilibrium is usually characterized by adsorption isotherms. Therefore, batch experiment is always performed to obtain adsorption isotherms. Column experiment is carried out after taking the optimized parameter obtained from batch experiment such as type of resin, pH, initial concentration, temperature, reaction time, etc. Hence, it is also necessary to predict the adsorption behavior of solute on sorbent by using non – linear chromatography method.

In solution, the concentration $c(x, t)$ of a sorbing chemical per unit pore volume of mobile phase is described by the advection-dispersion equation (Schweich and Sardin. 1981; Buergisser *et al.*, 1993; Sigg *et al.*, 2014).

$$\frac{\partial c_{tot}}{\partial t} = D \frac{\partial^2 c}{\partial x^2} - v \frac{\partial c}{\partial x} \quad \text{EQ 1.14}$$

with D is dispersion coefficient and \mathcal{V} is the mean pore velocity

$$\mathcal{V} = \frac{q}{\theta} = \frac{F}{A\theta} \quad \text{EQ 1.15}$$

whereas q is Darcy flow velocity (solvent volume per unit area A and time), θ is kinematic porosity of sorbent, F is overall flow rate through the column (mL min^{-1}), A is the total cross-sectional area of the column.

In case of no adsorption

The total concentration of solute is the concentration of solute in solution

$$C_{tot} = C \quad \text{EQ 1.16}$$

In this case, the solute species is called conservative tracer. The travel time distribution of the tracer in the column of the length L can be characterized by an average time t_0 and a standard deviation δ :

$$t_0 = \frac{L}{\mathcal{V}} \quad \text{EQ 1.17}$$

The standard deviation value is directly related to the column Péclet number, Pe , and the theoretical plate number J (for approximately $J > 100$)

$$Pe = \frac{L \cdot v}{D} = 2 \cdot \frac{t_0^2}{\delta^2} = 2J \quad \text{EQ 1.18}$$

In case of having adsorption

The total concentration of adsorbed species is the sum of the concentration in solution C and the concentration on sorbate, C_a :

$$C_{\text{tot}} = C + \rho C_a \quad \text{EQ 1.19}$$

whereas C_a is the amount of adsorbed species per unit mass of sorbent and ρ is the density of sorbent per unit pore volume

$$\rho = \rho_s \frac{1-\theta}{\theta} \quad \text{EQ 1.20}$$

ρ_s is the density of sorbent matrix with respect to the liquid, which is in the column.

For the local equilibrium assumption (LEA), the concentration of the adsorbed species C_a is a unique function of the concentration of the dissolved species C .

- For simplest case of linear adsorption isotherm

$$C_a = K_D \cdot C \quad \text{EQ 1.21}$$

K_D is the partition coefficient. The breakthrough curve is the same as that of conservative tracer.

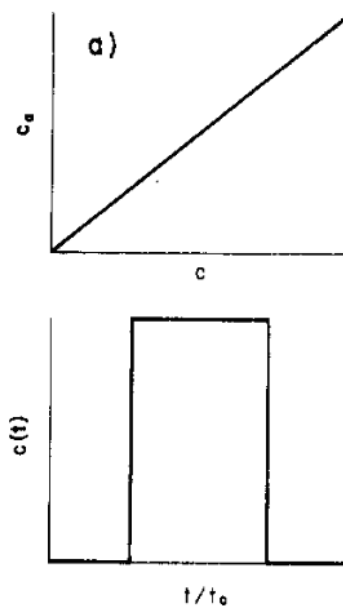


Fig. 1.17. Schematic representation of the response of the chromatographic column for linear adsorption isotherms.

From (Buergisser *et al.*, 1993)

The breakthrough curve is delayed in time by the retardation factor

$$R = 1 + \rho \cdot K_D$$

$$\text{EQ 1.22}$$

So, due to the linearity of the adsorption isotherm, the retardation factor is not dependent on the concentration of solute.

- **For the non-linear adsorption isotherm**

Three possible shapes of isotherm give three breakthrough curves (neglect the effect of dispersion). This derivation is achieved by using the Golden rule (Schweich and Sardin, 1981).

The Golden's rule states the relationship between the shape of the non-linear isotherm and the shape of a breakthrough curve due to the step of injection of the solute:

A piece of string is laid along the isotherm anti-clockwise from the point I (the initial state of the column) to the point F (the final state of the column) and then pulled straight. If the string lies on the isotherm, a self-sharpening or diffuse front is observed. If the string does not touch the isotherm, the breakthrough curve has a sharp boundary.

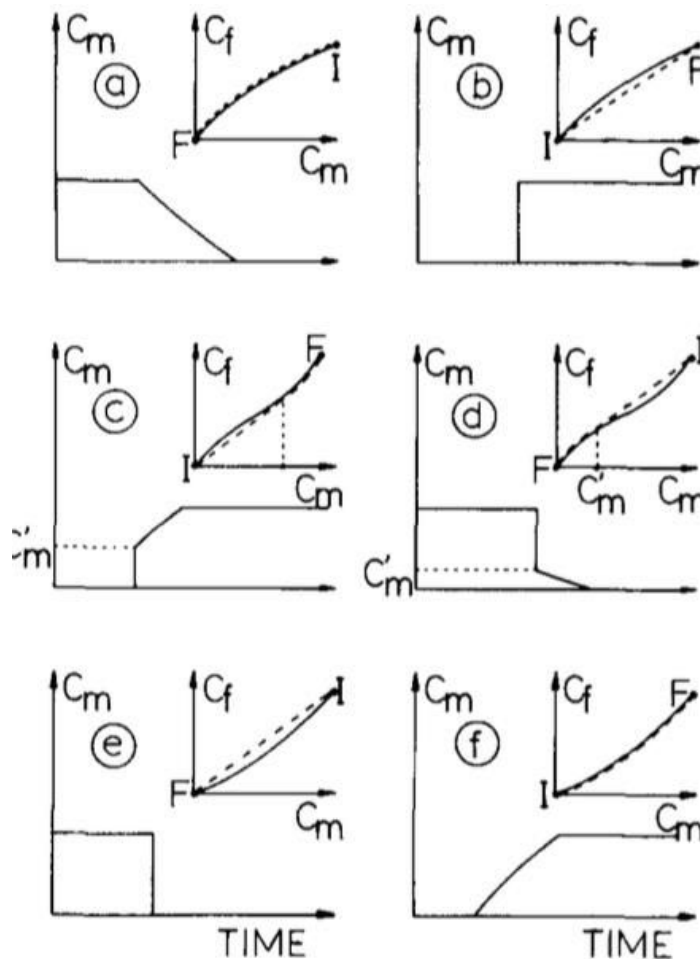


Fig. 1.18. Examples of Golden's rule: The column is previously equilibrated with the solute (state I). A step composition change is performed at the inlet of the column and the column progressively reaches the final state F.

From (Schweich and Sardin, 1981)

Suppose the isotherm is convex (i.e. FIG. 1.19a), according to Golden's rule, the string lies on the isotherm (as FIG. 1.18.a), so self-sharpening or diffuse front can be observed. In the step

concentration increases at the column input, a self – sharpening breakthrough curve will be obtained. If, that concentration decreases, a diffuse front will be formed. This is due to the fact that the retention time of solute decreases with the increase of concentration in solution. For adsorption process, concentration in solution is increasing in time, so the retention decreases, leads to a narrow, self-sharpening front. In contrast, for the desorption process, the retention increases in time then causes a broad, diffuse front. The reverse behavior is observed in the case of concave adsorption isotherm (FIG. 1.19 b).

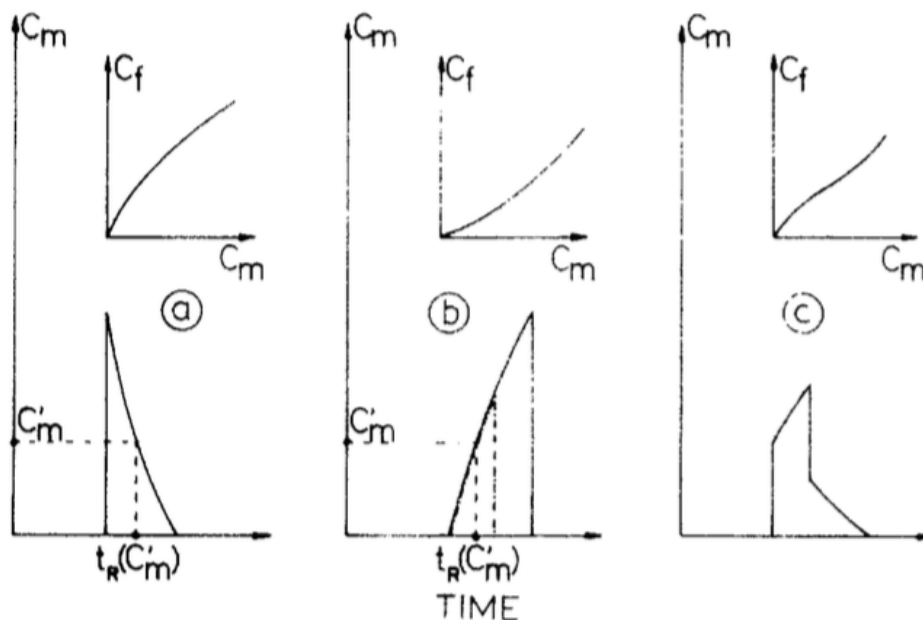


Fig. 1.19. Relation between the shape of an adsorption isotherm and the shape of the breakthrough curve. $C_f = C_a$, $C_m = C$

From (Schweich and Sardin, 1981)

- Self-sharpening front with convex adsorption isotherm
- Diffuse front with concave adsorption isotherm
- Both self-sharpening front and diffuse front with sharp boundaries. Isotherm with an inflection point

1.4.3. Optimized modeling of breakthrough curves

The comparison between batch and continuous trials can be achieved by kinetic or isotherm modeling.

1.4.3.1. Pseudo first order modeling

The Yoon and Nelson theoretical model was utilized to predict the breakthrough curve of boron concentration during adsorption process (Aksu and Gönen, 2004; Köse and Öztürk, 2008). In the column, the feed solution flows through the stationary bed of the resin and a portion of boron in the aqueous solution was retained within the resin bed. Let the fraction of boron adsorbed is A and the fraction of boron remained in aqueous solution, passing through the stationary resin bed is P . This model is based on the assumption that the decrease in adsorption fraction is proportional to A and P as presented in the following equation.

$$-\frac{dA}{dt} = k A P \quad \text{EQ 1.23}$$

Replacing $P = 1 - A$ and integrating the equation with condition of $A = A_a$ at $t = t_a$, it comes:

$$\ln \left| \frac{A(1-A_a)}{A_a(1-A)} \right| = k (t_a - t) \quad \text{EQ 1.24}$$

It is also written in the form of P as follow:

$$\ln \left| \frac{Pa(1-P)}{P(1-Pa)} \right| = k (t_a - t) \quad \text{EQ 1.25}$$

When $P = 0.5$ (one-half of the adsorption capacity), the adsorption time t_a is denoted as τ . The equation EQ 1.25 becomes:

$$P = \frac{1}{1 + e^{k(\tau - t)}} \quad \text{EQ 1.26}$$

or in a linear form

$$t = \tau + \frac{1}{k} \ln \left(\frac{P}{1-P} \right) \quad \text{EQ 1.27}$$

The boron fraction that passes through the resin bed: $P = C/C_0$, in which C is the boron concentration of solution exiting the adsorption column at time t while C_0 is the boron concentration of the inlet boron solution. The equation EQ 1.27 becomes:

$$t = \tau + \frac{1}{k} \ln \left(\frac{C}{C_0 - C} \right) \quad \text{EQ 1.28}$$

From the linear plot of adsorption time t versus $\ln [C/(C_0 - C)]$ as described in equation EQ 1.28, it can be obtained the values of adsorption time τ at $C = \frac{1}{2} C_0$, and the rate constant k (min^{-1}). By using these defined parameters, a complete breakthrough curve described the relationship between adsorption time and boron concentration of exiting solution C will be constructed and compared to the experimental breakthrough curve.

As definition, 50% breakthrough curve of adsorption process is obtained at τ . Therefore, the resin bed should be completely saturated at 2τ due to the sigmoid nature of the breakthrough curve. The amount of boron adsorbed by the resin is one-half of the total boron entering the adsorption column within the period of 2τ .

The adsorption capacity of the column is determined as following equation:

$$Q_0 = \frac{1}{2} C_0 F 2\tau = C_0 F \tau \quad \text{EQ 1.29}$$

where Q_0 is the adsorption capacity of the column (mg), F is flow rate of solution passing through the column (L min^{-1}), τ is 50 % breakthrough time.

1.4.3.2. Pseudo second order modeling

The Thomas model assumes Langmuir kinetics of adsorption-desorption, no axial dispersion, the rate driving force obeys the second-order reversible reaction kinetics (Aksu and Gönen, 2004). The model is presented by the following form:

$$\frac{C}{C_0} = \frac{1}{1 + e^{\left[\frac{K_T}{F}(q_0 m - C_0 V)\right]}} \quad \text{EQ 1.30}$$

where K_T is Thomas rate constant ($\text{mL min}^{-1} \text{mg}^{-1}$), F is flow rate (mL min^{-1}), q_0 is sorption capacity (mg g^{-1}), m is amount of resin in column, C_0 is inlet boron concentration (mg L^{-1}), C is boron concentration of exiting solution (mg L^{-1}), V is effluent volume (L).

The linear form of the Thomas model follows:

$$\ln\left(\frac{C_0 - C}{C}\right) = \frac{q_0 K_T m}{F} - \frac{K_T C_0}{F} V \quad \text{EQ 1.31}$$

The Thomas rate constant K_T and sorption capacity q_0 can be determined by plotting the linear relationship between $\ln((C_0 - C)/C)$ against volume of solution at a given flow rate.

1.5. Pectins - New adsorbents

As discussion in part 1.3 (Study of boron removal technologies), it is necessary to find a new adsorbent, which is expected to be cheap, biodegradable and effective on boron removal. In this thesis, we propose a type of natural polymer named pectins, which are usually found in agriculture waste and that contains polyol groups bringing the properties for the complexation of boron. Moreover, the boron-pectins complex could be a new type of fertilizer containing the required quantity of boron for the plants. This would avoid the pollution of the regeneration step and would give to the pectin an attractive economical application.

1.5.1. Pectins

1.5.1.1. Pectins presentation and functions

Pectin has been recognized for at least 200 years and identified by the French chemist Nicholas Vauquelin in 1790. Further work on pectin was undertaken by Braconnot, who named pectin as gelling substance pectic acid in 1824. In 1924, Smolenski identified pectin as a polymer of galacturonic acid. After that, the first basic formula of pectin was established by Scheneider and Bock in 1937 (Cyber Colloids LTD, 2006). Nowadays, pectins are known as complex polysaccharides, which are found in cell walls of higher plants. They function as a hydrating agent and essential material for the cellulosic network. The exceptional case is the cell walls of the Graminae family, which contains very small amount of pectin in normal structure. The highest concentration of pectin is in the middle lamella, which accounted for one third of the cell walls, with a gradual decrease from primary cell wall toward the plasma membrane. Pectins are found in large amounts in soft plant tissues under condition of fast growth and higher

moisture content. It seems that pectins are important factor in control of the movement of water and plant fluids (Thakur *et al.*, 1997).

Pectins influence the texture of fruit, vegetables because they are the wall components which determine whether the extension growth will take place (Jarvis *et al.*, 1984). Pectins contribute to the strength and structure of plant tissue. Some pectin molecules make a glycosidical link with xyloglucan chains that can bind covalently to cellulose (Keegstra *et al.*, 1973; Jarvis *et al.*, 1981). The firming effect of pectins in tissues consist of two phenomena: in fresh tissue, the formation of free carboxyl groups increases the possibilities and the strength of calcium binding between pectin polymers and in heated tissue, there is a combination of increased calcium binding and a decrease in the susceptibility of the pectin to depolymerization by β -elimination (Sajjaanantakul *et al.*, 1989).

Limited source of fruit is used as commercial pectin production because of different gelling agent properties due to different molecular weight and chemical composition. Recently, apple pomace, citrus peels, sugar beet and residues from the seed heads of sunflower are have been studied as source of pectins. Usually, this is a waste material from another industry such apple pomace from a cider producer. The amount of pectin from these different sources varies considerably TABLE 1.4.

1.5.1.1. Pectins structure and properties

Pectin structures

Pectins are copolymer of D-galactorunic acid and rhamnogalacturonan. The molecule is formed by L-1,4 – glycosidic linkages between the pyranose rings of D-galactorunic acid units. Pectins contain branched block and unbranched block polymers in which branched blocks contain a main galacturonan chain interrupted and bent by frequent rhamnose units (carrying side chains) while unbranched blocks has several or no rhamnose. Rhamnogalaturonan is primarily responsible for the chemical and structural complexcity of the pectic substance. Rhamnosyl insertion acts as junction during gelation. Neutral sugars appear in the side chains of pectin, for example, D-galactopyranose, L – arabinofuranose, D-xylopyranose, D – glucopyranose, D – apiose, 2 – O – methyl – D – xylose, 2 – O – methyl – fucose. These natural sugars account for 10 to 15% pectin weight. Pectin is classified in two types of pectin base on solubility: Water – soluble and water – insoluble pectin. Solubility in water is dependent on degree of polymerization and the number and distribution of methoxyl groups. Normally, solubility increases with the decreasing of molecular weight and increasing of esterified cacboxyl groups (Thakur *et al.*, 1997).

Table 1.4. Pectin content of some fruits

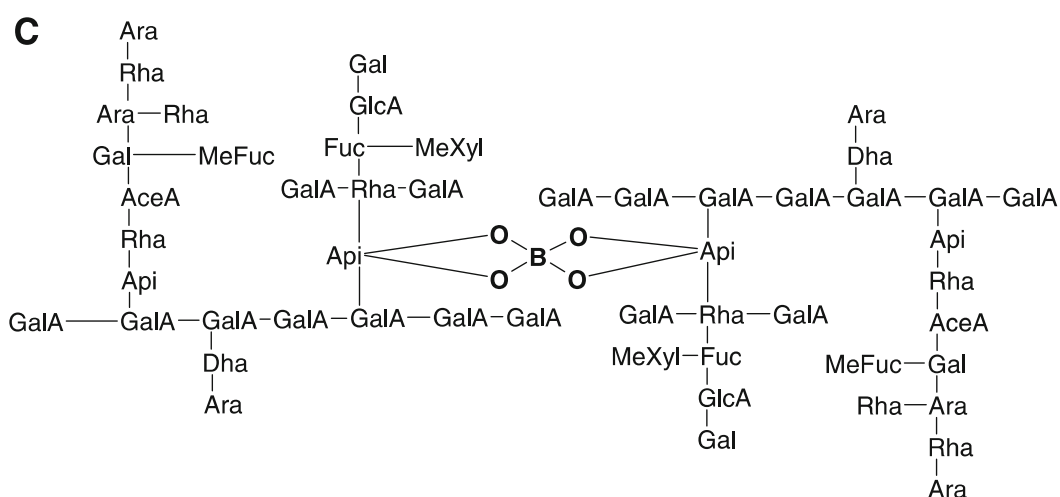
Data from (Renard and Thibault, 1993; Karr, 1976; Hodgson and Kerr , 1991)

Fruit	% pectic substances (wet weight)
Apple (Malus spp.)	0.5 – 1.6
Apple Pomace	1.5 – 2.5
Banana (Musa acuminata L.)	0.7 – 1.2
Beet pulp (Beta Vulgaris)	1.0
Carambola (Averrhoa carambola)	0.66
Carrot {Daucus carota}	0.2 – 0.5
Giant granadilla (Passiflora quadrangularis L)	0.4
Guava (Psidium guajava L.)	0.77 – 0.99
Lemon pulp (Citrus limon)	2.5 – 4.0
Lychee (Litchi chinesis S.)	0.42
Mango (Mangifera indica L.)	0.26 – 0.42
Orange peel (C. sinensis)	3.5 – 5.5
Papaya (Carcia papaya)	0.66 – 1.0
Passion fruit (Passiflora edulis S.)	0.5
Passion fruit rind	2.1 – 3.0
Peaches (Prunus persica)	0.1 -0.9
Pineapple (Ananas comosus L.)	0.04 – 0.13
Strawberries (Fragaria ananassa)	0.6 – 0.7
Tamarind (Tamarindus indica L.)	1.71
Thimbleberry (Rubus rosalfolius)	0.72
Tomato fruit (Lycopersicon esculentum)	0.2 – 0.6

Pectin structure contains of 4 different types of polysaccharides: Rhamnogalactorunan I, rhamnogalactorunan II, Homogalaturonan, xylogalactorunan. Homogalactorunan (HG) is the major type of pectin in cell walls, accounted for almost 60% of the total pectin. The HG polymer consists of a backbone of α -1,4-linked galactorunan acid (GalA) residues. The minimum estimated number of GalA residues is 72-100. Some of GalA in this backbone was esterified (C-6) and O-acetylated (O-2 and O-3) which define the physical properties of the pectin. A block of 10 non-esterified GalA residues make pectin molecule be sensitive with calcium cations crosslink (Daas *et al.*, 2001; Gee *et al.*, 1959; Mort *et al.*, 1993).

Xylogalacturonan (XGA) is the substitution of β -D-Xylp-(1-3) single unit side chain into the HG. The degree of xylosidation varies from 25% to 75% depending on different sources of pectin. Methyl esters are equally distributed among the substituted and unsubstituted GalA residues. Part of the GalA residues in XGA is methyl-esterified (Schols *et al.*, 1995). Rhamnogalactorunan I (RG-I) consists of a backbone, which is the repetition of [-> 2)- α -L-Rhap-(1 -> 4)- α -D-GalpA-(1 ->)] unit. Depending on the pectin source and extraction conditions, the number of repetitive unit can vary from 20 to 300 units. The rhamnosyl residues of RG-I can be substituted at O-4 with neutral sugars side chains. The sugar side chains usually compose of galactosyl and/or arabinosyl residues. The proportion of Rha residues is from 20 to 80%. RG-I contains 40% methyl esters but GalA residues of RG-I are presumably not methyl esterified because RG-I is not degraded under β -eliminative condition (Rihouey *et al.*, 1995; Lau *et al.*, 1987).

Rhamnogalactorunan II (RG-II): RG-II is a highly conserved structure in the plant and can be released by endopolygalacturonase action. RG-II structure is a cluster of four different side chains with very peculiar sugar residues such as, apiose, aceric acid, 3deoxy-lyxo-2-heptulosaric acid (DHA) and 3deoxy-mano-2-octulosonic acid (KDO). These side chains are attached to a HG fragment consists of nine galacturonic acid residues in which some are methyl-esterified (Ishii and Matsunaga, 2001; Ridley *et al.*, 2001). RG-II can complex with boron, forming a borate-diol ester, which can crosslink two HG molecules. Only the apiofuranosyl residues of the 2-O-methyl-D-xylose containing side chains in each of the subunits of the dimer participate in the cross-linking (Ishii *et al.*, 1999). The illustration of complex formation between RG-II and boron was shown in FIG. 1.20.



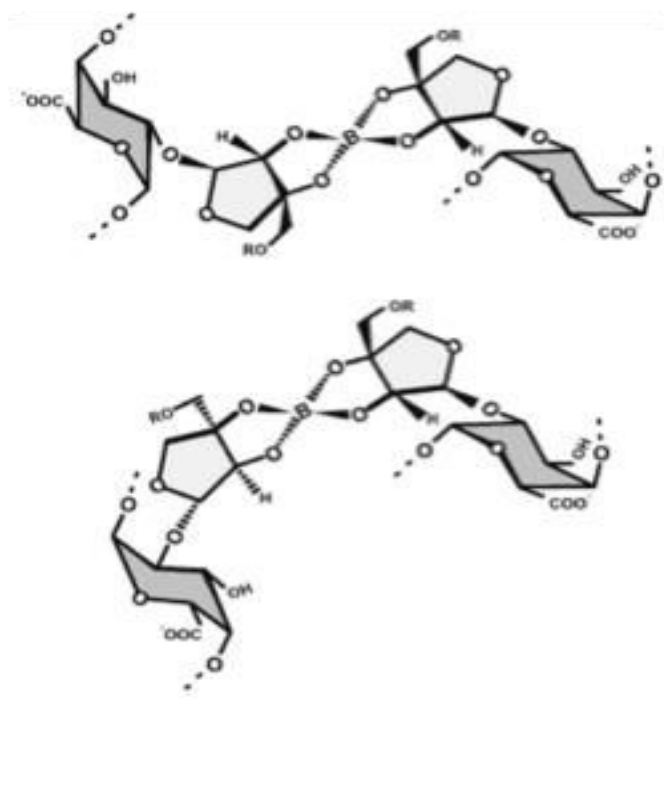


Fig. 1.20. The structures of two possible isomers of the reversible RG-II-Boron diester found in the walls of plant

From (Caffall and Mohnen, 2009; Voragen *et al.*, 2009)

Functional groups of pectin

Pectins carry nonsugar substituents, essentially methanol, acetic acid, phenolic acids and occasionally amide groups. The degree of methylation (DM) is determined by the percentage of carbonyl groups esterified with methanol. If more than 50% of the carboxyl groups are methylated, the pectins are called high-methoxy pectins (HM). Reversely, if the esterification percentage is less than 50%, the pectins are called low methoxy pectins (LM). Similar to the degree of acetylation (DAC), the same principle is applied although the DAC can be greater than 100% as galacturonosyl residues can be acetylated with more than one group per monosaccharide. Acetyl groups are generally presented in RG regions for apple and citrus pectins but found in higher amount in homogalacturonan from sugarbeet and potato pectins. Methyl esterification is common in native pectins but acetylation is rarer in natural extract (Sharma *et al.*, 2006). Overall the degree of substitution is known as the degree of esterification (DE). Depending on the isolation conditions, the remaining free carboxylic acid groups may be partly or fully neutralized. DE is the ratio of esterified D-galacturonic acid units to total D-galacturonic acid units. This degree strongly influences the solubility, gel forming ability, conditions required for gelation, gelling temperature, and gel properties (BeMiller, 1986).

Gelation of pectins

Low methoxy pectins (LM): LM pectin can gel in the presence of divalent cations, mainly calcium. The gelation is due to the formation of intermolecular junction zones between homogalacturonic smooth regions of different chains. Initial strong association of two polymers into a dimer is followed by the formation of weak interdimer aggregation, governed by

electrostatic interactions. Increase degree of methylation decreases the gel forming ability of LM pectins. LM pectins have a blockwise distribution of free carboxyl groups, which are very sensitive to low calcium levels. The gel formation with calcium ions is prohibited by the presence of acetyl groups but these groups give the pectins emulsion stabilising properties.

High methoxy pectins (HM): HM pectins have ability to form gel with sugar and acid. The gelation mechanism was affected by the degree of esterification (DE). For the LM pectins (DE < 50%), gelation results from specific non-covalent ionic interactions between blocks of galacturonic acid residues of pectin backbone and with divalent ions such as calcium. The affinity of pectin chains towards calcium is increased with the decrease in degree of esterification or ionic strength and with the increase of polymer concentration. In addition, the charge density of the polygalacturonate chain, the distribution of free and esterified carboxyl groups also has an important effect on the strength of calcium binding. Another factor influences the gel strength is molecular weight of the pectin used. Gel strength increases with the increase of molecular weights of pectins. Any treatment depolymerising the pectin chains results in weaker gels. Besides, rupture strength is dependent on the number of junction zones per single long chain molecule while the number of junction zones per unit gel volume determines rigidity. Acetyl groups prevent gelation. DM determines the setting temperature of a gel.

1.5.1.2. Application of pectins on industry

Because pectins have gelling ability so it has many application in human life such as food, pharmaceuticals, papers, edible films, etc. In the food industry, pectins are used in jams, jellies, frozen food, low – calorie foods as a fat or sugar replacer. In pharmaceutical industry, it is used to reduce blood cholesterol levels and gastrointestinal disorders. On the other hands, pectin is also used as a stabilizer in cosmetic products, oral drug delivery platforms, glue in cigar, foams, etc (Thakur *et al.*, 1997; Sriamornsak, 2011).

Among all of application, pectin has been widest applied in food industry. Some interaction between pectins and hydrocolloids were studied. LM pectins can be mixed with proteins to improve the strength of the gel or pectins can be mixed to gelatin in order to give the final product, which has a better stability at high temperature. Pectins are also combined with starch in jellybeans for example. Compared with jelly products, the texture of jellybeans is long and viscous. The appropriate texture level can be achieved by changing the pectin/starch ratio or by the choice of pectin and starch used.

1.5.2. Membrane filtration

The use of pectin as an adsorbent of boron removal in aqueous solution will produce a complex boron-pectin. In order to separate this complex from aqueous solution, membrane filtration is selected method.

A membrane is a permeable or semi - permeable, thin layer, which is capable of separating substances when a driving force is applied across the membrane. There are various driving forces to enable substances to transfer through a membrane, such as the application of a pressure

gradient, of a concentration gradient or of an electric potential. Membranes are manufactured in a variety of configurations including hollow fiber, spiral, and tubular shapes. There are four main membrane separation processes currently employed for liquid - solid separation:

- Microfiltration
- Ultrafiltration
- Nanofiltration
- Reverse osmosis

1.5.2.1. Principle and limiting factors

1.5.2.1.1. Principles

Microfiltration is applied for particles in range of 0.1 – 10 μm or molecular weight cut-off (MWCO) of 1000 kDa with low feed water pressure, 100 - 400 kPa. Materials can be retained by microfiltration filter such as sediment, algae, protozoa or large bacteria (Baker, 2012).

Ultrafiltration: Poresize of ultrafiltration membrane ranges from 0.002 to 0.1 μm , an MWCO of approximately 10 to 100 kDa, and an operating pressure of approximately 200 to 700 kPa. Ultrafiltration can contribute to a high removal capability of bacteria, virus's colloids. Therefore, ultrafiltration method is used mainly for drinking water treatment and protein concentration process (Clever *et al.*, 2000; Laine *et al.*, 2000).

Nanofiltration: is applied for the removal of molecules in ranges from 1-10 nm with MWCO of 100 Da to 1 kDa. Operating pressures are usually near 600 kPa and up to 1000 kPa. This method is mostly applied with low total dissolved solids water such as surface water and fresh groundwater to remove viruses, and humic materials.

Reverse osmosis: As introduced in previous part, reverse osmosis forces a solvent from a region with low concentration to the region with high concentration using high pressure 2–17 bar (30–250 psi). This method is specifically used for desalination process to produce fresh water from seawater or brackish water.

The classification of membrane separation techniques according to pore size and their application are summarized in the table below.

Table 1.5. The classification of membrane separation techniques (Pinnau *et al.*, 1999)

Separation techniques	Pore diameter	Driving force	Examples
Microfiltration	0.1 – 10 µm	Pressure driven force	Small particles, colloids, bacteria
Ultrafiltration	0.002 - 0.1 µm	Pressure driven force	Macromolecule emulsion
Nanofiltration	1 – 10 nm	Pressure driven force	Low molecular weight molecules (sugar, salt)
Osmose inverse	< 1 nm	Pressure driven force	Salt
Electrodialyse	< 5 nm	Electric potential gradient	Organic molecules
Electrofiltration	5 nm -10 µm	Electric potential gradient	Small particles, colloids, bacteria, Macromolecule emulsion
Dialyse	< 5 nm	Concentration gradient	Metabolites, mineral salts

1.5.2.1.2. Limiting parameters of membrane filtration

The operating principle for ultrafiltration is based on different parameters such as the transmembrane pressure, the permeate flux, the rejection rate and the concentration.

Among of them, the filtration performance is generally characterized by the permeate flux which is defined as the filtrate flow per unit of membrane filtration area, expressed by the Darcy equation:

$$J = \frac{TMP}{\mu R_h} \quad \text{EQ 1.32}$$

where

J: The flux (flow rate per membrane area) ($\text{kg}\cdot\text{s}^{-1}\cdot\text{m}^{-2}$) or ($\text{m}^3\cdot\text{s}^{-1}\cdot\text{m}^{-2}$)

TMP: The transmembrane pressure (Pressure difference between feed and permeate stream) (Pa)

μ : Viscosity of solution (Pa. s)

R_h : the hydraulic resistance of membrane (m^{-1})

Membrane filtration has some typical advantages compared to conventional method (thermal separation: distillation, sublimation, crystallization) such as energy saving, free-additives and chemical adding, therefore environmentally friendly. It is simple design, easy to coupled with other processes like microfiltration, RO, and high selectivity. However, it also shows some drawbacks, for example, concentration polarization and fouling which shorten membrane life time that cost money to replace (Clever *et al.*, 2000).

During filtration, the solvent and molecules are brought to the surface of the membrane under the effect of pressure. The solvent passes through the membrane while the molecules accumulate on the membrane's surface. Thus, the concentration of molecule in the vicinity of the membrane becomes greater than that of the feed solution. This is called concentration polarization. When solute concentration increases to very high value, a gel formation occurs with colloids. The concentration gradient creates a diffuse flux of solute which is in opposite direction to the filtration. So, when a decrease in permeate flux is observed, it can be attributed by the formation of a gel layer at a concentration C_g . The gel layer usually controls mass transfer and solvent flux in this case was determined by the following equation:

$$J = \frac{TMP}{\mu (R_g + R_h)} \quad \text{EQ 1.33}$$

where R_g is the resistance to flow through the gel (m^{-1})

The concentration polarization and gel formation illustration was presented in figure below.

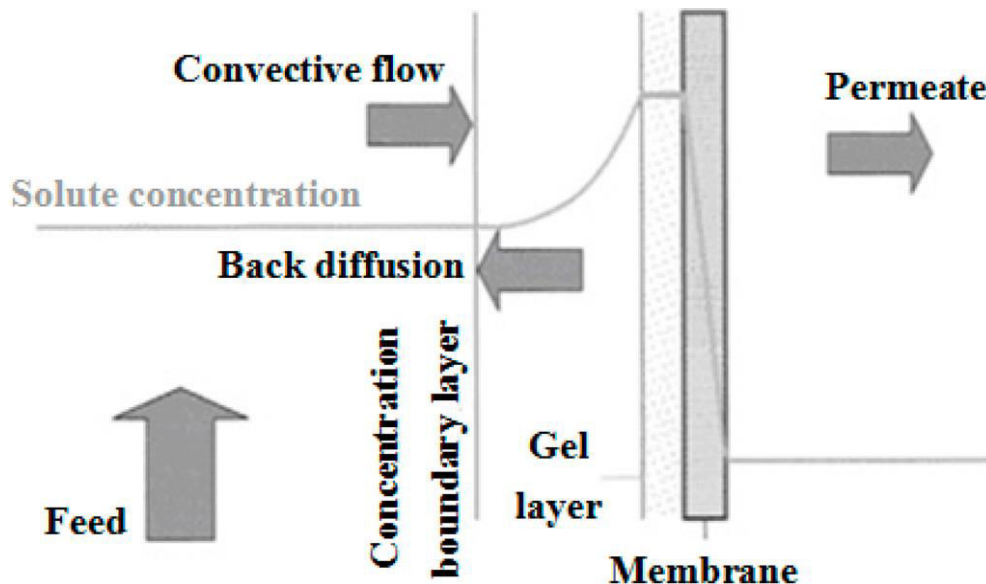


Fig. 1.21. The concentration polarization in filtration process.

From (Stephenson *et al.*, 2000)

Fouling is the phenomena in which sludge flocs, small particles and debris in bulk solution are migrated and accumulated to the channels inside the membrane. They block the convection flow through the membrane resulting in the reduction of permeation flux (Park *et al.*, 2015).

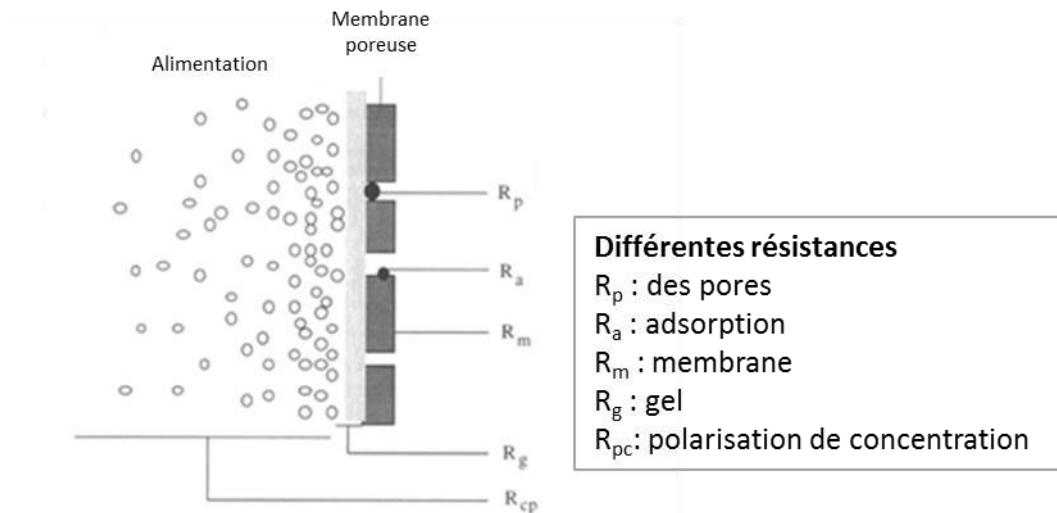


Fig. 1.22. Different resistances including concentration polarization and clogging.

From (Mulder, 1996)

Besides two main parameters, membrane filtration performance is also dependent on other operating parameters such as pressure, temperature, feed rate or agitation. The structural characteristics of the solutes also have direct influence on the membrane separation efficiency, for example, solubility, molecular size. During the experiment, these parameters should be considered to obtain the optimized values.

1.5.2.1.3. Membrane configurations and modules

There are two main flow configurations of membrane process: cross-flow (tangential flow) and dead-end filtrations FIG. 1.23.

In dead-end filtration, the direction of the flow is perpendicular with the surface of the membrane. This configuration is usually applied with low concentration solution or the packing tendency of the filter material does not produce a large pressure drop across the filter medium. Several examples of dead-end filtration are home water filters, vacuum cleaners, oil filters in automobiles.

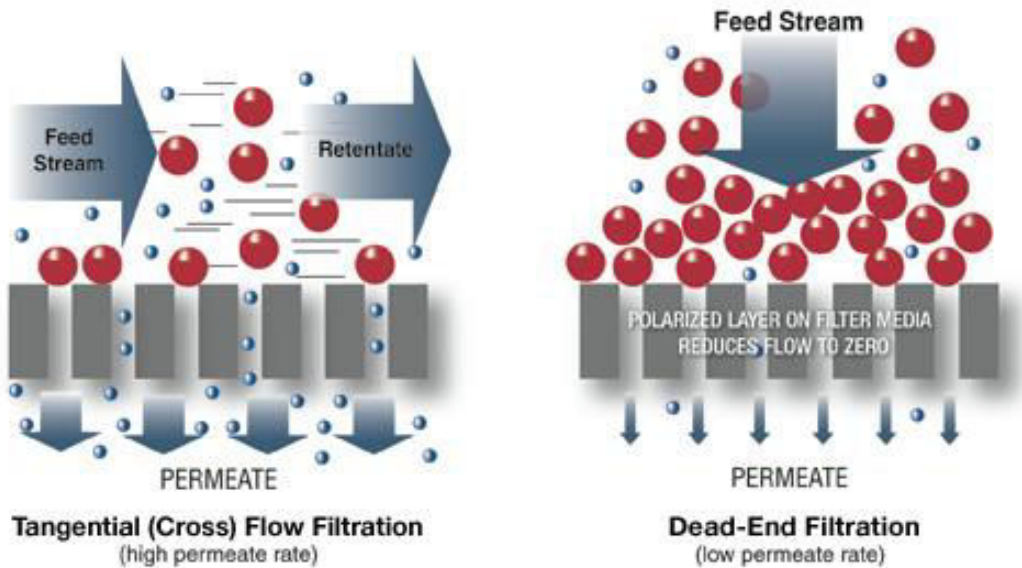


Fig. 1.23. The dead-end and cross-flow geometries

From (Spectrum Labs, n.d.)

In cross-flow filtration, the feed flow is tangential to the surface of the membrane, retentate is removed from the same side of the stream while permeate flow is tracked on the other side of the membrane. The cross-flow geometry is suitable for separation at high concentration of particles or macromolecules such as cells, proteins, and precipitated that rapidly compact on the surface membrane when operated with dead-end mode filter. The tangential flow device is more expensive but they can reduce fouling due to the sweeping effects and high shear rates of the passing flow. The most common modules for industrial uses are flat sheets, spiral wounds and hollow fibers (KOCH Membrane systems, 2012; Xu *et al.*, 2008).

Flat sheets are constructed as thin flat membrane surface to be used in dead-end geometry.

Spiral wound module is a sandwich arrangement of flat membrane sheets as a leaf wound around a central, perforated tube. A leaf consists of two membrane sheets placed back-to-back and separated by a permeate carrier. Three edges of the layers of the leaf are glued, the other edge is sealed around the perforated central tube. A single spiral-wound module may contain up to 20 leaves, each separated by a layer of plastic, which serves as the feed water channel. The purpose of wounding the leaves around the central tube is to create a tangential flow geometry to reduce membrane fouling (Oyama *et al.*, 2011).

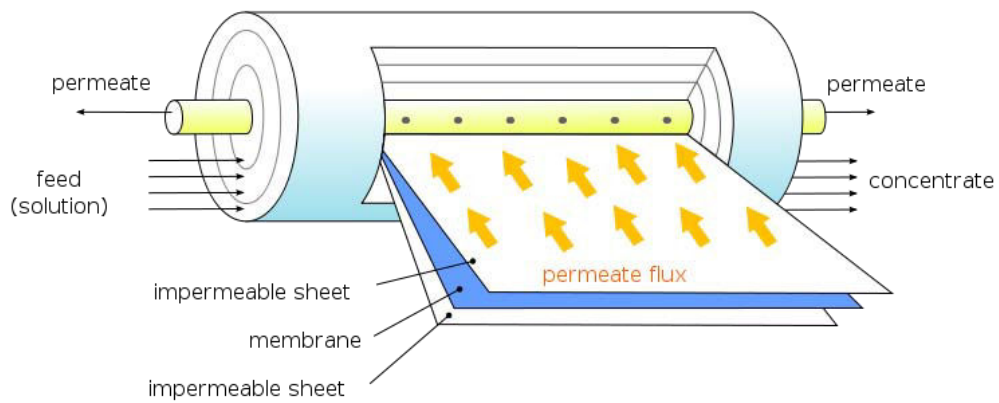


Fig. 1.24. Spiral wound membrane module

From (Oyama *et al.*, 2011)

Hollow fiber modules comprise of hollow fiber membranes, which are long and very narrow tubes. The hollow fiber modules can contain up to 10 000 fibers ranging from 200 to 2500 μm in diameter. The advantage of hollow fiber module compared to other modules is it has large surface area applying on an enclosed solute volume, therefore achieving high separation efficiency. A hollow fiber module can be operated with either “inside-out” or “outside-in” mode. In ‘inside-out’ mode, the separation layer is the inner surface of fiber. The feed water enters the fiber lumen (center or bore of the fiber) and is filtered through the fiber wall. The permeate flows outside of the fibers. The “outside-in” mode means the separation layer is on the outside surface of the fiber. The permeate is collected in the fiber lumen (Xu *et al.*, 2008). The illustration of hollow fiber module is presented in figure below.

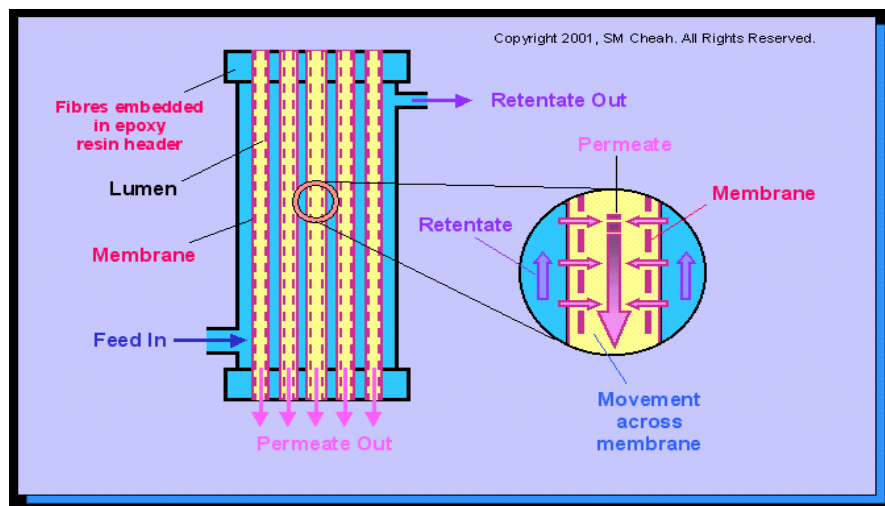


Fig. 1.25. Hollow fiber membrane modules (outside-in mode)

From (Membrane modules)

According to the high efficiency of hollow fiber module, it is selected to use to separate boron-pectin complex from the aqueous solution in this work.

1.5.3. Conclusion

Boron removal from water is usually performed by reverse osmosis or fixation on synthetic resins. Both methods present drawbacks that lead to the development of new methodologies. Among all, the combination of a sorbent to membrane filtration is very promising, either with particulates and microfiltration or polymers and ultrafiltration.

This bibliographic study shows that boron removal could be realized by the combination of a fixation step on a polysaccharide following by an ultrafiltration step to remove the polymers. This approach, called PEUF, is very attractive with a biodegradable polymer that could be applied after filtration in agriculture. Pectin material can be considered as promising polymers because they naturally play a role in plants by fixing boron.

The laboratory works on polysaccharides extraction from plants and has produced two different kinds of extracts from beet pulp, in stirred batch with ammoniac and in continuous conditions with sodium hydroxide. In order to define the conditions for applications of these pectins to boron removal it will be necessary first of all to understand how boron are fixed on industrial resin in batch and continuous conditions. In a second time fixation efficiency of the extracts will be defined and then how pectins can be removed by membrane filtration.

Chapter 2

MATERIAL AND METHODS

2.1. Boron analysis methods

There are plenty of methods for boron determination such as spectrophotometric methods, inometric methods, atomic spectrometric methods, mass spectrometry and nuclear reaction analytical methods. Among all, spectrophotometric method using azomethine-H is the most commonly used. This method is fast, simple, sensitive (detection limit 0.02 mg L^{-1}), high precision (relative standard deviation lower than 4%) (López *et al.*, 1993), and less interfered by other elements such as Fe, Cu, Al, V, Ti, Ta, Zn, W. Moreover, no concentrated acid is employed during color developing reaction like other spectrophotometric methods which usually use high concentrated sulfuric acid (96%) (Sah and Brown, 1997).

2.2. Experiments on batch system

2.2.1. Resins

The 4 resins used for experiments are all polystyrene-based resins. Amberlite IRA 743 (IRA 743), Diaion CRB 03 (CRB 03) are boron selective resins with N-methylglucamine functional group while Ambersep 900-OH and Amberlite IRA 402 Cl (IRA 402 Cl) have quaternary ammonium and trimethyl ammonium functional group, respectively (all purchased from Rohm and Haas Company, USA). Characteristics of these resins are reported in Table 2.1.

All adsorbents were pre-treated prior to use by washing 45 g resin sequentially with 1 L of Milli-Q water twice, NaOH solution at expected pH twice, 30 min for each. The pH and conductivity were measured by using a Mettler Toledo FiveEasy (pH electrode LE438 Mettler Toledo) and conductimeter WTW LF 320, respectively. pH-meter was calibrated every day or before measurement at room temperature with buffer solutions pH 4 and pH 7.

Stock and standard boron solutions were prepared from boric acid (99.99% purification) provided by Sigma Aldrich Company. 1 M NaOH (original in powder 97% purification, VWR) and 0.1 M HNO₃ (original solution of > 65% purification, Sigma Aldrich) were used to adjust pH of boron solutions. All other reagents such as L-ascorbic acid, azomethine-H monosodium salt, ethylenediaminetetraacetic acid (EDTA) was of analytical grade, supplied by Sigma Aldrich Company. Ammonium acetate (NH₄CH₃COO, > 99.8% purification, Sigma Aldrich) was used to prepare buffer solution at pH 4.5.

During the boron analysis, all tubes containing the reaction mixture were covered by aluminum foil to avoid external light that can degrade azomethine - H monosodium salt reagent. 250 mL plastic volumetric flasks were used to contain the mixture of solution and resins during adsorption reaction. HS 501 digital (IKA labortechnik) shaker machine was used to agitate mixture. Absorbance was measured with quartz cuvettes in a UV-1800 model spectrophotometer (Shimadzu Corporation, Japan).

All the solutions were prepared in plastic containers instead of glass because glass materials can contain boron silicate as their component (4% to 12%) and release boron to the solution from glass walls. Milli-Q water was used for diluting chemicals and rinsing stuffs of all experiment.

Table 2.1. Typical chemical and physical characteristics of four resins

Resin #	Physical form	Matrix	Functional group	Total exchange capacity	Particle size	Moisture holding capacity	Maximum operating temperature	Operating pH	Ionic form as shipped	Price and application	Dry resin mass (5.3 g wet resin)
Amberlite IRA 402 Cl	Pale yellow translucent spherical beads	Styrene divinylbenzene copolymer	Trimethyl ammonium	1.2 meq mL ⁻¹ by wetted bed volume	0.60-0.75 mm	49 to 60% (Cl ⁻ form)	60°C	0 - 14	Chloride	Price: 97.8 €/kg (Σ) Application: Treatment water	4.99
Ambersep 900-OH	Pink translucent spherical beads	Styrene divinylbenzene copolymer	Quaternary ammonium	0.8 meq mL ⁻¹ minimum	0.355-1.18 mm	66 to 75% (OH ⁻ form)	60°C	0 - 14	Hydroxide	Price: 152 €/kg (Σ) Application: Pure and drinking water	3.57
Amberlite IRA 743	Beige-coloured spherical beads	Styrene-divinylbenzene (macroporous)	N-methylglucamine	0.7 meq mL ⁻¹	0.500-0.700 mm	48 to 54%	75°C	0 - 14	Free Base (FB)	Price: 244 €/kg (Σ) Application: Pure, drinking, irrigation water	5.14
Diaion CRB 03	Beige-coloured spherical beads	Styrene-divinylbenzene (highly porous)	N-methylglucamine	0.95 meq mL ⁻¹ by wetted bed volume	0.35-0.55 mm	≤ 55%	79°C	0 - 14		Price: 203 €/kg (Σ) Application: Sea, brine water	4.84

2.2.2. Experiment procedures

All the batch experiments were carried out at room temperature (23 °C).

2.2.2.1. Kinetic experiments

Kinetic experiments were carried out with 250 mL plastic Erlenmeyer flasks using 2.0 g wet resin of IRA 402 Cl and 5.3 g of other wet resins. Resin was adjusted to pH 8 by first rinsing twice with Milli-Q water, and then rinsing twice with NaOH pH 8 solution, 30 min/rinsing. A volume of 100 mL of $10.38 \pm 0.84 \text{ mmol L}^{-1}$ (for CRB 03, IRA 402 Cl), and $9.49 \pm 0.14 \text{ mmol L}^{-1}$ (for IRA 743, Amb 900-OH) boron concentration was added into each flask after adjusting its pH to 8. All aqueous solutions were shaken at 260 rpm using shaker. After finishing shaking, each flask was put on the lab bench to settle down the resin on the bottom during 1 min, and then solution was transferred into another plastic beaker. The reaction time was varied from 2 min until 24 h, calculating from adding boron solution on resin until finishing separation.

2.2.2.1. pH effect experiments

Solutions of $9.30 \pm 0.33 \text{ mmol L}^{-1}$ (for CRB 03, IRA 402 Cl), $8.44 \pm 0.14 \text{ mmol L}^{-1}$ (for IRA 743, Amb 900-OH) and $4.59 \pm 0.33 \text{ mmol L}^{-1}$ (for Ambersep 900-OH) boron concentrations were used to investigate the dependence of pH on the adsorption. Resin and solutions were controlled at appropriate pH value by adding NaOH or HNO₃ solutions. A volume of 95 mL (for CRB 03, IRA 402 Cl) and 100 mL (for IRA 743, Amb 900-OH) of each aqueous boron solution was added in flask containing 5.3 g wet resin. Right after, pH was measured in each flask (initial pH). After measuring pH, the suspended mixture was shaken at 260 rpm by the mechanical shaker for 2 h. Then, after the resin was settled down on the bottom of the flasks during 1 min, boron solution and resin was separated manually like in kinetic experiment. The boron solution after adsorption was brought to measure pH (final pH) and determined remaining boron concentration by azomethine-H method. Results were plotted as the relationship between the amounts of sorbed boron with final pH.

2.2.2.2. Isotherm experiments

For the adsorption isotherm experiments, 5.3 g wet of each resin was in contact with 100 mL (Ambersep 900-OH) and 95 mL (IRA 743, CRB 03, IRA 402 Cl) of boric acid solution at concentration range: 4.6, 6.5, 9.3, 18.5, 27.8, 55.5, 92.5 mmol L^{-1} . Both resin and boron solutions were adjusted to pH 8 by adding NaOH or HNO₃ solutions. Samples were continuously mixed by the shaker at 260 rpm for 2 h. Boron solution after adsorption and resin were separated the same way as pH and kinetic experiments.

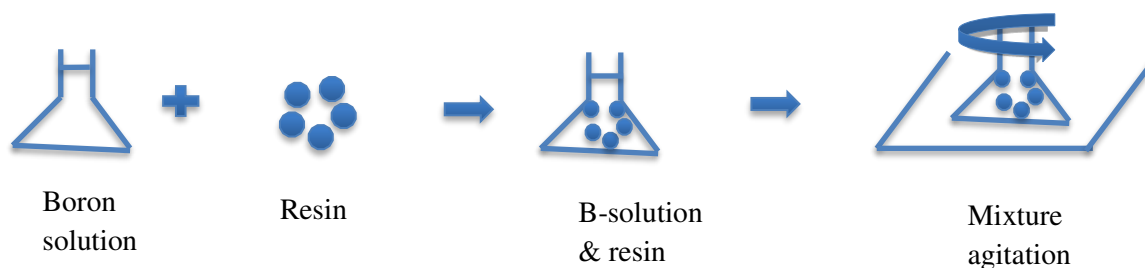


Fig. 2.1. Batch experiment design

2.3. Experiments on column system

2.3.1. Material and experimental set-up

Material

All the chemicals and reagents were prepared by Milli-Q water and stored in plastic containers similar to batch experiments. A plastic graduated cylinder was used to take 100 mL of dry resin. Two resins were used for column experiment: Anionic resin Ambersep 900-OH and boron selective resin Amberlite IRA 743.

Boron solution, NaOH, HNO₃ used to adjust pH of boron solutions and other reagents such as L-ascorbic acid, azomethine-H monosodium salt, ethylenediaminetetraacetic acid (EDTA), ammonium acetate (NH₄CH₃COO, > 99.8% purification, Sigma Aldrich) was of analytical grade. NaCl (99% purity) provided by ESCO - European salt company, was employed to determine pore volume of resin. Besides, H₂SO₄ 72% from Sigma Aldrich is also prepared to use for desorption process of Amberlite IRA 743 resin.

A column with diameter of 5 cm, length of 50 cm was used. A Manostat Vera peristaltic pump (Barnant Company) was utilized to control the flow rate. Boron solution was stored in 10 L plastic cans. Samples were collected in 100 mL plastic bottles, which is rinsed carefully by tap water, then Milli-Q water and dried. A timer was used to measure flow rate of the experiment. Sample was weighed on an OHAUS portable balance after collection. pH meter (Mettler Toledo), a conductimeter (WTW LF 320) are used to follow the pH and conductivity of the samples.

Experimental set-up

Volume of each resin was measured with a graduated cylinder, 100 mL or 400 mL, and the mass was recorded. All the resin was transferred in a beaker and mixed with Milli-Q water, shaking during 15 min. This step was repeated 4 times to eliminate all contaminants. After that, resin was collected and packed all in the column. When the resin bed was correctly packed, all Milli-Q water was exited out of the column, until reaching resin surface.

The resin column was connected to a 10 L feed tank by a peristaltic pump with a variator to control the flow rate. The resin was conditioned to pH 8 before starting experiment.

Table 2.2. Mass and length in column of 100 ml each resin

Resin	Mass (g)	Resin length in column (cm)
Ambersep 900-OH	64.33	6.4
Amberlite IRA 743	75.02	4.5

2.3.2. Experimental procedure

2.3.2.1. Pore volume (V_p) determination

Two concentrations of NaCl were prepared and conditioned to pH 8 (2 L of 0.05 M and 1 L of 0.1 M) were prepared for V_p determination experiment.

In the case of Ambersep 900-OH, V_p determination has been made three times using the same resin dose. The first time, 10 L of NaOH pH 8.30 solution were percolated through the column in order to condition the resin into pH 8. Percolation has been stopped when pH of the solution from the column was stable at 8.55. Then 2 L of the 0.05 M NaCl solution has been flowed at a flow rate of 10 BV h^{-1} . The solution exiting the column was continuously collected in fractions of 3 min. Mass, pH and conductivity were measured on each sample. Characteristics of the solutions are presented in TABLE 2.3.

Table 2.3. Properties of the sodium chloride solutions before elution

Concentration	pH	Conductivity ($mS\ cm^{-1}$)
NaCl 0.05 M	8.8 (after exp: 6.9)	14.5 (after exp: 15.0)
NaCl 0.1 M	9.0 (after exp: 7.3)	23.3 (after exp: 28.9)

The second time, 1 L of 0.1 M NaCl solution was continued to percolate through the previous resin dose using the same flow rate (1 L h^{-1}) in order to re-equilibrate the resin in the column. After that, 2 L of 0.05 M NaCl solution was again flowed through the column until reaching the equilibrium, so from this step the second V_p was determined. The third time, 1 L of 0.1 M NaCl solution was passed through the same resin bed with the same flow rate (1 L h^{-1}) in the column. Consequently, the third V_p was calculated from experimental data.

To desorb NaCl, 10 L of NaOH pH 8 and 2 L of pH 13 (0.1M) NaOH was used to pass through the column at the flow rate of 10 BV h^{-1} . The samples were collected and measured pH and conductivity. When these values reached values of the original NaOH solution, column was continued to rinse and conditioned by pH 8 NaOH solution.

In the case of Amberlite IRA 743, resin was conditioned with pH 8.3 NaOH solution. 2 L 0.05 M NaCl and 1 L of 0.1 M NaCl were prepared at pH 8 and the percolation was managed at flow rate of 30 BV h⁻¹ (3 L h⁻¹). Sample was collected each 30 seconds, weighed, and immediately measured pH and conductivity. To elute NaCl, 4 L of 0.5 M H₂SO₄ and 4 L of 0.25 M NaOH were run through the column at the same flow rate, respectively. Samples were collected, weighed, and measured pH and conductivity. The desorption stopped when samples got pH and conductivity values similar to those of feed solution. The bed resin was rinsed by Milli-Q water and reconditioned to pH 8 by pH 8 NaOH solution.

2.3.2.2. Boron adsorption experiment

Boron experiments on Ambersep 900-OH resin have been done with two bed volume sizes, 100 mL and 400 mL, while it was only 100 mL with Amberlite IRA 743. Adsorption was managed by the percolation of different boron concentration solutions (20 and 100 mg L⁻¹) through the column at the different flow rates (10, 16 and 60 BV h⁻¹). Then desorption was performed in two steps. For Ambersep 900-OH resin, column was first rinsed with pH 8 NaOH solution, then, boron was continued to elute with pH 13 NaOH solution. For Amberlite IRA 743, the resin was first rinsed by 0.5 M H₂SO₄, and then regenerated by 0.25 M NaOH solutions. At the end, both resins were reconditioned in pH 8 NaOH solution for further experiments.

Samples were continuously collected during each phase, every minute for a flow rate of 60 BV h⁻¹, every 10 min for the flow rate of 16 BV h⁻¹, every 3 minutes for a flow rate of 10 BV h⁻¹. Mass, conductivity and pH was measured immediately while boron concentration was determined by azomethine – H method after the end of each phase (adsorption, rinse and elution).

All the tested conditions that have been performed are presented in .

Table 2.4. Boron adsorption column experiment planning

Resin	[B] (mg L ⁻¹)	Flow rate (BV h ⁻¹)	Adsorption by	Desorption by
Amb 900-OH	100	16		
	20	60	Boric acid pH 8	NaOH pH 8 & pH 13
	100	10		
	20	10		
Amb IRA 743	100	60		
	100	10	Boric acid pH 8	0.5 M H ₂ SO ₄ & 0.25 M NaOH

2.4. Experiments on hybrid system

The hybrid system is the combination of an adsorption step of the boron on pectin extract powder followed by a water/pectin separation process by ultrafiltration.

2.4.1. Material

The two types of pectin evaluated have been produced in the laboratory. The first one (batch extracted pectin) has been produced from beet pulp in batch reactor in ammoniac conditions (Jorda, 2003) while the second one (twin-screw extracted pectin) has been produced by twin-screw extrusion with sodium hydroxide (Mogni, 2015).

The composition of these pectin extract powders, in sugars and galactorunic acid, were determined. An acid hydrolysis and HPLC analytical process was used, according to the NREL method. Hydrolysis was performed in pressured tube in a water bath with Teflon stir rod. Neutralization was achieved with CaCO_3 powder (Merk Chemicals). Centrifugation machine 6-16K Sigma centrifuge (Osteode, Gemany) is used to separate sample mixture and 0.2 μm filter and autosampler vials are used for sample injection in HPLC machine (Varian). Standard sugars, glucose, arabinose, xylose, arabinose (Sigma Aldrich), galactose (VWR), galacturonic acid (Fluka Chemie), were prepared to determine the samples concentration.

To determine viscosity of the pectin extract solution, a capillary a viscometer (CANNON No. 75) was employed. A water bath accompanying with a heat control system and a thermometer were utilized to keep the temperature of water bath as constant at 40 °C.

To study the pectin filtration efficiency of the using membranes, two kinds of ultrafiltration apparatus were used. At the first time, a stirred ultrafiltration cell (Amicon), with a volume of 100 mL, was employed for the screening of the membranes. A gauge, on the pressured air feed, controlled the pressure cell while a mixer is used to limit the creation of a polarization layer. Three types of flat sheet membranes with a MWCO of 10, 30, 100 kDa (Millipore) were studied.

At the second time, filtration was performed at a larger scale with a polyethersulfone membrane with a MWCO of 30 kDa (Ge Healthcare) with a filtration area of 0.085 m². This membrane was hollow-fiber type and the fibers had an internal diameter of 0.5 mm and a length of 60 cm and the module contained 50 fibers. Filtration was done by recycling both permeate and retentate to maintain constant concentration in the feed tank. Different trans-membrane pressures, from 0.4 to 2 bars, were tested with the same solution. At each pressure, mass flux was recorded until getting steady state. A sample was taken at each steady condition for further analysis. This ultrafiltration module was used with a tri-piston pump, a valve to control the pressure and pressure gauges on

feed, retentate and permeate. Both retentate and permeate was recycled in the 5 L feed tank in order to work under steady state conditions.

2.4.2. Experimental procedure

2.4.2.1. Pectin characterization

Pectins have been characterized according to the NREL protocol defined for sugar analysis in lignocellulosic plant. The procedure includes a polymer hydrolysis step, followed by an HPLC analysis step.

2.4.2.1.1. Pectin hydrolysis

300.0 ± 10.0 mg of dry pectin were weighed in a pressure tube. 3.00 ± 0.01 mL 72% sulfuric acid was added in each pressure tube (sample & blank). Mixture was mixed using Teflon stir rod during 1 min. Pressured tubes were introduced in a water bath set 30 ± 3 °C during 60 ± 5 min. Every five minutes the sample was stirred without removing it out of the bath. This step was essential to get a uniform hydrolysis. After removal from water bath, 84.00 ± 0.04 mL Milli-Q water was added in order to dilute to 4% acid and the tube covered by a Teflon cap. The tubes were placed in an autoclave for one hour at 121 °C and then allowed to slowly cool to near room temperature before removing the caps.

A sugar recovery standards (SRS) set was prepared in order to correct for losses due to destruction of sugars during dilute acid hydrolysis. SRS should include, D-(+)glucose, D-(+)xylose, D-(+)galactose, L-(+)arabinose, D-(+)mannose. SRS sugar concentrations has been chosen to most closely similar concentrations of sugars in the evaluated samples. The SRS set was submitted to the same treatment than the samples.

2.4.2.1.2. Sugar and galacturonic acid analysis

20 mL of the hydrolyzed liquor was transfer in a 50 mL Erlenmeyer flask and CaCO₃ powder was added to neutralize the sample to pH 5 – 6. After decantation of the insoluble salts, the liquid was filtered through a 0.2 µm filter into an autosampler vial. This solution was used as the sample for HPLC analysis.

50 µL of sample was injected in the HPLC system (Varian) composed of a polar column (Phenomenex Rezex RHM H⁺). Sample was eluted with 0.005 M H₂SO₄ mobile phase at flow rate of 0.6 mL min⁻¹ and a column temperature of 65 °C. Detection was performed by refractive index. Analysis duration is 50 min, and each sample was analyzed in triplicate. A series of calibration standards have been prepared (TABLE 2.5).

Table 2.5. Suggested concentration ranges for calibration standards

Component	Suggested concentration range (mg mL ⁻¹)
D-cellobiose	0.1-4.0
D(+)glucose	0.1-4.0
D(+)xylose	0.1-4.0
D(+)galactose	0.1-4.0
L(+)arabinose	0.1-4.0
D(+)mannose	0.1-4.0
CVS	Middle of linear range, concentration not equal to a calibration point

2.4.2.1.3. Viscosity measurement

Diluted pectin solution viscosity was measured with a capillary a viscometer (CANNON No. 75) while the non-Newtonian parameters have been defined for high concentration solutions. The kinetic viscometer was measured at 40 °C in a water bath and pectin solution was collected before and after filtration.

As polarization concentration could appear leading to high concentrations at the membrane surface, solutions with a concentration of 20 g L⁻¹ and 40 g L⁻¹ was prepared. Rheological properties of these solutions were measured with a disk viscometer (MC301, Anton Paar).

2.4.2.2. Boron fixation on hybrid method

2.4.2.2.1. Ultrafiltration evaluation on Amicon cell and hollow-fiber system

At small scale (Amicon cell), permeability of the three flat sheet membranes (10, 30, 100 kDa) was evaluated with water by measuring the permeate flux at different pressure. Then filtration efficiency has been characterized with batch extracted pectin solution at 1 bar pressure and different stirring rates. Pectin extract solution was prepared by adding 5 g of pectin extract powder into 100 mL Milli-Q water in an Erlenmeyer flask, then agitated in 2 h at 260 rpm. The mixture then was introduced in the filtration cell. Pressure was adjusted with the valve to the desire value. Permeate was continuously recovered, leading to the reduction of the volume of the solution remaining in the cell and therefore to the concentration of the retained molecules. Filtration was managed with membrane of 0.003 m² of filtration area. Samples were regularly taken in order to follow the evolution of the membrane performance. Mass of each sample was measured in order to get a mass flux. As the permeate flux was low, the recovered mass was very low compare to the initial volume and it has been assumed that there was no change in pectin concentration. Tests were done at different transmembrane pressures with all types of membranes.

At larger scale (hollow fiber system) filtration was done by recycling both permeate and retentate to maintain constant the concentration in the feed tank. It is therefore possible to reach pseudo-steady state. Different transmembrane pressures, from 0.4 to 2 bars, were tested with the same solution. At each pressure, mass flux was recorded until getting the steady state. A sample was taken at each steady condition for further analysis.

2.4.2.2.2. Boron fixation at different pH

2.4.2.2.2.1. Pectin with Milli-Q water

This experiment was designed to determine how much boron was already stored by pectin extract. 100 mL Milli-Q water was introduced in each Erlenmeyer flask. pH of each solution has been adjusted using sodium hydroxide or nitric acid to get pH from 2 to 12. 2.0 g of dry batch extracted pectin or 0.5 g of dry twin-screw extracted pectin was added and the flasks were then agitated during 2 h at 260 rpm using HS 501 digital (IKA labortechnik) agitation machine. pH measurement was performed before mixing in order to get the initial pH and after 2 h, the solution pH was measured in order to get final pH. Each sample was then centrifuged during 15 min at 8000 rpm using centrifugation machine 6-16 K (Sigma), $T = 20\text{ }^{\circ}\text{C}$. The solution was separated from the residues in centrifugation tubes, then filtered using a syringe and PTFE 0.45 μm filter. The solution after filtration was brought to determine non-fixed boron in pectin.

2.4.2.2.2.2. Pectin with boron solution

100 mL of 100 mg L^{-1} boron solution was introduced in each Erlenmeyer flask. pH of each solution has been adjusted using sodium hydroxide or nitric acid to get pH from 2 to 12. 2.0 g of dry batch extracted pectin or 0.5 g of dry twin-screw extracted pectin was added. pH measurement was performed before mixing in order to get the initial pH. Similar procedure was repeated as in experiment between pectin and water. Final pH and filtered solution was obtained to determined boron concentration.

All the chemicals using for all experiments in this thesis have been listed in the table below.

Table 2.6. List of chemicals

Chemicals	Providers
Amb 900-OH, IRA 743, IRA 400 Cl, CRB 03	Rohm and Haas – Dow company
Ammonium acetate (> 99.8% purity)	Sigma Aldrich
Azomethine-H monosodium salt,	Sigma Aldrich
Batch extracted pectin	LCA
Boric acid (99% purity)	Sigma Aldrich
CaCO ₃ powder	Merk Chemicals
Ethylenediaminetetraacetic acid (EDTA),	Sigma Aldrich
Galactose	VWR
Galacturonic acid	Fluka Chemie
Glucose, arabinose, xylose, arabinose	Sigma Aldrich
H ₂ SO ₄ 72%	Sigma Aldrich
HNO ₃ (Solution of > 65% purity)	Sigma Aldrich
L-ascorbic acid	Sigma Aldrich
NaCl (99% purity)	ESCO
NaOH (powder, 97% purity)	VWR
Polyethersulfone membrane (10, 30, 100 kDa)	GE Healthcare
Twin-screw extracted pectin	LCA

Chapter 3

BORON FIXATION ON SYNTHETIC RESINS WITH BATCH-MODE SYSTEM

(This chapter corresponds to a manuscript which has been submitted to *Desalination*)

3.1. Introduction

Boron is an element, which is necessary as nutrient for living organisms, especially for plants where it is involved in cell wall composition. But its excess can cause some health or ecotoxicological problems. The main bad influences are on the development of plants, humans and animals such as nausea, diarrhea, dermatitis, lethargy and defoliation, decay and fall unripe fruits (Murray, 1995; Melnyk et al., 2005). In particular, mammalian organisms, which have excessive boron, are suffered from problems of cardiovascular, coronary, nervous and reproductive systems. Boron toxicity also changes blood composition, caused disorder in neurological, physical, intellectual development (Wolska and Bryjak, 2013). As the result, the World Health Organization (WHO) has recommended a guideline of 0.5 mg L^{-1} B in drinking water and a maximum limit of 0.3 mg L^{-1} B in fresh water used for irrigation (WHO, 1998; WHO, 2011). The increasing use of boron in industries and its discharge to the environment has led to the contamination of not only surface water but also of ground water (Davidson and Bassett, 1993; Barth, 1998; Devirian and Volpe, 2003; Pennisi *et al.*, 2006; Kot, 2008; Grassi *et al.*, 2014). On the other hand, due to the shortage of fresh water sources, mainly in countries where fresh water is missing or population is strongly increasing, seawater desalination has been becoming an alternative fresh water supply. However, the presence of boron in seawater is quite high (5 mg L^{-1}) (Tu *et al.*, 2010).

Boron removal from fresh water or seawater would be a prerequisite to produce water having the standard guideline levels as recommended by WHO. Several separation technologies are often used such as adsorption, precipitation, coagulation, reverse osmosis, solvent extraction and ion exchange (Simonnot *et al.*, 2000; Wolska and Bryjak, 2013; Tagliabue *et al.*, 2014). Reverse osmosis (RO) and adsorption processes are the most extensively used, particularly in desalination plants because of high efficiency up to 99% for RO for pH higher than 10 (Simonnot *et al.*, 2000; Glueckstern and Priel, 2003).

Boron speciation in water depends on the acid-base reaction, with $\text{pK}_a = 9.2$:



This means that the boron species is mainly the neutral H_3BO_3 form at pH below 9.2 (Woods, 1994). At such conditions, it is necessary to pre-treat the water by increasing pH with alkaline solution addition to be efficient with reverse osmosis (Glueckstern and Priel, 2003). Acid needs to be added after filtration to decrease pH to acceptable pH (6.5 – 8.5) for drinking or irrigation water, which is a strong limitation from the point of view of application. Boron adsorption is therefore widely used in water production. The most common materials used for boron adsorption are either anionic or specific resins. The specific resins have three or more hydroxyl groups, which are located in cis position. Strong chelate complexes are formed between boric acid and/or borate present in solution and the surface sites of the resins as described in FIG. 3.1 (Smith *et al.*, 1999; Wolska and Bryjak, 2013).

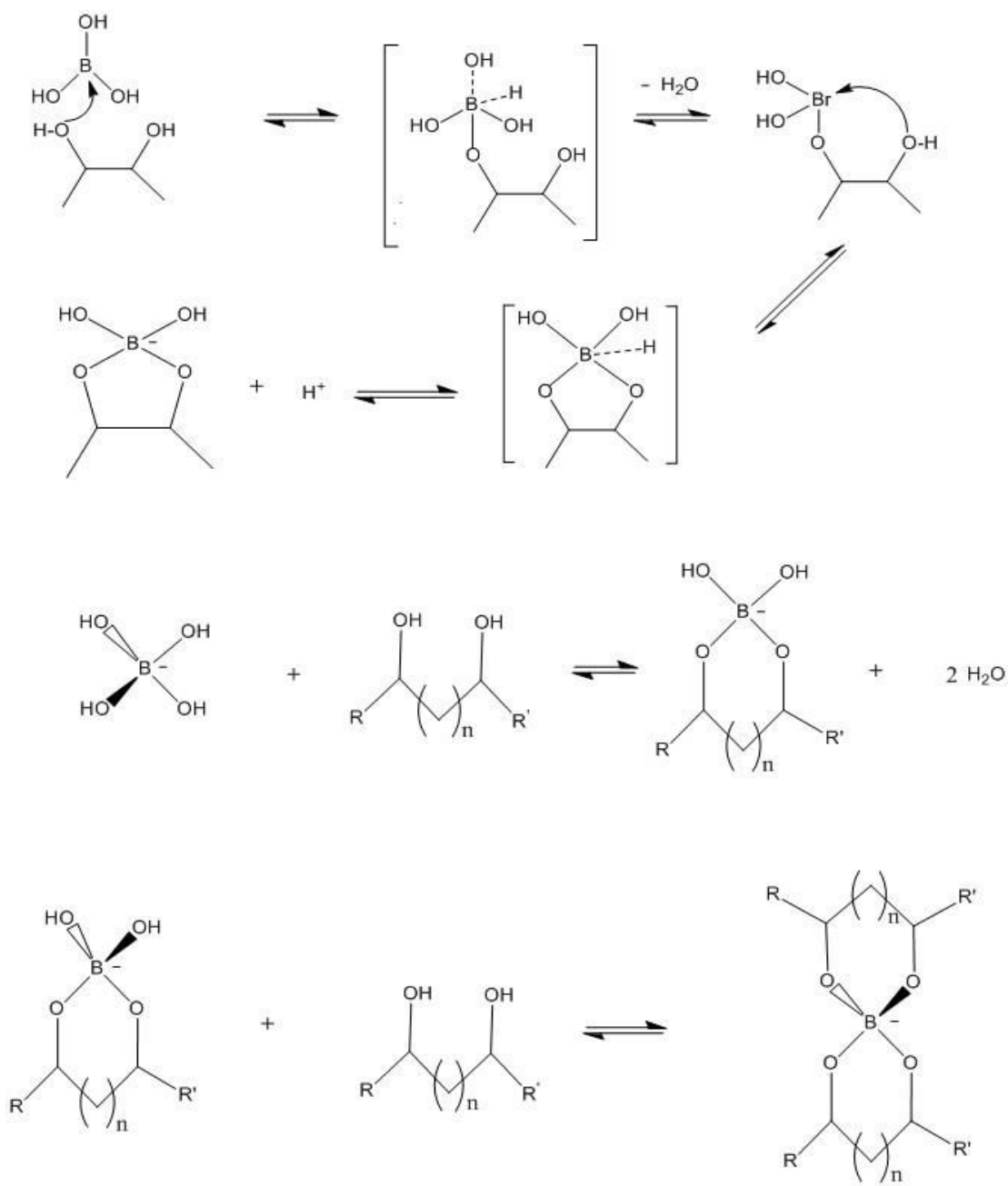


Fig. 3.1. Proposed mechanisms for the binding of boron by chelating resins

Adapted from (Smith *et al.*, 1999; Wolska and Bryjak, 2013)

Different authors have studied the kinetics and mechanisms of fixation of boron on different resins. Adsorption equilibrium can be obtained within 180 min in batch shaken condition with the specific resin Diaion CRB 02. The kinetics has been well described by pseudo-second order rate law (Kabay *et al.*, 2008). These authors (Kabay *et al.*, 2007) have reported that the removal efficiency increases when particle size decreases since the diffusion rate is improved due to the increase in the adsorption surface area. The retention has been described as a surface complexation reaction between two vicinal hydroxyl groups with the boric acid and borate. Other works have showed that

the adsorption isotherm fit well with linear relationship of Langmuir-type mechanism for three materials such as the CRB 03, CRB 05 resins and Chelest fiber (Chelest Fiber® GRY-HW) (Nishihama *et al.*, 2013). But it is important to remind that Langmuir-type reaction means reversibility of sorption, which has been shown to be not always the case (Simonnot *et al.*, 2000).

Anionic resin has not been much studied because it has been often considered to be inefficient at pH below 9, which is high pH value compare to the pH range of natural fresh or marine waters. Indeed, in most of natural waters, the most predominant species of boron is boric acid, which is not favorable for ion exchange process. Anionic resins are positively charged at their surface. Anions can exchange with other anions such as borate present in the aqueous solution. Experiment has been done with the Dowex 2x8 chloride (Köse and Öztürk, 2008; Öztürk and Köse, 2008), which is a strong basic anion exchanger. It does not contain N-methylglucamine (FIG. 3.2) like boron selective resins but OH⁻ groups, which are located on the functional groups. Maximum adsorption has been observed at pH 9 but the efficiency is rather low, 60% for the given experimental conditions [600 mg L⁻¹, 1 g of dry resin, 50 mL solution, contact time: about 8 h] (Öztürk and Köse, 2008). In order to get pH 9, NaOH has to be added to increase the solution pH, and then enhance boron sorption due to an improvement of borate ions. pH modification by chemical addition has the problem of increasing the treatment cost.

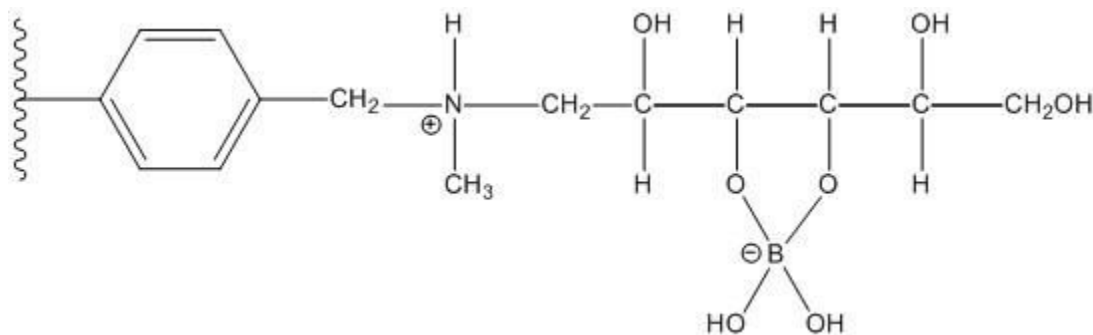


Fig. 3.2. N-methylglucamine group

Adapted from (Wolska and Bryjak, 2013)

Since boron removal from sea water or contaminated surface waters has been becoming very crucial due to its potential effect in the environment at high concentration, investigation of efficient materials for removal of boron at low cost is being more and more concerned. As reported above, two types of resins, *i.e.* anionic and selective ones can be used. The aim of our work was thus to compare the behavior of the two types of resins with respect to their retention capacity. Heading to this objective, experiments were performed to study and compare the mechanisms of boron surface exchange *vs.* time and at equilibrium depending on physicochemical parameters such as contact time, pH, initial boron concentration, using batch system with the set of resins.

3.2. Sorption kinetic and isotherm theory

Kinetic models

Several kinetic models can be used to predict the mechanism of sorption processes such as Lagergren pseudo-first order, the pseudo-second order of equation and parabolic diffusion model (Stone and Morgan, 1990; Ho and McKay, 1999; Öztürk and Kavak, 2005). Among them, the pseudo-first and pseudo-second order models are the most frequently used (Stone and Morgan, 1990; Kabay *et al.*, 2007; Sigg *et al.*, 2014; Yang *et al.*, 2014).

The pseudo-first order rate equation of Lagergren has been applied in the cases of diffusion through a boundary liquid film and adsorption kinetics as a chemical phenomenon. If film diffusion is rate controlling, the constant of the equation will vary inversely with the particle size and the film thickness. If the exchange is chemically rate controlled, the constant of the equation will be independent of particle diameter and flow rate and will depend only on the concentrations of the ions in solutions (Stone and Morgan, 1990; Ho and MacKay, 1999).

The pseudo-first order model is based on the following equation:

$$\frac{dq_t}{dt} = k_1(q_e - q_t) \quad \text{EQ 3.2}$$

where q_t and q_e represent the amounts of boron adsorbed (mmol g^{-1}) at time t and equilibrium, respectively; k_1 is the sorption rate constant (min^{-1}); q_e is estimated by taken the maximum value of experimental data.

Equation EQ 3.2 can be re-written as:

$$\frac{dq_t}{(q_e - q_t)} = k_1 dt \quad \text{EQ 3.3}$$

Taking the integral of EQ 3.3 with respect to the boundary conditions:

$q = 0$ when $t = 0$, and

$q = q_t$ when $t = t$,

we obtained the following relationship:

$$\log(q_e - q_t) = \log(q_e) - \frac{k_1}{2.303} t \quad \text{EQ 3.4}$$

Sorption rate constant k_1 (min^{-1}) can be estimated by plotting $\log(q_e - q_t)$ with time.

Multiple pseudo-first order kinetics has been used in some sorption systems such as protein silica (Ho and McKay, 1999). Basically, it means that a plot of $\ln(q_e - q_t)$ vs. time can be divided into two or three linear sections, each linear section meaning a pseudo-first order reaction mechanism. One

step is assumed to correspond to the initial binding of the molecules with the active site of the solid surface by removal or organization of surface bound water. The other step represents the denaturation and reorganization of the bound polymer (Ho and McKay, 1999). In the case of two kinetic steps, the first sorption step is faster than the second one. The sorption rate is controlled by either film diffusion or an intraparticle diffusion mechanism. Intraparticle diffusion was found to be a rate limiting step following the pseudo-first order sorption rate expression of Lagergren (Ho and Mac Kay, 1999).

The pseudo-second order kinetics is described as follows:

$$\frac{dq_t}{dt} = k_2(q_e - q_t)^2 \quad \text{EQ 3.5}$$

where q_t and q_e represent the amounts of boron adsorbed (mmol g^{-1}) at time t and equilibrium, respectively; k_2 is the sorption rate constant ($\text{g mmol}^{-1} \text{min}$). Rearranging the variables in the equation EQ 3.5 and integrating in the boundary as above, one gets:

$$q_t = \frac{k_2 q_e^2 t}{1 + k_2 q_e t} \quad \text{EQ 3.6}$$

Parameters can be estimated either by non-linear regression by using dedicated software or by re-writing equation EQ 3.6 as the reverse ratio of both sides multiplied then by t . In the latter case, it comes:

$$\frac{t}{q_t} = \frac{1}{k_2 q_e^2} + \frac{1}{q_e} t \quad \text{EQ 3.7}$$

The sorption rate constant k_2 ($\text{g mmol}^{-1} \text{min}$) and q_e (mmol g^{-1}) can be calculated by plotting q_t with t .

Sorption isotherm models

The Langmuir model (Langmuir, 1918): has been developed to study the equilibrium at gas-solid interface. Owing to similar shaped isotherms, this model has been extended for probing the sorption phenomenon at liquid-solid interface (Stumm, 1992). Some mathematic relationships have been adopted for fitting the experimental data (Sigg *et al.*, 2014). Monolayer adsorption between liquid and solid phases is usually described by Langmuir-type isotherm model with the following assumptions (Farley *et al.*, 1985; Sontheimer *et al.*, 1985; Sigg *et al.*, 2014)

- Homogeneous surface sites (same energy)
- Each site can occupy at most one molecule (all sites are identical and equivalent)
- No repulsion or attraction due to molecules already adsorbed
- A maximum of a monolayer can be formed at the surface of the adsorbent

The adsorption process can be expressed as follow:



where A is solute, =S is for surface sites, =S-A the adsorbate occupying one surface site.

The Langmuir-type coefficient (K_L) is expressed as (Sigg *et al.*, 2014):

$$K_L = \frac{\{=S-A\}}{[A]\{=S\}} \quad \text{EQ 3.9}$$

The total surface site is expressed as:

$$S_{\text{tot}} = \{=S\} + \{=S-A\} \quad \text{EQ 3.10}$$

Using equation EQ 3.9 and EQ 3.10, it comes:

$$\{=S-A\} = S_{\text{tot}} \frac{K_L[A]}{1 + K_L[A]} \quad \text{EQ 3.11}$$

with [A] is solute concentration in aqueous solution at equilibrium (mol L^{-1}), $\{=S-A\}$ the concentration of solute adsorbed on the resin at equilibrium (mol g^{-1}), S_{tot} the total adsorption capacity (or total surface site concentration) (mol g^{-1}), and K_L the Langmuir-type coefficient (L mol^{-1}).

As shown in Sigg *et al.* (2014) and Charrière *et al.* (2015), the Langmuir-type relationship can be deduced from physical-chemical reactions at solid-liquid interfaces such as surface complexation or ionic exchange reactions.

BET sorption model: Multilayer adsorption has been often described by Brunauer-Emmett-Teller isotherm (BET) (Brunauer *et al.*, 1938). It has been applied for liquid-solid interface (Foo and Hameed, 2010) as BET-type isotherm, especially if surface precipitation is assumed to occur at the solid-liquid interface (Farley *et al.*, 1985; Lützenkichen, 1996; Sigg *et al.*, 2014).

$$q_e = \frac{q_s K_{\text{BET}} C_e}{(C_s - C_e) \left[1 + (K_{\text{BET}} - 1) \left(\frac{C_e}{C_s} \right) \right]} \quad \text{EQ 3.12}$$

where K_{BET} is the BET-type coefficient (-), C_e the solute concentration in aqueous at equilibrium (mol L^{-1}), q_e the solute concentration on resin (mol g^{-1}), C_s the solute monolayer saturation concentration (mol L^{-1}), and q_s the equilibrium adsorption capacity (mol L^{-1}).

As K_{BET} and $K_{\text{BET}} (C_e/C_s)$ are usually much greater than 1, equation EQ 3.12 becomes:

$$q_e = \frac{q_s}{1 - \left(\frac{C_e}{C_s} \right)} \quad \text{EQ 3.13}$$

For both models, different ways can be used for parameter estimation, either by linearizing equation or by using specific software dedicated to solve non-linear equations.

3.3. Material and methods

3.3.1. Materials

The 4 resins used for experiments are all polystyrene-based resins. Amberlite IRA 743 (IRA 743), Diaion CRB 03 (CRB 03) are boron selective resins with N-methylglucamine functional group while Ambersep 900-OH and Amberlite IRA 402 Cl (IRA 402 Cl) have quaternary ammonium and trimethyl ammonium functional group, respectively (all purchased from Rohm and Haas Company, USA). Characteristics of these resins are reported in Table 2.1. All adsorbents were pre-treated prior to use by washing 45 g resin sequentially with 1 L of Milli-Q water twice, NaOH solution at expected pH twice, 30 min for each. The pH and conductivity were measured by using a Mettler Toledo FiveEasy (pH electrode LE438 Mettler Toledo) and conductimeter WTW LF 320, respectively. pH-meter was calibrated every day or before measurement at room temperature.

Stock and standard boron solutions were prepared from boric acid (99.99% purification) provided by Sigma Aldrich Company. 1 M NaOH (original in powder 97% purification, VWR) and 0.1 M HNO₃ (original solution of > 65% purification, Sigma Aldrich) were used to adjust pH of boron solutions. All other reagents such as L-ascorbic acid, azomethine-H monosodium salt, ethylenediaminetetraacetic acid (EDTA) were of analytical grade, supplied by Sigma Aldrich Company. Ammonium acetate (NH₄CH₃COO, > 99.8% purification, Sigma Aldrich) was used to prepare buffer solution at pH 4.5. Suspension solutions were shaken by a HS 501 digital (IKA Labortechnik) shaker during adsorption process.

All flasks and containers used were polypropylene plastic because glass materials can contain boron silicate as their component (4% to 12%) and release boron to the solution from glass walls.

3.3.2. Methods

All the batch experiments were carried out at room temperature (23 °C).

3.3.2.1. Kinetic experiments

Kinetic experiments were carried out with 250 mL plastic Erlenmeyer flasks using 2.0 g wet resin of IRA 402 Cl and 5.3 g of other wet resins. Solution containing resin was adjusted to pH 8 by first rinsing twice with Milli-Q water, and then rinsing twice with NaOH pH 8 solution, 30 min/rinsing. A volume of 100 mL of 10.38 ± 0.84 mmol L⁻¹ (for CRB 03, IRA 402 Cl), and 9.49 ± 0.14 mmol L⁻¹ (for IRA 743, Amb 900-OH) boron concentration was added into each flask after adjusting its pH to 8. All aqueous solutions were shaken at 260 rpm using shaker. After finishing shaking, each flask was put on the lab bench to settle down the resin on the bottom during 1 min, and then solution was transferred into another plastic beaker. The reaction time was varied from 2 min until 24 h, calculating from adding boron solution on resin until finishing separation.

3.3.2.2. pH effect experiments

Solutions of $9.30 \pm 0.33 \text{ mmol L}^{-1}$ (for CRB 03, IRA 402 Cl), $8.44 \pm 0.14 \text{ mmol L}^{-1}$ (for IRA 743, Amb 900-OH) and $4.59 \pm 0.33 \text{ mmol L}^{-1}$ (for Ambersep 900-OH) boron concentrations were used to investigate the dependence of pH on the adsorption. Resin and solutions were controlled at appropriate pH value by adding NaOH or HNO₃ solutions. A volume of 95 mL (for CRB 03, IRA 402 Cl) and 100 mL (for IRA 743, Amb 900-OH) of each aqueous boron solution was added in flask containing 5.3 g wet resin. Right after, pH was measured in each flask (initial pH). After measuring pH, the suspended mixture was shaken at 260 rpm by the mechanical shaker for 2 h. Then, after the resin was settled down on the bottom of the flasks during 1 min, boron solution and resin was separated manually like in kinetic experiment. The boron solution after adsorption was brought to measure pH (final pH) and determined remaining boron concentration by azomethine-H method. Results were plotted as the relationship between the amounts of sorbed boron with final pH.

3.3.2.3. Isotherm experiments

For the adsorption isotherm experiments, 5.3 g wet of each resin was in contact with 100 mL (Ambersep 900-OH) and 95 mL (IRA 743, CRB 03, IRA 402 Cl) of boric acid solution at concentration range: 4.6, 6.5, 9.3, 18.5, 27.8, 55.5, 92.5 mmol L⁻¹. Both resin and boron solutions were adjusted to pH 8 by adding NaOH or HNO₃ solutions. Samples were continuously mixed by the shaker at 260 rpm for 2 h. Boron solution after adsorption and resin were separated the same way as pH and kinetic experiments.

All the sorbed boron concentrations are expressed in mol per g of dry resin.

3.3.3. Boron analysis

The boron analysis was performed spectrophotometrically using azomethine-H method (Spencer and Erdmann, 1979). Boron standard solutions (0.046, 0.093, 0.19, 0.28, 0.37, 0.46 mmol L⁻¹) were prepared from 92.5 mmol L⁻¹ boron stock solution. A 0.01 M azomethine-H solution was prepared by dissolving 0.45 g azomethine-H into 100 mL 1% (w/w) ascorbic solution. A buffer solution of pH 4.5 was prepared by dissolving 50 g NH₄CH₃COO in 100 mL Milli-Q water, 100 mL of CH₃COOH and adding 3.0 g EDTA sodium salt. The color development reaction was carried out by adding 1 mL of standard solution (Milli-Q water for blank) or samples, 2 mL of azomethine-H and 2 mL of acetate buffer, shaking in 10 s, and then waiting for the reaction 1 h. Wavelength of 410 nm was used to measure the absorbance of sample by means of UV-1800 model spectrophotometer (Shimadzu Corporation, Japan). All dilutions were made using plastic flasks and pipets. With high concentration sample from 9.25 mmol B to 92.51 mmol B, adsorbed samples were diluted by Milli-Q water to the linear range.

Error bars are used on the graph to indicate the uncertainty in the measurement. It gives us the idea of how far from the reported value the true value might be, or in other words, error bars show the accuracy of the reported measurement. Error bars are usually calculated by dividing standard deviation, s , by the square roots of the measurements number. Reproducibility or precision indicates the experiments are repeated under unchanged condition and give the similar results. The limit of detection (LOD) is the smallest quantity of analyte that is significantly different from the blank, which is analyte-free. Limit of quantitation (LOQ) is the smallest amount of analytes that can be measured with reasonable accuracy (IUPAC, 1987) . LOD and LOQ are determined according to the formulas in EQ 3.14 and EQ 3.15 below.

Minimum detectable concentration:

$$LOD = \frac{3s}{m} \quad \text{EQ 3.14}$$

Lower limit of quantitation:

$$LOQ = \frac{10s}{m} \quad \text{EQ 3.15}$$

where s is standard deviation from the signal of the blank, and m is the slope of calibration curve.

According to calibration curves, LOD and LOQ were 0.015 mg L^{-1} ($0.0014 \text{ mmol L}^{-1}$) and 0.050 mg L^{-1} ($0.0046 \text{ mmol L}^{-1}$), respectively.

Parameters were estimated by using non-linear regression using the Sigmaplot software version 11.0.

3.4. Results

3.4.1. Kinetic sorption experiments

The sorption of boron on 4 resins was studied to define kinetics behavior and to determine the time to get equilibrium. The evolution of boron concentration in solution with time is plotted in Fig. 3.3

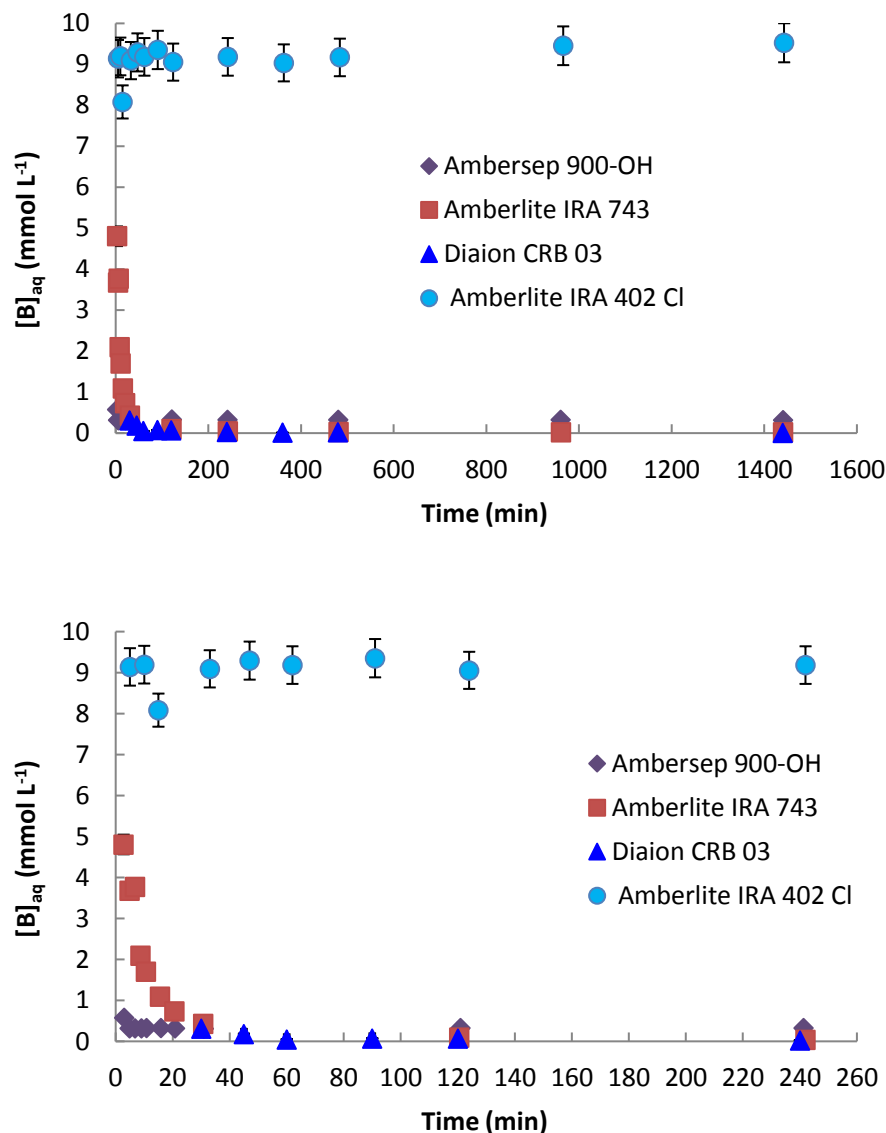


Fig. 3.3. Kinetic experiments of boron fixation on the four resins: IRA 743, CRB 03, IRA 402 Cl and Ambersep 900-OH at initial pH 8 (Final pH was increased to pH 10 for Amb 900 OH and decreased to pH 7 for others). Initial concentration of boron solution: $9.90 \pm 0.74 \text{ mmol L}^{-1}$

Results show that fast reaction occurred between solid and liquid phases within 30 min for IRA 743, CRB 03 and Ambersep 900-OH with remained boron concentration in aqueous solution of 0.43 , 0.31 , 0.31 mmol L^{-1} , corresponding to 98%, 98% and 96%, respectively (Fig. 3.3). Sorption reaction continues slower with the two specific resins and reaches closed to 0 after 2 h while adsorption reaction gets equilibrium just after 5 min with 96% adsorption for Ambersep 900-OH ($[B]_{aq} = 0.52 \text{ mmol L}^{-1}$). The sorption efficiency of Amberlite IRA 402 Cl is rather low (about 10%), sorption value fluctuating between 3% and 10%. For the three other resins, Amberlite IRA 743, Diaion CRB 03 and Ambersep 900, equilibrium can be assumed to be reached after 2 h while boron fixation efficiency is very high under the given experimental conditions.

Modeling of kinetics of boron sorption

Results were fitted with the two rates EQ 3.4 and EQ 3.6 in order to estimate the kinetic parameters with respect to the pseudo-first order and pseudo-second order rate laws, respectively.

A. Pseudo-first order kinetics

From equation EQ 3.4, the calculated regression coefficients were rather low, below 0.7, for the four resins, if kinetic data were fitted for the whole range of time (data not shown). However the fitting was much better if we considered only experimental data up to 15 min for Amberlite IRA 743 and Ambersep 900-OH (Fig. 3.4, TABLE 3.1).

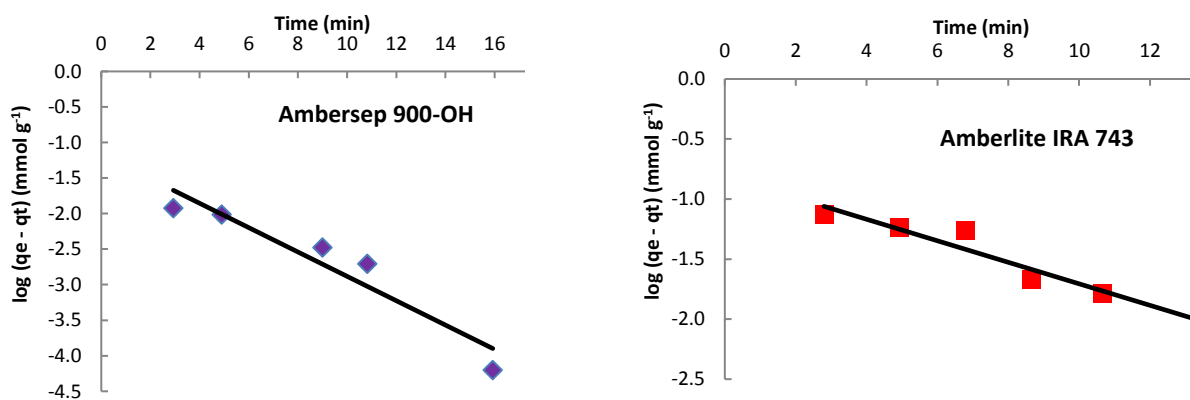


Fig. 3.4. Fitting of sorption boron kinetic experiments with the pseudo-first order kinetic model from 0 to 15 min the anionic Ambersep 900-OH resin and for the boron selective resin Amberlite IRA 743. Initial boron concentration: $9.90 \pm 0.74 \text{ mmol L}^{-1}$ at initial pH 8

The rate constant k_1 and amount of boron adsorbed at equilibrium q_e are reported in TABLE 3.1.

Table 3.1. Rate constant k_1 , amount of boron adsorbed at equilibrium q_e and half-time of boron sorption reaction for initial boron concentration of $9.90 \pm 0.74 \text{ mmol L}^{-1}$ and initial pH 8

Resin #	k_1 (min^{-1})	q_e (mmol g^{-1})	$t_{1/2}^*$ (min)	R^2
IRA 743	0.21	0.15	3.3	0.8859
Ambersep 900-OH	0.39	0.068	1.8	0.9079

- Reaction half-time: $t_{1/2} = \ln 2/k_1$

B. Pseudo-second order kinetics

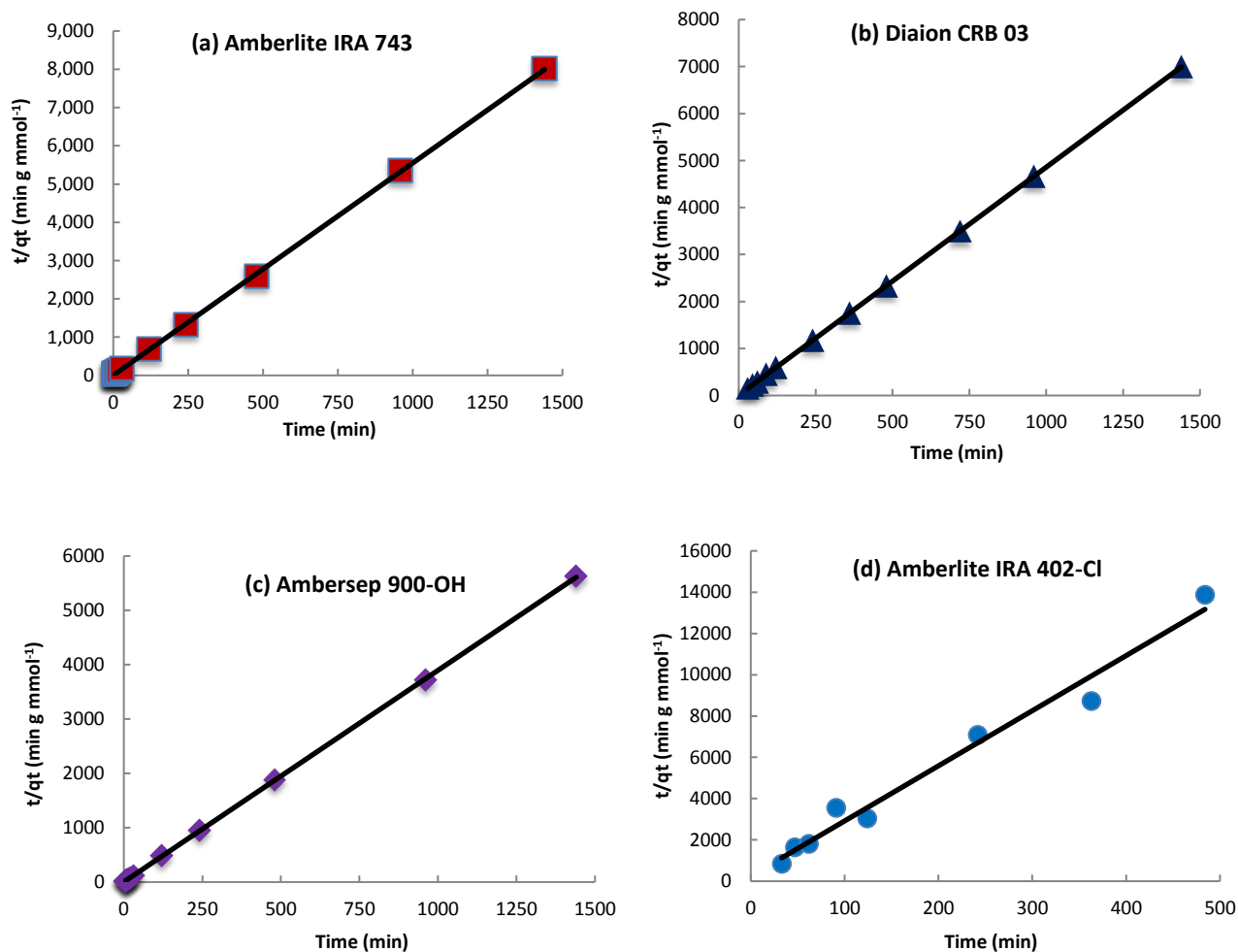


Fig. 3.5. Fitting of sorption boron kinetic experiments with the pseudo-second order kinetic model for B sorption on the 4 resins. Initial boron concentration: $9.90 \pm 0.74 \text{ mmol L}^{-1}$ at initial pH 8

Comparing Fig. 3.4 and Fig. 3.5, it appears that the pseudo-second order kinetic model better fits the sorption data for the four resins. The rate constant k_2 and amount of boron adsorbed at equilibrium q_e are reported in TABLE 3.2. It appears that the estimated k_2 for Amberlite IRA 743 is the highest, followed by Ambersep 900-OH and Diaion CRB 03. Amberlite IRA 402 Cl has the lowest rate constant. The maximum boron sorption concentration, q_e , is for Ambersep 900-OH, followed by Diaion CRB 03 and Amberlite IRA 743, when equilibrium is reached. The reaction half-time shows that Ambersep 900-OH and Amberlite IRA 743 has faster kinetics than Diaion CRB 03. Amberlite IRA 402 Cl showed very slow reaction rate meaning that either our experimental conditions or the uncertainty are not enough accurate for such a resin, or this resin is not a good sorbent for aqueous boron.

Table 3.2. Rate constant k_2 , amount of boron adsorbed at equilibrium q_e and half-time of boron sorption reaction for initial boron concentration of $9.90 \pm 0.74 \text{ mmol L}^{-1}$ and initial pH 8

Resin #	k_2 ($\text{g mmol}^{-1} \text{ min}$)	q_e (mmol g^{-1})	$t_{1/2}^*$ (min)	R^2
IRA 743	7.0	0.18	0.8	0.9999
CRB 03	3.7	0.21	1.3	0.9999
Ambersep 900-OH	5.7	0.26	0.7	0.9999
IRA 402 Cl	2.9	0.037	9.3	0.9771

• Reaction half-time from EQ 3.6: $t_{1/2} = (k_2 q_e)^{-1}$

3.4.2. Effect of pH on the boron adsorption

Influence of the pH on the boron adsorption was investigated in order to better understand the sorption mechanisms for the 4 selected resins. Depending on the resins and except for the Amberlite IRA 402 Cl, it was observed an increase in pH of the solution after adsorption.

As shown in Fig. 3.6, it appears that the two boron selective resins IRA 743 and CRB 03 had similar behaviour. Furthermore the boron adsorption does not depend on pH, On the other hand for the anionic resin Ambersep 900-OH, the maximum boron sorption is observed at pH 8.0 with a sorbed boron concentration of 0.08 mmol g^{-1} for 4.6 mmol L^{-1} total boron concentration, and at pH 9.5 with a sorbed boron concentration of 0.24 mmol g^{-1} for 8.4 mmol L^{-1} total boron concentration. For Amberlite IRA 402 Cl as seen in Fig. 3.6, the maximum measured sorption was observed at final pH close to 10.

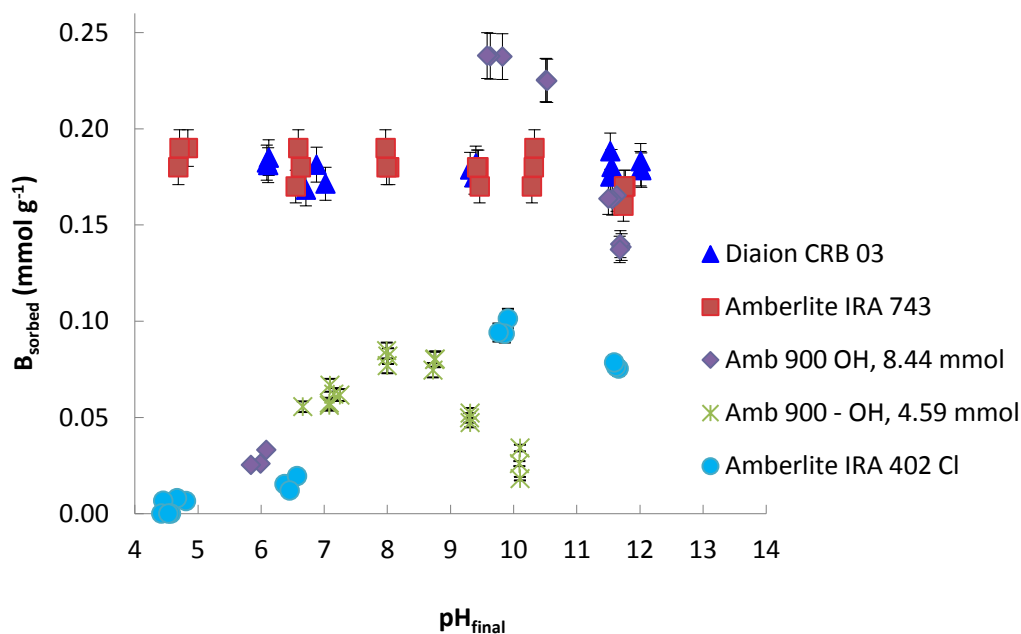


Fig. 3.6. pH Adsorption-edge experiments of boron adsorbed on the 4 resins, Amb 900-OH, CRB 03, IRA 743, IRA 402 Cl at pH 8. $9.30 \pm 0.33 \text{ mmol L}^{-1}$ (for CRB 03, IRA 402 Cl), $8.44 \pm 0.14 \text{ mmol L}^{-1}$ (for IRA 743, Amb 900-OH) and $4.59 \pm 0.33 \text{ mmol L}^{-1}$ (for Ambersep 900-OH) at pH 8

3.4.3. Isotherm experiments

The influence of the initial concentration of boron solution was studied for the 4 resins at initial pH 8 (FIG. 3.7).

The influence of the initial concentration of boron solution was studied for the 4 resins at initial pH 8. As shown in FIG. 3.7, the amount of boron adsorbed on the resin increased non-linearly for increasing aqueous boron concentration. A plateau is observed for the 2 resins, Diaion CRB 03 & Ambersep 900-OH, while the boron adsorption increased linearly with Amberlite IRA 402 Cl and two sorption steps are identified for the specific resin Amberlite IRA 743. The affinity sequence for boron is the following one, from the highest to the lowest one: the ionic Ambersep 900-OH resin, the specific Diaion CRB 03 and Amberlite IRA 743 resins, the ionic Amberlite IRA 402 Cl resin. This sequence is consistent with the one estimated from the pseudo-second order kinetic model (TABLE 3.2). On the other hand, efficiency of boron removal for the resin CRB 03 seems to get plateau from 10 to 50 mmol L^{-1} boron concentrations while the sorption concentration seems to continue to increase for the three other resins.

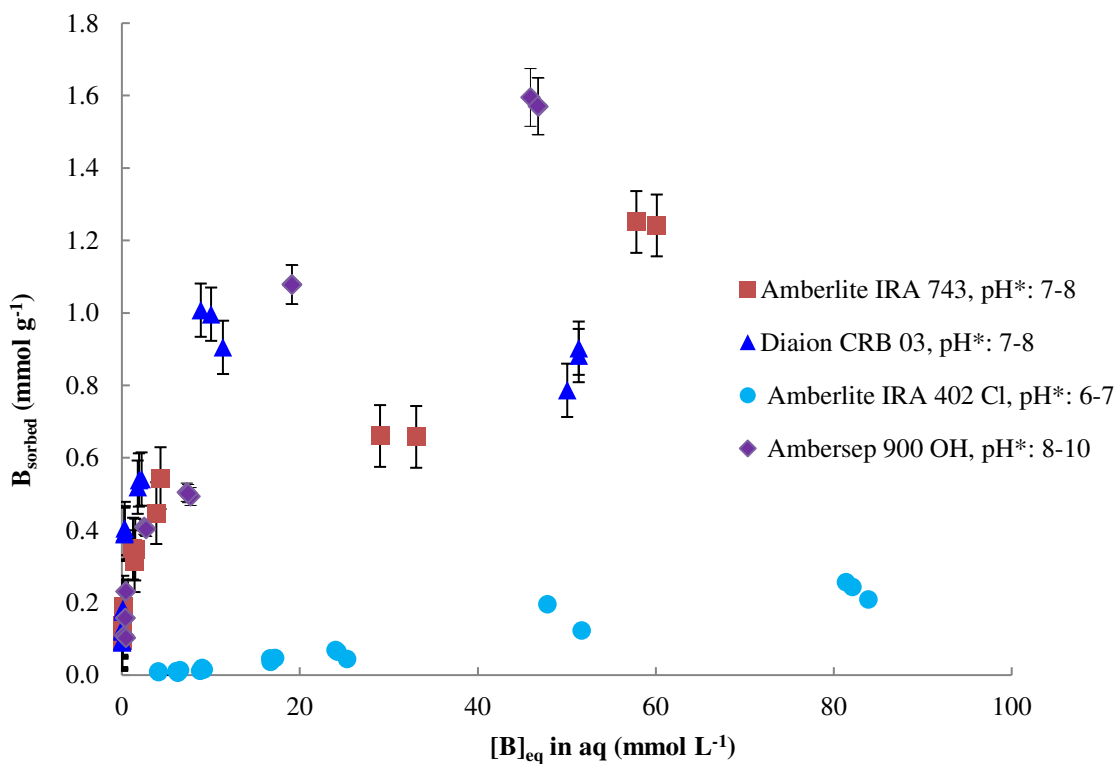


Fig. 3.7. Adsorption isotherms of boron with the selective and anionic resins for initial pH 8. Experimental conditions: mass of wet resin = 5.3 g; volume of boric acid solution = 100 ml (Ambersep 900-OH) and 95 ml (IRA 743, CRB 03, IRA 402 Cl). pH* corresponds to final pH

Modelling of sorption isotherms

Different models were used to fit the experimental adsorption isotherms: linear-type, Langmuir-type and BET-type relationships. It comes that:

- The resins CRB 03 and Ambersep 900-OH can be better fitted with a Langmuir-type isotherm relationship; it can be used for boron concentration lower than 35 mmol L⁻¹ for the specific resin IRA 743;
- For the anionic resin IRA 402 Cl, sorption isotherm can be better described by a linear-type relationship in the range of the studied concentration;
- The isotherm of the specific resin IRA 743 exhibits a BET-type shape with a first step corresponding to Langmuir-type behavior and a second step, which could be due to surface precipitation of boron.

Fitted parameters of Langmuir-type and BET-type models are reported for the three non-linear isotherms, for the IRA 743 in the boron concentration range < 35 mmol L⁻¹ (Table 3.3). In the case of the specific resin IRA 743 and for the full range of studied boron concentration, the BET-type estimated parameters are: $C_s = 90 \text{ mmol L}^{-1}$; $q_s = 0.43 \text{ mmol g}^{-1}$; and $K_{\text{BET}} = 1010 (-)$. The obtained values were used to plot the modeled isotherm curves and compared to experimental (Fig. 3.8).

Table 3.3. Maximum adsorption capacity, Langmuir-type coefficient, distribution coefficient and correlation coefficients estimated from the Langmuir-type relationship for the two selective resins and the anionic resin Ambersep 900-OH (data from Fig. 3.8). For the Amberlite IRA 402-Cl, linear-type relationship was applied

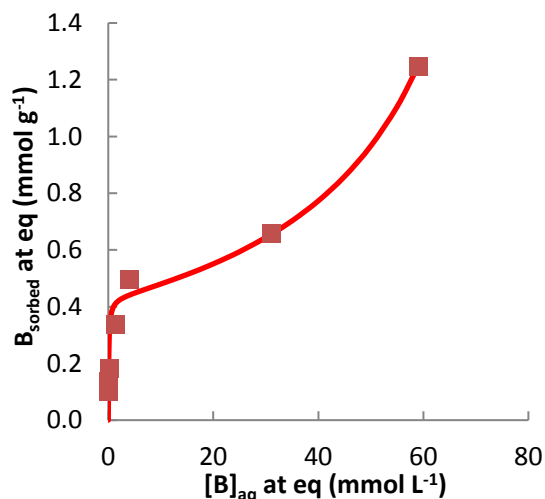
Resin #	S_{tot} [mmol g ⁻¹]	K_L [L mmol ⁻¹]	K_d [L g ⁻¹] [§]	R^2
Amberlite IRA 743*	0.62	1.5	0.90	0.8850
Diaion CRB 03	0.87	3.6	3.1	0.9987
Ambersep 900-OH	2.2	0.051	0.11	0.9517
Amberlite IRA 402-Cl [£]	–	–	0.003	0.9921

* For boron concentration < 35 mmol L⁻¹

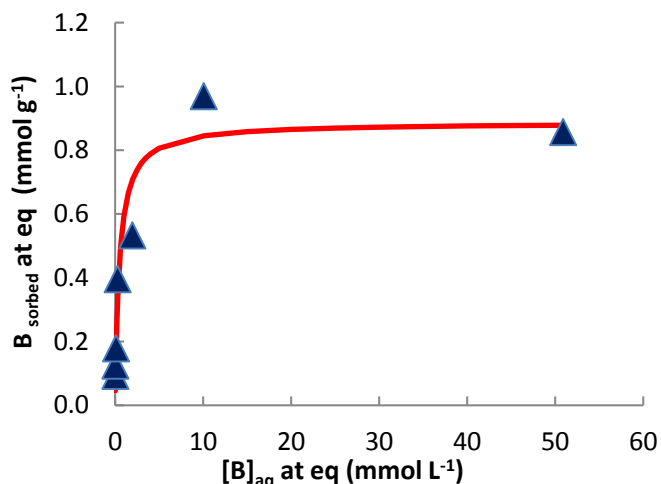
§ Distribution coefficient $K_d = S_{\text{tot}} K_L$

£ Linear-type fitting

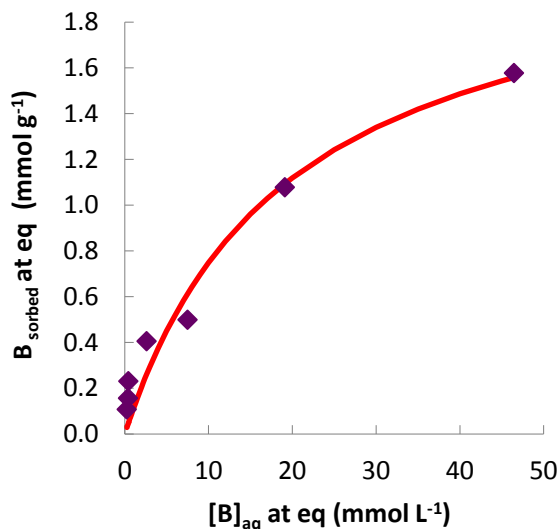
(a) Amberlite IRA 743



(b) Diaion CRB 03



(c) Ambersep 900-OH



(d) Amberlite IRA 402 Cl

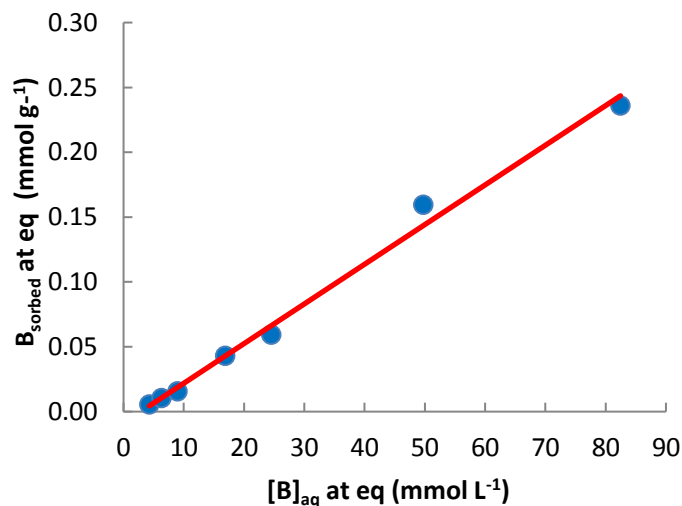


Fig. 3.8. Comparison between Langmuir-type fitting (line: —) and experimental data (dots) for boron sorption on the resins: (a) Amberlite IRA 743, (b) Diaion CRB 03, (c) Ambersep 900-OH; and (d) linear-type fitting for the anionic resin Amberlite IRA 402 Cl.

3.5. Discussion

Fitting with the pseudo-first order law shows rather low regression coefficient, below 0.7, meaning that the kinetic law cannot be applied for the four resins for the whole range of time (data not shown). But the fitting is much better for time up to 15 min as seen on Fig. 3.4.

The sorption kinetic was better fitted by the pseudo-second order kinetic model for 4 resins as shown in (Fig. 3.4) compared to (Fig. 3.5). The pseudo-second order chemical reaction kinetics provides the best correlation of the experimental data, if chemical reaction is significant in the rate

controlling step, while the proposed pseudo-first order model fits the experimental data well for an initial step of the first reaction only. However, over a long period the pseudo-second order model provides the best correlation for all the systems studied (Ho and Mac Kay, 1999). Reaction half-times for the different resins are reported in TABLE 3.1 and TABLE 3.2, indicating that the sorption kinetics is rather fast. But the question will be to compare them to the residence time when performing column experiments and to estimate if the kinetics which is observed in batch reactors can be a limiting step for flow-through reactors, as described by Ipek et al. (2013).

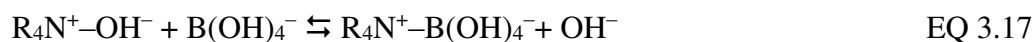
The results indicate that mass transfer is limiting the adsorption at the beginning. But after a long time, the adsorption efficiency is chemically controlled. The study of the pH influence on the adsorption rate has been used to identify the chemical reaction occurring during adsorption.

Boron speciation could play an important role in the boron behavior depending on the functional groups used for sorption as almost boron species is mainly as the molecular one H_3BO_3 at solution pH 6, while boron remains principally in borate form, $B(OH)_4^-$ at pH 12.

It is shown in Fig. 3.6 an independence of the boron adsorption on pH for the two boron selective resins. That could be due to the involvement of both neutral and anion forms in boron complexation reaction as shown in FIG. 3.1. The increase in pH of the solution after adsorption by the two boron selective resins Amberlite IRA 743 and Diaion CRB 03 can be assumed to be due to the capture of protons during adsorption on the N-methylglucamine group of the resins as in the EQ 3.16. The exceptional case of decreasing at initial pH ~ 7 for Diaion CRB 03 is still being studied.



On the other hand for the anionic resin Ambersep 900-OH, the maximum adsorption values is close to the pK_a of boric acid, meaning possible effect of boron species distribution in aqueous solution. The ion exchange reaction of the resin can be written as an ion exchange between borate ion and hydroxyl ion:



As the charge of the Ambersep 900-OH resin is positively charged at $\text{pH} < pK_a$, ion exchange is not efficient since the affinity of the major neutral species, H_3BO_3 , is rather low while the low OH^- concentration should favor sorption. For $\text{pH} > pK_a$, borate ion is predominant and resin surface are positively charged. But borate and hydroxyl ions compete for adsorption sites. The increasing presence of OH^- when pH increases limits the boron exchange reaction. But as it was observed for the experiments performed at total boron concentration of 4.6 and 8.4 mmol L^{-1} , the variation in pH from 8.0 to 9.5 corresponding to the maximum adsorption shows that the boron sorption affinity is quite high for this anionic resin. Exchange reaction (EQ 3.17) explains why the solution pH rose up with resin Ambersep 900-OH after boron adsorption.

For Amberlite IRA 402 Cl, the anion exchange was expressed as



In sorption process between resin Amberlite IRA 402 Cl and boron solution, borate ion is favorable for the ion exchange reaction like Ambersep 900-OH. As the results, the amount of adsorbed boron increased with increasing pH due to increase in borate ions. However, the sorption decreased for pH greater than 10 because of the competition between OH^- group and borate group in ion exchange reaction. The decrease in pH after adsorption could be explained by the involvement of borate ion into the ion exchange (EQ 3.18), more protons will be produced from reversible dissociation process from equation (EQ 3.1), and hence it caused a dropdown in pH.

The difference in boron adsorption behavior between 2 boron selective resins, Amberlite IRA 743 and Diaion CRB 03, 2 anion resins, resin Ambersep 900-OH and Amberlite IRA 402 can be explained according to the difference in the structure of the resins and adsorption mechanism. First, both forms of boron, boric acid and borate, can be involved in the adsorption reaction of the 2 boron selective resins, since their structures have 2 OH^- groups on the same plane and located next to each other. The complex between the resin and boric acid or borate, in tetrahedral form that is very stable, is easily done. For ion exchange resin, Ambersep 900-OH, only borate can take part in the ion exchange process between resin and boron solution. Second, the stable products formed between Amberlite IRA 743 and Diaion CRB 03 with boron can lower activation energy and force the direction of the adsorption reaction toward to produce more complex. On the contrary, for the ion exchange reaction of resin Ambersep 900-OH and Amberlite IRA 402 Cl, the ion exchanged product is less stable, with a competition between borate and OH^- ions in solution, leading to less boron adsorption.

Diaion CRB 03 got adsorption plateau from 10 to 50 $mmol L^{-1}$ since the exchange process reached exchange capacity of the resin. This resin has a behavior comparable to other Diaion resins such as CRB 02 and 05 (Recepoglu et al., 2017). Different with Diaion CRB 03, the isotherm of resin Amberlite IRA 743 displayed two plates. The first plateau was observed at lower equilibrium boron concentration ($< 40 mmol L^{-1}$) with an adsorption capacity of $0.7 mmol g^{-1}$ while the second plateau was appeared at higher equilibrium boron concentration ($\sim 60 mmol L^{-1}$) with adsorption capacity of $2.2 mmol g^{-1}$. It can be explained that the first plateau was established by the hydrophilic bonding between boron species with hydroxyl group on the surface of the resin, as observed by other authors such as Wei et al. (2011). When the first plateau ended, at high equilibrium concentration, borate was attached the surface and form H-bonding ($-O-H-O-$) with the adsorbed boron in the first layer, resulted in the second plateau (Hubbard, 2002). On the other hand, several steps can be assumed to explain the BET-type sorption behavior of boron. The two-first steps are reported in : first, borate forms complex with 2 resin sites, *i.e.* 2 hydroxyl functional groups. By analogy with the surface precipitation model proposed by Farley et al. (1985), this adsorbed borate could be considered as a new surface site where the boron could adsorb; the second step corresponds to the reaction of borate with the neo-surface boron complex site, mainly when the boron concentration increases. For the highest boron concentration, boron clusters made of

polyborate ions supported by bond analyses of borates (Yu and Xue, 2006) could be formed explaining the BET-type shape of the isotherm.

The higher the initial boron concentration was, the larger the amount boron was adsorbed on the surface of the resin. It is due to the probability of contact and occupy between boron species and adsorption sites increased when the initial boron concentration increased. The parameters of Langmuir-type model were identified for each isotherm (Table 3.3).

The obtained values were used to plot the modeled isotherm curves and compared to experimental (Fig. 3.8). The Langmuir-type relationship correctly describes the results obtained with Diaion CRB 03, Ambersep 900-OH but fails to describe correctly the results obtained with resin IRA 743 because it is the double fixation mechanism, as BET-type sorption.

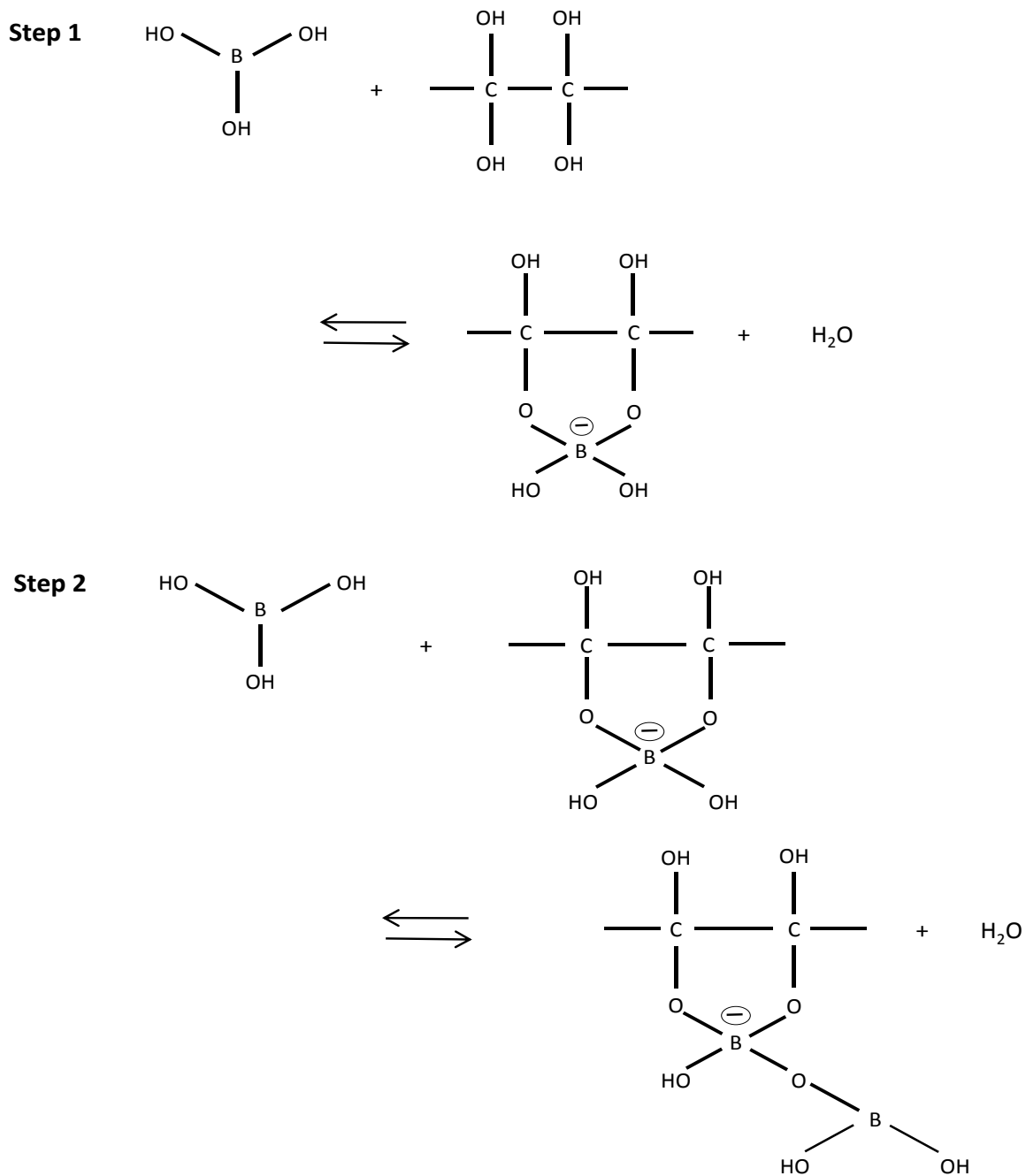


Fig. 3.9. Two first-step mechanisms for explaining BET-type behavior of boron sorption on the specific resin Amberlite IRA 743 taking into account diborate ion complexation supported by bond analyses of borates (Yu and Xue, 2006)

3.6. Conclusion

The adsorption of boron solution using 2 boron selective resins Amberlite IRA 743, Diaion CRB 03 and 2 ion exchange resins, Ambersep 900-OH and Amberlite IRA 402 Cl, as adsorbents was studied by the effect of kinetics, pH effect and sorption isotherm.

At initial pH 8, high percentage of boron adsorption was obtained within a half-hour, which showed a fast reaction between solid and liquid interface for the three resins, Amberlite IRA 743 (98%), Diaion CRB 03 (98%), Ambersep 900-OH (96%). Equilibrium was reached after 2 h reaction time for the four resins. The Amberlite IRA 402 Cl resin showed a slow rate and low boron sorption with only 10% removal even after 24 h adsorption. The pseudo second-order kinetic model was used to estimate kinetic parameters.

At equilibrium, boron sorption on specific boron resins did not depend on pH from 6 to 12, due to formation of surface complexes between boron and the polyhydroxyl functional groups present at the resin surface in this pH range. The anionic resins, Ambersep 900-OH and Amberlite IRA 402 Cl, exhibited the highest sorption capacity at pH 8 and 10, respectively. Ionic exchange is controlled by competition with OH^- ions at high pH for both resins and mainly by competition with Cl^- ions at low pH for the Amberlite IRA 402 Cl resin. At initial pH 8, the boron affinity for resins decreased as follow: Ambersep 900-OH (1.6 mmol g^{-1}), Amberlite IRA 743 (1.3 mmol g^{-1}), Diaion CRB 03 (0.9 mmol g^{-1}) and Amberlite IRA 402 Cl (0.2 mmol g^{-1}). In the range of boron concentrations studied, (i) the Langmuir-type relationship was applied to the Ambersep 900-OH and Diaion CRB 03 resins for fitting the maximum sorption capacity and the Langmuir-type coefficient which are 2.2 and 0.87 mmol g^{-1} respectively; (ii) the BET-type relationship was used for describing the boron behaviour in the presence of the Amberlite IRA 743 resin and for estimating the BET-type coefficient and the boron sorption capacity (0.43 mmol g^{-1}); and (iii) the Henry-type model was used for fitting boron sorption behaviour in the case of the Amberlite IRA 402 Cl. From this study and for the given experimental conditions used, the anionic resin Ambersep 900-OH appears to be the most efficient one compared to the specific ones.

Chapter 4

**BORON FIXATION ON SYNTHETIC
RESINS WITH FLOW - THROUGH
REACTOR**

(Written as a publication)

4.1. Introduction

The increasing use of boron in industries and its discharge to the environment has led to the contamination of not only surface water but also of ground water (Devirian and Volpe, 2003; Davidson and Bassett, 1993; Kot, 2008; Grassi *et al.*, 2014; Barth, 1998). On the other hand, due to the shortage of fresh water sources, mainly in countries where fresh water is missing or population is strongly increasing, seawater desalination has been becoming an alternative fresh water supply. However, the presence of boron in seawater is quite high (5 mg L^{-1}) (Tu *et al.*, 2010).

Boron is an element that is necessary as nutrient for living organisms, especially for plants where it is involved in cell wall composition. But its excess can cause some health or ecotoxicological problems. Boron toxicity has brought lots of negative influence on the development of plants, humans and animals such as nausea, diarrhea, dermatitis, lethargy and defoliation, decay and fall unripe fruits (Murray, 1995; Melnyk *et al.*, 2005). WHO has recommended a guideline of 0.5 mg L^{-1} B in drinking water and a maximum limit of 0.3 mg L^{-1} B in fresh water used for irrigation (WHO, 2011; WHO, 1998). Different boron removal methods has been developed such as adsorption, precipitation, reverse osmosis, solvent extraction and ion exchange (Simonnot *et al.*, 2000; Wolska and Bryjak, 2013; Tagliabue *et al.*, 2014). Reverse osmosis and adsorption by resin have been popular used in which reverse osmosis (RO) is extensively employed, particularly in desalination plants, because of a high efficiency up to 99% for RO for pH higher than 10 (Simonnot *et al.*, 2000; Glueckstern and Priel, 2003). Anionic and specific resins have widely used as boron adsorption materials. Specific resin has more priority in use because it has higher boron removal efficiency due to the selective complex formation between cis-diol groups on the structure of resin with boric acid and/or borate in solution (Smith *et al.*, 1999; Wolska and Bryjak, 2013).

Different authors have studied the kinetics and mechanisms of fixation of boron on different resins. The kinetics has been well described by pseudo-second order rate law (Kabay *et al.*, 2008). These authors (Kabay *et al.*, 2007) have reported that the removal efficiency increases when particle size decreases since the diffusion rate is improved due to the increase in the adsorption surface area. The retention has been described as a surface complexation reaction between two vicinal hydroxyl groups with the boric acid and borate. Other works have showed that the adsorption isotherm fit well with linear relationship of Langmuir-type mechanism for three materials such as the CRB 03, CRB 05 resins and Chelest fibre (Nishihama *et al.*, 2013). But it is important to remind that Langmuir-type reaction means reversibility of sorption, which has been shown to be not always the case (Simonnot *et al.*, 2000). Anionic resin has not been much studied because it has been often considered to be inefficient at pH below 9, which is high pH value compare to the pH range of natural fresh or marine waters. Indeed, in most of natural waters, the most predominant species of boron is boric acid, which is not favorable for ion exchange process. In continuous mode, increasing the flow rate leads to boron removal decreasing with specific resin XUS – 800 (Yan *et al.*, 2008).

The aim of our work is to compare the behavior of the two types of resins with respect to their retention capacity. Heading to this objective, experiments were performed to study the influence of

concentration and flow rate on the boron adsorption and resin capacity.

4.2. Materials and methods

4.2.1. Materials

All the chemicals and reagents were prepared by Milli-Q water and stored in plastic containers similar to batch experiments. A plastic graduated cylinder was used to take 100 mL of dry resin. Two resins used for column experiment: Anionic resin Ambersep 900-OH and boron selective resin Amberlite IRA 743.

Stock and standard boron solutions were prepared from 99.99% boric acid (Sigma Aldrich Company) in Milli-Q water. NaOH solutions were prepared from 97% powder (VWR) while HNO₃ from > 65% original solution (Sigma Aldrich). All other reagents, such as L-ascorbic acid, Azomethine-H monosodium salt, ammonium acetate (NH₄CH₃COO, > 99.8% purification) and EDTA were of analytical grade (Sigma Aldrich Company). Acetic acid (> 99.8%) (Sigma Aldrich) was used to make buffer solution pH 4.5. NaCl (99% purity) provided by ESCO - European salt company, was employed to determine pore volume of resin. H₂SO₄ 72% from Sigma Aldrich is also prepared to use for desorption process of Amberlite IRA 743 resin.

Boron solution was stored in 10 L plastic cans. Samples were collected in 100 mL plastic bottles, which is rinsed carefully by tap water, then Milli-Q water and dried. A timer was used to measure flow rate of the experiment. Sample was weighed on an OHAUS portable balance after collecting. pH meter (Mettler Toledo), a conductimeter (WTW LF 320) are used to follow the pH and conductivity of the samples.

4.2.2. Methods

4.2.2.1. Boron analysis

Calibration curve was first built using different boron concentration solution (0.5 and 5.0 mg L⁻¹). A 0.01 M azomethine - H solution was used as the color developing reagent. This solution was prepared by dissolving 0.45 g azomethine-H into 100 mL 1% (w/w) ascorbic acid solution. Ammonium pH 4.5 buffer solution was prepared by dissolving 50 g NH₄CH₃COO and 3 g EDTA sodium salt in a mixture containing 100 mL Milli-Q water and 100 mL of CH₃COOH (> 99.8%). The reaction was carried out by mixing of buffer, azomethine-H, boron solution or Milli-Q water with the ratio 2:2:1 (mL). The mixtures were stirred by a vortex during 10 s, and then standing for 1 h. Samples were measured by UV-Vis spectrophotometer at wavelength of 410 nm.

During the boron analysis, all tubes containing the reaction mixture were covered by aluminium foil to avoid external light that can degrade azomethine-H monosodium salt reagent. Absorbance was measured with quartz cuvettes in a UV-1800 model spectrophotometer (Shimadzu Corporation, Japan).

4.2.2.2. Column experiments

Two resins were employed for column experiments, Ambersep 900-OH and Amberlite IRA 743. Volume of resin was measured with a graduated cylinder, 100 mL or 400 mL, and the mass was recorded. All the resin was transferred in a beaker and mixed with Milli-Q water during 15 min. This step was repeated 4 times to eliminate all contaminants.

Resin was then packed in a column filled with Milli-Q water. When the resin beads were correctly packed, all Milli-Q water was passed through the column, until reaching resin surface (Water was kept on resin surface to avoid air bubbles can go into the resin that can break the tightness of column and change the flow rate after that). The column had a diameter of 5 cm and a length of 50 cm while the length of the resin bed was about 6.4 cm (Ambersep 900-OH) and 4.5 cm (Amberlite IRA 743). The resin column was connected to a 10 L feed tank by a peristaltic pump (Manostat Vera) with a variator to control the flow rate.

4.2.2.2.1. Pore volume (V_p) Determination

Two concentrations of NaCl were prepared and conditioned to pH 8 (2 L of 0.05 M and 1 L of 0.1 M) were prepared for V_p determination experiment.

In the case of Ambersep 900-OH, V_p determination has been made three times. The first time, 10 L of NaOH pH 8.30 solution were percolated through the column in order to condition the resin into pH 8. Percolation has been stopped when pH of the exiting solution from the column was stable at 8.55. Then 2 L of the NaCl solution has been flowed at a flow rate of 10 BV h^{-1} . The solution exiting the column was continuously collected in fractions of 3 min. Mass, pH and conductivity were measured on each sample.

The second time, 1 L of 0.1 M NaCl solution was continued to percolate through the previous resin dose using the same flow rate (1 L h^{-1}) in order to re-equilibrate the resin in the column. After that, 2 L of 0.05 M NaCl solution was again flowed through the column until reaching the equilibrium, so from this step the second V_p was determined.

The third time, 1 L of 0.1 M NaCl solution was continued to pass through the same resin dose with the same flow rate (1 L h^{-1}) in the column. The solution exiting the column was continuously collected in fractions of 3 min. Mass, pH and conductivity were measured on each sample.

To desorb NaCl, 10 L of NaOH pH 8 and 2 L of pH 13 (0.1M) NaOH was used to pass through the column at the flow rate of 10 BV h^{-1} . The samples were collected and measured pH and conductivity. When these values reached values of the original NaOH solution, column was continued to rinse and conditioned by pH 8 NaOH solution.

In the case of Amberlite IRA 743, resin was conditioned with pH 8.3 NaOH solution. 2 L 0.05 M NaCl and 1 L of 0.1 M NaCl were prepared at pH 8 and the percolation was managed at flow rate of 30 BV h^{-1} (3 L h^{-1}). Sample was collected each 30 s, weighed, and immediately measured pH and

conductivity. To elute NaCl, 4 L of 0.5 M H₂SO₄ and 4 L of 0.25 M NaOH were run through the column at the same flow rate, respectively. Samples were collected, weighed, and measured pH and conductivity. The desorption stopped when samples got pH and conductivity values similar to those of original NaOH solutions. The bed resin was rinsed by Milli-Q water and reconditioned to pH 8 by pH 8 NaOH solution.

4.2.2.2. Boron experiments

Boron experiments on Ambersep 900-OH resin have been done with two bed volume sizes, 100 mL and 400 mL, while it was only 100 mL with Amberlite IRA 743. Adsorption was managed by the percolation of different boron concentration solutions (20 and 100 mg L⁻¹) through the column at the different flow rates (10, 16 and 60 BV h⁻¹). Then desorption was performed in two steps. For Ambersep 900-OH resin, column was first rinsed with pH 8 NaOH solution, then, boron was continued to elute with pH 13 NaOH solution. For Amberlite IRA 743, the resin was first rinsed by 0.5 M H₂SO₄, and then regenerated by 0.25 M NaOH solutions. At the end, both resins were reconditioned in pH 8 NaOH solution for further experiments.

Samples were continuously collected during each phase, every minute for a flow rate of 60 BV h⁻¹, every 10 min for the flow rate of 16 BV h⁻¹, every 3 min for a flow rate of 10 BV h⁻¹. Conductivity and pH was measured immediately while boron concentration was determined after the end of each phase (adsorption, rinse and elution).

4.3. Results

4.3.1. Pore volume (V_p) determination

4.3.1.1. Ambersep 900-OH resin

The pore volume of the column has been defined in order to get better insight on the dynamic of the system. 2 L NaCl 0.05 M and 1 L NaCl 0.1 M was prepared using NaCl 99% purity and conditioned at pH 8 using 1.0 M NaOH solution as in TABLE 4.1. The change in the conductivity was followed and defined the pore volume of the system. The record of hydroxide anions was followed to study the reaction mechanism.

Table 4.1. Properties of the sodium chloride solutions before elution

Concentration	pH	Conductivity (mS cm ⁻¹)
NaCl 0.05 M	8.8 (after exp: 6.9)	14.5 (after exp: 15.0)
NaCl 0.1 M	9.0 (after exp: 7.3)	23.3 (after exp: 28.9)

The results obtained during this test are reported in Fig. 4.1

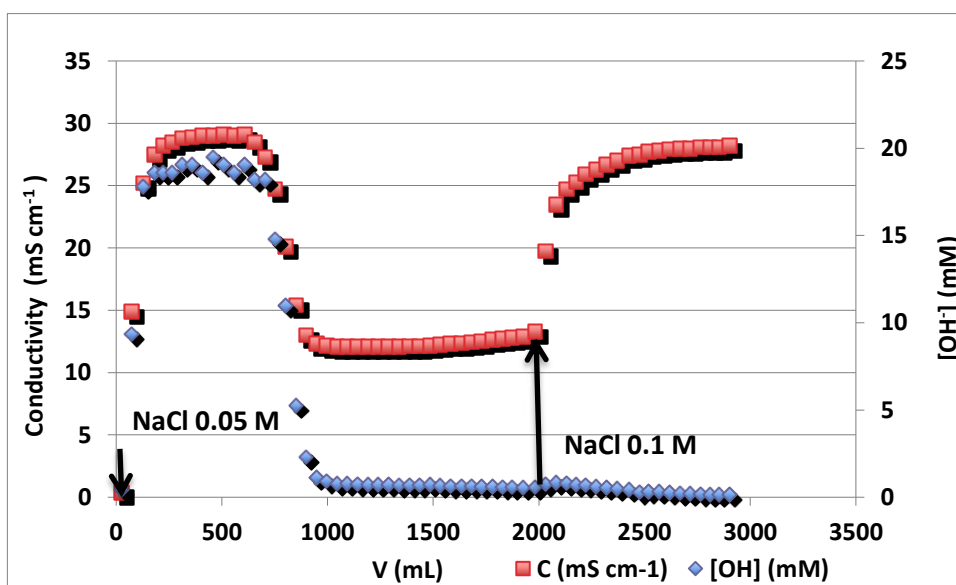
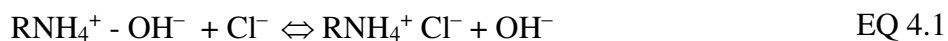


Fig. 4.1. Adsorption of NaCl 0.05 M, pH 8.8 and NaCl 0.1 M, pH 9.0 on 100 mL Ambersep 900-OH resin, the first time, flow rate of 10 BV h⁻¹ (1 L h⁻¹). (Black arrow indicates injection of adsorption solution)

Fig. 4.1 shows a similar behavior for [OH⁻] and conductivity. At the beginning, [OH⁻] and conductivity increased considerably ([OH⁻] = 19 mM, C = 29 mS cm⁻¹), and start to decrease since 0.5 L of 0.05 M NaCl was introduced. Steady state is gradually reached when 1 L to 2 L of solution injection. The rapid increase in pH and conductivity at the first part could be explained by the exchange between Cl⁻ and OH⁻ anions. OH⁻ anion is released in the solution and raised pH of samples.



The exchange reached steady state after 1 L 0.05 M NaCl was introduced; [OH⁻] and conductivity of solution was 0.6 mM and 13.3 mS cm⁻¹, respectively. Conductivity of solution rose strongly after addition of 0.1 M NaCl solution, due to the replacement of 0.1 M NaCl for 0.05 M NaCl into the pore of the resin. [OH⁻] decreased slightly at steady state. Fig. 4.2 shows how V_p was determined from experimental data.

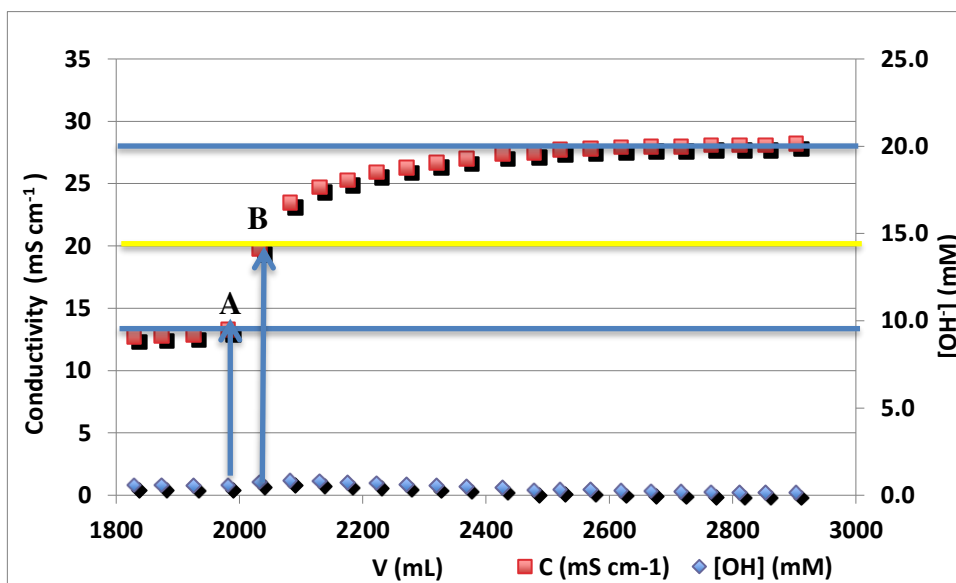


Fig. 4.2. Determination of V_p of 100 mL Ambersep 900-OH dry resin

V_p was determined based on the change of conductivity from 0.05 M NaCl to 0.1 M NaCl. Two steady states were symbolized with two blue offset horizontal lines, the higher one for 0.1 M NaCl and the lower one for 0.05 M NaCl. The yellow horizontal line divided the distance between two steady state lines in to two halves. This yellow line cuts the breakthrough curve of conductivity at B. A is the point 0.1 M NaCl was injected.

$$V_p = V_B - V_A \quad \text{EQ 4.2}$$

From experimental result, V_{p1} was determined at 51.1 mL.

Another set of 0.05 M NaCl and 0.1 M NaCl was prepared for the second and the third V_p determination times. The properties of these solutions were recorded as in TABLE 4.2.

Table 4.2. Properties of the NaCl solutions for the second and third elutions

Solutions	pH	C (mS cm ⁻¹)
2 L NaCl 0.05 M	8.8 (after exp. 7.6)	14.5 (after exp. 14.9)
2 L NaCl 0.1 M	8.9 (after exp. 7.8)	28.2 (after exp. 28.5)

Elution has been managed with 1 L of 0.1 M NaCl solution, then with 2 L of 0.05 M NaCl and finally with 1 L of 0.1 M NaCl solution. The behavior of OH^{-1} ions and conductivity of the second and the third experimental run was presented in Fig. 4.3.

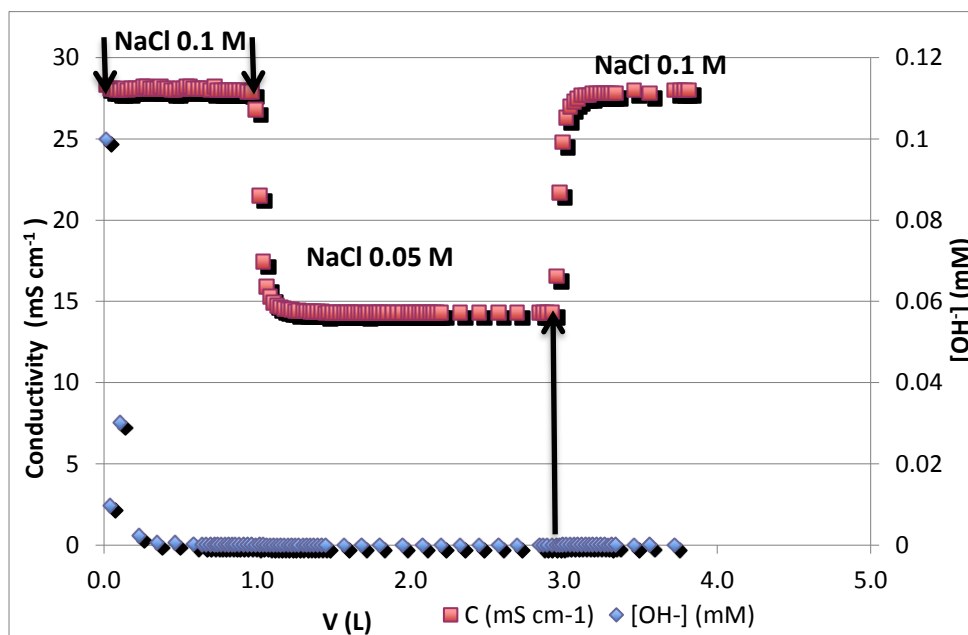


Fig. 4.3. Adsorption of NaCl 0.05 M, pH 8.8 and NaCl 0.1 M, pH 8.9 on 100 mL Ambersep 900-OH resin, the second and the third time, flow rate of 10 BV h^{-1} (1 L h^{-1}). (Black arrow means adsorption solution was injected).

Conductivity decreased from 30 to 15 mS cm^{-1} and then come back to 30 mS cm^{-1} , confirming in each case that the steady state was reached. The change in OH^- is not clear because the concentration is very closed to zero. The sharp form of the increase and the decrease indicates the low deviation due to hydrodynamic perturbations.

Two values of V_p were determined from two breakthrough curves of this experiment.

$$V_{p2} = 49.8 \text{ mL}; V_{p3} = 48.3 \text{ mL}$$

The mean value obtained from this two experiment is 49.1 while it is 49.7 from the three trials. The mean value used for pore volume of 100 mL Ambersep 900-OH resin has been 49.7 mL .

4.3.1.2. Amberlite IRA 743 resin

IRA 743 resin was prepared under the same protocol as Ambersep 900-OH. 100 mL of dry resin was weighted, cleaned, and packed tightly in the column. Resin after all was conditioned using pH 8.3 NaOH solution.

2 L 0.05 M NaCl and 1 L of 0.1 M NaCl were also prepared at pH 8. The properties of these solutions were reported in TABLE 4.3. The percolation was managed at flow rate of 30 BV h^{-1} (3 L h^{-1}). Sample was collected each 30 seconds, weighed, and immediately measured pH and conductivity (Fig. 4.4).

Table 4.3. Properties of the NaCl solutions for V_p determination of IRA 743

Solutions	pH	C (mS cm^{-1})
2 L NaCl 0.05 M	8.0 (after exp. 7.3)	13.2 (after exp. 13.4)
1 L NaCl 0.1 M	8.9 (after exp. 8.1)	25.8 (after exp. 26.0)

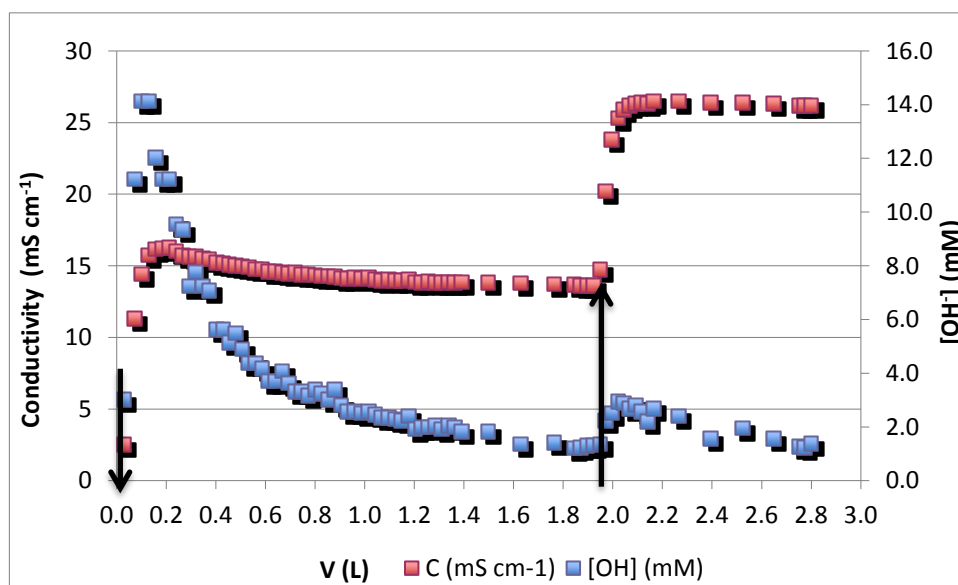


Fig. 4.4. Adsorption of 0.05 M NaCl, pH 8.0 and 0.1 M NaCl, pH 8.9 on 100 mL Amberlite IRA 743 resin, flow rate of 30 BV h^{-1} (3 L h^{-1}).

2 L of 0.05 M NaCl solution was percolated to ensure that the steady state is reached. pH and conductivity of solution increased strongly at the beginning due to the exchange between chloride and hydroxide ions, then reduced gradually to steady state. 0.1 M NaCl solution was introduced in the column that leads to a sharp increase in the conductivity and a little increase in OH^- anion concentration.

It is therefore possible to calculate the pore volume, V_p of Amberlite IRA 743 at the value of 76.2 mL compared to pore volume of IRA 743 in (Simonot et al., 2000) which is 68.0 mL. Those values are not so far from each other. The small difference could be due to the error from column experiment.

4.3.2. Boron fixation experiments

4.3.2.1. Ambersep 900-OH

4.3.2.1.1. Influence of boron concentration

Two experiments using the same resin bed (100 mL), same flow rate (10 BV h⁻¹), pH 8 and different boron concentrations (9.0 and 1.8 mM) were carried out to see the influence of boron concentration on boron adsorption behavior in continuous system.

Retardation factor of 1.8 mM boron solution is larger than this of 9.0 mM boron solution (FIG. 4.5). At higher boron concentration, the adsorption site on the surface of resin has more opportunities to contact with boron, thus increase ion exchange rate. Therefore, breakthrough curve of boron at higher concentration gets steady state sooner than that at lower concentration. This result is in concordance with isotherm results obtained with this resin in batch and the non-linear theory where the low concentrations increase the affinity, slowing boron transport for low concentration. On the same way, during desorption, the peak is wider for the lower concentration and sharper for the high concentration.

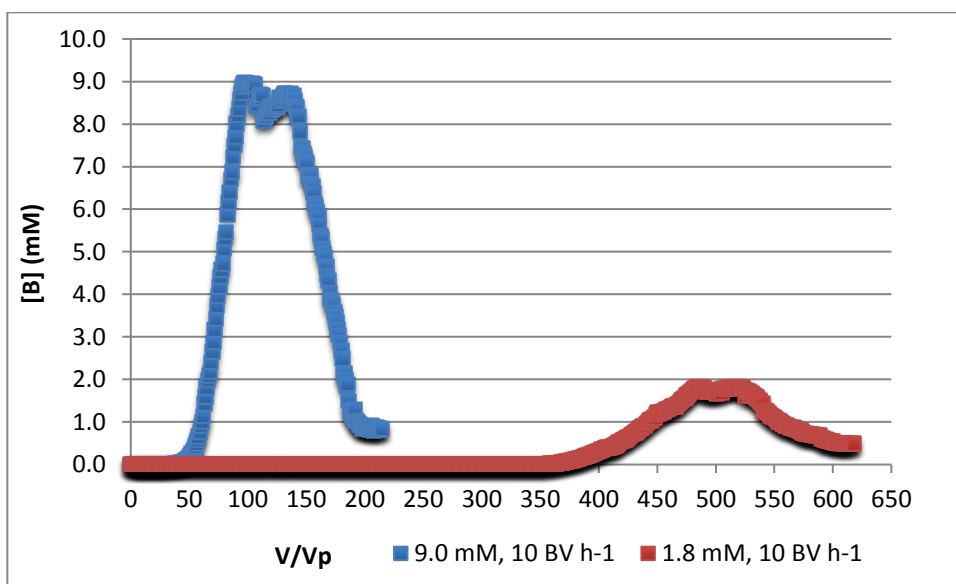


Fig. 4.5. Effect of boron concentration on boron breakthrough in the presence of Ambersep 900-OH.

Experimental conditions: 9.0 mM and 1.8 mM boron solutions, 10 BV h⁻¹ (1 L h⁻¹), pH 8

The boron sorption capacity for experiment of 1.8 mM was 0.40 mmol B mL⁻¹ resin, and increased to 0.51 mmol B mL⁻¹ resin for the trial at 9.0 mM. This result is in accordance with the batch results.

4.3.2.1.2. Influence of flow rate

In order to study the influence of flow rate on the boron adsorption of resin Ambersep 900-OH, two experiments using the same resin bed (100 mL), same boron concentration solution pH 8 (2.0 mM B) with different flow rates (10 and 60 BV h⁻¹) were carried out FIG. 4.6.

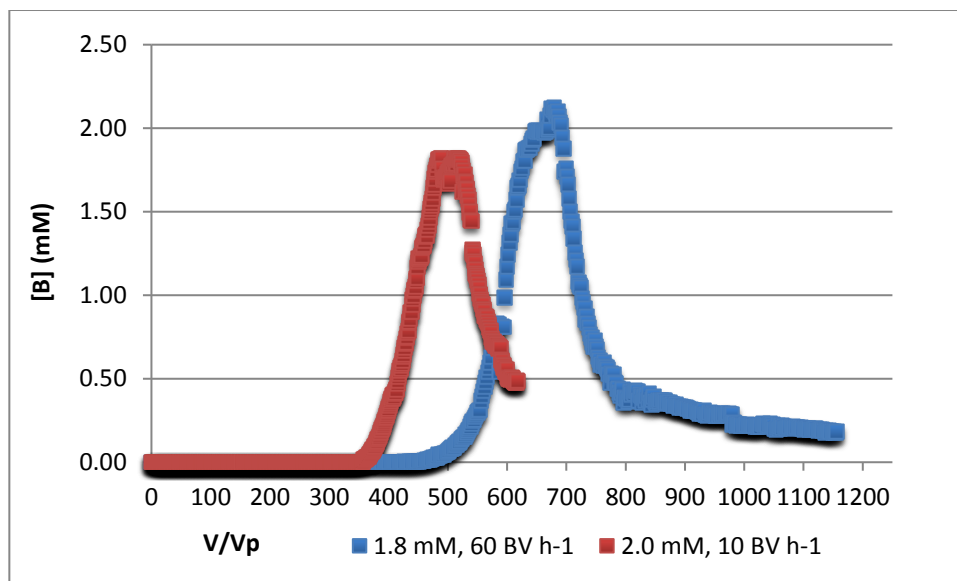


Fig. 4.6. Effect of flow rate on boron breakthrough in the presence of Ambersep 900-OH. Experimental conditions: 1.8 mM boron solution, 60 BV h⁻¹ (6.0 L h⁻¹), and 2.0 mM boron solution, 10 BV h⁻¹ (1 L h⁻¹), pH 8

The forms of the breakthrough curves are similar for the two flow rates, with a compressive form during adsorption and dispersive form during desorption. This result is in accordance with the Langmuir type of the isotherm determined during the batch experiments.

The analysis of the curves indicates that when the flow rate is increased, the retention factor also increased. From experimental result, the higher flow rate, the bigger amount of boron was adsorbed. The capacity of the resin increases from 0.40 mM B mL⁻¹ resin at 10 BV h⁻¹ to 0.59 mM B mL⁻¹ resin at 60 BV h⁻¹. This result is opposed to that obtaining from anion resin Dowex 2x8 (Köse and Öztürk, 2008). These primary results are also contradictory with theory that proposes that when flow rate is increased, fixation is less efficient and thus retention factor decrease.

A possible explanation could come from the presence of chloride ions on the resin that would have changed the capacity of the resin. The resin bed, in the case of the flow rate of 60 BV h⁻¹, has been used previously for pore volume determination and part of chloride ions may have been remained in the resin and modified the interactions intensity and the resin capacity.

4.3.2.1.3. Influence of resin bed volume

Four hundred milliliters, 211 g, of resin was conditioned in column (20 cm bed height) with pH 8.2 NaOH solution. 30 L of 103 mg L⁻¹ (9.54 mM) boric acid was prepared and conditioned at pH 8.1. Adsorption process was started with passing boric acid solution through the column at flow rate of 6.4 L h⁻¹ (16 BV h⁻¹). Desorption process was performed in two steps. First step, for rinsing, used about 30 L of NaOH solution pH 7.9 was eluted for rinsing, in a second step. Boron elution is performed with about 2 L of NaOH pH 12.9 (Fig. 4.7).

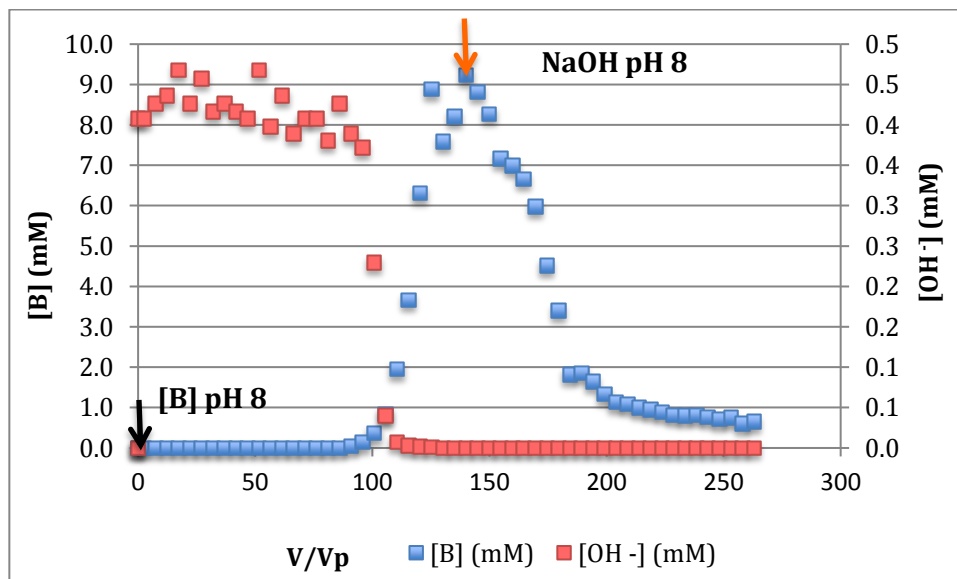


Fig. 4.7. Breakthrough curve for adsorption and desorption of 9.54 mM B solution, at flow rate of 16 BV h⁻¹ (6.4 L h⁻¹), pH 8. (Black arrow means adsorption solution was injected. (Orange arrow indicates when elution solution was injected).

There is no boron in the solution exiting the column until a volume of 100 V_p when the concentration starts to increase. This means that there is a large interaction between boron and resin. Thus hydroxide ions are exchanged and released in the solution. Hence its concentration in the solution is about 0.45 mM during the first 100 V_p and then started to decrease. It appears that ion exchange reached steady state at 140 V_p . Boron retardation factor has been evaluated at 117. This value is very similar to the results presented in FIG. 4.6. Rinsing process, operated with NaOH pH 7.9, showed a rapid decrease of the boron concentration from 9.2 mM to 0.6 mM with very little change in hydroxide concentration.

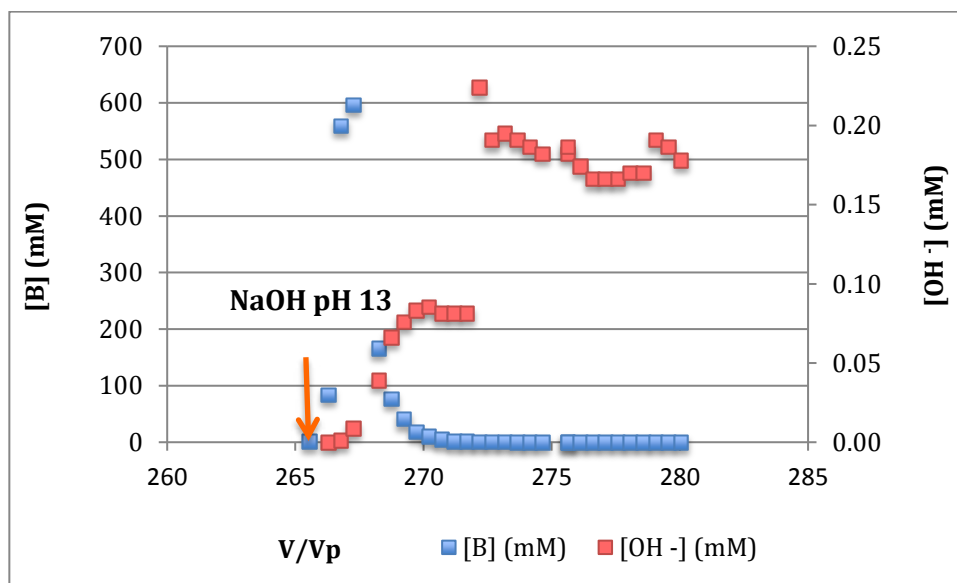


Fig. 4.8. Breakthrough curve for desorption of 9.54 mM B solution, at flow rate of 16 BV h⁻¹ (6.4 L h⁻¹), pH 13. (Orange arrow indicates when elution solution was injected).

Boron elution with pH 13, NaOH solution showed a sharp peak of boron between 265 V_p and 270 V_p with a maximum concentration of 600 mM.

The boron sorption capacity is 0.63 mmol B mL⁻¹ resin, which is higher than sorption capacity of experiment of 9.0 mM [B], 10 BV h⁻¹, pH 8 (0.51 mmol B mL⁻¹ resin) even this experiment was carried out at a little higher flow rate (16 BV h⁻¹). Hence, it is necessary to suppose that the residence time in the column was too short in 100 mL bed. But the characteristic time in the column was about 3 min in the two experiments, above the 0.7 min for half fixation calculated with pseudo-second order model.

4.3.2.2. Amberlite IRA 743

4.3.2.2.1. Influence of flow rate

Two experiments using the same Amberlite IRA 743 resin bed (100 mL), same boron concentration pH 8 (~ 9.0 mM) and different flow rates, 10 and 60 BV h⁻¹, were performed.

Boron breakthrough curves obtained for the two flow rates have been compared (FIG. 4.9). The results show that the slower the flow rate is, the higher the retardation factor is. This result is similar to which obtained from previous research on IRA 743 at three different flow rates (10, 20, 30 mL min⁻¹) (Yılmaz *et al.*, 2005). The result also confirms that when the flow rate is too high, the curve become width. The peak is sharper at 10 BV h⁻¹ and more widen at 60 BV h⁻¹, which indicates that 60 BV h⁻¹ is too fast flow rate and limits the fixation reaction. This result also fits with the suggestion of operating condition of Amberlite IRA 743 resin, which prefers the flow rate range of 4 BV h⁻¹ to 30 BV h⁻¹.

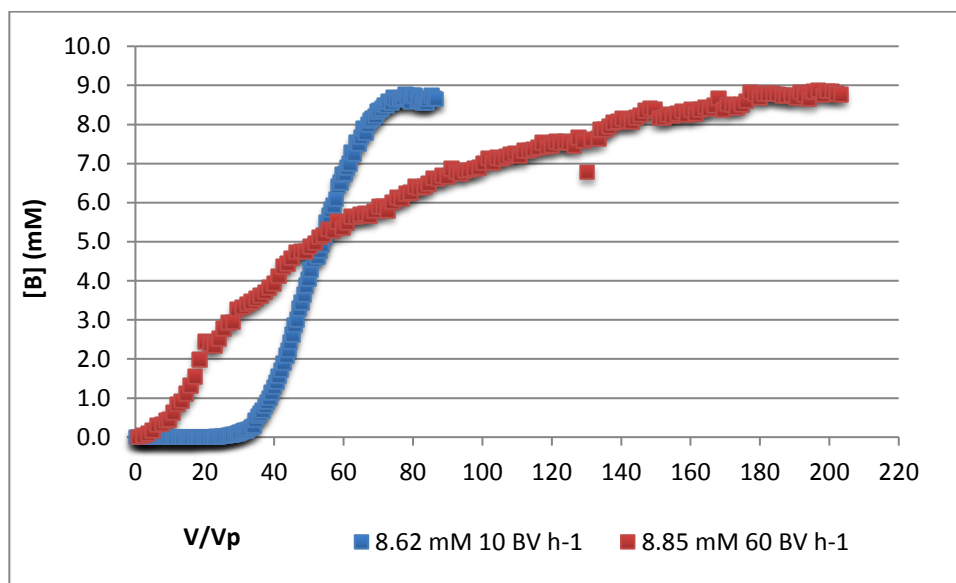


Fig. 4.9. Effect of flow rate on boron breakthrough in the presence of Amberlite IRA 743. Experimental condition: 8.62 mM boron solution, 10 BV h⁻¹ (1.0 L h⁻¹), 8.85 mM boron solution, 60 BV h⁻¹ (6.0 L h⁻¹), pH 8

The capacity of the resin does not change with the flow, 0.41 mmol B mL⁻¹ resin at 60 BV h⁻¹ and 0.36 mmol B mL⁻¹ resin at 10 BV h⁻¹. The boron amount adsorbed in experiment of 60 BV h⁻¹ is higher probably due to a pause at V/Vp = 130 for one hour. After pause, the equilibrium of reaction is re-established, more boron was adsorbed on the resin. It can be seen from FIG. 4.9 in the breakthrough curve of 60 BV h⁻¹, the boron concentration in sample is lower at pause point (the experiment was paused for 1h due to technical problem).

4.3.2.3. Comparison between two resins

Adsorption process of two resins with 8.62 mM B (IRA 743) & 9.0 mM B (Amb 900-OH), 10 BV h⁻¹, pH 8 was illustrated in Fig. 4.10.

The breakthrough curve for Amberlite IRA 743 appeared to be more quickly than that of Ambersep 900 – OH. This could be explained by the participation of both particles (boric acid and borate) in complex formation reaction with resin IRA 743 while only borate exchanges with OH⁻ ions on Ambersep 900 – OH resin in ion exchange reaction. Therefore, kinetics of experiment with IRA 743 was faster than that of experiment with Ambersep 900 – OH, hence the breakthrough curve getting steady state faster than that of Amb 900 – OH.

Sorption capacity of resin Ambersep 900-OH (0.51 mmol B mL⁻¹ resin) is higher than that of Amberlite IRA 743 (0.36 mmol B mL⁻¹ resin) at the same operating condition. Moreover, the breakthrough curves show that the capacity of treatment with Ambersep 900 is twice higher than that of IRA 743 for the production of water with maximum boron concentration of 0.5 mg L⁻¹. This result proves that Ambersep 900-OH is an interesting resin for boron removal in aqueous solution in the experimental condition, meaning for the removal of boron in demineralized water.

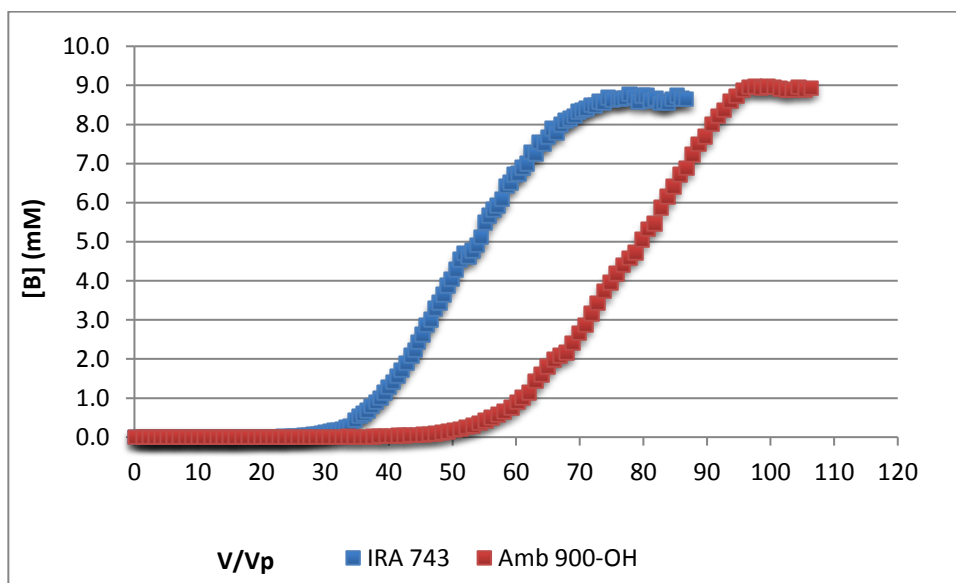


Fig. 4.10. Comparison of boron breakthrough for the two types of resin, the specific IRA 743 and the anionic Ambersep 900-OH ones. Experimental conditions: 8.62 mM B (IRA 743) & 9.0 mM B (Amb 900-OH), 10 BV h⁻¹(1.0 L h⁻¹), pH 8

From the TABLE 4.4, it is indicated that the column utilization of Ambersep 900-OH resin is quite good, approximate 90% for all experiment, however this value is not good for resin Amberlite IRA 743, especially with the experiment of 60 BV h⁻¹. This proved that this flow rate is not applicable for this resin. Boron capacity data in mmol g⁻¹ are reported in Table 4.4.

Table 4.4. Column utilization performance for each resin

Resin bed	Experiment condition	Amb 900-OH (mmol mL ⁻¹)			Amb IRA 743 (mmol mL ⁻¹)		
		C _{Total}	C _{Break-through}	Column Utilization (%)	C _{Total}	C _{Break-through}	Column Utilization (%)
		100 mL (Amb 900-OH)	1.8 mM, 10 BV h ⁻¹	0.45	0.40	88.6	
	1.8 mM, 60 BV h ⁻¹	0.67	0.59	87.9			
100 mL (Amb IRA 743)	9.0 mM, 10 BV h ⁻¹	0.59	0.51	86.3	0.57	0.36	63.3
	9.0 mM, 60 BV h ⁻¹				1.37	0.41	29.6
400 mL (Amb 900-OH)	9.5 mM B, 16 BV h ⁻¹	0.69	0.63	91.4			

Table 4.5. Boron adsorption capacities on each resin

Experiment condition	Amb 900-OH (mmol g ⁻¹)	Amb IRA 743 (mmol g ⁻¹)
1.8 mM, 10 BV h ⁻¹	0.62	
1.8 mM, 60 BV h ⁻¹	0.92	
9.0 mM, 10 BV h ⁻¹	0.79	0.48
9.0 mM, 60 BV h ⁻¹		0.55
9.5 mM B, 16 BV h ⁻¹	1.19	

4.3.2.4. pH and conductivity evolution

4.3.2.4.1. Ambersep 900-OH

pH and conductivity of samples in column experiment are followed to study the behavior of the solution during adsorption and desorption process. One example of experiment using Ambersep 900-OH resin was chosen to present the pH and conductivity changes.

The characteristic of feed solution was presented in TABLE 4.6.

Table 4.6. Properties of the boron feed solutions used for adsorption on Ambersep 900-OH, 10 BV h⁻¹(1.0 L h⁻¹), pH 8

Original B solution	pH	[B] (mM)	C (μS cm ⁻¹)
1	7.9	1.76	9.0
2	7.9	1.79	9.7
3	7.9	1.81	9.0

The behavior of hydroxide ions and conductivity compared to that of boron concentration in sample solution was illustrated in Fig. 4.11 and Fig. 4.12 below. In this experiment, desorption process was performed at the same flow rate using NaOH pH 8.6 at the first stage and NaOH pH 12.6 solution at the second stage.

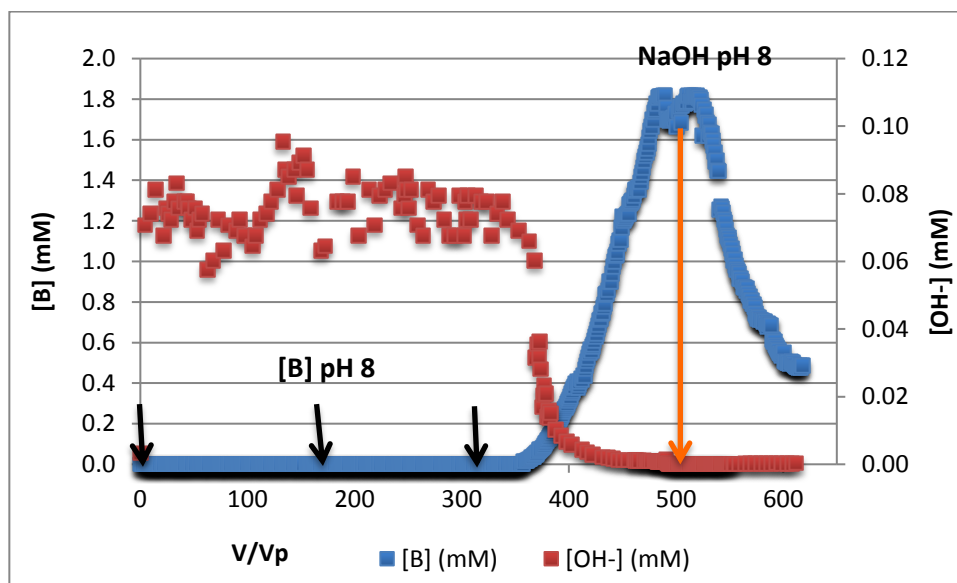


Fig. 4.11. Breakthrough curves of [B] versus $[OH^-]$ for adsorption and desorption process of 1.8 mM boron solution, 10 BV h^{-1} (1.0 L h^{-1}), pH 8. (Black arrow means adsorption solution was injected. Orange arrow means elution solution was injected).

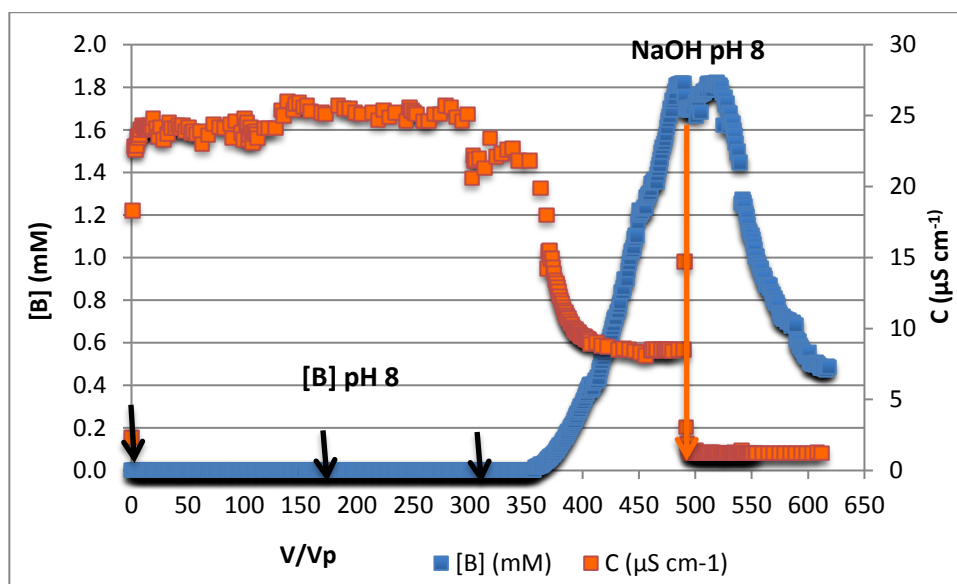


Fig. 4.12. Breakthrough curves of [B] versus C for adsorption and desorption process of 1.8 mM boron solution, 10 BV h^{-1} (1.0 L h^{-1}), pH 8. (Black arrow means adsorption solution was injected. Orange arrow means elution solution was injected).

From Fig. 4.11 and Fig. 4.12, it can be easily observed that boron concentration breakthrough curve matches very well with breakthrough curves of hydroxide ions and conductivity. At the beginning,

there was exchange between borate and hydroxide anions in solution; all boron was adsorbed in the resin. Hence there was no boron in the solution exiting the column while the hydroxide concentration increased to 0.07 mM. As the boron concentration was low, only few hydroxides are liberated which induced a small pH variation at the limit of the capacity of the pH probe. This explains the variability in the hydroxide concentration. Furthermore, as hydroxide has a higher conductivity than boron, exchange between the two ions leads to the increasing of the conductivity of the exiting solution.

From $V = 358 V_p$, boron started to appear in solution, that means the ion exchange was gradually reaching steady state. At the same time, hydroxide concentration and conductivity were also lowering to initial value of feed boron solution ($\text{pH } 8, C = 8.5 \mu\text{S cm}^{-1}$).

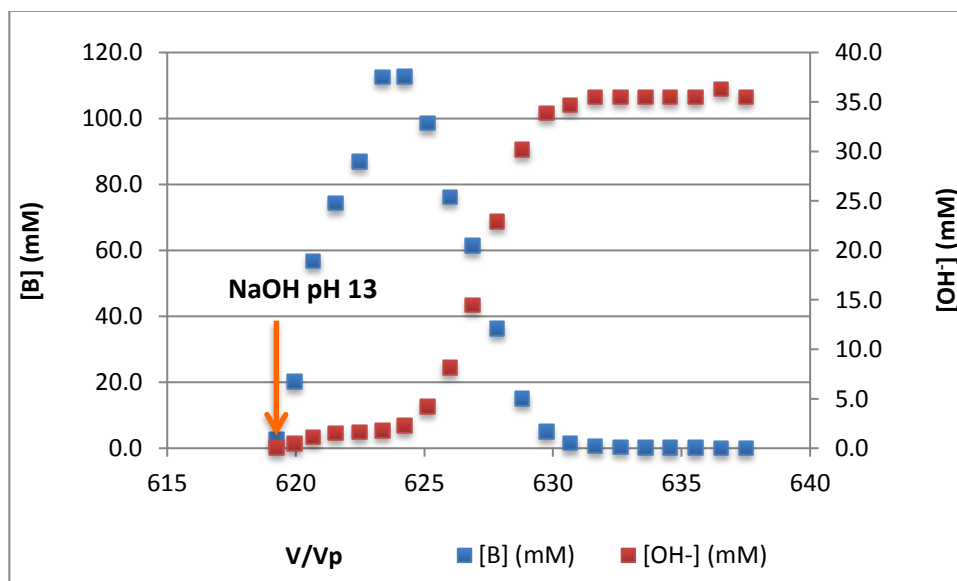


Fig. 4.13. Breakthrough curves of [B] versus [OH⁻] for desorption process of 1.8 mM boron solution, 10 BV h^{-1} (1.0 L h^{-1}), $\text{pH } 12.6$.

Boron concentration increased sharply during desorption using NaOH $\text{pH } 12.6$. The maximum of the peak is obtained with a boron concentration of 112 mM and then decreased to zero after about 10 V_p . Simultaneously, [OH⁻] gradually increased and get a stable value, indicated that the steady state is reached.

The monitoring of pH (or [OH⁻]) and conductivity of sample solution strongly supports us to explain the behavior of boron concentration, to make sure that the adsorption and desorption were completed and have a better understanding about the ion exchange process during column experiment.

4.3.2.4.2. Amberlite IRA 743

The follow of pH and conductivity of experiment with Amberlite IRA 743 resin also selected. The characteristic of feed solution was presented in TABLE 4.7.

Table 4.7. Properties of the boron feed solution used for adsorption on Amberlite IRA 743, 10 BV h⁻¹ (1.0 L h⁻¹), pH 8.

Boron solution	[B] (mM)	pH	Conductivity ($\mu\text{S cm}^{-1}$)
Feed solution	8.62	7.8	29.8

The evolution of hydroxide ions concentration and conductivity have been followed and compared to boron concentration in sample solution (Fig. 4.14, Fig. 4.15).

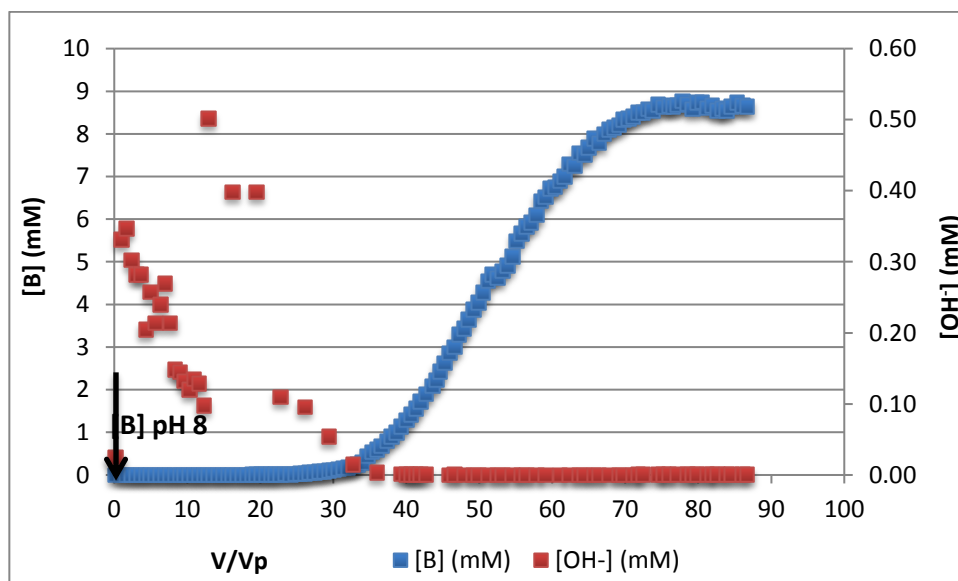


Fig. 4.14. Breakthrough curves of boron and hydroxide versus elution volume for adsorption process of 8.62 mM boron solution, 10 BV h⁻¹(1.0 L h⁻¹), pH 8. (Black arrow means adsorption solution was injected).

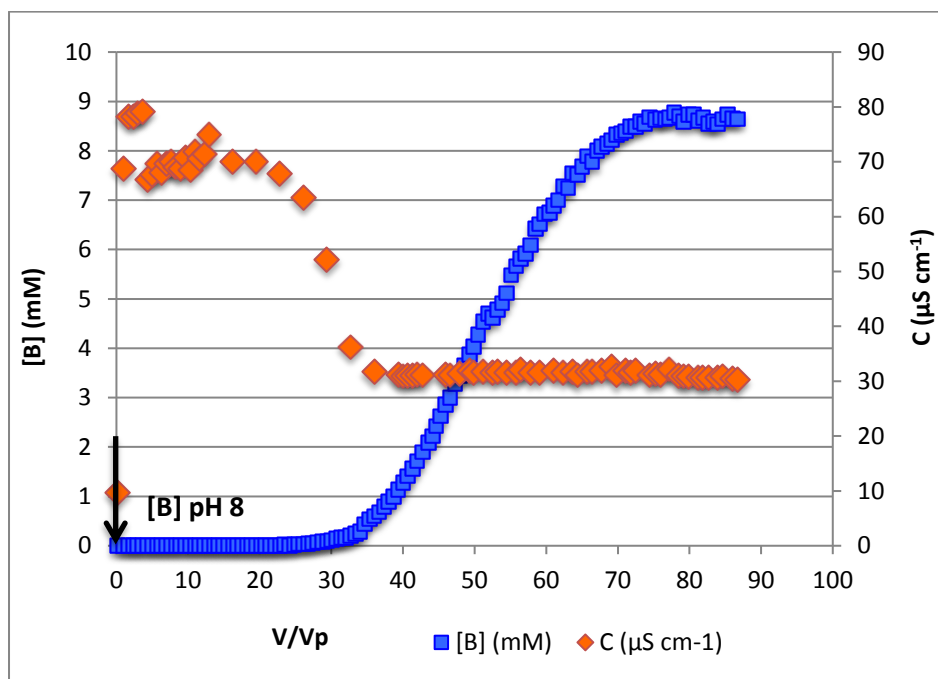


Fig. 4.15. Breakthrough curves of boron and conductivity versus elution volume for adsorption process of 8.62 mM boron solution, 10 BV h^{-1} (1.0 L h^{-1}), pH 8. (Black arrow means adsorption solution was injected).

The results show that the boron concentration remained non detectable in the samples until the volume of $18 V_p$, and then progressively increased to the feed concentration at the volume of $75 V_p$. The form of the curve is smooth indicating that advection is high compare to the fixation processes.

Hydroxide concentration sharply increased at the beginning, then fluctuated between 0.1 and 0.5 mM, after that approached to zero concentration (pH 8). This unstable phenomenon might be explained by the liberation of proton during adsorption process when borate ions participated into complex reaction. These protons during reaction were also captured by NMDG group on the resin. Therefore, it could cause the fluctuation of sample solutions. When the ion exchange reaction was going to be steady state, the proton gradually stopped liberation and the pH of solution tended to that of feed solution.

Similar to hydroxide ions, the change in conductivity of sample solution appeared to be varied at the beginning due to the presence and capture simultaneously of the protons, started to decrease when boron appeared in the sample solution and remained stable when equilibrium was reached.

In this experiment, desorption process was started using strong sulfuric acid and then sodium hydroxide (TABLE 4.8).

The results showed that boron was almost immediately released from the resin when acid enters in the column Fig. 4.16. There is a sharp peak of boron until $10 V_p$ with a maximum of 150 mM at $4 V_p$. Then there is no boron in the eluate after this volume. The pH of the eluate started at a value of 7 and then progressively decreases to pH of the sulfuric acid feed solution.

Table 4.8. Properties of the desorption solutions

Solution	Concentration		Conductivity (mS cm ⁻¹)	Volumic mass (kg m ⁻³)
	(M)	pH		
H ₂ SO ₄	0.5	0.63	203	1026
NaOH	0.25	12.42	45	1004

Sodium hydroxide is used after to wash the acid and regenerate the resin. Sodium hydroxide elution does not recover any boron.

The pH and conductivity of this experiment helped us to understand more deeply and confirm the phenomena happening during the experiment, explained the difference in adsorption mechanism between two resins.

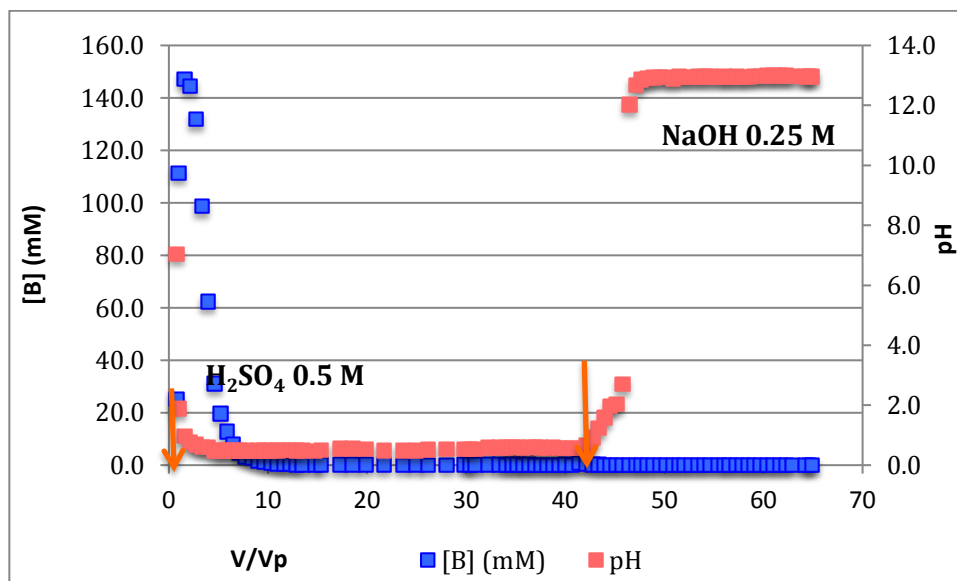


Fig. 4.16. Breakthrough curves of boron and pH versus elution volume for desorption process 8.62 mM boron solution, 10 BV h⁻¹, using 0.5 M H₂SO₄ and 0.25 M NaOH. (Orange arrow means elution solution was injected).

4.3.3. Optimized models

4.3.3.1. Pseudo first order breakthrough curve modeling

Two continuous experiments with the two resins, Ambersep 900-OH and Amberlite IRA 743, were chosen to fit with Yoon and Nelson model. In a first time the results obtained during the percolation at 16 BV h⁻¹ of a 9.54 mM boron solution using Ambersep 900-OH were used for the model

parameter identification by plotting time versus $\ln(C/(C_0-C))$ (FIG. 4.17). The parameters were then used to build up the theoretical breakthrough curve and compared with the observed one from experiment (FIG. 4.18).

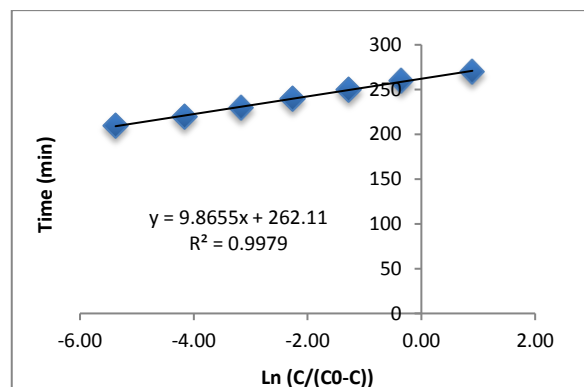


Fig. 4.17. Linear plot of time vs. $\ln(C/(C_0-C))$ at 9.54 mM, 400 mL resin, 16 BV h^{-1} , Amb 900-OH resin

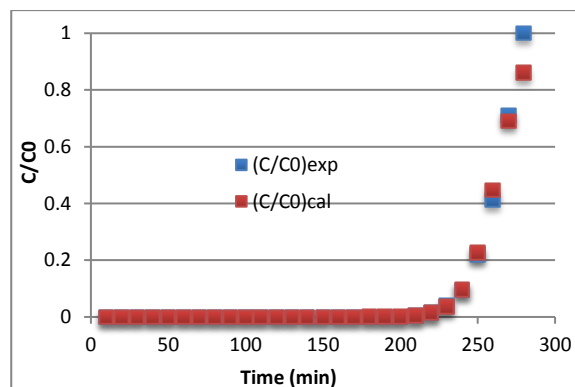


Fig. 4.18. Comparison between experimental and predicted breakthrough curves according to Yoon and Nelson model ([B]: 9.54 mM, 400 mL resin, 16 BV h^{-1} , Amb 900-OH resin)

Similarly, the relationship between time and $\ln(C/(C_0-C))$ was also plotted to estimate model parameters for Amberlite IRA 743 resin, from the experiment managed with an 8.62 mM boron solution at a flow rate of 10 BV h^{-1} .

The rate constant (min^{-1}), 50% breakthrough time (min) and adsorption capacity ($mmol g^{-1}$) parameters for the model were calculated and used to construct the predicted breakthrough curve and compared with the experimental (FIG. 4.19, FIG. 4.20).

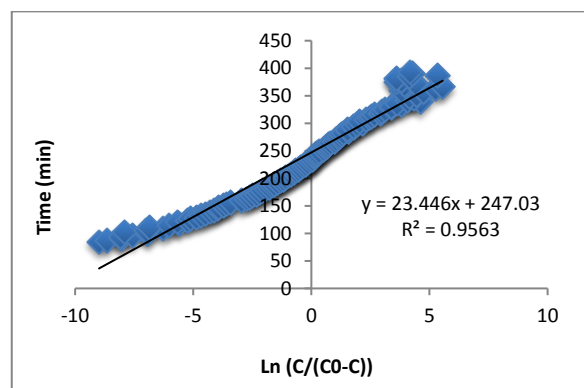


Fig. 4.19. Linear plot of time vs $\ln(C/(C_0-C))$ at 8.62 mM, 100 mL resin, 10 BV h^{-1} , Amb IRA 743

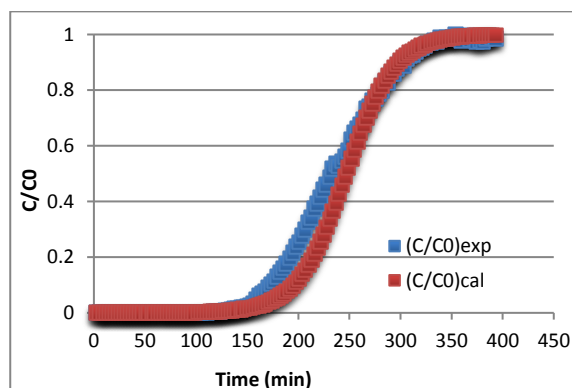


Fig. 4.20. Comparison between experimental and predicted breakthrough curves according to Yoon and Nelson model ([B]: 8.62 mM, 100 mL resin, 10 BV h^{-1} , Amb IRA 743)

From the results and figures, it can be seen that there is a small difference in 50% breakthrough time and adsorption capacities between prediction and experiment. Yoon and Nelson model is adequate to describe the variation of boron concentration in the experiment of adsorption of ~ 9.0 mM boron

solution on 100 mL Amberlite IRA 743 and Ambersep 900-OH resins. Hence, the values of the parameters are compared to the values obtained in batch with pseudo-first order model (TABLE 4.9)

Table 4.9. Yoon and Nelson model parameters compared to pseudo-first order model parameters

	Yoon and Nelson model			Pseudo first order model		
	k (min ⁻¹)	□ (min)	q ₀ (mmol g ⁻¹)	k (min ⁻¹)	t _{1/2} (min)	q ₀ (mmol g ⁻¹)
Ambersep 900	0.1	260	1.1	0.39	1.8	0.07
IRA 743	0.04	247	0.5	0.21	3.3	0.15

The results of the model show a large difference in the capacities of the resins that are higher at in continuous conditions than in batch. This result is due to hydrodynamic of the column that can modify the retardation factor, and thus the quantity of boron retained in the column. But the value of the retardation factor is multiply by 180 for both resins between batch and continuous. Such difference cannot solely be explained by hydrodynamic, and another explanation could be the influence of the pH. During batch experiment, pH changed with released hydroxide, and this hydroxide can compete with boron for fixation. During continuous experiments, hydroxide are continuously removed from the column and do not enter in competition with boron.

4.3.3.2. Pseudo-second order breakthrough curve modeling

First, in order to determine Thomas model parameters, the plot of the relationship between volume of exiting solution and $\ln((C_0-C)/C)$ was established for experiment with Ambersep 900-OH at a flowrate of 16 BV h⁻¹ of 9.54 mM boron solution. The rate constant (mL min⁻¹ mg⁻¹) and adsorption capacity (mg g⁻¹) parameters for the model were estimated and used to plot a model breakthrough curve (FIG. 4.21, FIG. 4.22).

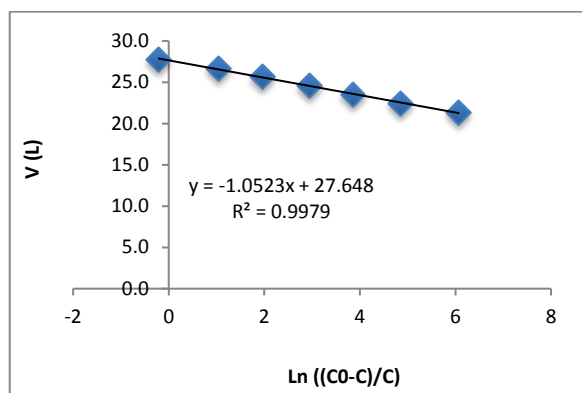


Fig. 4.21. Linear plot of volume vs $\ln((C_0-C)/C)$ at 9.54 mM, 400 mL resin, 16 BV h^{-1} , Amb 900-OH

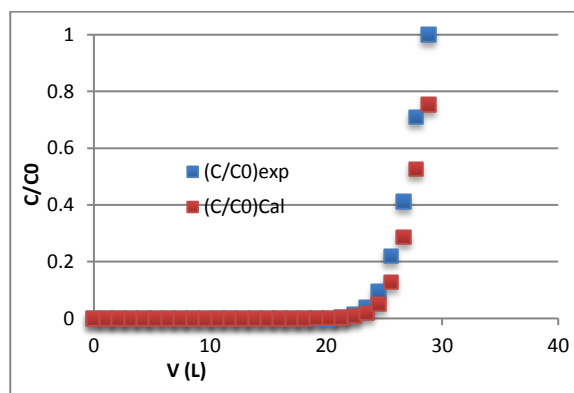


Fig. 4.22. Comparison between experimental and predicted breakthrough curves according to Thomas model ([B]: 9.54 mM, 400 mL resin, 16 BV h^{-1} , Amb 900-OH)

A similar procedure has been used for experiment with Amberlite IRA 743 resin at a flow rate of 10 BV h^{-1} and 8.62 mM boron solution. The plot between volume of exiting solution and $\ln((C_0-C)/C)$ was built and the parameters used to draw the theoretical breakthrough curve (FIG. 4.23, FIG. 4.24).

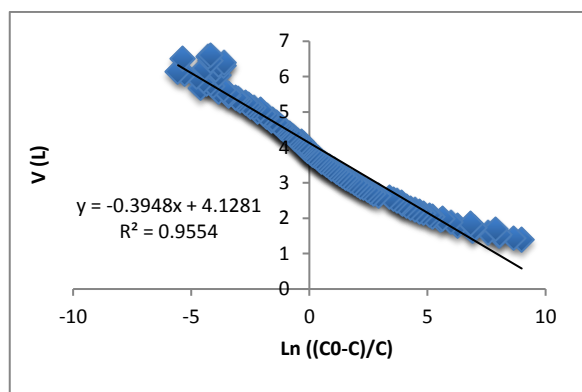


Fig. 4.23. Linear plot of volume vs $\ln((C_0-C)/C)$ at 8.62 mM, 100 mL resin, 10 BV h^{-1} , Amb IRA 743

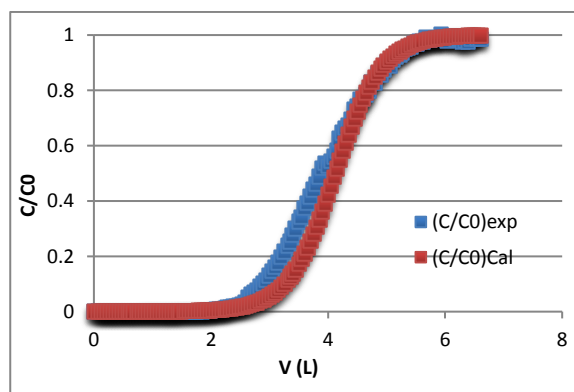


Fig. 4.24. Comparison between experimental and predicted breakthrough curves according to Thomas model ([B]: 8.62 mM, 100 mL resin, 10 BV h^{-1} , Amb IRA 743)

From the results and figures, it can be seen that there is a small difference in 50% breakthrough time and adsorption capacities between prediction and experiment. Thomas model is adequate to describe the variation of boron concentration in the experiment of adsorption of ~ 9.0 mM boron solution on 100 mL Amberlite IRA 743 and Ambersep 900-OH resins. Hence, the values of the parameters are compared to the values obtained in batch with pseudo-second order model (TABLE 4.10).

Table 4.10. Thomas model parameters compared to pseudo-second order model parameters

	Thomas model		Pseudo-second order model	
	K_T (mL mg ⁻¹ min ⁻¹)	q_0 (mmol g ⁻¹)	k_2 (g mmol ⁻¹ min ⁻¹)	q_0 (mmol g ⁻¹)
Ambersep 900-OH	1.1	1.2	5.7	0.7
IRA 743	0.45	0.5	7.0	0.8

4.3.4. Non-linear chromatography modeling

4.3.4.1. Non-linear model

The non-linear model is based on a mass balance calculated from a column experiment:

$$u\epsilon C_{tot}x + u(1-\epsilon)Qy - [u\epsilon C_{tot}x_0 + u(1-\epsilon)Qy_0] = tFC_{tot}x - t_0FC_{tot}x_0 \quad \text{EQ 4.3}$$

with

x: molar fraction of the solute in the liquid phase

y: molar fraction of the solute in the solid phase

ϵ : void fraction or porosity of the resin bed

t: time to exit out of the column (s)

t_0 : residence time of non-reactive tracer (s)

u: velocity (m s⁻¹)

Q: resin capacity (mol m⁻³)

$$F = \frac{u}{t_0 \epsilon} \text{ (m s}^{-2}\text{)}$$

C_{tot} : total solution concentration (mol L⁻¹)

The residence time for the exit of the front can be calculated from:

$$t_s = t_0 \left(1 + \frac{1-\epsilon}{\epsilon} \frac{Q}{C_{tot}} \frac{y}{x} \right) \quad \text{EQ 4.4}$$

Table 4.10. Thomas model parameters compared to pseudo-second order model parameters

	Thomas model		Pseudo-second order model	
	K_T (mL mg ⁻¹ min ⁻¹)	q_0 (mmol g ⁻¹)	k_2 (g mmol ⁻¹ min ⁻¹)	q_0 (mmol g ⁻¹)
Ambersep 900-OH	1.1	1.2	5.7	0.7
IRA 743	0.45	0.5	7.0	0.8

4.3.4. Non-linear chromatography modeling

4.3.4.1. Non-linear model

The non-linear model is based on a mass balance calculated from a column experiment:

$$u\epsilon C_{totX} + u(1 - \epsilon)Qy - [u\epsilon C_{totX0} + u(1 - \epsilon)Qy_0] = tFC_{totX} - t_0FC_{totX0} \quad \text{EQ 4.3}$$

with

x: molar fraction of the solute in the liquid phase

y: molar fraction of the solute in the solid phase

ϵ : void fraction or porosity of the resin bed

t: time to exit out of the column (s)

t_0 : residence time of non-reactive tracer (s)

u: velocity (m s⁻¹)

Q: resin capacity (mol m⁻³)

$$F = \frac{u}{t_0 \epsilon} \text{ (m s}^{-2}\text{)}$$

C_{tot} : total solution concentration (mol L⁻¹)

The residence time for the exit of the front can be calculated from:

$$t_s = t_0 \left(1 + \frac{1}{C_{tot}} \frac{Q}{x} \frac{y}{x} \right) \quad \text{EQ 4.4}$$

Hence the velocity of the front is described by the equation:

$$W_s = \frac{Z}{t_s} = \frac{u}{1 + \frac{1-\epsilon}{\epsilon} \frac{Q}{C_{tot}}} = \frac{u}{1 + \rho \frac{1-\epsilon}{\epsilon} \frac{Q}{C_{tot}} \frac{C_s}{C}} \quad \text{EQ 4.5}$$

W_s : front velocity (m s^{-1})

Z : length of the resin bed (m)

ρ : apparent volumic mass of the resin bed (kg m^{-3})

C_s : boron concentration sorbed on the resin (mol g^{-1})

C : boron in aqueous solution at equilibrium (mol L^{-1})

Each concentration front has its own velocity in the column and this value is constant.

The evolution of the velocity depends on the interactions of the molecules with the supports. The batch experiments indicated that the Langmuir-type model could describe the boron fixation with the following parameters (Table 3.3). According to the form of the model, breakthrough curve can be described from the compressive equation while desorption is described by the dispersive equation.

$$R = 1 + \rho_s \frac{\Delta\{C_s\}}{\Delta[C]} \quad (\text{compressive or sharp front}) \quad \text{EQ 4.6}$$

$$R = 1 + \rho_s \frac{S_{\text{Tot}} K_L}{(1 + K_L [C])^2} \quad (\text{dispersive front}) \quad \text{EQ 4.7}$$

The apparent density and the porosity have been calculated from experimental measurements.

Table 4.11. Mass and length in column of 100 mL each resin

Resin	Mass (g)	Volume (mL)	Apparent volumic mass (kg m^{-3})	Porosity
Ambersep 900- OH	64.33	100	643	0.497
Amberlite IRA 743	75.02	100	750	0.762

Boron fixation has been modeled according to the Langmuir parameters determined during the batch experiments (Table 3.3).

Table 3.3. Maximum adsorption capacity, Langmuir-type coefficient, distribution coefficient and correlation coefficients estimated from the Langmuir-type relationship for the two selective resins and the anionic resin Ambersep 900-OH (data from Fig. 3.8). For the Amberlite IRA 402-Cl, linear-type relationship was applied

Resin #	S_{tot} [mmol g^{-1}]	K_L [L mmol $^{-1}$]	K_d [L g^{-1}] [§]	R^2
Amberlite IRA 743*	0.62	1.5	0.90	0.8850
Diaion CRB 03	0.87	3.6	3.1	0.9987
Ambersep 900-OH	2.2	0.051	0.11	0.9517
Amberlite IRA 402-Cl [£]	–	–	0.003	0.9921

* For boron concentration $< 35 \text{ mmol L}^{-1}$

§ Distribution coefficient $K_d = S_{\text{tot}} K_L$

£ Linear-type fitting

4.3.4.2. Non-linear modeling

Ambersep IRA 900-OH Resin

Simulation has been realized in a first time for a concentration of 9 mM and the results compare to experimental results (FIG. 4.25). The calculated retardation factor is of 56 while the experimental one is 76. The difference is really small and can be obtained for a S_{tot} of 2.4 mmol g⁻¹ instead of 2.2 mmol g⁻¹ and a K_L of 0.08 L mmol⁻¹ instead of 0.06 L mmol⁻¹ (optimized model in FIG. 4.25). The dispersive front also correctly described the experimental results, but there is difference due to a shift difficult to explain (FIG. 4.26). The concentration starts to decrease at the same time for experiment and model, but during the experimental elution remained stable at 8.5 mM before finally decreasing with the same trend than describe by the model. It can be also seen that the model is not able to describe the very low concentrations, at the end of the front.

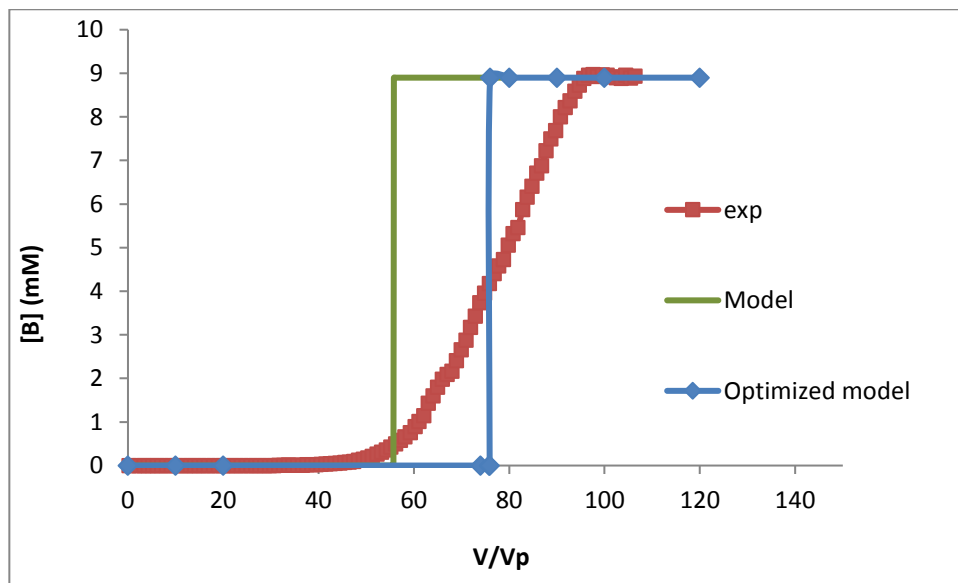


Fig. 4.25. Comparison of boron fixation fronts of model, optimized model and experiment with Ambersep 900-OH using a boron solution of 8.9 mM and a flow rate of 10 BV h⁻¹. Model used the Langmuir-type parameters obtained from batch experiment

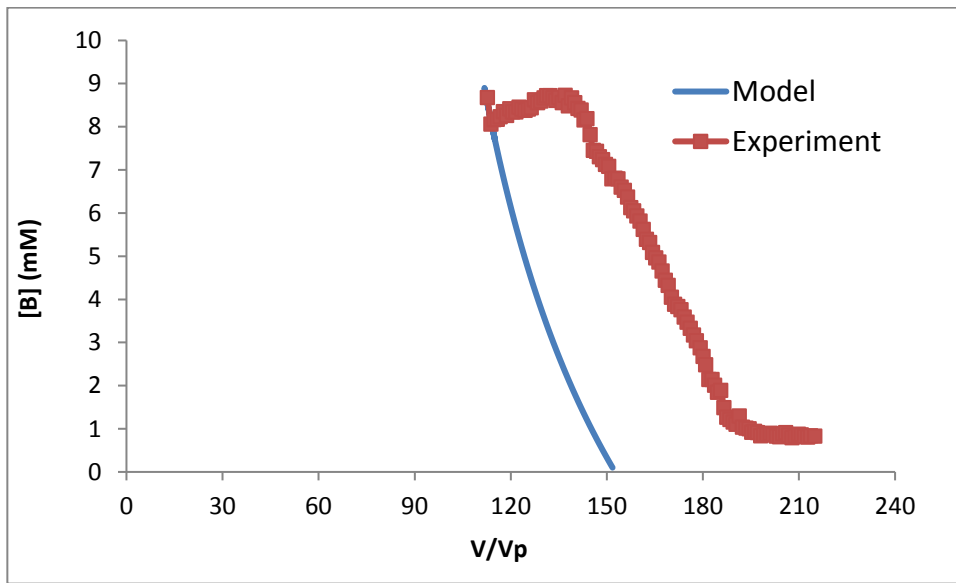


Fig. 4.26: Comparison of boron elution of of model, optimized model and experiment with Ambersep 900-OH using a boron solution of 8.9 mM and a flow rate of 10 BV h^{-1} . Model used the Langmuir-type parameters obtained from batch experiment

Table 4.12: Calculation of the influence of the concentration on the boron retardation factor on the resin Ambersep IRA 900-OH. The model used the Langmuir-type parameters determined from the batch experiments

Concentration (mM)	Retardation factor
1	74
2	70
3	67
4	64
5	61
6	59
7	57
8	54
9	51
10	49

The modeling result indicates that the boron resin interactions can be described according to the Langmuir-type model. Influence of concentration inlet has been therefore modeled and compared to experimental results (TABLE 4.12). Experimental influence of concentration cannot be explained by isotherm theory, since the calculated value for the retardation factor is about 100 at the concentration of 2 mM while the obtained values are about 500 to 600. This large difference shows that other mechanisms are involved in the boron fixation efficiency, and these mechanisms largely increase the boron affinity for the Ambersep 900-OH resin.

Amberlite IRA 743 resin

Simulation has been realized for a concentration of 9 mM and the results compared to experimental (FIG. 4.27). The results show a large difference between the calculated retardation factor (16) and the experimental (50). This difference can be explained by the fixation mechanism that might be not completely described by the Langmuir-type model since the correlation coefficient r^2 was only 0.88. To obtain the same retardation factor, it is necessary to use a value of 2 for S_{tot} instead of 0.62, calculated from batch experiments.

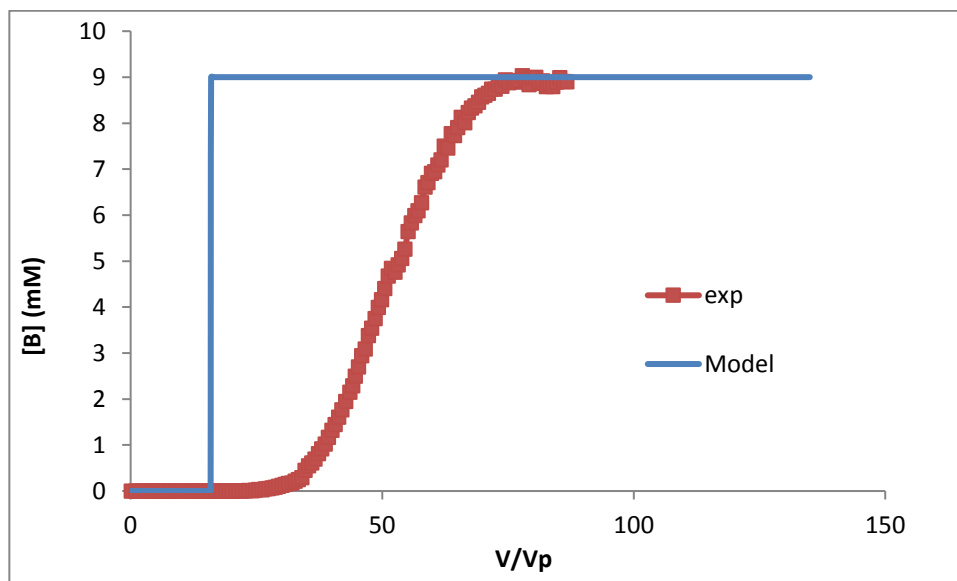


Fig. 4.27. Comparison of model and experiment for boron fixation front with Ambersep IRA 743 with a boron solution of 9 mM and a flow rate of 10 BV h⁻¹. Model used the Langmuir-type parameters obtained from batch experiment.

Another factor that can explain the difference between model and experiment is the value of the pore volume, V_p that is very high (0.76) compare to the results obtained for Ambersep 900-OH that is 0.50. Model could fit experimental results for IRA 743 if the V_p value was 0.54 instead of 0.76.

Bibliographic analysis of previous studies indicates that the V_p has been evaluated to 0.68 (Simonnot *et al*, 2000). The model, using Langmuir-type parameter values from our batch experiments and the V_p value from works of Simonnot and co-workers, presents a better fitting of our experiment results. Furthermore, this model can correctly fit the Simonnot and co-workers experiment results. The description is good for the concentrations above 1 mM but failed for the concentrations below, particularly for the concentration of 0.1 mM (TABLE 4.13). This trend is similar to the conclusion obtained during the simulation of the dispersive front with Ambersep 900-OH.

Table 4.13: Comparison of the influence of the concentration on the boron retardation factor for model and experiment results of Simonnot and co-workers. Models used the Langmuir-type parameters obtained from batch experiments

Concentration (mM)	Retardation factor		
	Simonnot	Model with V_p of 0.68	Model with V_p of 0.54
0.1	2000	300	530
0.3	650	230	420
0.5	400	192	346
1	200	134	241
2	85	84	150
5	45	40	71
10	25	22	38

This large difference could be explained by the fact that two mechanisms would be involved in boron fixation, at low concentration and high concentration.

4.3.5. Conclusion

Boron fixation was studied on both resins with different influence factors. The research on influence of flow rate for Amb 900-OH is not successful because of unreasonable result obtaining from experiment of 1.8 mM, 60 BV h⁻¹, pH 8 which probably due to the remaining of chloride ions in the resin. For Amb IRA 743, it is indicated that at higher flow rate, the breakthrough curve appears more quickly than that of slower flow rate. At slower flow rate, boron has more time to contact with adsorption sites of resin and ion exchange process proceeds longer, then the retardation remains later. The influence of resin bed volume for Amb 900-OH resin also showed that the sorption capacity increased with an increase of resin dose. Similar results achieved with the study of inlet boron concentration on boron removal of Amb 900-OH resin. The sorption capacity of experiment using 9.0 mM B (0.51 mmol B mL⁻¹ resin) is higher than that of experiment using 1.8 mM (0.40 mmol B mL⁻¹ resin) at the same given experiment condition. However, a repetition of experiment using 9.0 mM should be done to obtain the mass balance between adsorption and desorption and make sure the result. pH and conductivity of each experiment was also followed to have better understanding about the ion exchange process, to explain the change in behavior of boron breakthrough curves. A comparison about the boron fixation efficiency between two resins at the same experimental condition was presented. The Amb 900-OH resin has higher capacity of boron fixation (0.51 mmol B mL⁻¹ resin) with the anionic-exchange mechanism than that of Amb IRA 743 (0.36 mmol B mL⁻¹ resin) even boron under the tested conditions was on neutral form. In the case of seawater, with a large competition between all the anions, it maybe supposed that the efficiency of Amb 900-OH would sharply decrease while it will not change for the specific resin. Tests with mixture solutions would assess this hypothesis. High column utilization (90%) was observed for resin Amb 900-OH at all flow rate while maximum 63% column utilization was reached for Amb IRA 743 at flow rate of 10 BV h⁻¹. The flow rate 60 BV h⁻¹ is not applicable for this resin.

Yoon and Nelson model and Thomas model were chosen to fit with the experimental data of two resins. It is concluded that both models are well fitted with experiments with similar sorption capacities. These models can be used to optimize the breakthrough curves for experiments using both resins. Non-linear model using Langmuir parameters from batch experiment can be used to simulate well for the compressive front of Amb 900-OH. There is a small shift between the dispersive fronts of experiment and simulation but they showed the same trend. Boron concentration influence cannot be explained by isotherm theory, which is supposed to have another mechanism that largely increases boron affinity on resin. Non-linear model does not simulate well the compressive front of experiment using Amb IRA 743 resin due to a large difference in calculated and experimental retardation factor. Possible reasons should be Langmuir isotherm only fits for a small range of boron concentration in solution (< 35 mmol L⁻¹) and a large value of pore volume. Calculated retardation factor using smaller V_p from Simonot's publication showed a better-fitted simulation with our experiment.

Chapter 5

PECTIN EXTRACTS FOR BORON

REMOVAL IN WATER

(Written as a publication)

5.1. Introduction

Seawater desalination is usually performed by reverse osmosis, but it is ineffective to reject boron from seawater under normal pH conditions. Elevation of the pH produces borate ions that can be rejected by the membrane, but it leads to scaling, corrosion and higher costs. An alternative is the use of specific resins that contain polymers with the vicinal polyalcohol function groups, which are reportedly the most efficient ligands for the complexation of boron in aqueous solutions. Amberlite IRA-743 with the N-methylglucamine function has possibly been one of few commercial resins for the boron-specific removal since the 1970's (Wei *et al.*, 2011). The operational cost and capacity loss during the regeneration make the resin less economically attractive. Furthermore, most polymer-supported resins are based on the copolymers of styrene and divinylbenzene, which often limit their efficiencies due to their strong hydrophobic properties (Wei *et al.*, 2011).

The principle of boron selective resins is the use of a complexation reaction. Boric acid and borate ions react with compounds possessing multihydroxyl groups (polyols) to form a variety of borate esters. The esters formed rapidly, liberating protons into the solution, which are then partially captured by N-methylglucamine group on the resin. Thus, the amount of acidification produced upon the addition of the polyols is proportional to the extent of ester formation (Hilal *et al.*, 2011).



Adapted from (Hilal *et al.*, 2011)

It is also possible to combine two separation mechanisms, sorption on fine bodies and membrane separation of boron-loaded bodies. Adsorption membrane filtration systems can combine microspherical sorbents and microfiltration membranes or polymer adsorption followed by separation on ultrafiltration/nanofiltration membranes. Polymers, selective for boron removal have been synthesized by the attachment of sugar-like ligands to the polymeric chains and separated by ultrafiltration. The profit of this method is high efficiency and fast kinetic but limited by membrane fouling and regeneration of water-soluble polymers (Wolska & Bryjak, 2013). A solution would be the use of biodegradable polymers like chitosan. The amine and hydroxyls groups of chitosan usually serve as the primary sites for the surface modification. The produced bead of chitosan had a maximal capacity of 3.25 mmol g⁻¹ with an optimum at neutral pH (Wei *et al.*, 2011). Boric acid reacts with alcohols forming boron esters and/or neutral cis-diol monoborate esters or monoborate complexes with sugars (Dembitsky *et al.*, 2002). Boron also interacts with polyhydroxy polymers to form borate-polymer cross-links. Large polysaccharide molecules have many boron-binding sites and produce a multinet complex, cross-linked by the borate groups (Loomis & Durst, 1992).

Matoh *et al.* (1992) presented evidence that boron is localized in the cell wall, where it may be largely bounded to cellular pectins (Yamauchi *et al.*, 1986) (Matoh *et al.*, 1992). Research on squash and tobacco indicated that under boron limiting conditions, boron in cell wall represented 95% of cellular boron. The majority of this cell wall boron (70%) was associated with pectin (Hu and Brown, 1994) (Hu *et al.*, 1996).

Pectins are known as complex polysaccharides, which are found in cell walls of higher plants. They function as a hydrating agent and essential material for the cellulosic network. The highest concentration of pectin is in the middle lamella, which accounted for one third of the cell walls, with a gradual decrease from primary cell wall toward the plasma membrane. Pectins are found in large amounts in soft plant tissues under condition of fast growth and higher moisture content. It seems that pectin is important factor in control of the movement of water and plant fluids (Thakur *et al.*, 1997).

The firming effect of pectins in tissues consist of two phenomena: in fresh tissue, the formation of free carboxyl groups increases the possibilities and the strength of calcium binding between pectin polymers and in heated tissue, there is a combination of increased calcium binding and a decrease in the susceptibility of the pectin to depolymerization by β -elimination (Sajjaanantakul *et al.*, 1989). The softening during the ripening of fruits is explained by the enzymatic degradation and solubilization of the protopectin. The textural changes occur when cell wall pectins are hydrolyzed by polygalacturonases (Dellapenna *et al.*, 1986). Besides formation of plant cell walls, pectin also influences various cell wall properties such as porosity, surface charge, pH, and ion balance and therefore are important to the ion transport in the cell wall (McNeil *et al.*, 1984).

Pectins are copolymer of D-galactorunic acid and rhamnogalacturonan. The molecule is formed by L-1,4-glycosidic linkages between the pyranose rings of D-galactorunic acid units. Pectins contain branched block and unbranched block polymers in which branched blocks contain a main galacturonan chain interrupted and bent by frequent rhamnose units (carrying side chains) while unbranched blocks has several or no rhamnose. Rhamnogalaturonan is primarily responsible for the chemical and structural complexcity of the pectic substance. Rhamnosyl insertion acts as junction during gelation. Neutral sugars occur in the side chains of pectin, for example, D-galactopyranose, L-arabinofuranose, D-xylopyranose, D-glucopyranose, D-apiose, 2-O-methyl-D-xylose, 2-O-methyl-fucose. These natural sugars account for 10 to 15 % pectin mass.

Pectin structure contains of 4 different types of polysaccharides: Rhamnogalactorunan I, rhamnogalactorunan II, homogalaturonan, xylogalacturonan. RG-II is known as self-associated by forming RG-II dimers via a boron ester bond (FIG. 5.1).

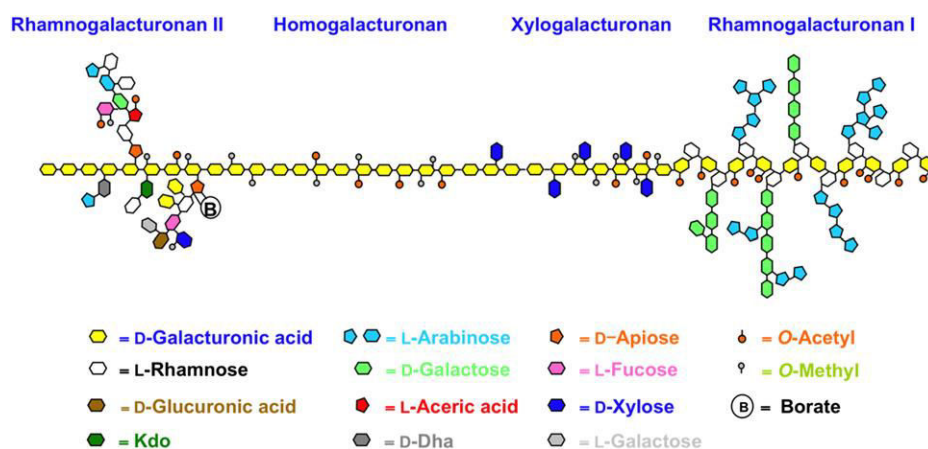


Fig. 5.1. Description of the interaction between pectin and boron.

From (Harholt, Suttangkakul, scheller, 2010).

Homogalacturonan (HG): HG is the major type of pectin in cell walls, accounted for almost 60% of the total pectin. The HG polymer consists of a backbone of α -1,4-linked galacturonic acid (GalA) residues. Some of GalA in this backbone was esterified (C-6) and O-acetylated (O-2 and O-3) which decided the physical properties of the pectin. A block of 10 non-esterified GalA residues make pectin molecule be sensitive with calcium cations crosslink (Daas *et al.*, 2001) (Gee *et al.*, 1959) (Mort *et al.*, 1993).

Xylogalacturonan (XGA): XGA is the substitution of β -D-Xylp-(1-3) single unit side chain into the HG. The degree of xylosidation varies from 25% to 75% depending on different sources of pectin. Methyl esters are equally distributed among the substituted and unsubstituted GalA residues. Part of the GalA residues in XGA is methyl-esterified (Schols *et al.*, 1995).

Rhamnogalacturonan I (RG-I): RG-I consists of a backbone, which is the repetition of [\rightarrow 2)- α -L-Rhap-(1 \rightarrow 4)- α D-GalpA-(1 \rightarrow)] unit. Depending on the pectin source and extraction conditions, the number of repetitive unit can vary from 20 to 300 units. The rhamnosyl residues of RG-I can be substituted at O-4 with neutral sugars side chains. The sugar side chains usually compose of galactosyl and/or arabinosyl residues. The proportion of Rha residues is from 20 to 80%. RG-I contains 40% methyl esters but GalA residues of RG-I are presumably not methyl esterified because RG-I is not degraded under β -eliminative condition (Rihouey *et al.*, 1995) (Lau *et al.*, 1987).

Rhamnogalacturonan II (RG-II): RG-II is a highly conserved structure in the plant and can be released by endopolygalacturonase action. RG-II structure is a cluster of four different side chains with very peculiar sugar residues such as, apiose, aceric acid, 3deoxy-lyxo-2-heptulosaric acid (DHA) and 3deoxy-mano-2-octulosonic acid (KDO). These side chains are attached to a HG fragment consists of nine galacturonic acid residues in which some are methyl-esterified (Ishii and Matsunaga, 2001) (Ridley *et al.*, 2001). RG-II can complex with boron, forming a borate-diol ester,

arabinose (Sigma Aldrich), galactose (VWR), galacturonic acid (Fluka Chemie), were prepared to determine the samples concentration.

The viscosity of the pectin extract solution was measured with a capillary a viscometer (Cannon No. 75) was employed. A water bath accompanying with a heat control system and a thermometer were utilized to keep the temperature of water bath as constant at 40 °C.

To study the pectin filtration efficiency of the using membranes, two kinds of ultrafiltration apparatus were used. At the first time, a stirred ultrafiltration cell (Amicon), with a volume of 100 mL, was employed for the screening of the membranes. A gauge, on the pressured air feed, controlled the pressure cell while a mixer is used to limit the creation of a polarization layer. Three types of flat sheet membranes with a MWCO of 10, 30, 100 kDa (Millipore) were evaluated.

At the second time, filtration was performed at a larger scale using a polyethersulfone membrane with a MWCO of 30 kDa (GE Healthcare) and a filtration area of 0.085 m² was used. This membrane was hollow-fiber type whose fibers had an internal diameter of 0.5 mm, a length of 60 cm and the module contained 50 fibers. This ultrafiltration system was built in the laboratory with a tri-piston pump, a valve to control the pressure and pressure gauges on feed, retentate and permeate. Both retentate and permeate was recycled in the 5 L feed tank in order to work under steady state conditions. Different trans-membrane pressures, from 0.4 to 2 bar, were tested with the same solution. At each pressure, mass flux was recorded until getting steady-state. A sample was taken at each steady condition for further analysis.

5.2.2. Methods

5.2.2.1. Pectins characterization

Pectins have been characterized according to the NREL protocol defined for sugar analysis in lignocellulosic plant. The procedure includes a polymer hydrolysis step, followed by an HPLC analysis step.

5.2.2.1.1. Pectin hydrolysis

300.0 ± 10.0 mg of dry pectin were weighed in a pressure tube. 3.00 ± 0.01 mL 72% sulfuric acid was added in each pressure tube (sample & blank). Mixture was mixed using Teflon stir rod during 1 min. Pressured tubes were introduced in a water bath set 30 ± 3 °C during 60 ± 5 min. Every five minutes the sample was stirred without removing it out of the bath. This step was essential to get a uniform hydrolysis. After removal from water bath, 84.00 ± 0.04 mL Milli-Q water was added in order to dilute to 4% acid and the tube covered by a Teflon cap. The tubes were placed in an autoclave for one hour at 121°C and then allowed to slowly cool to near room temperature before removing the caps.

A sugar recovery standards (SRS) set was prepared in order to correct for losses due to destruction of sugars during dilute acid hydrolysis. SRS should include, D-(+)glucose, D-(+)xylose, D-(+)galactose, L-(+)arabinose, D-(+)mannose. SRS sugar concentrations has been chosen to most closely similar concentrations of sugars in the evaluated samples. The SRS set was submitted to the same treatment than the samples.

5.2.2.1.2. Sugar and galactorunic acid analysis

20 mL of the hydrolyzed liquor was transfer in a 50 mL Erlenmeyer flask and CaCO₃ powder was added to neutralize the sample to pH 5 – 6. After decantation of the insoluble salts, the liquid was filtered through a 0.2 µm filter into an autosampler vial. This solution was used as the sample for HPLC analysis.

50 µL of sample was injected in the HPLC system (Varian) composed of a polar column (Phenomenex Rezex RHM H⁺). Sample was eluted with 0.005 M H₂SO₄ mobile phase at flow rate of 0.6 mL min⁻¹ and a column temperature of 65 °C. Detection was performed by refractive index. Analysis duration is 50 min, and each sample was analyzed in triplicate.

A series of calibration standards have been prepared in TABLE 5.1.

Table 5.1. Suggested concentration ranges for calibration standards

Component	Suggested concentration range (mg/mL)
D-cellobiose	0.1-4.0
D(+)-glucose	0.1-4.0
D(+)-xylose	0.1-4.0
D(+)-galcatose	0.1-4.0
L(+)-arabinose	0.1-4.0
D(+)-mannose	0.1-4.0
CVS	Middle of linear range, concentration not equal to a calibration point

5.2.2.1.3. Viscosity measurement

Diluted pectin solution viscosity was measured with a capillary a viscometer (Cannon No. 75) while the non-Newtonian parameters have been defined for high concentration solutions. The kinetic viscosity was measured at 40 °C in a water bath. Pectin solution was collected before and after filtration.

Procedure (see more in appendices)

Prepare a clean viscometer. Charge the sample by inverting the viscometer, apply suction to tube arm L, immersing tube N in the sample solution and draw liquid to mark G. Turn the viscometer in the normal direction. Put viscometer vertically in the water bath 40 °C, make sure that most of the viscometer is under the water. Allow the sample flow through capillary R and approximately half-

filled bulb A, stop the meniscus in bulb A by placing a rubber stopper in tube N. Allow the viscometer in the water about 10 min for sample to get 40 °C, make sure the meniscus in bulb A does not reach line E. Remove the rubber stopper and allow the meniscus to pass from mark E to F, from F to I. Record the passing time in seconds (efflux time).

$$\text{Kinetic viscosity} = \text{Efflux time} * \text{viscometer constant}$$

The viscometer constant at 40 °C for bulb C and D: 0.007769 (mm² s⁻²), 0.007257 (mm² s⁻²).

As polarization concentration could appear leading to high concentrations at the membrane surface, solutions with a concentration of 20 g L⁻¹ and 40 g L⁻¹ was prepared. Rheological properties of these solutions were measured with a disk viscometer (MC301, Anton Paar).

5.2.2.1. Boron fixation on hybrid method

5.2.2.1.1. Ultrafiltration evaluation on Amicon cell and hollow-fiber system

At small scale (Amicon cell), permeability of the three membranes was evaluated with water by measuring the permeate flux at different pressure. Then filtration efficiency has been characterized with batch extracted pectin solution at 1 bar pressure and different stirring speeds. Pectin extract solution was prepared by adding 5 g of pectin extract powder into 100 mL Milli-Q water in an Erlenmeyer flask, then agitated in 2 h at 260 rpm. The mixture then was introduced in the filtration cell. Pressure was adjusted with the valve to the desire value. Permeate was continuously recovered, leading to the reduction of the volume of the solution remaining in the cell and therefore to the concentration of the retained molecules. Filtration was managed with membrane of 0.003 m² of filtration area. Samples were regularly taken in order to follow the evolution of the membrane performance. Mass of each sample was measured in order to get a mass flux. As the permeate flux was low, the recovered mass was very low compare to the initial volume and it has been assumed that there was no change in pectin concentration. Tests were done at different transmembrane pressures with all types of membranes.

At larger scale (hollow fiber system) filtration was done by recycling both permeate and retentate to maintain constant the concentration in the feed tank. It is therefore possible to reach pseudo-steady state. Different transmembrane pressures, from 0.4 to 2 bars, were tested with the same solution. At each pressure, mass flux was recorded until getting the steady state. A sample was taken at each steady condition for further analysis.

5.2.2.1.2. Boron fixation at different pH

5.2.2.1.2.1. Pectin with Milli-Q water

This experiment was designed to determine how much boron was already stored by pectin extract. 100 mL Milli-Q water was introduced in each Erlenmeyer flask. pH of each solution has been adjusted using sodium hydroxide or nitric acid to get pH from 2 to 12. 2.0 g of dry batch extracted pectin or 0.5 g of dry twin-screw extracted pectin was added pH measurement was performed before mixing in order to get the initial pH. The flasks were then agitated during 2 h at 260 rpm using HS 501 digital (IKA Labortechnik) agitation machine. After 2 h, the solution pH was measured in order to get final pH. Each sample was then centrifuged during 15 min at 8000 rpm using centrifugation machine 6-16 K (Sigma), T = 20 °C. The solution was separated from the residues in centrifugation tubes, then filtered using a syringe and PTFE 0.45 µm filter. The solution after filtration was brought to determine non-fixed boron in pectin.

5.2.2.1.2.2. Pectin with boron solution

100 mL of 100 mg L⁻¹ boron solution was introduced in each Erlenmeyer flask pH of each solution has been adjusted using sodium hydroxide or nitric acid to get pH from 2 to 12. 0.5 g of dry batch extracted pectin or 2.0 g of dry twin-screw extracted pectin was added. pH measurement was performed before mixing in order to get the initial pH. Similar procedure was repeated as in experiment between pectin and water. Final pH and filtered solution was obtained to determined boron concentration.

5.3. Results and discussion

5.3.1. Pectin characterization

Two kinds of pectin above (batch extracted and twin-screw extracted) have been used for boron fixation. These pectins were produced by specific procedures developed in the laboratory. They have been characterized by their sugar composition, but their purities are very low because it was crude extract.

The extracts have been produced for the valorization of residue and were not industrially produced. Their compositions are quite different, particularly the galacturonic acid is twice higher for batch extracted sample but without glucose compared to those in twin-screw extracted pectin. The galactose concentration is very similar (8 and 10%). The sugar purity is low in both cases at about 47% and the other molecules are still not identified. Part of these molecules can be phenolic and polyphenolic compounds that may also fixe boron molecules.

Table 5.2. Composition of the pectin extracts used for the boron fixation.

Components	Twin-screw extracted pectin (%)	Batch extracted pectin (%)
Glucose	9.8	Non detected
Galactose	10.2	8.0
Arabinose	15	17.3
Galacturonic acid	11.9	22.7

5.3.2. Ultrafiltration

5.3.2.1. Membranes screening

5.3.2.1.1. Membrane permeability

It is necessary to characterize the water membrane permeability of the three membranes in a first time. Flow rate is usually given for one square meter filtration area in order to compare membranes that might have different size (EQ 5.2):

$$J = \frac{Q_p}{S} \quad \text{EQ 5.2}$$

where J is the permeate flux ($\text{kg h}^{-1}\text{m}^{-2}$), Q_p is the permeate flow rate (kg h^{-1}) and S (m^2) is the filtration area.

The permeability is usually calculated from EQ 5.3:

$$J = L_p \Delta P \quad \text{EQ 5.3}$$

where L_p is the hydraulic permeability ($\text{kg h}^{-1}\text{m}^{-2}\text{bar}^{-1}$) and ΔP the transmembrane pressure (bar).

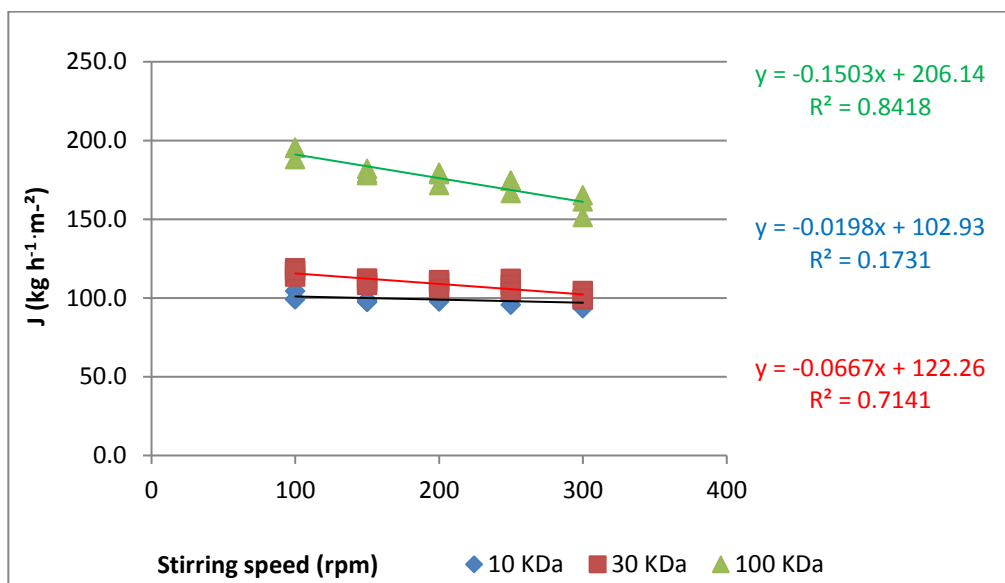


Fig. 5.3. Influence of the stirring velocity on the membrane permeability during the filtration of water with three membranes with a MWCO of 10, 30 and 100 kDa.

The obtained fluxes slightly decreased when the stirring velocity is increased (Fig. 5.3). These results are usually explained by hydrodynamic influence over the membrane. The bigger the MWCO is, the higher the permeate flux is. 100 kDa membrane has a flux of about $170 \text{ kg h}^{-1} \text{ m}^{-2}$ while it is only about $100 \text{ kg h}^{-1} \text{ m}^{-2}$ for the two other membranes. The difference in permeate flux between the two later membranes is small but this can be explained by the conditions of fabrication (Jorda *et al.*, 2002)

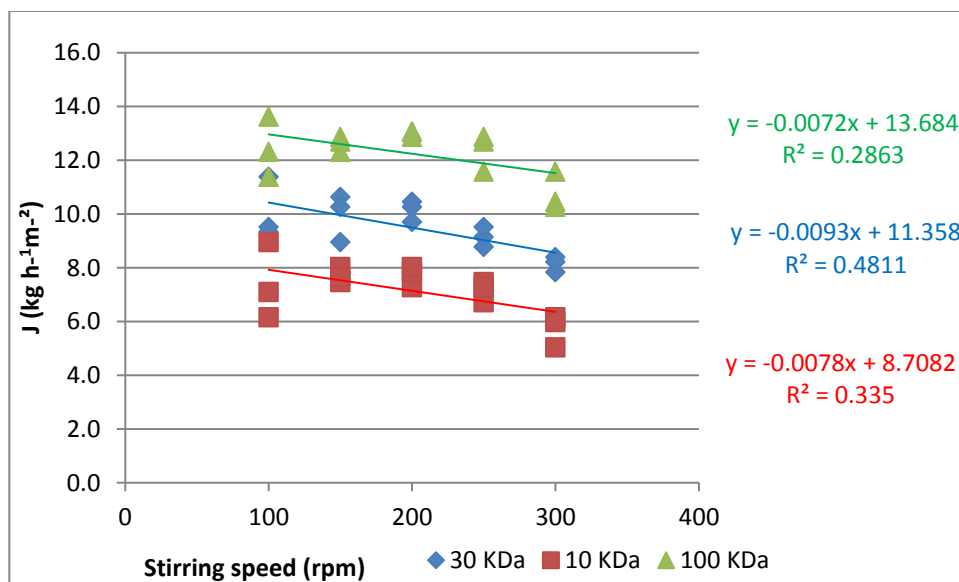


Fig. 5.4. Permeate flux evolution versus the stirring velocity during the filtration of a 5 g L^{-1} pectin solution with three membranes with a MWCO of 10, 30 and 100 kDa at the temperature of $25 \text{ }^\circ\text{C}$ and the transmembrane pressure of 1 bar.

The permeate flux sharply decreases during the filtration of pectic solutions, compared with water. The obtained values are around $10 \text{ kg h}^{-1} \text{ m}^{-2}$. The highest value, ($12 \text{ kg h}^{-1} \text{ m}^{-2}$) is obtained with

the 100 kDa membrane, followed by the permeate flux of the 10 kDa membrane with value of about $10 \text{ kg h}^{-1} \text{ m}^{-2}$. There is almost no difference between all the membranes. This result is regularly presented during polymer filtration because of limitations, polarization concentration layer over the membrane and the viscosity increasing just above the membrane that does not depend on the membranes. The polarization layer appears difficult to remove, therefore, the mixing velocity does not changes the value of permeate flux (Fig. 5.4).

From EQ 1.32 ($J = \frac{TMP}{\mu R_h}$), it comes:

$$\frac{J_{water}}{J_{pectin}} = \frac{\mu_{pectin}}{\mu_{water}} \quad \text{EQ 5.4}$$

$$J_{pectin} = J_{water} * \frac{\mu_{water}}{\mu_{pectin}} \quad \text{EQ 5.5}$$

At $40 \text{ }^\circ\text{C}$, $\mu_{water} = 0.6579 \text{ (mm}^2 \text{ s}^{-1}\text{)}$. Kinematic viscosity of pectin solution was measured in a hot water bath ($40 \text{ }^\circ\text{C}$) by using capillary viscometer Cannon N₀. 75, its value is $0.87 \text{ (mm}^2 \text{ s}^{-1}\text{)}$.

In addition, the hydraulic permeability of the membranes is calculated from the water fluxes according to the EQ 5.3. The hydraulic permeabilities of three membranes with water, pectin solution and calculated value were presented in TABLE 5.3.

Table 5.3. The hydraulic permeabilities of the membrane with water and pectic solutions

Membrane	Water ($\text{kg h}^{-1} \text{m}^{-2} \text{bar}^{-1}$)	Pectic solution ($\text{kg h}^{-1} \text{m}^{-2} \text{bar}^{-1}$)	Calculated ($\text{kg h}^{-1} \text{m}^{-2} \text{bar}^{-1}$)
10 kDa	100	7	75
30 kDa	110	9	83
100 kDa	170	12	129

The permeabilities obtained with the pectin solutions are smaller than those obtained with water filtration (TABLE 5.3). This difference could be explained by the viscosity difference between water and pectin solutions, but the results indicate that experimental values are far below than the theoretical one. The difference could be due to the apparition of a concentration polarization layer. During the filtration, the concentration polarization over the membrane induces a large change of the viscosity of the solution at the membrane surface and creates an extra resistance to mass transfers that could explain the low permeability values.

5.3.2.1.2. Influence of the pressure

The influence of the pressure has been studied in order to confirm the existence of the concentration polarization layer. The results show that the permeate flux increases with the increase of the trans-membrane pressure until a limit value of 1 bar (Fig. 5.5).

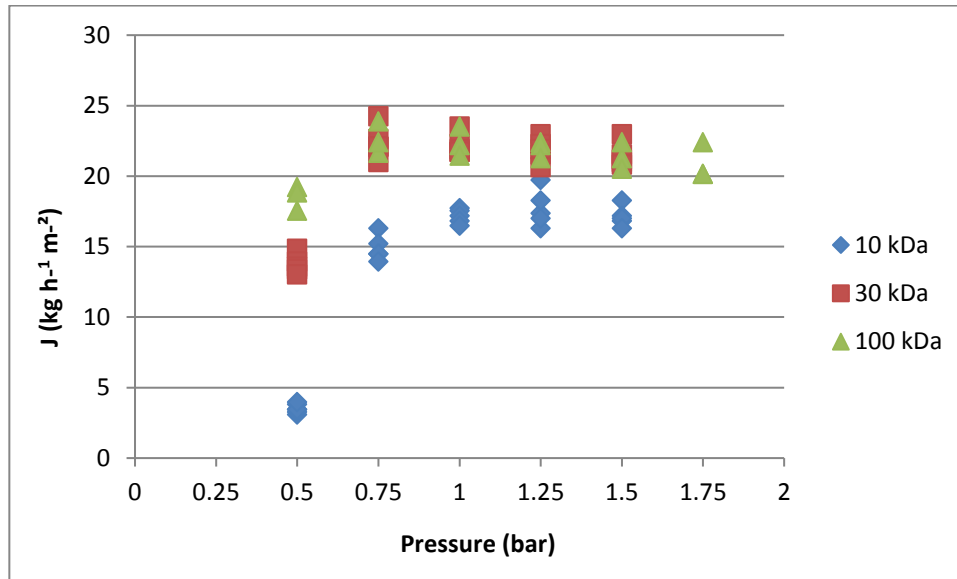


Fig. 5.5. Influence of the pressure during the filtration of pectin solution

Above the limit value of 1 bar, the flux does not increase with increased pressure. This result is usually described during the filtration of polysaccharide that tends to form a gel layer during ultrafiltration. The structure of the gel often has a large influence on the filtration performances (Jorda *et al.*, 2002). This hypothesis could explain the low difference between the three membranes.

This result confirms the conclusions obtaining in previous studies and also proves that the most efficient membrane is the 30 kDa membrane. This membrane allows getting more similar fluxes than the other membranes with a higher rejection rate of the pectin, far higher than the rejection obtained during the ultrafiltration with a 100 kDa membrane (Jorda, 2003).

5.3.2.2. Membrane performance evaluation

A continuous filtration experiment has been managed with a larger size system, with membrane having MWCO of 30 kDa, surface area of 0.085 m^2 , in order to confirm the initial results. The filtration has been realized with a hollow-fiber membrane of 0.5 mm of lumen. This kind of membrane has been used in order to reduce the thickness of the gel layer and to obtain the highest permeate flux. The tests have been realized with the two kinds of pectin. The tested solution has a concentration of 5 g L^{-1} .

5.3.2.2.1. Batch extracted pectin

Filtration has been started at the pressure of 0.4 bar, and flux measured regularly until the values became constant. Samples were taken, then the pressure in the system increased to 0.6 and pressure remained constant until steady state. This procedure has been repeated until 2 bar. The permeate fluxes obtained for each steady state are presented in Fig. 5.6 for two tangential velocities (0.25 and 1.5 m s⁻¹).

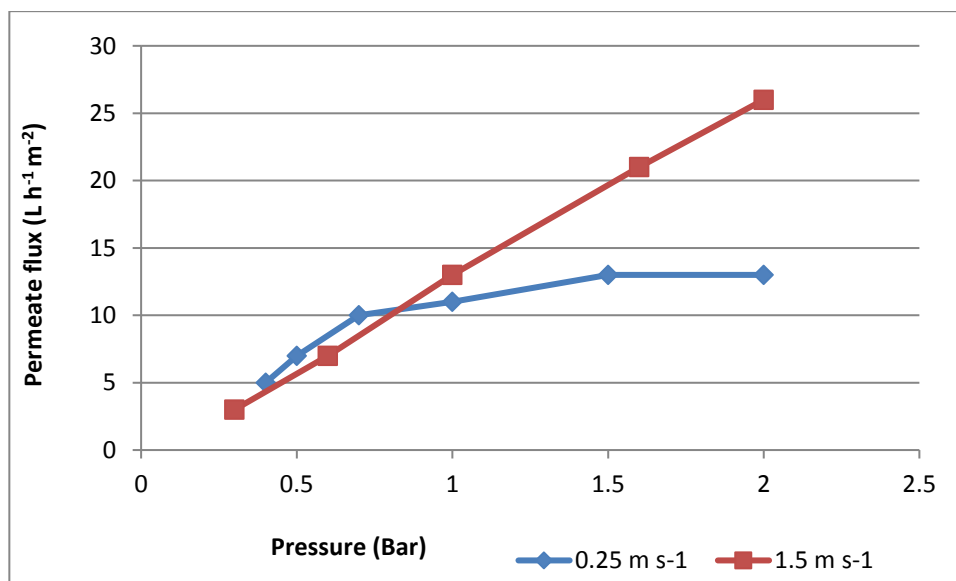


Fig. 5.6. Influence of the pressure on the permeate flux at steady state during the filtration of a 5 g L⁻¹ pectin solution at 25 °C. Pectin has been extracted in batch condition.

The permeate flux increased linearly with pressure until a maximum value of 26 L h⁻¹ m⁻² for the transmembrane pressure of 2 bars when filtration was performed with the highest tangential velocity. This result indicates that there is no polarization limitation. The flux evolution was completely different when filtration was operated at low tangential velocity. Increased permeate is non-linear and became unchanged from the pressure of 1.5 bar, indicating the apparition of a gel layer at the surface of the membrane. This pressure is defined as the limit pressure under these conditions. The polarisation layer was removed when filtration was performed at a higher shear rate with the velocity of 1.5 m.s⁻¹.

5.3.2.2.2. Twin-screw extracted pectin

Filtration has been managed in the same condition with the pectin extracted by twin-screw extrusion at the tangential velocity of 1.5 m s⁻¹.

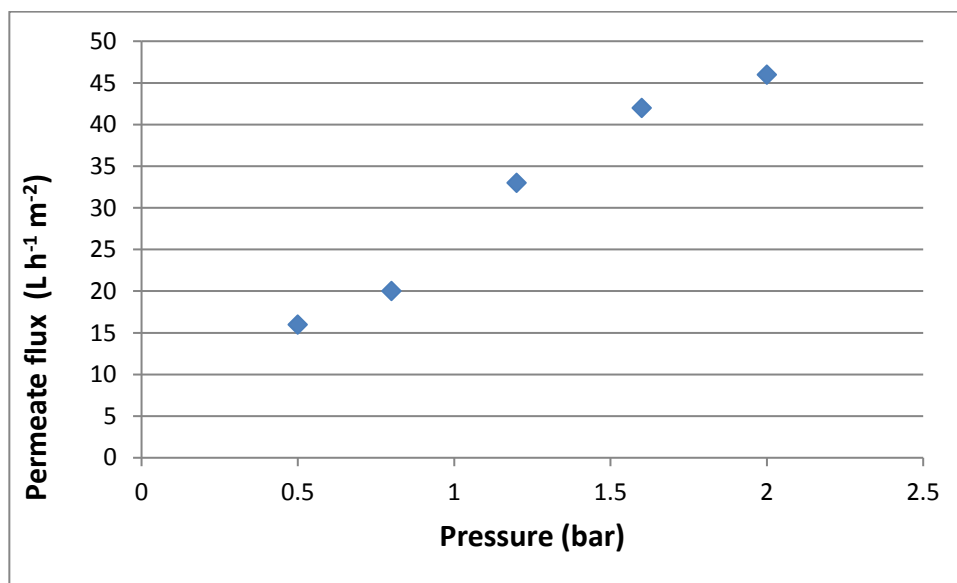


Fig. 5.7. Influence of the pressure on the permeate flux at steady state during the filtration of a 5 g L⁻¹ pectic solution at 25 °C. Pectin have been extracted by twin-screw extrusion.

The results show that the permeate flux increased almost linearly from 15 L h⁻¹ m⁻² at 0.4 bar to 46 L h⁻¹ m⁻² at 2 bar (Fig. 5.7). The value obtained at 0.4 bar is little higher than that obtained with the cell filtration, but increased to the value of twice higher at 2 bar without any asymptotic form. This result indicates that there was almost no concentration polarization layer on the surface of the membrane, which appeared in the cell experiment. The lumen of the membranes allows having a shear effect, high enough to limit the apparition of the gel layer.

5.3.2.3. Discussion

The results obtaining from filtration showed that pectin filtration could be managed with an ultrafiltration membrane of 30 kDa molecular weight cut-off. Filtration of the pectin solution required to be managed at high shear rate in order to avoid the apparition of a gel layer that would limit the membrane performance. The permeate flux of this membrane is of 26 L h⁻¹ m⁻² and 46 L h⁻¹ m⁻² at 2 bar for the batch extracted and twin-screw extracted pectin, respectively. The difference between the two solutions can be explained by the composition of the extract, and its influence on the rheological properties. The batch extracted pectin presents a higher tendency to form a gel, at lower concentration, which could induce a larger flux limitation.

5.3.3. Boron fixation

5.3.3.1. Fixation experiment

5.3.3.1.1. Twin-screw extracted pectin

Tests have been first managed on the twin-screw extracted pectin at different pH values, from pH 5 to pH 12. Two grams of pectin were mixed in 100 mg Milli-Q water to determine the amount of boron that already exists in extracted pectin (B_1). The same amount of twin-screw extracted pectin was also added to 100 mL of 100 mg L^{-1} boron solution and then the boron concentration in aqueous solution after adsorption was determined (B_2). Finally, amount of sorbed boron per mass of pectin was calculated (TABLE 5.4).

The results show that the boron fixation efficiency is low in a large range of pH (from 5 to 12), ranging from 3% to 14%, corresponding to sorption capacity from 0.1 to 0.6 mg g^{-1} which is lower compared to that obtaining from batch experiment of boron selective resin IRA 743 (6.7 mg g^{-1}), CRB 03 (9.4 mg g^{-1}), and anionic resin Amb 900-OH (23.8 mg g^{-1}). This low removal efficiency may be explained by the heterogeneity of the produced powder because pectin content only accounted for 47% of the extracted pectin component, other part could be the impurities, which have no contribution on boron removal process. pH after adsorption strongly reduced with solutions having high initial pH (initial pH 12) and remained unchanged with low initial pH (initial pH 5). This could be due to the highest contribution of galacturonic acid in pectin extract component, which exposed acid property when mixing into solution.

In addition, low boron fixation can be due to the high selectivity of boron with only small available content of RG-II in pectin. Boron plays a very important role in development of plant because boron forms borate ester with rhamnogalacturonan-II (RG-II) by a covalent cross-link to strengthen and grow the cell wall. Normally, plants have 95% of the RG-II molecules in the dimer form that means 95% RG-II in cell wall already made complex with boron, only 5% of RG-II is free for boron adsorption (Caffall and Mohnen, 2009).

Table 5.4. Boron in pectin, boron adsorbed by pectin, initial & final pH of adsorption experiment between boron solution and dry twin-screw pectin (2.0 g).

pH _{initial}	pH _{final}	B ₁ (mg L ⁻¹)	B ₂ (mg L ⁻¹)	B _{remained} (mg L ⁻¹)	[B] _{initial} (mg L ⁻¹)	[B] _{adsorbed} (mg L ⁻¹)	B] _{adsorbed} (mg g ⁻¹)	% Removal
5.49	5.45	1.27	91.89	90.63	102.2	11.6	0.58	11.4
5.57	5.51	1.30	92.54	91.24	98.27	7.04	0.35	7.16
5.43	5.54	1.26	85.90	84.64	98.27	13.6	0.68	13.8
5.49	5.45	1.13	96.02	94.89	98.27	3.38	0.17	3.44
6.05	6.02	0.97	96.02	95.04	97.90	2.86	0.14	2.92
9.65	7.15	1.13	95.95	94.82	97.73	2.91	0.15	2.98
9.61	7.29	1.36	96.33	94.97	97.73	2.76	0.14	2.82
9.64	7.55	1.61	96.76	95.15	97.73	2.58	0.13	2.64
11.5	7.45	1.24	89.93	88.68	102.3	13.5	0.68	13.2
11.4	7.53	1.71	100.4	98.73	102.3	3.55	0.18	3.47

To check if boron was already fixed in RG-II of pectin, boron concentration in pectin has been determined by extraction in water at different pH (TABLE 5.5).

Table 5.5. Initial pH, final pH, boron content in pectin solution and powder.

pH _{controlled}	pH _{initial}	pH _{final}	B _{pectin} (mg L ⁻¹)	B _{pectin} (mg g ⁻¹)
3.40	5.29	5.56	1.27	0.06
5.30	5.41	5.68	1.24	0.06
7.00	5.65	5.75	1.26	0.06
8.50	5.72	5.70	1.75	0.08
9.20	5.92	5.71	1.24	0.06
9.80	6.18	5.73	1.36	0.06
10.40	7.37	5.87	1.24	0.06
11.46	11.65	9.44	1.71	0.08

Boron content in pectin has been determined at about 0.06 mg g⁻¹ or 60 mg kg⁻¹, which is not far way from boron content of carrot roots cell wall (38.8 mg kg⁻¹) and beet (42.1 mg kg⁻¹) (Matoh *et al.*, 1996).

This result confirms that a certain amount of boron was fixed on the extracted pectin. Furthermore, the pectin extract was not pure and contained other carbohydrates components as well such as cellulose, hemicelluloses and impurities like salt. Moreover, according to previous published result, borate ester in dimer RG-II-B is stable above pH 4 (O'Neill *et al.*, 1996). Therefore, the fixation reaction was not studied in the optimal conditions. The combination of all these causes can explain the low fixation efficiency.

5.3.3.1.2. Batch extracted pectin

Similar to twin-screw pectin extract, determination of the boron content in the batch extracted powder has also been done in different pH (TABLE 5.6).

Table 5.6. Initial pH, final pH, boron content in pectin (0.5 g)

pH _{initial}	pH _{final}	B _{pectin} (mg L ⁻¹)	B _{pectin} (mg g ⁻¹)
2.13	2.07	0.74	0.148
6.25	6.10	0.42	0.084
8.02	7.98	0.36	0.072
10.21	10.03	0.31	0.062
12.30	12.10	0.43	0.086

Boron content ranges from 62 to 84 mg kg⁻¹ at pH above 6, which is higher than that in twin-screw extracted pectin. Especially, this value is much higher at pH 2 (148 mg kg⁻¹). This can be explained by the hydrolysis of borate ester into boric acid and monomer RG-II at pH 2 is better than that at higher pH, therefore higher amount of boron was released.

First, pH of solution before and after adsorption seemed to be unchanged which is different with the strong reduction of pH in solution with twin-screw pectin extract. The content of galacturonic acid in batch extracted pectin is twice higher than that in twin-screw extracted pectin that could explain this difference.

Table 5.7. Boron in pectin, boron adsorbed by pectin, initial & final pH of adsorption experiment between boron solution and dry batch extracted pectin.

pH _{initial}	pH _{final}	[B] _{remained} (mg L ⁻¹)
2.25	2.15	254.07
6.23	6.3	315.80
8.31	8.2	377.28
10.12	10.1	354.81
11.98	12.01	50.90

The results of the boron fixation experiment are difficult to analyze since the final concentration is much higher than the initial concentration (100 mg L⁻¹), except the last value. This may be due to dilution problems. Nevertheless, the final value of the concentration obtained after adsorption, can be compared. It indicates that fixation is better in acid condition, 30% better than in neutral conditions. However, to valid this conclusion, the repetition of this experiment is necessary.

5.3.3.2. Discussion

The fixation results indicate that raw pectin extracts has low boron capacities. The purity and the form of the extracted molecules can explain these results. The capacity that can be calculated is low, at about 0.5 mg g⁻¹ of powder, but considering the purity to be about 50%, it gives a potential capacity of 1 mg g⁻¹ of pectin. This value is still low compared to the capacity of the IRA 743 resin that was about 6.7 mg g⁻¹ of resin. However, an improvement in sorption capacity of pectin can be achieved if a better extraction process was developed to get pectin with a higher purity. Additionally, a hydrolysis of extracted pectin to liberate RG-II from RG-II-B, before carrying out boron adsorption, may be a solution to get higher boron sorption capacity.

5.3.4. Conclusion

The best membrane type for pectin filtration is 30 kDa molecular weight cut-off membrane. In order to avoid the appearance of gel layer and the influence of solution viscosity, the filtration of pectin solution required to be managed at high enough shear rate using hollow-fiber module continuous system. At the same experimental condition (5 g L⁻¹ pectin solution, 2 bar pressure, 2 L min⁻¹ velocity), the permeate flux obtained from batch extracted pectin is twice lower than that of twin-screw extracted pectin, because the batch extracted pectin has more tendency to form gel

layer on the surface of membrane. This difference could be due to the difference in the components of two extracts.

The results on boron fixation by pectin showed that boron adsorption is possible but requires more powder with higher purity to have a high enough RG-II concentration. It should be also necessary to active it, in acid condition, for example, in order to release the fixed boron and liberate RG-II as well as other sugars in monomer form which is more favorable to boron complex reaction. Another solution would be the chemical modification in order to increase the number of reactive site. Hence these considerations show that boron fixation by pectin could be an interesting way for water treatment.

Ultrafiltration of the pectin solution is an attractive solution for pectin recovery from water. Even if the flow rate is lower than during water ultrafiltration, the hybrid system could allow removing boron and producing an interesting agriculture fertilizer at the same time.

CONCLUSIONS AND PERSPECTIVES

Conclusions and perspectives

Boron removal by ion exchange is a challenging issue for desalination industry as well as water treatment. Enhanced boron removal has been investigated and applied on various materials however they still expose some limitation about low efficiency, high pH requirement, and expensive cost. So in this study, we aimed to find an alternative low cost material, which can be efficient on boron removal. This work was conducted to achieve a better understanding of surface exchange mechanisms on different materials *vs.* time and at equilibrium depending on different physicochemical parameters such as pH, reaction time, and different boron concentrations, on batch experiments.

Batch experiments were carried out using 4 resins in which there are 2 anionic resins (Ambersep 900-OH & Amberlite IRA 402 Cl) and 2 boron selective resins (Amberlite IRA 743 & Diaion CRB 03). Different parameters such as, pH (from 6 to 12), reaction time (from 2 min to 24 h), boron concentration (5 to 92.5 mmol L⁻¹), were employed to study kinetics, pH influence, isotherm of the adsorption. The pseudo first and second-order kinetic model was used to fit with experimental data. Langmuir-type, BET-type and Henry-type models were used for fitting boron sorption behavior of 4 resins. Isotherm parameters then were used to draw the theoretical model, which is compared with the obtaining experimental models.

Boron removal was studied on continuous system as a function of boron concentration and flow rate. Column experiments were operated using 2 resins: one anionic resin (Ambersep 900-OH) and one boron selective resin (Amberlite IRA 743). Two concentrations of boron (9.25 mmol L⁻¹ and 1.85 mmol L⁻¹) and two flow rates (60 BV h⁻¹ and 10 BV h⁻¹) were various investigated parameters. Two resin bed volumes (100 and 400 mL) of Ambersep 900-OH resin was used to carry out the boron adsorption experiment. Pore volume (V_p) determination experiment was operated using 0.05 M and 0.1 M NaCl solution. All the solutions were conditioned to natural pH (pH 8). Desorption process was performed using NaOH pH 13 solution for Ambersep 900-OH and 0.5 M H₂SO₄ and 0.25 M NaOH for Amberlite IRA 743 resin. A comparison of pH, conductivity, boron concentration breakthrough curves behavior and boron removal capacities between two resins were done. Kinetic models (Yoon and Nelson model, and Thomas model) were selected to fit with the experimental data of column experiment of two resins. A link between results obtaining in batch and column mode experiments was evaluated.

Two types of pectin were used in this thesis: Batch extracted pectin and twin-screw extracted pectin. Acid hydrolysis, HPLC analysis, viscosity measurement was used to characterize pectin contents. Membranes with three different MWCO (10, 30 and 100 kDa) were chosen to apply on hybrid system. Membrane filtration versus different pressures, stirring speeds was performed with both water and pectin solution to evaluate the permeable performance of the membranes. Two filtration systems including the dead – end geometry Amicon cell filtration system and the cross-flow geometry hollow fiber filtration system were utilized. Boron adsorption on pectin was conducted with two types of pectin at different pH. Boron adsorption capacities were determined and compared with that of synthetic resin.

Batch experiments on synthetic resins

Kinetics was fast at the beginning, proving by more than 96% boron removal obtaining after 30 min reaction for three synthetic resins (Amberlite IRA 743, Diaion CRB 03 & Ambersep 900-OH). The equilibrium reached after 2 h reaction with high efficiency with three above resins, but low efficiency (10 % removal) with Amberlite IRA 402 Cl. The pseudo-second order kinetic model well fits with sorption data of four resins with fastest reaction half time and highest rate constant are 0.8 min and $7.0 \text{ g mmol}^{-1} \text{ min}^{-1}$ for Amberlite IRA 743 and 0.7 min and $5.7 \text{ g mmol}^{-1} \text{ min}^{-1}$ for Ambersep 900-OH resin.

pH has a strong influence on adsorption process of Ambersep 900-OH and Amberlite IRA 402 Cl but insignificant effect on boron removal of two boron selective resins. Maximum boron adsorption was obtained at pH 8 and pH 10 for Ambersep 900-OH and Amberlite IRA 402 Cl, respectively. Ionic exchange is controlled by competition with OH^- ions at high pH for both resins and mainly by competition with Cl^- ions at low pH for the Amberlite IRA 402 Cl resin. Removal efficiency was independent on pH with Amberlite IRA 743 and Diaion CRB 03 resins due to the participation of both neutral and anionic forms of boron in complex formation reaction with diols structure on functional group. Furthermore, a significant increase in pH of adsorbed solution was observed with Amberlite IRA 743, Diaion CRB 03 due to the capture of protons on N-methylglucamine group on the resin. pH after adsorption also increased strongly with Ambersep 900-OH resin because of the release of OH^- in to the solution. Reversed phenomenon was seen with Amberlite IRA 402 Cl with a decrease in pH of solution after reaction.

The amount of adsorbed boron increased when the boron concentration increasing, but the forms of the isotherms are different according to the resin type. A plateau is observed for the two resins, Ambersep 900 - OH, Diaion CRB 03 while two plateaus was observed with Amberlite IRA 743 and the boron adsorption is linear with Amberlite IRA 402 Cl. The boron removal for Diaion CRB 03 seems to get plateau from 10 to 50 mmol L^{-1} boron concentration while it continues to increase with three others. Langmuir type relationship correctly describes the adsorption behavior for Diaion CRB 03, Ambersep 900-OH while BET type relationship better fits with double fix mechanism of Amberlite IRA 743. The calculated maximum sorption capacities obtaining for three resins Ambersep 900-OH, Diaion CRB 03 and Amberlite IRA 743 were 2.2, 0.87 and 0.43 mmol g^{-1} , respectively. The Henry-type model was best fitted with boron sorption in the case of the Amberlite IRA 402 Cl.

The results indicated that the ion exchange resin Ambersep 900-OH is the most efficient boron adsorption and the cheapest resin compared to the specific ones in our experimental conditions.

Column experiments with synthetic resins

Column experiment was carried out with two resins: one boron selective resin (Amberlite IRA 743) and one ion exchange resin (Ambersep 900-OH). Pore volume of Ambersep 900-OH and Amberlite IRA 743 are 49.7 mL and 76.2 mL, respectively.

Boron fixation on column experiment was studied at different flow rates, boron concentration, and resin bed volume. Results showed that the breakthrough curve of boron concentration reaches ahead at flow rate of 60 BV h⁻¹ compared to that at flow rate of 10 BV h⁻¹ for Amberlite IRA 743. This result is confirming to the theory, because when the flow rate is too high, mass transfer limits boron fixation. However, reverse result was obtained with resin Ambersep 900-OH, meaning that retardation factor at 60 BV h⁻¹ was higher than at 10 BV h⁻¹. In both cases, the boron sorption capacity at 60 BV h⁻¹ is greater than that at 10 BV h⁻¹. This result could be due to the remaining of chloride ions in resin that changes the structure of resin, and the ion exchange process for Ambersep 900-OH resin. The sorption capacity increased when resin bed volume increased for Ambersep 900-OH, indicating that the mean contact time was too short with the 100 mL bed. The contact time was calculated at 3 minutes that it was similar to the reaction time calculated from batch experiments.

Boron concentration in inlet solution also has a significant impact on boron adsorption. Breakthrough curve showed that the steady state was reached sooner with higher inlet boron concentration at the same flow rate. This can be explained by the higher contact probability between boron and adsorption sites at higher boron concentration, so that the adsorption rates occurred faster and got steady state sooner. The sorption capacity of experiment using ~ 9.0 mM B (0.51 mM B mL⁻¹ resin) is higher than that of experiment using 1.8 mM B L⁻¹ (0.40 mM B mL⁻¹ resin) however a repetition should be done with experiment using ~ 9.0 mM B solution to confirm the conclusion.

At the same condition (~ 9.0 mM boron concentration, 10 BV h⁻¹), Ambersep 900 - OH resin has higher capacity of boron fixation (0.51 mmol B mL⁻¹ resin) than that of Amberlite IRA 743 (0.36 mmol B mL⁻¹ resin) even boron was on neutral form under the tested conditions. Results could be changed if the adsorption process was carried out in seawater condition with the competition of other anions for Ambersep 900-OH but expectedly keep unchanged for Amberlite IRA 743. A test is recommended to valid the hypothesis. Column utilization for Ambersep 900-OH resin was high (> 90%) while for Amberlite IRA 743 was only 63%. This result confirms that best operational flow rate of the supplier for Amberlite IRA 743 is from 5 to 30 BV h⁻¹. Yoon and Nelson model and Thomas model were used to optimize the breakthrough curves with similar sorption capacities of two resins. Non-linear model built on Langmuir parameters from batch experiment, was used to simulate the breakthrough curves of experiment (9 mM, 10 BV h⁻¹) for two resins. For Ambersep 900-OH, the simulation fitted well with compressive fronts while it showed a small shift with dispersive front. Concentration influence was not explained by isotherm theory due to a large difference between calculated and experimental retardation factors. It supposed to have another mechanism involved in the reaction and increased boron affinity with resin. For Amberlite IRA 743, a significant difference between simulation and experimental breakthrough curves was observed. There are two possible reasons: Langmuir isotherm only fitted for a small range of boron concentration and pore volume is too high. Using smaller pore volume value from Simonnot's experiment resulted in a better-fitted breakthrough curve.

All these results indicate that Ambersep 900-OH should be recommended for the treatment surface water with low salt contents or for the post-treatment of desalted seawater. But specific resins should be most efficient for boron removal from water having high salt concentration.

Pectin experiments in batch and continuous system

Membrane permeability is studied with water and pectin solution at different stirring speed and pressures with three membranes having MWCO of 10, 30 and 100 kDa. The permeate flux of membrane is lower with pectin solutions than with water, may due to the appearance of polarization concentration layer, viscosity difference and fouling. As pressure increases, the permeability also increases, but reaches constant after 1 bar due to the gel layer formation. The filtration of the pectin solution required performing at high shear rate to avoid the appearance of gel layer that limited the membrane performance. Batch extracted pectin has more tendency to form gel layer on the surface of membrane than twin-screw extracted pectin. The composition of the two types of pectin is responsible for the difference in maximum permeates flux, due to the influence of rheological properties. But for both pectins, the best filtration performances were obtained with the 30 kDa membrane.

Two types of pectin contain similar components including of glucose, galactose, arabinose, galacturonic acid (47 %). However, there is difference in percentage of glucose and galacturonic acid between two pectins. The galacturonic acid is twice higher for batch-extracted sample but without glucose compared to those in twin-screw extracted pectin. This can be due to the different in production method. The non-defined component of two pectins can be phenolic, polyphenolic compounds, carbohydrates components, which may also fix boron.

Boron fixation was performed with 9.25 mM boric acid solution at different pH (from 5 to 12). The boron fixation efficiency is low, ranging from 3% to 14%. This can be due to the impurities of extracted pectin and the status of sorption sites. The pectin extract contained, reducing the number of available adsorption sites for boron fixation. Boron content in batch extracted and twin – screw extracted pectin are 84 mg kg⁻¹ and 60 mg kg⁻¹, respectively. Hence, the capacity of boron removal for pectin extract is 1 mg g⁻¹, smaller than that of IRA 743 (6.7 mg g⁻¹) but this capacity could be improved with purer pectin, used in optimized operation. Boron fixation by pectin is possible but requires more purified powder to have a high enough RG-II concentration or it should be necessary to active the extracted pectin, in acid condition (pH < 3) to release the fixed boron and liberate RG-II as well as other sugars in monomer form which is more favorable to boron complex reaction.

Boron fixation by pectin and the recovery of pectin from solution using ultrafiltration is feasible. In addition, the utilization of boron-pectin after adsorption as a boron rich fertilizer is a good way to recycle this sorbent without using any additional chemicals which harmful to the environment.

Future works

Many questions are remaining after all the experiments and it would be interesting to manage the following tests.

In real solution, for example, desalted water or drinking water, there are many other ions such as Ca²⁺, Mg²⁺, Fe²⁺, Fe³⁺, Cl⁻, NO₃⁻, SO₄²⁻ and they can change drastically the resins performances. It should be interesting in a first time to define the influence of anions on the sorption kinetics and the

adsorption capacity, particularly with Ambersep 900-OH. Anions could compete with boron for the fixation, reducing the resin efficiency, but other mechanisms could also appear and should be characterized by kinetics analysis. Moreover, temperature is another parameter, which has direct influence on boron fixation on resins. By changing temperature of experiment, it will change the movement of ions or molecules in the solution, then increase or decrease the opportunities of their contact with adsorption sites, consequently changing the reaction kinetics.

Furthermore, the boron fixation also needs to be performed with the presence of other ions such as Cl^- , NO_3^- , SO_4^{2-} which are usually found in real water samples. These ions will probably have a considerable influence on the ion exchange process due to the competition with borate ions, hydroxides.

Column experiment should be performed with some extra boron concentrations (5, 20, 30 mmol L^{-1}) with more flow rates (15, 20, 30 BV h^{-1}) to have more reliable results about the influence of flow rates as well as boron concentration on boron fixation process. The aim of these trials would be to understand the influence of advection and fixation kinetic on the fixation performances of the resin. In this case, it would be interesting to manage experiments with column of different diameters in order to separate the influence of contact time and advection on the fixation rate.

All the experiments realized during the PhD and the further proposed above require a long time, and it appears that modeling would be very attractive to reduce the number of experiments. It is therefore important that the laboratory develop competences in chromatographic modeling.

It has been demonstrated that the combination of pectin and ultrafiltration could be attractive, but the results are too superficial to really conclude. Many studies still have to be performed for the validation of the concept.

Ultrafiltration of pectin has been studied at bench scale, and even if the MWCO of the membrane has been selected, it will be necessary to confirm the optimal conditions with a larger membrane.

The larger part of work will concern the understanding of the fixation reaction. Boron fixation would have to be performed with different kind of refined fractions of pectin (RG-I, RG-II, etc.) in order to identify the polymers that can interact with boron, what are the mechanisms involved and the kinetic parameters. These results would help to define the required purity and composition of the extract to have an efficient boron fixation.

The extract compositions will have to accurately characterize in order to know the content in the different pectin polymers, but also the content in phenolic compounds (ferulic and coumaric acid) and hemicelluloses that can also fixed boron. They aim to have not only a pure expensive extract, but also an extract with a high fixation capacity. It will be therefore interesting to define the fixation capacity of these impurities by evaluating the sorption isotherm of model solutions.

Then boron adsorption on pectin extract should be investigated with different parameters such as different boron concentration, pectin dose, reaction time, temperature and influence of other ions. If necessary, it could be used a pretreatment in order to activate the extract and fixe a higher quantity of boron.

Finally, it will be important to contact a company that could used the final product containing pectin and boron for plant growth because it is necessary to define what would be the required properties of the product (solubility, composition, etc.).

References

- Abd, A. E. 2014. Determination of boron in water using neutron scattering and transmission, and prompt gamma ray neutron activation analysis methods: A comparative study. *Nucl. Instrum. Meth. B*, 337, 62–67.
- Akretche, D. E., Kerdjoudj, H., 2000. Donnan dialysis of copper, gold and silver cyanides with various anion exchange membranes. *Talanta*, 51, 281–289.
- Aksu, Z., Gönen, F., 2004. Biosorption of phenol by immobilized activated sludge in a continuous packed bed: prediction of breakthrough curves. *Process Biochem.*, 39, 599–613.
- Anderson, M. A., Cudero, A. L., Palma, J., 2010. Capacitive deionization as an electrochemical means of saving energy and delivering clean water. Comparison to present desalination practices: Will it compete? *Electrochim. Acta*, 55, 3845–3856.
- Aronoff, M. R., VanVeller, B., Raines, R. T., 2013. Detection of Boronic Acids through Excited-State Intramolecular Proton-Transfer Fluorescence. *Org. Lett.*, 15, 5382–5385.
- Avraham, E., Noked, M., Soffer, A., Aurbach, D., 2011. The feasibility of boron removal from water by capacitive deionization. *Electrochim. Acta*, 56, 6312–6317.
- Ayyildiz, H. F., Kara, H., 2005. Boron removal by ion exchange membranes. *Desalination*, 180, 99–108.
- Baker, 2012. *Microfiltration*. 3rd edition, John Wiley & Sons Ltd, California.
- Barth, S., 1998. Application of boron isotopes for tracing sources of anthropogenic contamination in groundwater. *Water. Res.*, 32, 685–690.
- BeMiller, J. N., 1986. An Introduction to Pectins: Structure and Properties. *Chemistry and Function of Pectins*. American Chemical Society. 310, 2–12.
- Biçak, N., Bulutçu, N., Şenkal, B. F., Gazi, M., 2001. Modification of crosslinked glycidyl methacrylate-based polymers for boron-specific column extraction. *React. Funct. Polym.*, 47, 175–184.

- Biçak, N., & Şenkal, B. F. (1998). Sorbitol-modified poly(N-glycidyl styrene sulfonamide) for removal of boron. *Journal of Applied Polymer Science*, 68(13), 2113–2119.
- Bick, A., Oron, G., 2005. Post-treatment design of seawater reverse osmosis plants: boron removal technology selection for potable water production and environmental control. *Desalination*, 178, 233–246.
- Blahušiak, M., Schlosser, Š., 2009. Simulation of the adsorption—microfiltration process for boron removal from RO permeate. *Desalination*, 241, 156–166.
- Boncukcuoğlu, R., A. E. Yilmaz, M. M. Kocakerim, M. Çopur, 2004. An empirical model for kinetics of boron removal from boron-containing wastewaters by ion exchange in a batch reactor. *Desalination*, 160, 159–166.
- Bonnélye, V., Sanz, M. A., Francisci, L., Beltran, F., Cremer, G., Colcuera, R., Laraudogoitia, J., 2007. Curacao, Netherlands Antilles: A successful example of boron removal on a seawater desalination plant. *Desalination*, 205, 200–205.
- Indian Minerals Yearbook, 2014. Part-III: Mineral Reviews. Boron Minerals. 53rd Edition. Indian bureau of mines, Nagpur.
- Bortolussi, S., Ciani, L., Postuma, I., Protti, N., Luca Reversi, null, Bruschi, P., Ferrari C., Cansolino L., Panza L., Altieri, S., 2014. Boron concentration measurements by alpha spectrometry and quantitative neutron autoradiography in cells and tissues treated with different boronated formulations and administration protocols. *Appl. Radiat. Isotopes: Including Data, Instrumentation and Methods for Use in Agriculture, Industry and Medicine*, 88, 78–80.
- Bouguerra, W., Mnif, A., Hamrouni, B., Dhahbi, M., 2008. Boron removal by adsorption onto activated alumina and by reverse osmosis. *Desalination*, 223, 31–37.
- B.R. Sharma, Naresh L., N.C. Dhuldhoya, S. U. Merchant, U. C. Merchant. 2006. An overview on pectins. *Times Food Processing Journal*, June-July, 44–45.

- Brunauer, S., Emmett, P. H., Teller, E., 1938. Adsorption of Gases in Multimolecular Layers. *J. Am. Chem. Soc.*, 60, 309–319.
- Buergisser, C. S., Cernik, M., Borkovec, M., Sticher, H., 1993. Determination of nonlinear adsorption isotherms from column experiments: an alternative to batch studies. *Environ. Sci. Technol.*, 27, 943–948.
- Bursali, E. A., Cavas, L., Seki, Y., Bozkurt, S. S., Yurdakoc, M., 2009. Sorption of boron by invasive marine seaweed: *Caulerpa racemosa* var. *cylindracea*. *Chem. Eng. J.*, 150, 385–390.
- C. Smallwood, 1998. Environmental Health Criteria 204. *Boron*. US Environmental Protection Agency, Ohio.
- Caffall, K. H., Mohnen, D., 2009. The structure, function, and biosynthesis of plant cell wall pectic polysaccharides. *Carbohydr. Res.*, 344, 1879–1900.
- Carlson, R.M., Paul, J. L., 1969. Potentiometric determination of boron in agricultural sample. *Soil Sci.*, 108, 266-272.
- Çelik, Z. C., Can, B. Z., Kocakerim, M. M., 2008. Boron removal from aqueous solutions by activated carbon impregnated with salicylic acid. *J. Hazard. Mater.*, 152, 415–422.
- Cengeloglu, Y., Arslan, G., Tor, A., Kocak, I., Dursun, N., 2008. Removal of boron from water by using reverse osmosis. *Sep. Purif. Technol.*, 64, 141–146.
- Charrière, D., Hernández Cortázar, M. de A., Behra, P., 2015. Effect of the presence of pyrite traces on silver behavior in natural porous media. *J. Colloid Interface Sci.* 446, 373-379.
- Clever, M., Jordt, F., Knauf, R., Rübiger, N., Rüdibusch, M., Hilker-Scheibel, R., 2000. Process water production from river water by ultrafiltration and reverse osmosis. *Desalination*, 131, 325–336.
- Cyber Colloids LTD, 2006. Introduction to Pectin. 72, 43.
- D. Schweich, M. S., 1981. Adsorption, partition, ion exchange and chemical reaction in batch reactors or in columns - A review. *J Hydrol*, 50, 1–33.

- Daas, P. J. H., Boxma, B., Hopman, A. M. C. P., Voragen, A. G. J., Schols, H. A., 2001. Nonesterified galacturonic acid sequence homology of pectins. *Biopolymers*, 58, 1–8.
- Damien Cividini., 2009. Thesis: *Contribution à l'étude du cycle géochimique du Bore*. Ecole et observatoire des sciences de la terre, Strasbourg, France.
- Damkjaer, A., 1981. Determination of boron in iron-based metallic glasses by neutron irradiation and alpha-particle track recording in cellulose nitrate. *Journal of Radioanalytical Chemistry*, 67, 413–419.
- Davidson, G. R., Bassett, R. L., 1993. Application of boron isotopes for identifying contaminants such as fly ash leachate in groundwater. *Environ. Sci. Technol*, 27, 172–176.
- Dellapenna, D., Alexander, D. C., Bennett, A. B., 1986. Molecular cloning of tomato fruit polygalacturonase: Analysis of polygalacturonase mRNA levels during ripening. *Proceedings of the National Academy of Sciences of the United States of America*, 83, 6420–6424.
- Davy H., 1809. An account of some new analytical researches on the nature of certain bodies, particularly the alkalies, phosphorus, sulphur, carbonaceous matter, and the acids hitherto undecomposed: with some general observations on chemical theory. *Philosophical Transactions of the Royal Society of London*, 99: 39–104.
- Dembitsky, V. M., Smoum, R., Al-Quntar, A. A., Ali, H. A., Pergament, I., Srebnik, M., 2002. Natural occurrence of boron-containing compounds in plants, algae and microorganisms. *Plant Sci.*, 163, 931–942.
- Demey, H., Vincent, T., Ruiz, M., Sastre, A. M., Guibal, E., 2014. Development of a new chitosan/Ni(OH)₂-based sorbent for boron removal. *Chem. Eng. J.*, 244, 576–586.
- Demir, B. S., Serindağ, O., 2009. Determination of Boron in Grape (*Vitis vinifera*) by Azomethine H Spectrophotometric Method. *Eurasian J. Anal. Chem+*, 1, 11–18.
- Devirian, T. A., & Volpe, S. L. (2003). The Physiological Effects of Dietary Boron. *CRC. CR. Rev. Food Sci.*, 43, 219–231.

- Deyhle, A., 2001. Improvements of boron isotope analysis by positive thermal ionization mass spectrometry using static multicollection of Cs_2BO_2^+ ions. *Int. J. Mass. Spectrom.*, 206, 79–89.
- Dilek, Ç., Özbelge, H. Ö., Biçak, N., Yılmaz, L., 2002. Removal of boron from aqueous solutions by continuous polymer-enhanced ultrafiltration with polyvinyl alcohol. *Separ. Sci. Technol.*, 37, 1257–1271.
- Duchateau, N. L., de Bièvre, P., 1983. Boron isotopic measurements by thermal ionization mass spectrometry using the negative BO_2^- ion. *Int. J. Mass Spectrom.*, 54, 289–297.
- El-Dessouky, H. T., Ettouney, H. M., 2002. Chapter 1 - Introduction. In *Fundamentals of Salt Water Desalination*. (1–17), Elsevier Science B.V, Amsterdam.
- Ezechi, E. H., Isa. M. H., Kutty S. R. B. M., 2012. Boron in Produced Water: Challenges and Improvements: A Comprehensive Review. *Journal of Applied Sciences*, 12, 402-415.
- Farhat, A., Ahmad, F., Arafat, H., 2013. Analytical techniques for boron quantification supporting desalination processes: A review. *Desalination*, 310, 9–17.
- Farley, K. J., Dzombak, D. A., Morel, F. M. M., 1985. A surface precipitation model for the sorption of cations on metal oxides. *J. Colloid Interf. Sci.*, 106, 226–242.
- Ferreira, O. P., de Moraes, S. G., Durán, N., Cornejo, L., Alves, O. L., 2006. Evaluation of boron removal from water by hydrotalcite-like compounds. *Chemosphere*, 62, 80–88.
- Foo, K. Y., Hameed, B. H., 2010. Insights into the modeling of adsorption isotherm systems. *Chem. Eng. J.*, 156, 2–10.
- Fujita, Y., Hata, T., Nakamaru, M., Iyo, T., Yoshino, T., Shimamura, T., 2005. A study of boron adsorption onto activated sludge. *Bioresource Technol.*, 96, 1350–1356.
- Gay Lussac, J.L. & Thenard, L.J., 1808. Sur la décomposition et la recomposition de l'acide boracique. *Annales de chimie*. 68: 169–174.
- Gazi, M., Shahmohammadi, S., 2012. Removal of trace boron from aqueous solution using iminobis-(propylene glycol) modified chitosan beads. *React. Funct. Polym.*, 72, 680–686.

- GE healthcare., 2010. Ion Exchange Chromatography & Chromatofocusing - Principles and Methods. AA Edition, Amersham Bisciences.
- Gee, M., Reeve, R. M., McCready, R. M., 1959. Measurement of Plant Pectic Substances, Reaction of Hydroxylamine with Pectinic Acids. Chemical Studies and Histochemical Estimation of the Degree of Esterification of Pectic Substances in Fruit. *J. Agr. Food Chem.*, 7, 34–38.
- Geffen, N., Semiat, R., Eisen, M. S., Balazs, Y., Katz, I., Dosoretz, C. G., 2006. Boron removal from water by complexation to polyol compounds. *J. Membrane Sci.*, 286, 45–51.
- Glueckstern, P., & Priel, M., 2003. Optimization of boron removal in old and new SWRO systems. *Desalination*, 156, 219–228.
- Grassi, S., Amadori, M., Pennisi, M., Cortecchi, G., 2014. Identifying sources of B and As contamination in surface water and groundwater downstream of the Larderello geothermal – industrial area (Tuscany–Central Italy). *J. Hydrol.*, 509, 66–82.
- WHO, 2011. *Guidelines for Drinking - water Quality*. 4th ed., World Health Organization, Geneva.
- Hayes, M. R., Metcalfe, J., 1962. The boron-curcumin complex in the determination of trace amounts of boron. *Analyst*, 87, 956–969.
- Higgs, D. G., 1960. The spectrophotometric determination of boron in molybdenum alloys with carmine. *Analyst*, 85, 897–904.
- Hilal, N., Kim, G. J., Somerfield, C., 2011. Boron removal from saline water: A comprehensive review. *Desalination*, 273, 23–35.
- Ho, Y. S., McKay, G., 1999. Pseudo-second order model for sorption processes. *Process Biochem.*, 34, 451–465.
- Hodgson, A. S., Kerr, L. H., 1991. *Tropical fruit products* (Walter, R. H.), Academic Press, New York.
- Hou, D., Wang, J., Sun, X., Luan, Z., Zhao, C., Ren, X., 2010. Boron removal from aqueous solution by direct contact membrane distillation. *J. Hazardous Mater.*, 177, 613–619.

- Hu, H., Brown, P. H., 1994. Localization of Boron in Cell Walls of Squash and Tobacco and Its Association with Pectin (Evidence for a Structural Role of Boron in the Cell Wall). *Plant Physiol.*, 105, 681–689.
- Hu, H., Brown, P. H., & Labavitch, J. M., 1996. Species variability in boron requirement is correlated with cell wall pectin. *J. Exp. Bot.*, 47, 227–232.
- Hubbard, A. T., 2002. *Encyclopedia of Surface and Colloid Science - Volume 2*. CRC Press.
- Indian Bureau of Mines, 2014. *Indian Minerals Yearbook, Part III: Mineral Reviews, Boron minerals*. 53rded. Indira Bhavan, Civil Lines, NAGPUR – 440 001.
- Inukai, Y., Tanaka, Y., Matsuda, T., Mihara, N., Yamada, K., Nambu, N., Itoh, O., Doi, T., Kaida, Y., Yasuda, S., 2004. Removal of boron (III) by N-methylglucamine-type cellulose derivatives with higher adsorption rate. *Anal. Chim. Acta*, 511, 261–265.
- Ipek, I.Y., Kabay, N., Yüksel, M., 2013. Modeling of fixed bed column studies for removal of boron from geothermal water by selective chelating ion exchange resins. *Desalination*, 310, 151–157.
- Ishii, T., Matsunaga, T., 2001. Pectic polysaccharide rhamnogalacturonan II is covalently linked to homogalacturonan. *Phytochemistry*, 57, 969–974.
- Ishii, T., Matsunaga, T., Pellerin, P., O'Neill, M. A., Darvill, A., Albersheim, P., 1999. The Plant Cell Wall Polysaccharide Rhamnogalacturonan II Self-assembles into a Covalently Cross-linked Dimer. *J. Biol. Chem.*, 274, 13098–13104.
- IUPAC., 1987. Recommendations for the definition, estimation and use of the detection limit, 112, 199–204.
- J. Mulder, 1996. *Basic Principles of Membrane Technology*. 2nd ed., Springer Science & Business Media.
- J. T. Hatcher, L. V. Wilcox, 1950. Colorimetric Determination of Boron Using Carmine. *Anal Chem.*, 22, 567-569.

- Jalali, M., Rajabi, F., Ranjbar, F., 2015. The removal of boron from aqueous solutions using natural and chemically modified sorbents. *Desalin. Water Treat.*, 57, 1–11.
- Jarvis, M. C., 1984. Structure and properties of pectin gels in plant cell walls. *Plant Cell Environ.*, 7, 153–164.
- Jarvis, M. C., Hall, M. A., Threlfall, D. R., Friend, J., 1981. The polysaccharide structure of potato cell walls: Chemical fractionation. *Planta*, 152, 93–100.
- Jorda, J., 2003. *Étude du procédé d'extraction alcaline et de purification des pectines de pulpe de betterave: étude des propriétés chimiques et physico-chimiques* (Thèse de doctorat). Institut national polytechnique, Toulouse, France.
- Jorda, J., Marechal, P., Rigal, L. Pontalier, P. -Y., 2002. Biopolymer purification by ultrafiltration. *Desalination*, 148, 187–191.
- Kabay, N., Güler, E., Bryjak, M., 2010. Boron in seawater and methods for its separation — A review. *Desalination*, 261, 212–217.
- Kabay, N., Sarp, S., Yuksel, M., Arar, Ö., Bryjak, M., 2007. Removal of boron from seawater by selective ion exchange resins. *React. Funct. Polym.*, 67, 1643–1650.
- Kabay, N., Sarp, S., Yuksel, M., Kitis, M., Koseoğlu, H., Arar, Ö., Bryjak, M., Semiat, R., 2008. Removal of boron from SWRO permeate by boron selective ion exchange resins containing N-methyl glucamine groups. *Desalination*, 223, 49–56.
- Kabay, N., Yilmaz, İ., Bryjak, M., Yuksel, M., 2006. Removal of boron from aqueous solutions by a hybrid ion exchange–membrane process. *Desalination*, 198, 158–165.
- Karr, A. L., 1976. *Cell wall bigenesis - Plant Biochemistry*. 3rd ed. Academic Press, New York.
- Kasemann, S., Meixner, A., Rocholl, A., Vennemann, T., Rosner, M., Schmitt, A. K., Wiedenbeck, M., 2001. Boron and Oxygen Isotope Composition of Certified Reference Materials NIST SRM 610/612 and Reference Materials JB-2 and JR-2. *Geostandards Newslett.*, 25, 405–416.

- Keegstra, K., Talmadge, K. W., Bauer, W. D., Albersheim, P., 1973. The Structure of Plant Cell Walls: III. A Model of the Walls of Suspension-cultured Sycamore Cells Based on the Interconnections of the Macromolecular Components. *Plant Physiol.*, 51, 188–197.
- Kentjono, L., Liu, J. C., Chang, W. C., Irawan, C., 2010. Removal of boron and iodine from optoelectronic wastewater using Mg–Al (NO₃) layered double hydroxide. *Desalination*, 262, 280–283.
- Kir, E., Gurler, B., & Gulec, A., 2011. Boron removal from aqueous solution by using plasma-modified and unmodified anion-exchange membranes. *Desalination*, 267, 114–117.
- Kıpçak, İ., Özdemir, M., 2012. Removal of boron from aqueous solution using calcined magnesite tailing. *Chem. Eng. J.*, 189–190, 68–74.
- KOCH Membrane systems, Inc., 2012. An Overview of Membrane Technology and Theory. Application bulletin.
- Köse, T. E., & Öztürk, N. (2008). Boron removal from aqueous solutions by ion-exchange resin: Column sorption–elution studies. *Journal of Hazardous Materials*, 152(2), 744–749.
- Koseoglu, H., Kabay, N., Yüksel, M., Kitis, M., 2008. The removal of boron from model solutions and seawater using reverse osmosis membranes. *Desalination*, 223, 126–133.
- Koseoglu, H., Kabay, N., Yüksel, M., Sarp, S., Arar, Ö., Kitis, M., 2008. Boron removal from seawater using high rejection SWRO membranes — impact of pH, feed concentration, pressure, and cross-flow velocity. *Desalination*, 227, 253–263.
- Kot, F. S., 2008. Boron sources, speciation and its potential impact on health. *Rev. Environ. Sci. Bio. Technol.*, 8, 3–28.
- Krejčová, A., Černohorský, T., 2003. The determination of boron in tea and coffee by ICP–AES method. *Food Chem.*, 82, 303–308.
- Laîné, J.-M., Vial, D., Moulart, P., 2000. Status after 10 years of operation — overview of UF technology today. *Desalination*, 131, 17–25.

- Langmuir, I., 1918. The adsorption of gases on plane surfaces of glass, mica and platinum. *J. Am. Chem. Soc.*, *40*, 1361–1403.
- Lau, J. M., McNeil, M., Darvill, A. G., Albersheim, P., 1987. Treatment of rhamnogalacturonan I with lithium in ethylenediamine. *Carbohydr. Res.*, *168*, 245–274.
- Laura Sigg, Philippe Behra, Werner Stumm, 2014. *Chimie des milieux aquatiques, cours et exercices corrigés* 5th ed, Dunod, Paris.
- Lawrence K. Wang, Jiaping Paul Chen, Yung-Tse Hung, Nazih K. Shammass, 2011. *Membrane and Desalination Technologies. Handbook of Environmental Engineering*. Vol. 13. New York, USA.
- Leeman, W. P., Tonarini, S., Pennisi, M., Ferrara, G., 2005. Boron isotopic variations in fumarolic condensates and thermal waters from Vulcano Island, Italy: Implications for evolution of volcanic fluids. *Geochim. Cosmochim. Ac.*, *69*, 143–163.
- Li, X., Liu, R., Wu, S., Liu, J., Cai, S., Chen, D., 2011. Efficient removal of boron acid by N-methyl-d-glucamine functionalized silica–polyallylamine composites and its adsorption mechanism. *J. Colloid Interf. Sci.*, *361*, 232–237.
- Liu, H., Ye, X., Li, Q., Kim, T., Qing, B., Guo, M., Ge, F., Wu, Z., Lee, K., 2009. Boron adsorption using a new boron-selective hybrid gel and the commercial resin D564. *Colloids and Surfaces A: Physicochemical and Engineering Aspects*, *341*, 118–126.
- Liu, R., Ma, W., Jia, C., Wang, L., Li, H.-Y., 2007. Effect of pH on biosorption of boron onto cotton cellulose. *Desalination*, *207*, 257–267.
- Loomis, W. D., Durst, R. W., 1992. Chemistry and biology of boron. *BioFactors (Oxford, England)*, *3*, 229–239.
- López, F. J., Giménez, E., Hernández, F., 1993. Analytical study on the determination of boron in environmental water samples. *Fresen. J. Anal. Chem.*, *346*, 984–987.

- Magara, Y., Tabata, A., Kohki, M., Kawasaki, M., Hirose, M., 1998. Development of boron reduction system for sea water desalination. *Desalination*, 118, 25–33.
- Matoh, T., Akaike, R., Kobayashi, M., 1997. A sensitive and convenient assay for boron in plant using chromotropic acid and HPLC. *Plant Soil*, 192, 115–118.
- Matoh, T., Ishigaki, K., Mizutani, M., Matsunaga, W., Takabe, K., 1992. Boron Nutrition of Cultured Tobacco BY-2 Cells I. Requirement for and Intracellular Localization of Boron and Selection of Cells that Tolerate Low Levels of Boron. *Plant Cell Physiol.*, 33, 1135–1141.
- Matoh, T., Kawaguchi, S., Kobayashi, M., 1996. Ubiquity of a Borate-Rhamnogalacturonan II Complex in the Cell Walls of Higher Plants. *Plant Cell Physiol.*, 37, 636–640.
- Maung Htun Oo, 2012. *Boron removal by reverse osmosis membranes*. National University of Singapore, Singapore.
- McIntosh, J. J., Cox, J. E., 1960. Colorimetric Determination of Boron in Porcelain Enamel Frits. *J. Am. Ceram. Soc.*, 43, 123–124.
- McNeil, M., Darvill, A. G., Fry, S. C., Albersheim, P., 1984. Structure and Function of the Primary Cell Walls of Plants. *Annu. Rev. Biochem.*, 53, 625–663.
- Melnyk, L., Goncharuk, V., Butnyk, I., Tsapiuk, E., 2005. Boron removal from natural and wastewaters using combined sorption/membrane process. *Desalination*, 185, 147–157.
- Mishra, H., Yu, C., Chen, D. P., Goddard, W. A., Dalleska, N. F., Hoffmann, M. R., & Diallo, M. S., 2012. Branched Polymeric Media: Boron-Chelating Resins from Hyperbranched Polyethylenimine. *Environ. Sci. Technol.*, 46, 8998–9004.
- Mogni, A., 2015. Fractionnement des complexes lignine-polysaccharides issus de différentes biomasses lignocellulosiques par extrusion bi-vis et séparation chromatographique [PhD Thesis]. Institut National Polytechnique de Toulouse.
- Mort, A. J., Qiu, F., Maness, N. O., 1993. Determination of the pattern of methyl esterification in pectin. Distribution of contiguous nonesterified residues. *Carbohydr. Res.*, 247, 21–35.

- Murray, F. J., 1995. A human health risk assessment of boron (boric acid and borax) in drinking water. *Regul. Toxicol. Pharm.*, 22, 221–230.
- Nielsen, F. H., 1997. Boron in human and animal nutrition. *Plant Soil*, 193, 199–208.
- Nishihama, S., Sumiyoshi, Y., Ookubo, T., Yoshizuka, K., 2013. Adsorption of boron using glucamine-based chelate adsorbents. *Desalination*, 310, 81–86.
- Onderková, B., Šchlosser, Š., Blahušiak, M., Búgel, M., 2009. Microfiltration of suspensions of microparticulate boron adsorbent through a ceramic membrane. *Desalination*, 241, 148–155.
- O'Neill, M. A., Warrenfeltz, D., Kates, K., Pellerin, P., Doco, T., Darvill, A. G., Albersheim, P., 1996. Rhamnogalacturonan-II, a pectic polysaccharide in the walls of growing plant cell, forms a dimer that is covalently cross-linked by a borate ester. In vitro conditions for the formation and hydrolysis of the dimer. *J. Biol. Chem.*, 271, 22923–22930.
- Oo, M. H., & Song, L., 2009. Effect of pH and ionic strength on boron removal by RO membranes. *Desalination*, 246, 605–612.
- Orlando, U. S., Okuda, T., Baes, A. U., Nishijima, W., & Okada, M., 2003. Chemical properties of anion-exchangers prepared from waste natural materials. *React. Funct. Polym.*, 55, 311–318.
- Oxspring, D. A., McClean, S., O'Kane, E., Smyth, W. F., 1995. Study of the chelation of boron with Azomethine H by differential pulse polarography, liquid chromatography and capillary electrophoresis and its analytical applications. *Anal. Chim. Ac.*, 317, 295–301.
- Öztürk, N., & Kavak, D., 2005. Adsorption of boron from aqueous solutions using fly ash: Batch and column studies. *J. Hazard. Mater.*, 127, 81–88.
- Öztürk, N., Kavak, D., 2008. Boron removal from aqueous solutions by batch adsorption onto cerium oxide using full factorial design. *Desalination*, 223, 106–112.
- Öztürk, N., & Köse, T. E., 2008. Boron removal from aqueous solutions by ion-exchange resin: Batch studies. *Desalination*, 227, 233–240.
- Pankratz, T., 2014. *The IDA Desalination Yearbook 2014-2015*. Topsfield, MA: IDA

- Park, H.-D., Chang, I.-S., Lee, K.-J., 2015. *Principles of Membrane Bioreactors for Wastewater Treatment*. 1st ed. CRC Press.
- Parschová, H., Mištová, E., Matějka, Z., Jelínek, L., Kabay, N., Kauppinen, P., 2007. Comparison of several polymeric sorbents for selective boron removal from reverse osmosis permeate. *React. Funct. Polym.*, 67, 1622–1627.
- Pennisi, M., Gonfiantini, R., Grassi, S., Squarci, P., 2006. The utilization of boron and strontium isotopes for the assessment of boron contamination of the Cecina River alluvial aquifer (central-western Tuscany, Italy). *Appl. Geochem.*, 21, 643–655.
- Pinnau, I., Freeman, B.D., 1999, Membrane Formation and Modification, volume 744, Division of Polymeric Materials: Science and Engineering, American Chemical Society.
- Pimentel, D., Berger, B., Filiberto, D., Newton, M., Wolfe, B., Karabinakis, E., Clark, S., Poon, E., Abbett, E., Nandaopal, S., 2004. Water Resources, Agriculture, and the Environment. Ithaca (NY): New York State College of Agriculture and Life Sciences, Cornell University. Environmental Biology Report 04-1.
- Polowczyk, I., Ulatowska, J., Koźlecki, T., Bastrzyk, A., Sawiński, W., 2013. Studies on removal of boron from aqueous solution by fly ash agglomerates. *Desalination*, 310, 93–101.
- Qi, T., Sonoda, A., Makita, Y., Kanoh, H., Ooi, K., Hirotsu, T., 2002. Synthesis and Borate Uptake of Two Novel Chelating Resins. *Ind. Eng. Chem. Res.*, 41, 133–138.
- Qin, J.-J., Oo, M. H., Wai, M. N., Cao, Y.-M., 2005. Enhancement of boron removal in treatment of spent rinse from a plating operation using RO. *Desalination*, 172, 151–156.
- Rajaković, L. V., & Ristić, M. D., 1996. Sorption of boric acid and borax by activated carbon impregnated with various compounds. *Carbon*, 34, 769–774.
- Rao, R. M., Parab, A. R., Sasibhushan, K., & Aggarwal, S. K., 2008. Studies on the isotopic analysis of boron by thermal ionisation mass spectrometry using NaCl for the formation of Na₂BO₂⁺ species. *Int. J. Mass Spectrom.*, 273, 105–110.

- Rao, R. M., Parab, A. R., Sasibhushan, K., Aggarwal, S. K., 2009. A robust methodology for high precision isotopic analysis of boron by thermal ionization mass spectrometry using Na_2BO_2^+ ion. *Int. J. Mass Spectrom.*, 285, 120–125.
- Redondo, J., Busch, M., De Witte, J.-P., 2003. Boron removal from seawater using FILMTECTM high rejection SWRO membranes. *Desalination*, 156, 229–238.
- Reid, R., 2010. Can we really increase yields by making crop plants tolerant to boron toxicity? *Plant Sci.*, 178, 9–11.
- Renard, C. M. G. C., Thibault, J.-F., 1993. Structure and properties of apple and sugar-beet pectins extracted by chelating agents. *Carbohyd. Res.*, 244, 99–114.
- Ridley, B. L., O'Neill, M. A., Mohnen, D., 2001. Pectins: structure, biosynthesis, and oligogalacturonide-related signaling. *Phytochemistry*, 57, 929–967.
- Rihouey, C., Morvan, C., Borissova, I., Jauneau, A., Demarty, M., Jarvis, M., 1995. Structural features of CDTA-soluble pectins from flax hypocotyls. *Carbohyd. Polym.*, 28, 159–166.
- Ristić, M. D., & Rajaković, L. V., 1996. Boron Removal by Anion Exchangers Impregnated with Citric and Tartaric Acids. *Separ. Sci. Technol.*, 31, 2805–2814.
- Rivas, B. L., Pereira, E. D., Palencia, M., Sánchez, J., 2011. Water-soluble functional polymers in conjunction with membranes to remove pollutant ions from aqueous solutions. *Prog. Polym. Sci.*, 36, 294–322.
- Rodríguez Pastor, M., Ferrándiz Ruiz, A., Chillón, M. F., Prats Rico, D., 2001. Influence of pH in the elimination of boron by means of reverse osmosis. *Desalination*, 140, 145–152.
- Rudnick RL, Gao S., (2005). Composition of the continental crust . *Treatise on Geochemistry*, 3, 1-64.
- S. Seyhan, Y. Seki, M. Yordakoc, M. Merdivan, 2007. Application of iron-rich natural clays in Camlica, Turkey for boron sorption from water and its determination by fluorimetric-azomethine-H method. *J. Hazard. Mater.*, 146, 180–185.

- Sabarudin, A., Oshita, K., Oshima, M., Motomizu, S., 2005. Synthesis of cross-linked chitosan possessing N-methyl-d-glucamine moiety (CCTS-NMDG) for adsorption/concentration of boron in water samples and its accurate measurement by ICP-MS and ICP-AES. *Talanta*, *66*, 136–144.
- Sah, R. N., Brown, P. H., 1997. Boron Determination—A Review of Analytical Methods. *Microchem. J.*, *56*, 285–304.
- Sajjaanantakul, T., Van Buren, J. P., Downing, D. L., 1989. Effect of Methyl Ester Content on Heat Degradation of Chelator-Soluble Carrot Pectin. *J. Food Sci.*, *54*, 1272–1277.
- Sato, S., Uchikawa, S., 1982. Spectrophotometric determination of boron by solvent extraction with hydrobenzoin and crystal violet. *Bunseki Kagaku*, *31*, 479–483.
- Sayiner, G., Kandemirli, F., Dimoglo, A., 2008. Evaluation of boron removal by electrocoagulation using iron and aluminum electrodes. *Desalination*, *230*, 205–212.
- Schols, H. A., Bakx, E. J., Schipper, D., Voragen, A. G. J., 1995. A xylogalacturonan subunit present in the modified hairy regions of apple pectin. *Carbohydr. Res.*, *279*, 265–279.
- Seki, Y., Seyhan, S., Yurdakoc, M., 2006. Removal of boron from aqueous solution by adsorption on Al₂O₃ based materials using full factorial design. *J. Hazard. Mater.*, *138*, 60–66.
- Senkal, B. F., & Bicak, N., 2003. Polymer supported iminodipropylene glycol functions for removal of boron. *React. Funct. Polym.*, *55*, 27–33.
- Shiklomanov, Igor A., 1993. *World fresh water resources - Water in crisis: A guide to the world's fresh water resources*. in Peter H. Gleick ed., Oxford University Press, New York.
- Shiklomanov, I. A., and J. C. Rodda. 2003. *World water resources at the beginning of the twenty-first century*. Cambridge, UK: Cambridge University Press.
- Simonnot, M.-O., Castel, C., Nicolaï, M., Rosin, C., Sardin, M., Jauffret, H., 2000. Boron removal from drinking water with a boron selective resin: is the treatment really selective? *Water Res.*, *34*, 109–116.

- Smith, B. F., Robison, T. W., Carlson, B. J., Labouriau, A., Khalsa, G. R. K., Schroeder, N. C., Jarvinen G. D., Lubeck C. R., Folkert S. L., Aguino, D. I., 2005. Boric acid recovery using polymer filtration: Studies with alkyl monool, diol, and triol containing polyethylenimines. *J. Appl. Polym. Sci.*, 97, 1590–1604.
- Smith, B. M., Todd, P., Bowman, C. N., 1999. Hyperbranched Chelating Polymers for the Polymer-Assisted Ultrafiltration of Boric Acid. *Separ. Sci. Technol.*, 34, 1925–1945.
- Sontheimer, H., Fettig, J., Hörner, G., Hubele, C., Zimmer, G., Frick, B.R., 1985. *Adsorptionsverfahren zur Wasserreinigung*. DVGW-Forschungsstelle am Engler-Bunte-Institut der Universität Karlsruhe (TH).
- Spectrum Labs. (n.d.). Tangential Flow and Hollow Fiber Benefits at Spectrum Labs.
- Spencer, R. R., Erdmann, D. E., 1979. Azomethine H colorimetric method for determining dissolved boron in water. *Environ. Sci. Technol.*, 13, 954–956.
- Spielholtz, G. I., Toralballa, G. C., Willsen, J. J., 1974. Determination of total boron in sea water by atomic absorption spectroscopy. *Microchim. Ac.*, 62, 649–652.
- Sriamornsak, P., 2011. Application of pectin in oral drug delivery. *Expert Opin. Drug Deliv.*, 8, 1009–1023.
- Stanton, R. E., McDonald, A. J., 1966. The colorimetric determination of boron in soils, sediments and rocks with methylene blue. *Analyst*, 91, 775–778.
- Stephenson, T., Brindle, K., Judd, S., Jefferson, B., 2000. *Membrane Bioreactors for Wastewater Treatment*. IWA Publishing.
- Stone, A.T., Morgan, J.J., 1990. *Kinetics of chemical transformations in the environment*. In *Aquatic Chemical Kinetics: Reactions rates of processes in natural waters*. W. Stumm Ed, Wiley-Interscience Pub, New York.
- Tagliabue, M., Reverberi, A. P., Bagatin, R., 2014. Boron removal from water: needs, challenges and perspectives. *J. Clean. Prod.*, 77, 56–64.

- Ted Oyama, Susan M. Stagg-Williams, 2011. Inorganic Polymer and Composite Membranes Structure, Function and other Correlations. *Membrane Science and Technology*, 14, 2-373.
- Teychene, B., Collet, G., Gallard, H., Croue, J., Acomparative study of boron and arsenic (III) rejection from brackish water by reverse osmosis membranes. *Desalination*, 310, 109-114
- Thakur, B. R., Singh, R. K., Handa, A. K., Rao, D. M. A., 1997. Chemistry and uses of pectin — A review. *CRC. CR. Rev. Food Sci.*, 37, 47–73.
- Thames Water, (2014). Section 4: Current and future water supply. Final water Resources Management Plan 2015-2040.
- Thangavel, S., Dhavile, S. M., Dash, K., Chaurasia, S. C., 2004. Spectrophotometric determination of boron in complex matrices by isothermal distillation of borate ester into curcumin. *Anal. Chim. Ac.*, 502, 265–270.
- Theiss, F. L., Ayoko, G. A., Frost, R. L., 2013. Removal of boron species by layered double hydroxides: a review. *J. Colloid Interf. Sci.*, 402, 114–121.
- Tonarini, S., Leeman, W. P., Ferrara, G., 2001. Boron isotopic variations in lavas of the Aeolian volcanic arc, South Italy. *J. Volcanol. Geoth. Res.*, 110, 155–170.
- Toray-Innovation by Chemistry, 2006. Flow Diagram/Models | seawater desalination | TORAY.
- Tu, K. L., Nghiem, L. D., Chivas, A. R., 2010. Boron removal by reverse osmosis membranes in seawater desalination applications. *Sep. Purif. Technol.*, 75, 87–101.
- Turek, M., Bandura-Zalska, B., Dydo, P., 2009. Boron removal by Donnan dialysis. *Desalin. Water Treat.*, 10, 53–59.
- Turek, M., Dydo, P., Trojanowska, J., Campen, A., 2007. Adsorption/co-precipitation—reverse osmosis system for boron removal. *Desalination*, 205, 192–199.
- Vasudevan, S., Lakshmi, J., Sozhan, G., 2013. Electrochemically assisted coagulation for the removal of boron from water using zinc anode. *Desalination*, 310, 122–129.

- Voragen, A. G. J., Coenen, G.-J., Verhoef, R. P., Schols, H. A., 2009. Pectin, a versatile polysaccharide present in plant cell walls. *Struct. Chem.*, 20, 263.
- Wang, B., Guo, X., Bai, P., 2014. Removal technology of boron dissolved in aqueous solutions – A review. *Colloids Surf. A: Physicochem. Eng. Asp.*, 444, 338–344.
- Ward, N. I., 1987. The determination of boron in biological materials by neutron irradiation and prompt gamma-ray spectrometry. *J. Radioanal. Nucl. Chem.*, 110, 633–639.
- Haden, E., (2005). Facts and Trends: Water. WBSCD - World Business Council for Sustainable Development,, Earthprint.
- Wei, Y.-T., Zheng, Y.-M., Chen, J. P., 2011. Design and fabrication of an innovative and environmental friendly adsorbent for boron removal. *Water Res.*, 45, 2297–2305.
- Stumm, W., 1992. Chemistry of the Solid-Water Interface: Processes at the Mineral-Water and Particle-Water Interface in Natural Systems. Wiley-Interscience Pub., New York.
- WHO. (1998). Boron. Environmental Health Criteria 204,. World Health Organization, Geneva.
- WHO. (2011). Guidelines for drinking-water quality. 4th ed.,. World Health Organization, Geneva.
- Winter, D., Koschikowski, J., Wieghaus, M., 2011. Desalination using membrane distillation: Experimental studies on full scale spiral wound modules. *J. Membrane Sci.*, 375, 104–112.
- Wolska, J., Bryjak, M., 2011. Preparation of polymeric microspheres for removal of boron by means of sorption-membrane filtration hybrid. *Desalination*, 283, 193–197.
- Wolska, J., Bryjak, M., 2013. Methods for boron removal from aqueous solutions — A review. *Desalination*, 310, 18–24.
- Wolska, J., Bryjak, M., Kabay, N., 2010. Polymeric microspheres with N-methyl-d-glucamine ligands for boron removal from water solution by adsorption–membrane filtration process. *Environ. Geochem. Hlth*, 32, 349–352.
- Woods, W. G., 1994. An introduction to boron: history, sources, uses, and chemistry. *Environ. Health Persp.*, 102, 5–11.

- Xu, J., Ruan, G., Gao, X., Pan, X., Su, B., Gao, C., 2008. Pilot study of inside-out and outside-in hollow fiber UF modules as direct pretreatment of seawater at low temperature for reverse osmosis. *Desalination*, 219, 179–189.
- Xu, Y., & Jiang, J.-Q., 2008. Technologies for Boron Removal. *Ind. Eng. Chem. Res.*, 47, 16–24.
- Yamauchi, T., Hara, T., Sonoda, Y., 1986. Distribution of Calcium and Boron in the Pectin Fraction of Tomato Leaf Cell Wall. *Plant Cell Physiol.*, 27, 729–732.
- Yan, C., Yi, W., Ma, P., Deng, X., Li, F., 2008. Removal of boron from refined brine by using selective ion exchange resins. *J. Hazard. Mater.*, 154, 564–571.
- Yang, C.-H., Shih, M.-C., Chiu, H.-C., Huang, K.-S., 2014. Magnetic Pycnopus sanguineus-loaded alginate composite beads for removing dye from aqueous solutions. *Molecules*, 19, 8276–8288.
- Yilmaz, İ., Kabay, N., Brjyak, M., Yüksel, M., Wolska, J., Koltuniewicz, A., 2006. A submerged membrane–ion-exchange hybrid process for boron removal. *Desalination*, 198, 310–315.
- Yilmaz, A. E., Boncukcuoglu, R., Yilmaz, M. T., Kocakerim, M. M., 2005. Adsorption of boron from boron-containing wastewaters by ion exchange in a continuous reactor. *J. Hazard. Mater.*, 117, 221–226.
- Yu, D., Xue, D., 2006. Bond analyses of borates from the Inorganic Crystal Structure Database. *Acta Crystallogr. B* 62, 702–709.
- Zaijun, L., Zhu, Z., Jan, T., Hsu, C.-G., Jiaomai, P., 1999. 4-Methoxy-azomethine-H as a reagent for the spectrophotometric determination of boron in plants and soils. *Anal. Chim. Ac.*, 402, 253–257.
- Zerze, H., Ozbelge, H. O., Bicak, N., Aydogan, N., Yilmaz, L., 2013. Novel boron specific copolymers with quaternary amine segments for efficient boron removal via PEUF. *Desalination*, 310, 169–179.

Appendices

1. Boron analysis methods

The study of characteristics, advantages, disadvantages and application of these methods are presented in this part of the thesis.

Spectrophotometric methods

Colorimetric methods & Fluorimetric method

Numerous spectrophotometric methods using different reagents for the color development are applied to determine boron concentration such as curcumin (McIntosh and Cox, 1960; Hayes and Metcalfe, 1962; Thangavel *et al.*, 2004), methylene blue (Stanton and McDonald, 1966), carmine (Hatcher, 1950; Higgs, 1960), crystal violet (Sato and Uchikawa, 1982) and azomethine-H (Demir and Serindağ, 2009; Oxspring *et al.*, 1995; Spencer and Erdmann, 1979) and others like quinalizarin, sorbitol, methyl orange, robocurcumin and rosocyanin (Zaijun *et al.*, 1999).

The main principle of colorimetric methods is to form color complex between boron and the reagent, for example, yellow complex with azomethine-H, blue complex with methylene blue, bluish red or blue with carmine, changing from pink to blue with quinalizarin or rose with curcumine. Then maximum absorbance of these complexes are measured at a define wavelength.

Beside spectrophotometric methods, fluorimetric method is utilized for boron determination through formation of fluorescent compounds between boron and number of reagents in concentrated acid or under milder condition as well. Aronoff (Aronoff *et al.*, 2013) reported boron and other boron-containing compounds can be detected readily by the interruption of the excited-state intramolecular proton transfer (ESIPT) of 10-hydroxybenzo[h]quinolone (HBQ). Another reagent, chromotropic acid (1,8-dihydroxynaphthalene-3,6-disulfonic acid), was used in a publication of Matol (T. Matoh *et al.*, 1997) which can react with boron to form the fluorescent B-chromotropic acid complex in an aqueous solution, and can be detected on HPLC. However, fluorimetric method is sensitive to pH and temperature and also suffered from interference of number of chemical species (Sah and Brown, 1997).

Ionometric Methods

Ionometric method is a non-spectrophotometric method where boron in the sample is reacted with HF and converted into tetrafluoroborate (BF_4^-) which is then measured by a selective electrode (Farhat *et al.*, 2013). The formation of tetrafluoroborate was greatly dependent on temperature. It is said that complete formation of tetrafluoroborate was in 5 min in 0.28 M hydrofluoric acid at 60°C but lasted 6 h in lower acid concentration and temperature. But this method was strongly influenced by nitrate and iodide anions. In order to eliminate this inconvenience, another work, which used a column of boron selective resin Amberlite XE-243 to isolate boron. Therefore this method is

interference free and suitable for boron analysis of some complicated matrix sample such as soil, plant (Carlson and Paul, 1969).

Atomic Spectrometric methods

Atomic emission/absorption spectrometry methods: AES and AAS use a flame (usually acetylene-air or acetylene-N₂O-air) to atomize the elements of the sample. AAS measurement is worked base on the principle that free atoms of an element in the ground state absorb photon from the discrete energy which is generated by a hollow cathode lamp containing that element. Reversely, AES technique measures the emission from the atomized and excited species when they fall down to the ground state. These methods often require separation and preconcentration of B from sample matrix (Sah and Brown, 1997). AAS method was used by Spielholtz (Spielholtz *et al.*, 1974) to determine B in seawater by using a boron hollow cathode, mixture of acetylene-N₂O-air as the fuel. Chelation and extraction was employed to preconcentrate boron concentration and increase the sensitivity. The accuracy of the method was reported to be consistent with the colorimetric carmine reagent method. Besides, boron was analyzed from Chinese tea and coffee hot water extract by using ICP-AES method (Krejčová and Černohorský, 2003). Introducing inductively couple plasma technique can increase the diversity of the sample from fresh to saline water, solid sample such as soil, rock, plant and biological sample (Leeman *et al.*, 2005; Tonarini *et al.*, 2001; Kasemann *et al.*, 2001). Moreover, by monitoring the ions based on their mass-to-charge ratio (*m/z*), ICP-AES can simultaneously measures boron concentration and its stable isotope abundance (Farhat *et al.*, 2013).

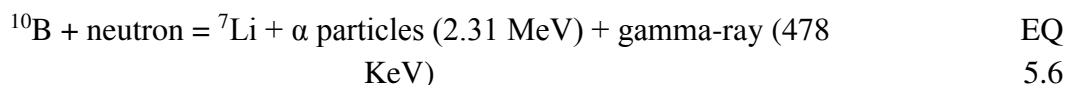
Other mass spectrophotometry

Thermal ionization mass spectrometry (TIMS)-based techniques: There are two types of TIMS methods: positive TIMS and negative TIMS. In PTIMS, boron in sample is converted into positive charged metaborate ions (BO₂⁺) which are present not only in BO₂⁺ but also in metal metaborate or alkali metaborate cation (MBO₂⁺), then measured by MS for *m/z* filtering (Deyhle, 2001; Rao *et al.*, 2008; Rao *et al.*, 2009). Negative TIMS operates in a similar way to PTIMS but produces and analyzes metaborate anions (BO₂⁻). Compare to PTIMS, in NTIMS, no alkali salt or metals are required, only metaborate anions are necessary, thus the simpler measurement is conducted (Duchateau and de Bièvre, 1983; Aggarwal and Palmer, 1995).

Nuclear reaction analytical methods (NRA)

Beside spectrophotometric methods, ionometric methods, atomic spectrometric method, nuclear reaction analytical methods are less popular technique which is using to analyze boron in solid samples with multi elements such as works of art or historical artifacts and generally low detection limit. Nuclear reaction analytical methods include neutron activation analysis, methods based on α -particle, methods based on measurement of γ -rays (Ward, 1987; Abd, 2014; Damkjaer, 1981; Bortolussi *et al.*, 2014). In NRA methods, the sample is bombarded with neutrons; the elements of interest are produced in form of radioactive isotopes. The radioactive emissions and radioactive decay paths for each element are well known. Using this information, it is possible to study spectra of the emissions of the radioactive sample, and determine the concentrations of the elements. For

boron samples, after bombarding with neutrons, the reaction produces α -particle and γ -particles which are monitored to correlate to ^{10}B stable isotope abundance (Farhat *et al.*, 2013).



In this work, we used azomethine-H method because of its advantages such as fast, simple and sensitive. It is appropriate for making a numerous number of sample analyses at once (about 20 samples) and stuff availability of the lab.

2. Viscosity measurement

Procedure

The sample is charged by inverting the viscometer and suction applied to tube arm L, while tube N was immersed in the sample solution and liquid drawled to mark G. The viscometer was then turned in the normal direction vertically in the water bath 40 °C. The sample was allowed to flow through capillary R and approximately half-filled bulb A, the meniscus was stopped in bulb A by placing a rubber stopper in tube N. The viscometer was introduced in the water about 10 min for sample to get 40 °C and the rubber stopper was removed to allow the meniscus to pass from mark E to F, from F to I. The passing time in seconds was recorded (efflux time).

$$\textit{Kinetic viscosity} = \textit{Efflux time} * \textit{viscometer constant}$$

The viscometer constant at 40°C for bulb C and D: 0.007769 ($\text{mm}^2 \text{ s}^{-2}$), 0.007257 ($\text{mm}^2 \text{ s}^{-2}$).



Fig. 1. The Cannon-Fenske opaque viscometer

RÉSUMÉ DE THÈSE

Introduction

L'eau douce est un élément essentiel à la vie et sa consommation se multiplie pour de nombreuses raisons: Les activités quotidiennes, l'élevage du bétail, la production d'agricultures ou la production d'énergie telles que l'électricité. La demande en eau augmente donc fortement avec le nombre de ces besoins, alors que les ressources diminuent à cause de la pollution industrielle et du changement climatique (Hilal *et al.*, 2011). Par conséquent, il est nécessaire de trouver des sources d'eau douce alternatives pour répondre à la forte demande d'eau de la société. L'eau potable produite à partir d'eau de mer par dessalement est l'une des solutions les plus utilisées (Karl *et al.*, 2009).

Normalement, la concentration de bore dans l'eau de mer est d'environ $4,6 \text{ mg L}^{-1}$, mais peut être supérieure, comme en Mer Méditerranée ($9,6 \text{ mg L}^{-1}$). Après le dessalement, la concentration de bore a diminué, mais reste toujours supérieur à $1,0 \text{ mg L}^{-1}$ selon le type de traitement utilisé. Ce problème se rencontre également lors du traitement de l'eau de surface ou des eaux souterraines, dont la concentration en bore peut être élevée en raison de contaminations par le rejet d'eaux usées des industries utilisant du bore (verre, engrais) ou du rejet des eaux domestiques contenant des produits de la vie quotidienne tels que les savons (Tu *et al.*, 2010), etc.

Le bore est un des éléments essentiels pour le développement des humains, des animaux et des plantes, mais l'excès de bore cause aussi des dommages à la santé et écologiques. La toxicité du bore limite la formation des cellules, affaiblit les os, retarde la croissance et crée des désordres du système de reproduction des personnes et des animaux. Chez les plantes, l'excès de bore se traduit, par exemple, par la réduction de la division cellulaire de la racine, l'inhibition de la photosynthèse, la diminution de la production de chlorophylle, etc. Par conséquent, il est très important de contrôler la concentration de bore dans l'eau pour obtenir une source d'eau assurant la vie humaine et l'irrigation. Des normes sur la concentration en bore ont été mises en place dans l'eau potable, elle doit être au maximum de $0,5 \text{ mg L}^{-1}$ selon l'OMS et $1,0 \text{ mg L}^{-1}$ par l'UE. Pour certaines plantations sensibles tels que les agrumes, la limitation de bore est abaissée à $0,3 \text{ mg L}^{-1}$ dans de l'eau d'irrigation (Redondo *et al.*, 2003).

L'élimination du bore est un problème difficile de nombreuses recherches ont été effectuées trouver les méthodes les plus efficaces. Mais chacun d'entre elles a ses avantages et inconvénients. Les technologies les plus utilisées ont été l'osmose inverse, l'échange d'ions ou une combinaison de procédés d'adsorption et de filtration. Ces méthodes peuvent éliminer le bore avec une efficacité de plus de 90%, mais ils ont encore gros inconvénients, comme l'obligation de fonctionner avec un pH élevé, le coût énergétique élevé, des matériaux coûteux, non biodégradable, etc.

L'objectif de cette thèse est d'étudier le développement d'un nouveau procédé, qui soit plus respectueux de l'environnement en utilisant un matériau d'origine biosourcé biodégradable comme support pour la fixation du bore. Afin de comprendre les mécanismes de fixation du bore, quatre résines synthétiques ont été choisies, deux résines d'échanges d'ions (Ambersep 900-OH et Amberlite IRA 402 Cl) et deux résines spécifiques du bore (Amberlite IRA 743 et Diaion CRB 03).

Ensuite, des pectines extraites à partir de déchets agricoles ont été évaluées comme adsorbant de bore. L'efficacité d'adsorption du bore des différents systèmes étudiés a ainsi pu être comparée.

Pour atteindre les objectifs, les travaux suivants ont été réalisés :

- Étudier l'influence du pH, de temps de réaction et de la concentration initiale de bore sur l'efficacité de fixation des résines synthétiques en système discontinu fermé.
- Etudier le comportement et comparer les courbes de percée d'adsorption du bore sur les différentes résines synthétiques appliqué dans un système ouvert en continu.
- Caractériser et analyser l'extrait de pectine: teneur en sucre neutre, acide galacturonique, la viscosité.
- Etudier le potentiel de filtration membranaire d'extrait de pectine à différents pH et la vitesse d'agitation.
- Effectuer la fixation de bore sur extraits de pectine avec deux systèmes d'ultrafiltration.

Cette thèse est organisée en 5 chapitres comprenant une introduction et une conclusion

Introduction: Présentation du contexte et des enjeux des travaux, puis des objectifs de la thèse

Chapitre 1: Etude bibliographique, faisant le bilan sur les différents procédés d'élimination du bore, puis sur les travaux actuels de recherche sur les nouvelles techniques. Une attention particulière est attachée à la description du mécanisme d'adsorption du bore et sur les premiers résultats de l'utilisation de matériaux naturels comme adsorbants

Chapitre 2: Matériels et méthodes, préparation et mise en place et des procédures d'expériences

Chapitre 3: Fixation du bore, par utilisation des résines synthétiques en mode batch. Présentation des résultats et discussion des points principaux.

Chapitre 4: Fixation du bore, par utilisation résines synthétiques en mode colonne. Présentation des résultats et discussion des points principaux.

Chapitre 5: Extraits de pectine pour l'élimination de bore dans l'eau, caractérisation et application des extraits de pectine sur l'élimination de bore.

Conclusion et travaux futurs: Bilan des résultats principaux de la thèse. Suggestion d'autres perspectives.

Chapter 1 ETAT DE L'ART

1.1. Présentation de bore

Le bore est un élément chimique rare sur la Terre, jamais sous la forme élémentaire (Rudnick and Gao, 2005). Le bore est un élément métalloïde, qui est légère mais très dur. Sa configuration électronique, $1s^2 2s^2 2p^1$, avec une orbite vide, fait qu'il y a tendance à opérer des liaisons avec d'autres éléments riches en électrons pour former différents composés (Cividini et al., 2009). La plupart des composés de bore naturels sont des minéraux sous forme de borate, qui sont déposés à partir de gaz volcaniques ou de sources d'eau chaude à proximité des activités volcaniques. Il existe plus de 200 minéraux dans le monde, avec deux dépôts prédominants (borax et sassolite), qui sont constitués de différents composés du bore avec le sodium, le calcium et le magnésium. Le bore peut être trouvée dans la roche (5 mg L^{-1}), dans le basalte ($<100 \text{ mg L}^{-1}$), dans le schiste sédimentaire ou dans le sol ($10 - 20 \text{ mg L}^{-1}$)

En milieu aquatique, le bore se trouve principalement dans les composés associés tels que le borate et d'acide borique. Sa concentration dans l'eau de mer a une valeur moyenne de $4,6 \text{ mg L}^{-1}$, dans l'eau douce de moins de $0,01 \text{ mg L}^{-1}$ à $1,5 \text{ mg L}^{-1}$, dans l'eau de pluie typiquement inférieure à $10 \text{ } \mu\text{g L}^{-1}$. En outre, le bore se trouve dans les plantes, des animaux et le corps humain comme élément essentiel, qui est nécessaire pour le développement structurel.

1.2. Boron dans la production de l'eau

Sans eau douce aucune société ne peut fonctionner. La surexploitation des ressources existantes en eau douce devient un problème dans de nombreuses régions du monde. Il y a un certain nombre de moyens qui traitent de l'augmentation du manque d'eau, par exemple, la réduction du gaspillage, l'augmentation du recyclage de l'eau, l'amélioration du réseau de transfert, le dessalement de l'eau de mer.

La production d'eau douce est généralement réalisée à partir d'eau souterraine mais de plus en plus à partir d'eau de mer ou d'eau de surface polluée. Au cours des processus industriels, de grandes quantités de bore ont été introduites dans l'environnement en tant que déchet. En effet, le bore est utilisé dans de nombreux domaines industriels, par exemple, la production de fibre de verre, production de porcelaine, le traitement du cuir, la production de savons de détergent et nettoyants, la production d'engrais, herbicides et insecticides. Le bore apparaît dans l'eau de surface comme la conséquence du rejet de ces eaux usées non traitées ou mal traitées.

Le bore est un élément nutritif essentiel pour la croissance des fruits et légumes et humain en raison de son rôle dans la formation et le renforcement de parois cellulaires et la synthèse d'hormones. La carence en bore inhibe la plante à partir de la croissance du tissu méristématique, la formation des cellules et des retards des réactions enzymatiques, la réduction de l'absorption des autres minéraux. La toxicité du bore est caractérisée par l'apparition chez les plantes de pointes jaunes aux feuilles ou la défoliation, la chute de fruits non mûrs pour les plantes. Chez les animaux, la toxicité se traduit par la réduction des systèmes nerveux et reproducteur, des problèmes dans le développement intellectuel et neurologique. L'OMS recommande donc une concentration de bore dans l'eau potable inférieure à $0,5 \text{ mg L}^{-1}$.

En solution aqueuse, le bore est normalement présent sous forme d'acide borique H_3BO_3 et des anions borate H_2BO_3 ($B(OH)_4^-$). L'équilibre de l'acide borique et du borate (pKa: 9.2) peut être exprimée comme suit:

L'équilibre de l'acide borique et du borate (pKa: 9,2) peut être exprimée comme suit:



.1

Lorsque le pH est inférieur à 9,2, le bore existe principalement dans la solution sous forme d'acide borique. Dans la région alcaline, l'ion borate devient la majeure partie.

Le dessalement de l'eau de mer est l'une des façons de produire de l'eau potable. Il y a environ plus de 23.000 usines de dessalement dans plus de 150 pays qui traitent plus de 85.000 m³ par jour. Il existe plusieurs types de configurations pour les usines de dessalement, celle qui se développe le plus utilise des membranes d'osmose inverse pour l'élimination des sels. Généralement une deuxième étape est alors nécessaire pour enlever le bore résiduel, soit encore par osmose inverse, après augmentation du pH, soit par des résines spécifiques pour le bore.

Les membranes d'osmose inverse sont des membranes denses où le transfert de solvant et de soluté à travers la membrane s'effectue par diffusion. Le transfert exige la dissolution de la molécule dans le matériau de la membrane avant sa diffusion. Par conséquent, les interactions entre la membrane et le soluté régissent l'efficacité de l'osmose inverse et permet d'expliquer leur grande sélectivité. Les résines spécifiques se composent de deux parties principales, un support macroporeux et des groupes fonctionnels greffés sur le polymère. Ces résines ont généralement au moins deux groupes hydroxyles adjacents, qui sont posés, en position cis, dite cis-diol qui a une sélectivité élevée en bore. Le principe de l'adsorption est un processus de complexation où l'acide borique est dissocié en solution aqueuse, libère des protons et réagit avec les diols pour former des esters de borate, qui sont alors immobilisés sur la résine. Les protons libérés lors de la réaction sont capturés par un groupe amine tertiaire, qui est fixé sur la matrice polymère, afin que le pH de l'eau reste constant (Li *et al.*, 2011).

Des procédés hybrides ont été développés en parallèle de l'osmose inverse et des résines spécifiques. Cette méthode est basée sur la combinaison du procédé d'adsorption et de filtration sur membrane. Les solutés comme le bore sont d'abord adsorbés par des sorbants fins puis filtrés sur membrane. Les avantages de cette technique sont meilleures performances, à moindre coût, pas de chute de pression.

1.3. Adsorbants récents à partir de matières liées aux plantes

Des échangeurs d'anions peuvent être construits à partir de déchets de matériaux naturels telles que la sciure de bois, la noix de coco, la canne à sucre, la bagasse, les feuilles de thé, la coque de riz, etc. Ils sont plus économiques que des échangeurs d'ions classiques, puisque cela permet d'élargir les applications de ces déchets agricoles. De plus, ces matériaux biodégradables ont un avantage

écologique par rapport aux produits dérivés du pétrole. Ces matériaux ont été utilisés comme échangeurs d'anions en raison de leur abondance des groupes diol qui ont des propriétés de chélation avec du bore en solution aqueuse.

1.4. Chromatographie sur colonne

La chromatographie sur colonne est étudiée depuis de nombreuses années, et ses performances sont décrites par différents types de modèles.

Théorie du modèle cinétique

L'équation cinétique du pseudo-premier ordre a été appliquée pour décrire les cas où la diffusion est limitée par le transfert au travers d'un film de liquide et l'adsorption est considérée comme un phénomène chimique.

$$\log(q_e - q_t) = \log(q_e) - \frac{k_1}{2.303} t \quad 1.2$$

L'équation cinétique pseudo-second ordre est décrit à partir de l'équation :

$$\frac{t}{q_t} = \frac{1}{k_2 q_e^2} + \frac{1}{q_e} t \quad 1.3$$

Où q_t et q_e représentent les quantités de bore absorbé (mmol g^{-1}) à l'instant t et à l'équilibre, respectivement; k_1 et k_2 sont la constantes de vitesses d'absorption ($\text{g mmol}^{-1} \text{min}$).

Théorie du modèle isotherme

L'adsorption monocouche entre les phases liquide et solide est généralement décrite par modèle isotherme de Langmuir avec les hypothèses suivantes (Foo and Hameed, 2010):

- Les sites de surface homogènes (même énergie)
- Chaque site peut occuper au plus une molécule (tous les sites sont identiques et équivalents)
- Pas de répulsion ou d'attraction due à des molécules déjà absorbées

$$\{=S-A\} = S_{\text{tot}} \frac{K_L [A]}{1 + K_L [A]} \quad 1.4$$

L'adsorption multicouche pour interface liquide-solide peut être décrit par le modèle BET.

$$q_e = \frac{q_s K_{\text{BET}} C_e}{(C_s - C_e) \left[1 + (K_{\text{BET}} - 1) \left(\frac{C_e}{C_s} \right) \right]} \quad 1.5$$

1.5. Pectines – Nouvelles adsorbants

Les pectines sont connues comme des polysaccharides complexes. Les pectines sont constituées de 4 types de polysaccharides différents : le rhamnogalacturonane I, le rhamnogalacturonane II, l'homogalacturonane et le xylogalacturonane. Le bore est présent dans la structure pectine par complexation avec le rhamnogalacturonane II (RG - II) sous forme d'un ester de bore. C'est pour cette raison qu'il a été envisagé de fixer le bore sur les pectines qui peuvent être extraites en grande quantité de la pulpe de betterave, résidu agricole mal valorisé. Les pectines sont biodégradables et pourraient être utilisées, après fixation du bore, comme compléments dans le cadre d'une agriculture biologique.

Néanmoins, il est nécessaire de récupérer les pectines après fixation du bore. Un procédé hybride devra donc être développé, par filtration sur membranes.

Il existe quatre procédés de séparation à membrane: Microfiltration, ultrafiltration, nanofiltration, osmose inverse. La filtration sur membrane présente certains avantages typiques (économies d'énergie, respectueux de l'environnement), mais aussi des limitations (encrassement et membrane avec courte durée de vie). La récupération des polysaccharides est généralement réalisée par ultrafiltration avec des membranes ayant un seuil de coupure compris entre 10 et 50 kDa.

Chapitre 2. MATÉRIELS ET MÉTHODES

2.1. Matériels

Solutions: Les solutions de bore ont été préparées à partir d'acide borique 99.99% (Sigma Aldrich Company) avec de l'eau Milli-Q. Les solutions ont été préparées avec du NaOH à 97% (VWR), du HNO₃ à 65% (Sigma Aldrich) et de l'acide acétique à 99,8% (Sigma Aldrich) Tous les autres réactifs, tels que l'acide L-ascorbique, azométhine-H et le sel monosodique de l'EDTA étaient de qualité analytique (Sigma Aldrich Company). Lors de l'analyse du bore, tous les tubes contenant le mélange réactionnel ont été couverts par une feuille d'aluminium pour éviter la lumière extérieure qui peut dégrader l'azométhine - sel H monosodique.

Résines: Quatre résines a été évaluées, deux résines anioniques, Ambersep 900-OH (Rohm & Haas) et Amberlite IRA 402 Cl (Rohm & Haas) et deux résines spécifiques du bore, Amberlite IRA 743 (Rohm & Haas) et Diaion CRB 03 (Rohm & Haas). Les principales caractéristiques de ces résines ont été rassemblées dans le tableau 2.1.

Pectines: Les deux types de pectine évalués ont été produits dans le laboratoire. La première a été produite à partir de la pulpe de betterave en réacteur discontinu avec de l'ammoniaque (Jorda, 2003) tandis que le second a été produit par extrusion à l'aide d'hydroxyde de sodium (Mogni, 2015).

Les standards de sucre (glucose, arabinose, le xylose, arabinose) étaient de qualité analytique (Sigma Aldrich), sauf le galactose (VWR). L'acide galacturonique était de Fluka Chemie.

Equipements: Les mesures de coloration pour le dosage du bore ont été réalisées avec un spectrophotomètre UV-1800 (Shimadzu Corporation, Japon). L'agitation des fioles a été réalisée avec un agitateur mécanique HS 501 digital (IKA Labor Technik). Les essais chromatographiques ont été réalisés avec une colonne de diamètre 5 cm, et de longueur de 50 cm. La solution d'alimentation était amenée dans la colonne par une pompe péristaltique Manostat Vera (Barnant Company).

La purification des échantillons a été réalisée avec une centrifugeuse 6-16K Sigma (Osteode, Allemagne). Une cellule d'ultrafiltration sous agitation Amicon a été utilisée pour les essais de filtration. Trois types de membranes en feuilles plates avec un MWCO de 10, 30, 100 kDa (Millipore) ont été placés dans la cellule de filtration. Un système de filtration à fibres creuses a été utilisé lors des essais de filtration à plus grande échelle. Les membranes étaient en polyéthèresulfone (GE Healthcare) avec un seuil de coupure de 30 kDa.

2.2. Procédures

L'analyse par la méthode de bore azométhine-H

Des solutions de bore, avec une concentration comprise entre 0,5 et 5,0 mg L⁻¹, ont été préparées pour réaliser la courbe d'étalonnage à partir d'une solution mère à 1000 mg L⁻¹. Une solution de azométhine – H 0,01 M a été préparée en dissolvant 0,45 g d'azométhine-H dans 100 ml de 1% (w / w) d'acide ascorbique. Une solution tampon 4,5 pH d'ammonium est préparée en dissolvant 50 g

$\text{NH}_4\text{CH}_3\text{COO}$ et 3 g de sel de sodium et de l'EDTA dans un mélange contenant 100 ml d'eau Milli-Q et 100 ml de CH_3COOH (> 99,8%). La réaction de décoloration a été réalisée en ajoutant 2 ml de tampon d'acétate d'ammonium, 2 ml d'azométhine-H réactif et de 1 ml d'une solution de bore ou de l'eau Milli-Q pour le blanc. Les mélanges ont été agités pendant 10 s, puis laissés au repos pendant 1 h. Les échantillons ont été analysés par spectrophotométrie à la longueur d'onde de 410 nm.

Caractérisation des pectines

Les pectines ont été caractérisées selon le protocole NREL définie pour l'analyse des sucres constitutifs. Le procédé comprend une étape d'hydrolyse du polymère, suivie d'une étape d'analyse par HPLC.

La viscosité a été mesurée avec un viscosimètre capillaire (CANNON n ° 75), tandis que les paramètres non-Newtoniens ont été définis pour les solutions à haute concentration avec un viscosimètre à disque (Paa Anton).

Expériences Batch

Expériences cinétiques: la résine humide conditionnée (2 g pour IRA 402 Cl et 5,3 g pour les autres) a été introduite dans un Erlenmeyer de 250 ml en plastique avec 95 ml de solution de bore, à un pH de 8 et à la concentration souhaitée. Le mélange a été agité mécaniquement à 258 tours par minute. Le temps d'adsorption étant comprise entre 30 min et 24 h.

Expériences de l'influence de pH: Les essais sont conduits de manière similaire aux expériences précédentes, mais le pH des solutions a été ajusté après introduction de la résine aux valeurs comprise entre pH 5 et pH 12. Le temps de contacts a été fixé à 2h.

Expériences isothermes: Elle est similaire à expérience cinétique, mais la solution de pH 8, (50 – 1000 mg L⁻¹) ont été agités dans 2h.

Expériences en colonne: Deux résines ont été utilisées pour des expériences de colonne, Ambersep 900-OH et Amberlite IRA 743. La résine a été préparée comme pour les essais en réacteur fermé et coulée dans la colonne de verre. Deux concentrations de bore (20 et 100 mg L⁻¹) et deux débits (10 et 60 BV h⁻¹) ont été utilisées.

Expérience de détermination de volume de pore: Deux concentrations de NaCl ont été préparées et conditionnées à un pH de 8, 2 L à 0,05 M et 1 L à 0,1 M. La colonne a été conditionnée à un pH de 8 par percolation d'une solution de soude. Ensuite les solutions de NaCl ont été éluées à un débit de 10 BV h⁻¹. Le pH et la conductivité ont été mesurés pour chaque échantillon.

Expérience d'adsorption de bore: Les expériences de bore sur Ambersep 900 - OH résine ont été réalisées avec deux lits, un de 100 ml et l'autre de 400 ml alors que pour l'Amberlite IRA 743 le lit était uniquement de 100 mL. L'adsorption a été opérée par la percolation d'une solution de bore à

travers la colonne au débit souhaité. La désorption a été réalisée en deux temps avec la résine Ambersep 900 - OH. Le lit a d'abord été rincé avec une solution de NaOH à pH 8, puis le bore a été élué avec une solution NaOH pH 13. Dans le cas de la résine IRA 743, l'éluion est réalisée directement avec une solution H₂SO₄ 0,5 M puis avec une solution de NaOH 0,25 M. A la fin, les deux résines ont été conditionnées dans une solution de NaOH à pH 8 pour être régénérées. Des échantillons ont été prélevés en continu chaque minute pour les débits de 60 BV h⁻¹ et 16 BV h⁻¹, toutes les 3 minutes pour un débit de 10 BV h⁻¹ flux. La conductivité et le pH ont été mesurés immédiatement, tandis que la concentration en bore a été déterminé après la fin de chaque phase (adsorption, rinçage et éluion).

Fixation de bore sur la méthode hybride:

À petite échelle: la solution de pectine (100 ml) a été introduite dans la cellule de filtration et la pression a été ajustée avec de l'air comprimé. La filtration a été réalisée avec une membrane de 0,003 m² de surface de filtration.

Des échantillons ont été prélevés périodiquement afin de suivre l'évolution des performances de la membrane au cours du temps. La masse de chaque échantillon a été mesurée afin d'obtenir un flux de massique.

À plus grande échelle: Une membrane de polyéthersulfone avec un seuil de coupure de 30 kDa (Ge Healthcare) avec une surface de filtration de 0,085 m² a été utilisée. La filtration a été effectuée à la fois par le recyclage du perméat et du rétentat pour maintenir une concentration constante dans le réservoir d'alimentation et travailler à l'état stationnaire. Différentes pressions transmembranaires, de 0.4 à 2 bars, ont été testées avec la même solution. A chaque pression, le flux de perméat a été mesuré jusqu'à obtenir l'état d'équilibre. Un échantillon a été prélevé à chaque état d'équilibre pour une analyse ultérieure.

Fixation de bore à différents pH

100 ml d'eau Milli-Q ou de solution de pectine ont été introduits dans chaque flacon, et le pH a été ajusté avec de l'hydroxyde de sodium ou l'acide nitrique. On a ajouté 2,0 g ou 0,5 g de pectine et la solution mélangées avant la mesure du pH afin d'obtenir la valeur initiale. Le flacon a été ensuite mélangé pendant 2 heures à 260 rpm par agitation mécanique. Au bout de 2 heures, le pH de la solution a été mesuré afin d'obtenir le pH final. Chaque échantillon a ensuite été centrifugé pendant 15 min à 8000 rpm à T = 20 °C. Le surnageant a été récupéré et filtré à l'aide d'une seringue et un filtre PTFE 0,45 µm. Le bore non fixé a été déterminé à partir de cette solution.

**Chapter 3. FIXATION DU BORE SUR RESINES SYNTHETIQUES AVEC
 SYSTEME BATCH-MODE**

L'adsorption du bore a été étudié sur deux résines spécifiques du bore, Amberlite IRA 743 et Diaion CRB 03 et deux résines échangeuses d'ions, Ambersep 900-OH et Amberlite IRA 402 Cl.

3.1. Cinétique

La cinétique est rapide au début, avec la fixation de plus de 98%, 98% and 96% du bore après 30 min de contact pour trois résines synthétiques IRA 743, CRB 03 and Amb 900-OH, respectivement. L'équilibre atteint après 2 h de réaction montre haute efficacité avec des résines ci-dessus, mais une faible efficacité (10% d'élimination) avec IRA 402 Cl. Les modèles cinétiques du pseudo-premier ordre et du pseudo-second ordre ont été utilisés pour tester les données expérimentales. Il a été confirmé que le modèle cinétique du pseudo second ordre correspond le mieux avec les données expérimentales des quatre résines. Les constantes de vitesse et la quantité d'adsorption du bore à l'équilibre ont alors pu être calculées (table 3.1).

Tableau 3.1. Constante de vitesse et quantité de bore adsorbé à l'équilibre pour une solution de bore à $9.90 \pm 0.74 \text{ mmol L}^{-1}$.

5.6.	Resin #	k_2 ($\text{g mmol}^{-1}\text{min}^{-1}$)	q_e (mmol g^{-1})
	IRA 743	7,0	0,18
	CRB 03	3,7	0,21
	Amb 900-OH	5,7	0,26
	IRA 402 Cl	2,9	0,037

3.2. Influence du pH

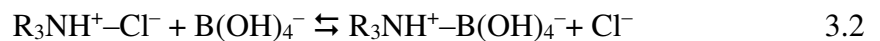
Le pH a une forte influence sur le processus d'adsorption avec la résine Ambersep 900-OH et Amberlite IRA 402 Cl, mais n'a pas d'impact sur l'élimination de bore des deux résines spécifiques du bore. L'adsorption maximale de bore a été obtenue à pH 8 et pH 10 pour Ambersep 900 - OH et IRA-OH 402 Cl, respectivement. Cependant, l'efficacité d'élimination était similaire à un pH différent avec les résines Amberlite IRA 743 et CRB 03. En outre, une augmentation significative du pH de la solution adsorbée a été observée avec l'IRA 743, CRB 03 et Ambersep 900 - OH. Le phénomène inverse a été observé avec IRA 402 Cl avec une diminution du pH de la solution après la réaction. Toutes les observations ci-dessus peuvent être expliqué par les mécanismes réactionnels:

- Adsorption maximale à un pH de 8 pour Ambersep 900-OH



Comme le pKa de l'acide borique est de 9,2, la plupart du bore est sous forme d'acide borique à pH <8, et sous forme de borate à pH > 8. La forme acide borique n'est pas favorable à un échange d'ions entre le bore et le groupe fonctionnel de la résine. Le borate participe à la réaction d'échange d'ions, mais à un pH supérieur à 8, il se retrouve en compétition avec les ions OH⁻ en solution. Par conséquent, c'est à pH = 8, quand 50% des borates sont en solution avec peu d'ions OH⁻ en compétition que la fixation de bore est maximale. L'augmentation du pH en solution après adsorption peut être clairement expliquée par l'équation en raison de la libération du groupe OH⁻ au cours du processus d'échange.

- Adsorption maximale à pH 10 pour Amb IRA 402 Cl



Les ions borates sont le principal facteur dans la réaction d'échange d'ions. A pH inférieur 10, les ions borates ne sont pas assez nombreux pour entrer en compétition avec les ions Cl⁻, mais à pH supérieur 10, la compétition entre les ions borate et les ions OH⁻ réduit l'adsorption. Ainsi, l'adsorption maximale est obtenue à un pH de 10. La diminution du pH en solution après adsorption est due à la protonation qui apparaît dans le processus de dissociation lorsque plus d'ions borate ont été impliqués dans une réaction d'échange d'ions.

- L'adsorption du bore est indépendante du pH pour IRA 743 et CRB 03: Ceci peut être expliqué par la participation des deux formes neutres et anioniques dans la réaction de formation du complexe avec les groupes fonctionnels. L'augmentation du pH de la solution après l'adsorption peut être due à la capture de protons sur le groupe N-méthylglucamine sur la résine.

3.3. Isotherms

Le comportement de l'adsorption du bore a été étudié sur les quatre résines. En général, la quantité de bore adsorbée augmente lorsque la concentration de bore augmente. Un plateau est observé pour les deux résines, Ambersep 900 – OH et CRB 03 tandis que deux plateaux sont observés avec IRA 743. L'adsorption du bore augmente de façon linéaire avec l'IRA 402 Cl. La relation de Langmuir décrit correctement le comportement d'adsorption pour CRB 03, Ambersep 900 - OH tandis que le type de relation BET correspond mieux au double mécanisme de l'IRA 743. Les résultats indiquent que la résine échangeuse d'ions 900 Ambersep - OH est très efficace avec une capacité de sorption double par rapport à celle de la résine spécifique de bore CRB 03 à pH naturel (pH 8).

La capacité d'adsorption et le coefficient de corrélation sont présentés dans le tableau 3.2.

Tableau 3.2. La capacité d'adsorption et le coefficient de corrélation de résines

Resin #	S_{tot} [mmol g ⁻¹]	K_L [L mmol ⁻¹]
Amb IRA 743	0,62	1,5
Diaion CRB 03	0,87	3,6
Amb 900-OH	2,2	0,051

**Chapter 4. FIXATION DE BORE SUR RESINES SYNTHETIQUES AVEC UN
REACTEUR TRAVERSANT TEL QUE LE SYSTEME DE COLONNE**

Il y a deux résines utilisées pour l'expérience colonne: une résine échangeuse d'anions (Ambersep 900 - OH) et une résine de bore sélective (Amberlite IRA 743)

4.1. Résine Ambersep 900 - OH

Détermination de pore volume (V_p)

L'expérience de détermination du V_p a été répétée plusieurs fois et a permis d'obtenir trois valeurs: 51,1 mL; 49,8 mL et 48,3 mL. La valeur moyenne (49,7 mL) a été utilisée.

L'expérience de fixation du bore

L'Influence de la concentration de bore: facteur de retardement de l'expérience d'une solution de 1,8 mM de bore est supérieure à celle d'une solution de bore 9,2 mM. Au cours de la désorption, le pic est plus large pour la concentration plus faible et plus nette pour la concentration élevée. L'augmentation de la concentration conduit à une augmentation de la masse de bore fixe. La capacité de sorption du bore pour l'expérience de 1.8 mM était de 0,40 mmol de résine B mL⁻¹, et on l'a augmentée à 0,51 mmol de résine B mL⁻¹ pour l'essai à 9,0 mM. Ce résultat est en accord avec les résultats des lots.

L'Influence du débit: Des expériences ont été réalisées des solutions utilisées à une concentration de 2 mM. Lorsque le débit augmente, le facteur de rétention a également augmenté. La capacité de la résine augmente de 0,40 mM de résine B mL⁻¹ à 10 BV h⁻¹ à 059 mM de résine B mL⁻¹ à 60 BV h⁻¹. Ceci est opposé à la théorie. Ce résultat pourrait être expliqué par la présence d'ions chlorure resté dans la résine qui aurait pouvoir changer la capacité de la résines

Influence du volume du lit de résine: La capacité de sorption du bore pour l'expérience de 9,54 mM B, 400 mL de résine, le débit de 16 BV h⁻¹ est de 0.63 mmol de résine B mL⁻¹, qui est supérieure à la capacité de sorption de l'expérience de 9,2 mM [B], 100 mL de résine, 10 BV h⁻¹, pH 8 (0,51 mmol de résine B mL⁻¹), même cette expérience a été réalisée à un débit légèrement supérieur (16 BV h⁻¹). Par conséquent, il est nécessaire de supposer que le temps de séjour dans la colonne était trop court dans 100 ml de lit. Mais le temps caractéristique dans la colonne était d'environ 3 min dans les deux expériences, au-dessus de 0,7 min pour la demi-fixation calculée avec le modèle de pseudo-deuxième ordre

4.2. Résine Amberlite IRA 743

Détermination de pore volume (V_p)

Le volume de pore (V_p) a été déterminé, avec des solutions de chlorure de sodium comme pour la résine précédente et avec un lit de 100 ml de résine sèche, a la valeur de 76,20 mL.

L'expérience de fixation du bore

Comparaison entre les deux débits: Les courbes de percée du bore, obtenues pour les deux débits (10 & 60 BV h⁻¹), ont été comparées. Les résultats montrent que lorsque le débit est plus faible, le facteur de retard est plus élevé. Mais ils confirment aussi que, lorsque le débit est trop élevé, la courbe devient linéaire. Le pic est plus net à 10 BV h⁻¹, mais ce flux est encore trop élevé et la réaction limite toujours la fixation du bore. La capacité de la résine ne change pas avec le flux, 0,41 mmol de résine B mL⁻¹ à 60 BV h⁻¹ et 0,36 mmol de résine B mL⁻¹ à 10 BV h⁻¹. La différence de 10% reste dans les limites de la précision de la méthode.

4.3. Comparaison entre les deux résines

L'efficacité d'adsorption des deux résines a été réalisée avec une solution de bore de 8,62 mM (IRA 743) et 9,2 mM (Ambersep 900 - OH) à un débit 10 BV h⁻¹ et pH 8. Le facteur de retard, obtenu à partir de la courbe de percée de bore pour Amberlite IRA 743 est inférieur à celle de Ambersep 900 - OH. Ceci s'explique par le fait que la cinétique de fixation limite l'efficacité de la résine spécifique, qui laisse alors sortir plus rapidement le bore. Néanmoins, la masse de bore adsorbé pour les deux expériences est similaire, 0,36 mmol B mL⁻¹ de résine (IRA 743) et 0,51 mmol B mL⁻¹ de résine (Ambersep 900 - OH), à moins de 10% de différence. Mais dans le cas d'un fonctionnement où la concentration en bore en sortie de traitement doit être inférieure à 0,5 mg L⁻¹, la résine Ambersep 900 - OH permettrait de traiter un volume deux fois plus grand que la résine IRA 743. Néanmoins, la résine IRA 743 pourrait avoir la même efficacité si le débit était réduit à moins de 10 BV h⁻¹.

4.4. Modélisation des courbes de percée

Le modèle de Yoon et Nelson et le modèle de Thomas sont adaptés choisis pour correspondre aux données expérimentales de deux résines. Les deux modèles sont bien équipés d'expériences avec des capacités de sorption similaires. En conclusion, ces modèles peuvent optimiser les courbes de percée pour les expériences des deux résines. Le modèle non linéaire utilisant les Langmuir paramètres à partir de l'expérience discontinue, peut être utilisé pour simuler correctement le front compressif d'Amb 900-OH. Il y a un petit décalage entre le front dispersif de l'expérience et la simulation, mais ils ont montré la même tendance. L'influence de la concentration de bore ne peut pas être expliquée par la théorie de l'isotherme, qui a un autre mécanisme qui augmente largement l'affinité du bore sur la résine. Le modèle non linéaire ne simule pas bien le front compressif de l'expérience avec la résine Amb IRA 743 en raison d'une grande différence dans le facteur de retardement calculé et expérimental. Les raisons possibles doivent être l'isotherme de Langmuir qui ne correspond qu'à une petite gamme de concentration de bore en solution (< 35 mmol L⁻¹) et une grande valeur du volume des pores. Le facteur de retardement calculé utilisant un V_p plus petit à vérifier la publication de Simonot a montré une simulation mieux ajustée avec notre expérience.

Chapter 5. EXTRAIT DE PECTINE POUR LE RETRAIT DE BORE DANS L'EAU

5.1. Ultrafiltration

La perméabilité de la membrane

L'influence de la vitesse d'agitation sur la perméabilité de la membrane au cours de la filtration de l'eau a été étudiée sur trois membranes avec un seuil de coupure (MWCO) de 10, 30 et 100 kDa. Les flux obtenus ont légèrement diminué lorsque la vitesse d'agitation est augmentée, mais surtout plus le MWCO est élevé plus le flux de perméat est grand. La membrane 100 kDa a un flux d'environ $170 \text{ L h}^{-1} \text{ m}^{-2}$ alors qu'elle est seulement d'environ $100 \text{ L h}^{-1} \text{ m}^{-2}$ pour les deux autres membranes.

L'influence de la vitesse d'agitation sur le flux de perméat lors de la filtration d'une solution de 5 g L^{-1} de pectine a alors été étudiée avec ces trois membranes. Le flux de perméat obtenu au cours de la filtration des solutions pectiques est beaucoup plus faible que ceux obtenus avec de l'eau. En revanche, il n'y a presque pas de différence entre les flux des membranes, les valeurs obtenues sont de l'ordre de $10 \text{ kg h}^{-1} \text{ m}^{-2}$. Ce résultat est régulièrement présenté lors de la filtration de solutions de polymères en raison de la création d'une couche de polarisation de concentration. Cette couche de polarisation de concentration donne les propriétés filtrantes et tend à niveler les différences entre les membranes. Cette couche est difficile à enlever car la vitesse d'agitation ne modifie pas la valeur du flux de perméat. La perméabilité expérimentale des solutions de pectine est beaucoup plus faible que la valeur que l'on peut calculer à partir de la viscosité de la solution et de la perméabilité de la membrane. Cette différence confirme l'influence de la couche de polarisation sur les performances de filtration. Lors de la filtration, la couche de polarisation de concentration au-dessus de la membrane provoque une modification importante de la viscosité de la solution à la surface de la membrane et crée une résistance supplémentaire au transfert de masse.

L'Influence de la pression

L'influence de la pression a été réalisé afin de confirmer l'existence de la couche de polarisation de concentration. Les résultats montrent que le flux de perméat augmente avec la pression transmembranaire jusqu'à une valeur limite de 1 bar. Au-dessus de cette valeur limite, le flux n'augmente plus en raison de la formation d'une couche de gel dont l'épaisseur augmente avec la pression.

5.2. Évaluation des performances à l'échelle pilote

Pectine extraite en réacteur discontinu

La filtration a été lancée à la pression de 0,4 bar, et le flux mesuré régulièrement jusqu'à ce que les valeurs soient devenues constantes. Une fois l'état stationnaire atteints, les prélèvements ont été effectués et la pression augmentée. Les flux de perméat obtenus pour chaque état d'équilibre de chaque pression sont présentés pour deux vitesses tangentielles. Le flux de perméat augmente de façon linéaire avec la pression jusqu'à une valeur maximale de $26 \text{ L h}^{-1} \text{ m}^{-2}$ pour la pression transmembranaire de 2 bars. Ce résultat indique qu'il n'y a pas de limitation par la couche de polarisation de concentration. A basse vitesse tangentielle, l'évolution du flux n'a pas augmenté au-dessus de la

pression limite de 1,5 bar, ce qui indique l'apparition d'une couche de gel à la surface de la membrane. Les résultats montrent donc que la couche de polarisation de concentration peut être partiellement éliminées aux fortes vitesses tangentielles ce que ne permettait pas la cellule de filtration.

Pectine extraite par extrusion bi-vis

La filtration a été fait dans les mêmes conditions que pour l'étude avec l'extrait en réacteur fermé. Les débits augmentés presque linéairement de 15 L h⁻¹ m⁻² à 0,4 bar à 46 L h⁻¹ m⁻² à 2 bars. Ce résultat indique qu'il n'y a pas de couche de polarisation de concentration. La lumen des membranes permet d'avoir un effet de cisaillement, suffisamment élevé pour limiter l'apparition de la couche de gel et permet d'obtenir des valeurs de flux élevées. Le flux obtenu est deux fois supérieur, à 2 bars, avec l'extrait par extrusion qu'avec le cell obtenu avec l'extrait en réacteur fermé. Cette différence s'explique par la pureté de l'extrait discontinu qui contient plus de pectine et donc qui présente des propriétés gélifiantes plus élevées.

5.3. Fixation de bore

Caractérisation de pectine

Les deux types de pectine testés lors de la filtration ont été utilisés pour la fixation de bore. Ces extraits qui n'ont pas été purifiés présente une pureté relativement faible (tableau 5.1).

Tableau 5.1. La composition des extraits pectiques utilisés pour la fixation du bore

Composants	Pectine extraite par extrusion (%)	Pectine extraite par réacteur fermé (%)
Glucose	9,8	Non détecté
Galactose	10,2	8,0
Arabinose	15	17,3
Galacturonic acid	11,9	22,7

Essais de fixation

Pectine extraite en continu

Des essais ont été réalisés à différents pH (5-12), avec 2 g de pectine dans 100 ml de solution à 100 mg L⁻¹ en bore. Les résultats montrent que le rendement de fixation du bore est faible, allant de 3% à 14% correspondant à une capacité de sorption de 0,1 à 0,6 mg g⁻¹ qui est inférieure à celle obtenue pour la résine IRA 743 (6,7 mg g⁻¹), CRB 03 (9,4 mg g⁻¹) et Amb 900-OH (23,8 mg g⁻¹). Ceci peut être expliqué par l'hétérogénéité de la poudre produite parce que la teneur en pectine ne représentait que 47% du composant de pectine extrait, l'autre partie pourrait être les impuretés.

La faible concentration en RG-II dans l'extrait pectique est aussi une raison à cette faible efficacité. En effet, le bore forme l'ester de borate uniquement avec le RG-II par une réticulation covalente.

Comme de plus, les plantes ont 95% des molécules de RG-II impliquées dans un dimère avec du bore, et seulement 5% de RG-II libre pour l'adsorption du bore. La teneur de bore en pectine a été déterminée à environ 0.06 mg g⁻¹ ou 60 mg kg⁻¹, ce qui confirme cette hypothèse, les pectines contiennent du bore et donc seule une faible proportion du RG-II est disponible pour la fixation du bore.

Enfin, un pH élevé n'est pas favorable à la fixation du bore par la pectine. Le borate dans le dimère RG-II-B est stable au-dessus de pH 4. Par conséquent, la réaction de fixation n'a pas été étudiée dans les conditions optimales.

Pectine extraite par extrusion bi-vis en discontinu

La teneur de bore, 62 à 84 mg kg⁻¹, est supérieure à celle dans l'extrait pectique obtenu par extrusion continue. Surtout, cette valeur est beaucoup plus élevée à pH 2 qu'à pH 6, peut être par l'hydrolyse de l'ester de borate en acide borique et monomère RG-II à pH 2. Les résultats de l'essai de fixation du bore sont difficiles à analyser, car la concentration finale est supérieure à la concentration initiale, en raison de problèmes de dilution.

Chapter 6. CONCLUSIONS ET FUTURES DES TRAVAUX

CONCLUSIONS

6.1. L'expériences des lots sur résines synthétiques

Cinétique: La cinétique est rapide avec fixation de plus de 96% de bore après 30 min de contact pour trois résines synthétiques (IRA 743, CRB 03 & Ambersep 900 -OH) mais une faible efficacité avec IRA 402 Cl. L'équilibre est atteint après 2 h de réaction. Le modèle cinétique pseudo second ordre permet la meilleure description des résultats expérimentaux.

L'influence du pH: le pH a une forte influence sur le processus d'adsorption avec les résines Ambersep 900 - OH et Amberlite IRA 402 Cl, mais n'a pas d'impact sur la fixation du bore par les deux résines spécifiques. L'adsorption maximale de bore a été obtenue à pH 8 et pH 10 pour Ambersep 900 et IRA-OH 402 Cl respectivement.

Isotherme: La quantité de bore adsorbée augmente lorsque la concentration en bore augmente. Un plateau est observé pour les deux résines, Amb 900 - OH, CRB 03 tandis que deux plateaux ont été observés avec IRA 743. L'adsorption du bore augmente de façon linéaire avec l'IRA 402 Cl. La relation de type de Langmuir décrit correctement le comportement d'adsorption pour CRB 03, Amb 900-OH tandis que le type de relation de BET correspond mieux avec double mécanisme de l'IRA 743. La résine Amb 900-OH est très efficace avec une capacité de sorption doublée par rapport à celle du CRB 03 à pH naturel (pH 8).

6.2. L'expériences de colonnes avec des résines synthétiques

Deux résines ont été évaluées, une résine spécifique du bore (Amberlite IRA 743) et une résine échangeuse d'ions (Ambersep 900 - OH). Le volume de pore des lits a été évaluée à 49,7 mL pour Ambersep 900 - OH et 76,2 mL pour IRA 743.

Pour la résine Ambersep 900-OH : Le facteur de retard et la capacité qui augmentent que le débit diminue. La présence d'ions chlorure dans la résine au fort débit liée à une mauvaise régénération après la mesure du V_P peut expliquer ce résultat. Quand le débit est constant, le facteur de retard diminue quand la concentration augmente de 1,8 mM à 9,2 mM.

Pour la résine IRA 743: Le facteur de retard diminue quand le débit augmente de 10 BV h⁻¹ à 60 BV h⁻¹, mais la capacité reste assez similaire, 0,36 mmol B mL⁻¹ resin à 10 BV h⁻¹ et 0,41 mmol B mL⁻¹ resin à 60 BV h⁻¹.

La comparaison des deux résines, à même concentration (9,0 mM) et même débit (10 BV h⁻¹) montre que l'état d'équilibre est atteint plus rapidement avec la résine IRA 743. La courbe de percée de cette résine à une forme linéaire qui montre que les débits utilisés étaient trop élevés pour permettre la fixation efficace du bore. La réaction de fixation était l'étape limitant. Néanmoins, les capacités des deux résines sont similaires. Mais la forme des courbes de percée montre que pour la production d'eau à une concentration en bore maximale de 0,5 mg L⁻¹, la capacité de traitement de l'Ambersep 900 - OH est deux fois plus grande que celle de Amberlite IRA 743.

Table 6.1. Résumé de l'expérience de la colonne avec des résines synthétiques

Resin bed	Experiment condition	Amb 900-OH (mmol mL ⁻¹)			Amb IRA 743 (mmol mL ⁻¹)		
		C _{Total}	C _{Break-through}	Column Utilization (%)	C _{Total}	C _{Break-through}	Column Utilization (%)
		100 mL (Amb 900-OH)	1.8 mM, 10 BV h ⁻¹	0.45	0.40	88.6	
	1.8 mM, 60 BV h ⁻¹	0.67	0.59	87.9			
100 mL (Amb IRA 743)	9.0 mM, 10 BV h ⁻¹	0.59	0.51	86.3	0.57	0.36	63.3
	9.0 mM, 60 BV h ⁻¹				1.37	0.41	29.6
400 mL (Amb 900-OH)	9.5 mM B, 16 BV h ⁻¹	0.69	0.63	91.4			

Le modèle de Yoon et Nelson et le modèle Thomas ont été utilisés pour optimiser les courbes de percée avec des capacités de sorption similaires de deux résines. Le modèle non linéaire construit sur les paramètres de Langmuir à partir d'expériences par lots a été utilisé pour simuler les courbes de percée de l'expérience (9 mM, 10 BV h⁻¹) pour deux résines. Pour Ambersep 900-OH, la simulation s'est bien équipée avec des front compressif mais qu'il présentait un petit décalage avec le front dispersé. L'influence de la concentration n'a pas été expliquée par la théorie de l'isotherme en raison d'une grande différence entre les facteurs de retardement expérimental et calculés. Il est censé avoir un autre mécanisme qui a impliqué dans la réaction et augmenté l'affinité au bore avec la résine. Pour Amberlite IRA 743, une différence significative entre la simulation et les courbes de percée expérimentale a été observée. Il existe deux raisons possibles: l'isotherme de Langmuir n'est adaptée qu'à une petite gamme de concentration de bore et le volume des pores est trop élevé. L'utilisation d'une plus petite valeur de volume de pores provenant de l'expérience de Simonot, a entraîné une courbe de percée mieux adaptée.

6.3. L'expérience de pectine dans les lots et le système continu

La filtration de la pectine peut être gérée avec une membrane d'ultrafiltration ayant un MWCO de 30 kDa. Mais pour être efficace, la filtration de la solution de pectine a besoin d'être réalisée à un taux de cisaillement élevé afin d'éviter l'apparition d'une couche de gel qui limiterait les performances de la membrane. Le flux de perméat de membrane à 2 bars est de $26 \text{ L h}^{-1} \text{ m}^{-2}$ pour la pectine extraite en discontinu et il est de $46 \text{ L h}^{-1} \text{ m}^{-2}$ pour la pectine extraite en continu. La différence entre les deux solutions peut être expliquée par la composition de l'extrait, et son influence sur les propriétés rhéologiques. La pectine extraite en discontinu présente une plus forte tendance à former un gel, à une concentration plus faible, ce qui pourrait provoquer une limitation du flux plus importante.

Les extraits de pectine ont de faibles capacités de fixation du bore, mais la pureté et la structure des molécules extraites peuvent expliquer cela. La capacité qui peut être calculée faible, à environ $0,5 \text{ mg g}^{-1}$ de poudre, mais compte tenu de la pureté d'environ 50%, il donne une capacité potentielle de 1 mg g^{-1} de pectine. Cette valeur est encore faible par rapport à la capacité de la résine IRA 743 qui était d'environ 6.7 mg g^{-1} de résine. Les résultats montrent donc que la fixation du bore par les pectines est possible mais nécessite d'utiliser une poudre raffinée pour avoir une concentration suffisamment élevée en RG-II. De plus, l'extrait pourra être activé par libération du bore fixé avec un traitement acide. Une autre solution serait la modification chimique afin d'augmenter le nombre de site réactif.

FUTURES DES TRAVAUX

Il devrait dans un premier temps de définir l'influence des anion Ca^{2+} , Mg^{2+} , Fe^{2+} , Fe^{3+} , Cl^- , NO_3^- , SO_4^{2-} sur la cinétique de sorption et la capacité d'adsorption, en particulier avec Ambersep 900-OH. Deuxièmement, il faut apprendre de l'influence de la température sur l'efficacité d'adsorption. En modifiant la température de l'expérience, elle modifie le mouvement des ions ou des molécules dans la solution, puis augmente ou diminue les possibilités de leur contact avec les sites d'adsorption, modifiant par conséquent la cinétique de la réaction.

L'expérience de la colonne doit être effectuée avec des concentrations de bore supplémentaires (5, 20, 30 mmol L^{-1}) avec des débits plus élevés (15, 20, 30 BV h^{-1}) pour obtenir des résultats plus fiables quant à l'influence des débits et concentration de bore sur le processus de fixation du bore. L'objectif de ces essais serait de comprendre l'influence de l'advection et de la fixation cinétique sur les performances de fixation de la résine. Dans ce cas, il serait intéressant de gérer des expériences avec une colonne de différents diamètres afin de séparer l'influence du temps de contact et de l'advection sur le taux de fixation.

La fixation du bore doit également être réalisée avec la présence d'autres ions tels que Cl^- , NO_3^- , SO_4^{2-} qui sont habituellement présents dans des échantillons d'eau réels. Ces ions auront probablement une influence considérable sur le processus d'échange d'ions en raison de la compétition avec les ions borate, les hydroxydes.

Plus grande membrane doit être appliquée pour trouver les conditions optimales. La fixation du bore doit être réalisée avec différents types de fractions raffinées de pectine (RG-I, RG-II, etc.) afin d'identifier les polymères pouvant interagir avec le bore, quels sont les mécanismes impliqués et les paramètres cinétiques. Ces résultats permettront de définir la pureté et la composition requises de l'extrait pour une fixation efficace du bore.

Les compositions d'extraits devront caractériser avec précision afin de connaître la teneur en différents polymères de pectine, mais aussi la teneur en composés phénoliques (acide férulique et coumarique) et en hémicelluloses qui peuvent également fixer le bore.

L'adsorption de bore sur l'extrait de pectine doit être étudiée avec différents paramètres tels que la concentration de bore, la dose de pectine, le temps de réaction, la température et l'influence d'autres ions. Un prétraitement est utilisé pour activer l'extrait et fixer une plus grande quantité de bore.